Electronic Supplementary Material (ESI) for Organic & Biomolecular Chemistry.

Supporting Information

In-Flow Photooxygenation of Aminothienopyridinones Generates Iminopyridinedione PTP4A3 Phosphatase Inhibitors

Nikhil R. Tasker,[a] Ettore J. Rastelli,[a] Isabella K. Blanco,[b] James C. Burnett,[a] Elizabeth R. Sharlow,[b] John S. Lazo[b] and Peter Wipf[a]*

[a]Department of Chemistry, University of Pittsburgh, Pittsburgh, PA 15260, United States
[b]Department of Pharmacology, University of Virginia, Charlottesville, VA 22908, United States

1. Scheme S1. Synthesis of compounds **5**, **6**, and **7** ..... Page 2
2. Scheme S2. Synthesis of compounds **8a**, **9a**, **8b**, **9b**, **8c**, and **9c** ..... Page 2
3. Scheme S3. Synthesis of compounds **8d**, **9d**, **8e**, **9e**, **8g**, **9g**, **8j**, **9j**, **8p**, **2** and **3** ..... Page 3
4. Scheme S4. Synthesis of compounds **8f**, **9f**, **8h**, **9h**, **8i**, **9i**, **8k**, **9k**, **8l**, **9l**, **8m**, **9m**, **8n**, and **9n** ..... Page 4
5. Scheme S5. Synthesis of compounds **8o** and **9o** ..... Page 5
6. Scheme S6. Synthesis of compounds **9p**, **9q**, and **40** ..... Page 5
7. Scheme S7. Synthesis of compounds **15**, **16**, and **17** ..... Page 5
8. Scheme S8. Synthesis of compounds **18** and **19** ..... Page 6
9. Figure S1. Sketch of flow apparatus ..... Page 6
10. Figure S2. Picture of flow apparatus in operation and additional experimental details ..... Page 7
11. Figure S3. Concentration-PTP4A3 phosphatase inhibition response curves ..... Page 9
12. Table S1. General procedure and results for optimization of photooxygenation ..... Page 10
13. Table S2. Purification methods of **2**:**3** mixture ..... Page 11
14. Table S3. Computational drug-likeness estimates for derivatives of **2** ..... Page 12
15. Single crystal x-ray diffraction data; Table S4 ..... Page 13
16. Spectrofluorometry and UV-VIS data; Figures S4-S8 ..... Page 14
17. PTP4A3 Phosphatase assay methods ..... Page 20
18. Molecular modeling methods; Figures S9-S12 ..... Page 21
19. Spectra (^{1}H NMR, ^{13}C NMR, ^{19}F NMR) ..... Page 25

1. Scheme S1. Synthesis of compounds **5**, **6**, and **7**

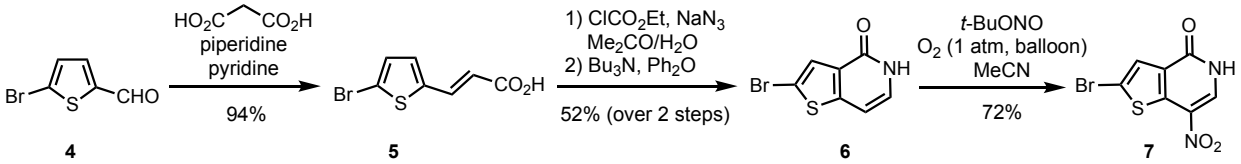

2. Scheme S2. Synthesis of compounds **8a**, **9a**, **8b**, **9b**, **8c**, and **9c**

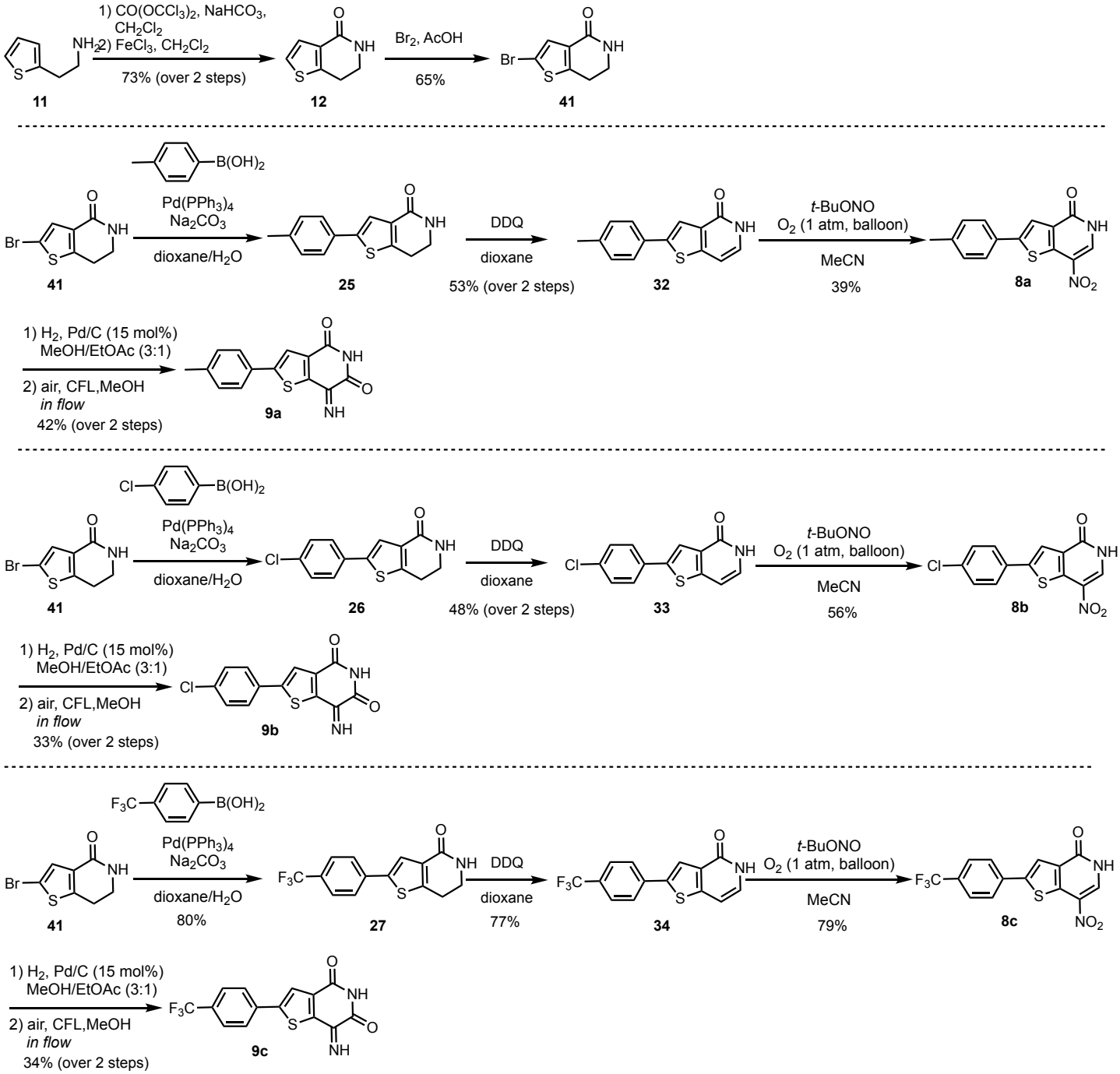

3. Scheme S3. Synthesis of compounds **8d**, **9d**, **8e**, **9e**, **8g**, **9g**, **8j**, **9j**, **8p**, **2** and **3**

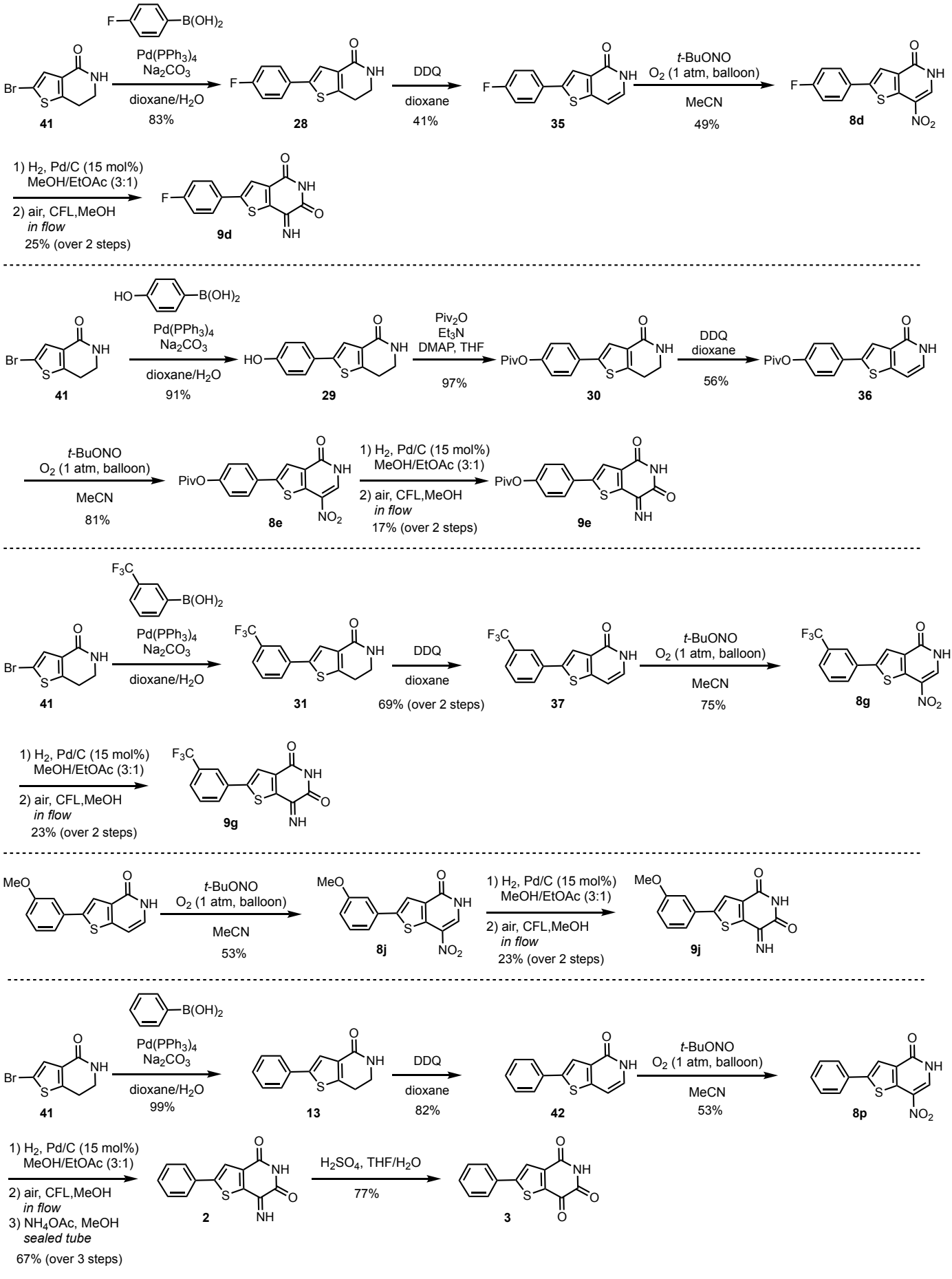

4. Scheme S4. Synthesis of compounds **8f**, **9f**, **8h**, **9h**, **8i**, **9i**, **8k**, **9k**, **8l**, **9l**, **8m**, **9m**, **8n**, and **9n**

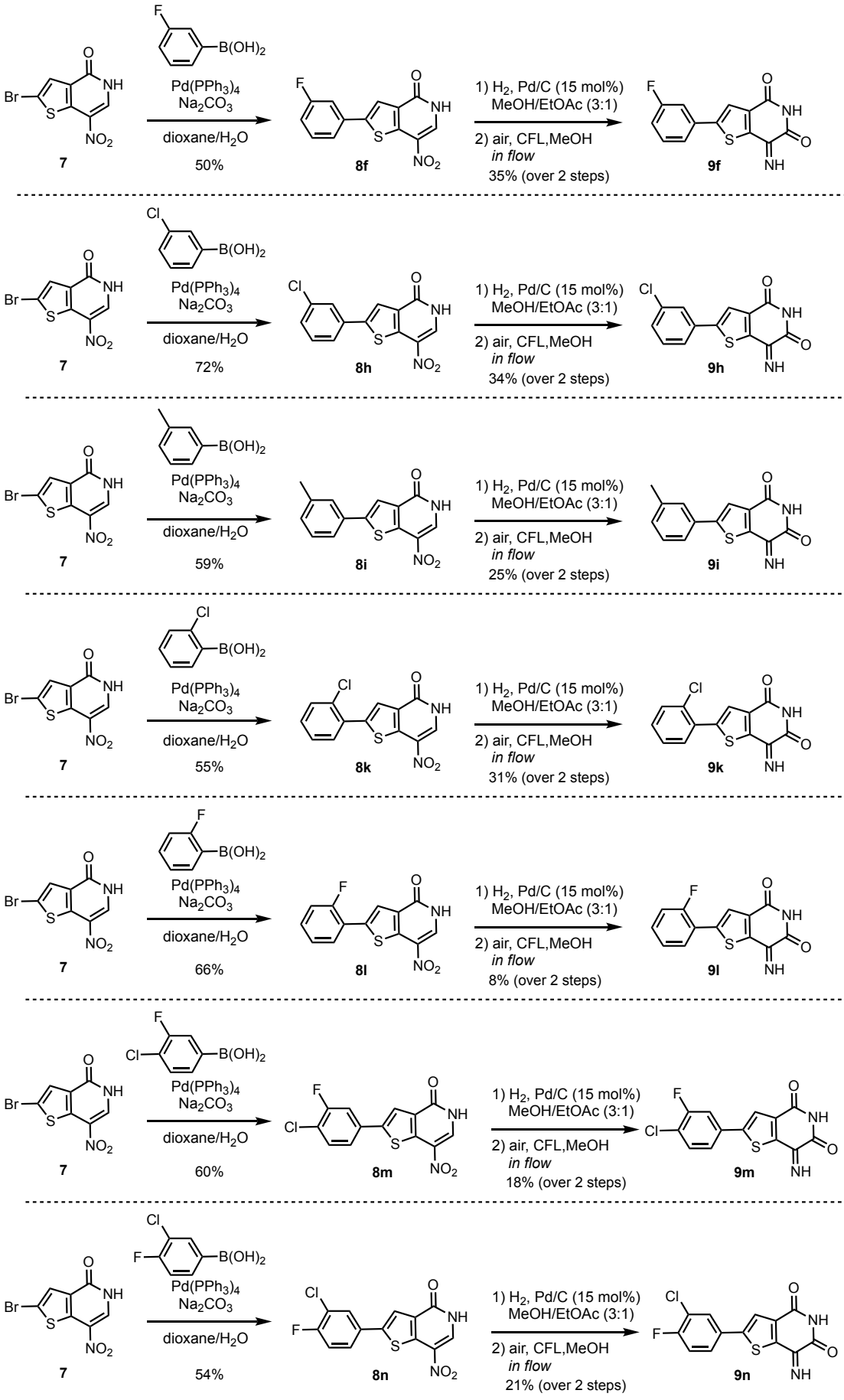

5. Scheme S5. Synthesis of compounds **8o** and **9o**

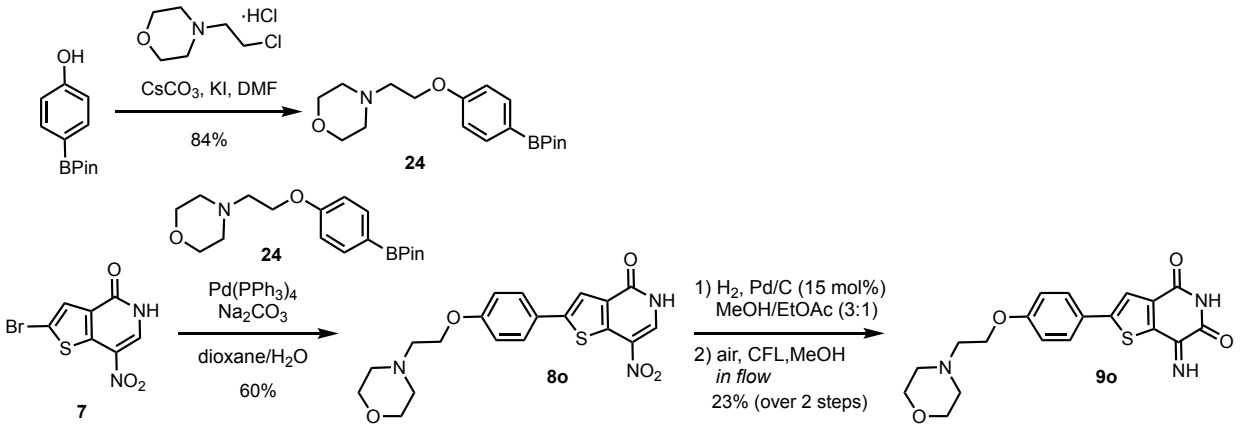

6. Scheme S6. Synthesis of compounds **9p**, **9q**, and **40**

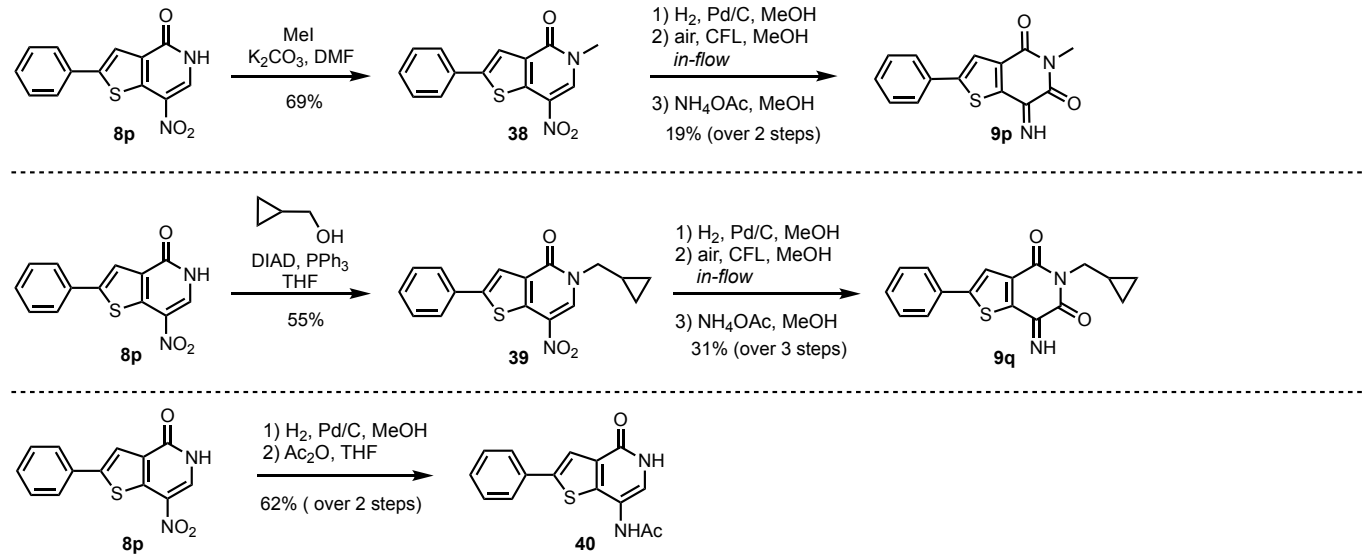

7. Scheme S7. Synthesis of compounds **15**, **16**, and **17**

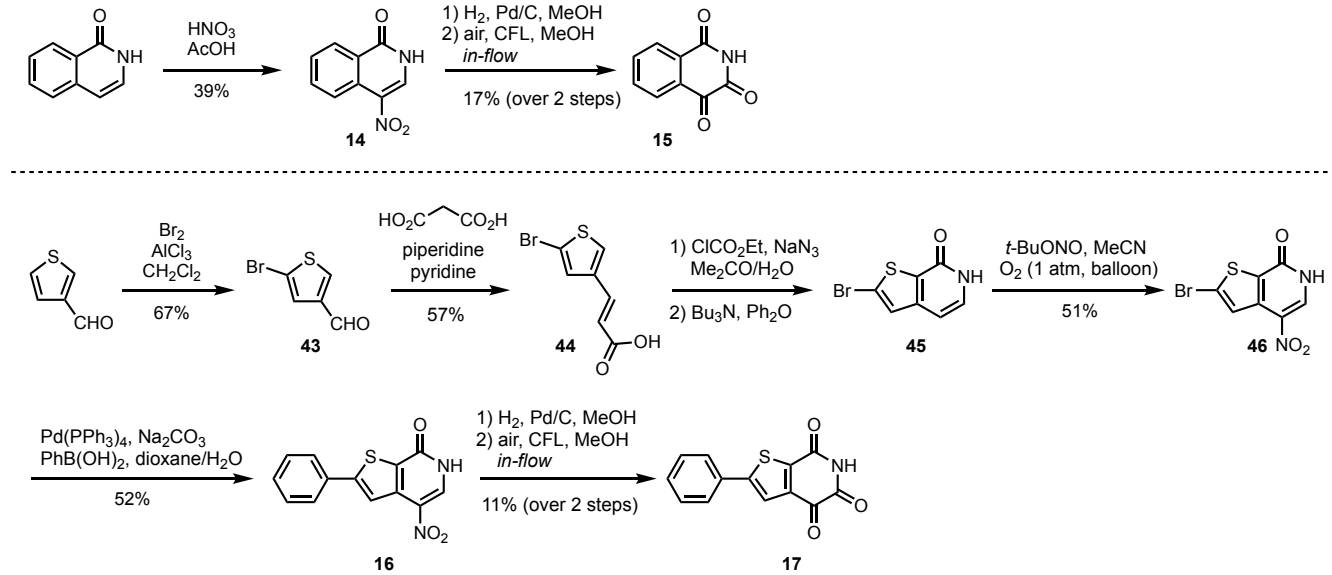

8. Scheme S8. Synthesis of compounds **18** and **19**

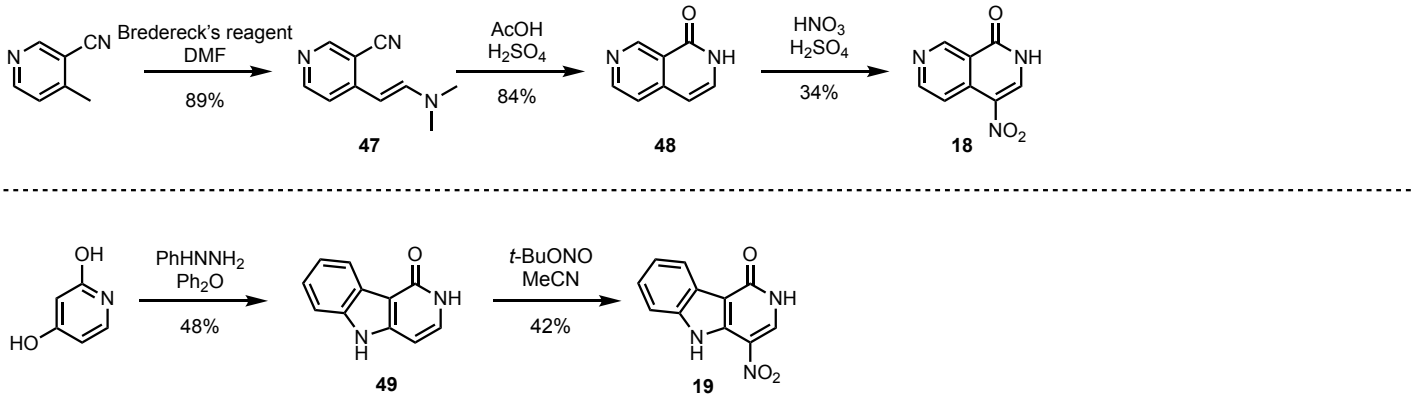

9. Figure S1. Sketch of flow apparatus

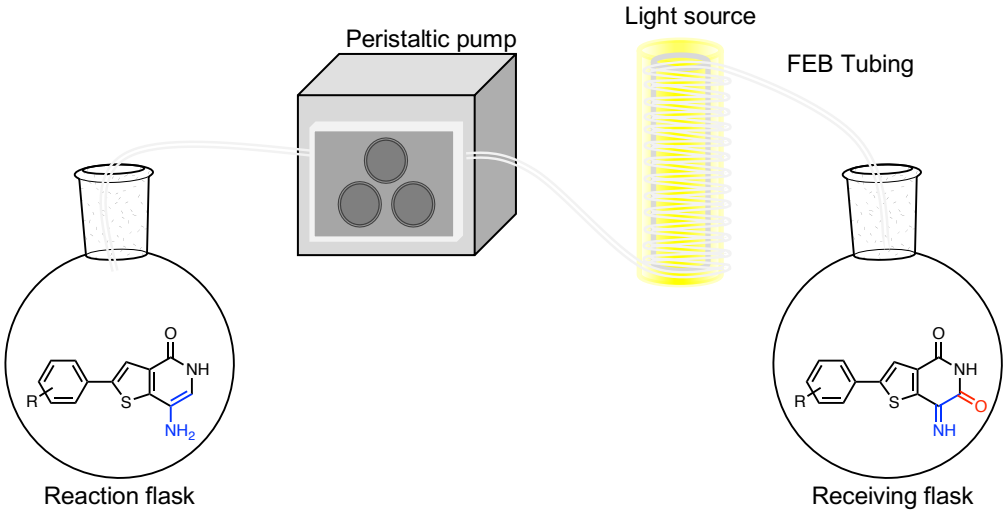

10. Figure S2. Picture of flow apparatus in operation, and additional experimental details

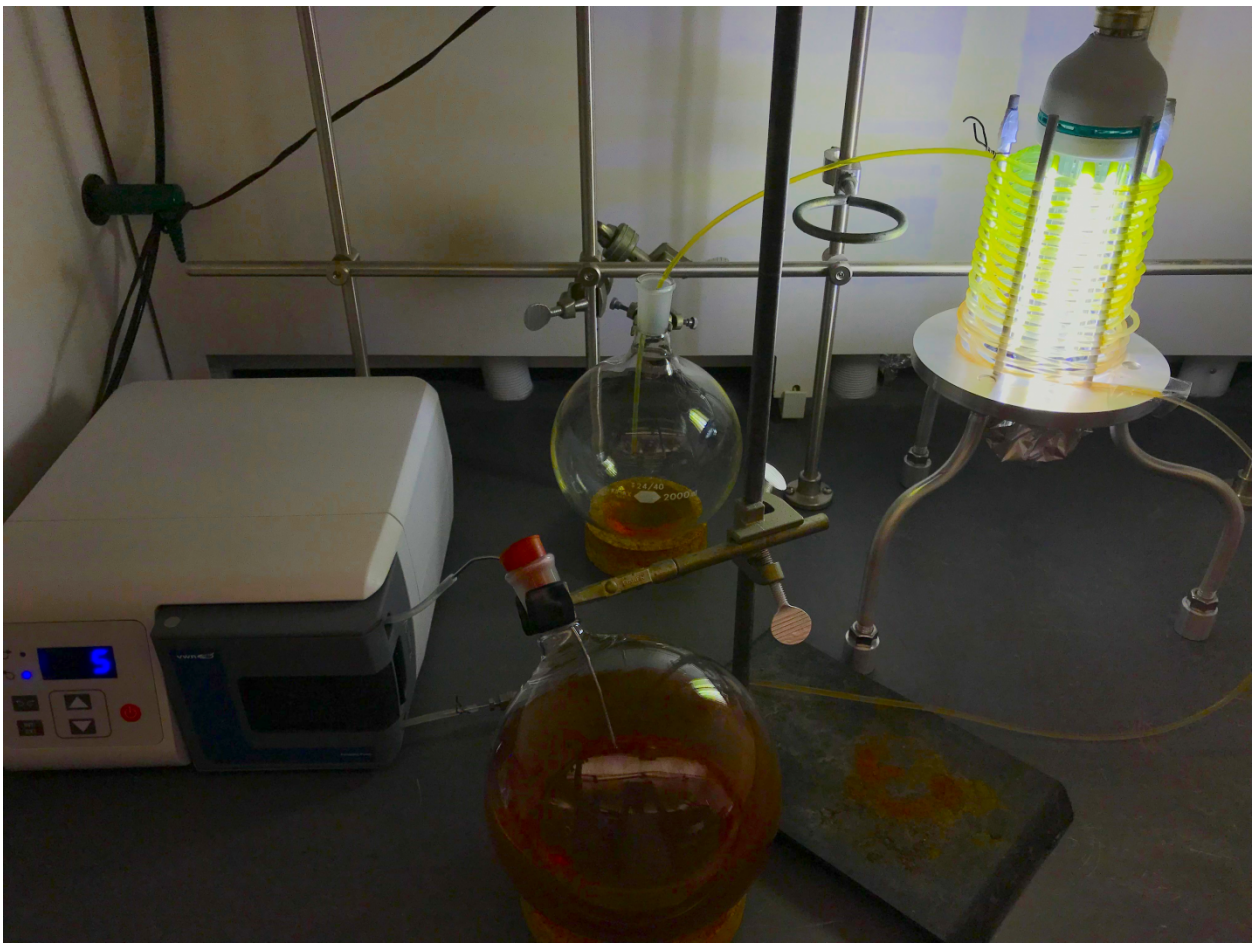

For preliminary experiments, air was bubbled through the solution for 15 minutes prior to photooxygenation *in-flow*. However, we found that this was unnecessary, and solvent was subsequently used directly from 20 L bulk solvent cans without supplementary treatment with air or oxygen. The photooxygenation reactions were performed in an open system; the beginning and the end of the tubing were open to the ambient atmosphere (i.e. in an oxygen partial pressure of 0.2 atm). While we did not have access to a mass flow controller for gases, at a mole fraction of oxygen in MeOH equal to $4.15 \cdot 10^{-4}$ in 1 atm of O_2, and an O_2/N_2 solubility ratio of 1.5,[1] we estimate the concentration of O_2 in our flow system at any time to be at least 2 times higher than the concentration of the substrate of 1.4 mM. The flow rate was adjusted empirically to 1.4 mM and 1.9 mL/min, resulting in a residence time in the flow reactor of 42 min to ensure complete conversion. Since a peristaltic pump is used, we did not install a back-pressure regulator and estimate the internal pressure to be about 1.05 atm. For the white CFL and white LED lights, the external temperature of the capillary tubing did not exceed 42 ºC. The flow system was a 14 cm tall coil of capillary tubing with 36 turns, an internal diameter of 10 cm, and a nominal distance of 2 cm from the light source to the coil.

The white LED used was rated 6500K and has a blue peak wavelength at ~458 ± 40 nm.[2] The white CFL has discrete peaks at various intensities around 450 nm,[3] and was also rated 6500K. If a standard white light is unavailable, blue LED lights will also result in conversion. For additional information, please see: https://www.digikey.com/en/articles/techzone/2013/apr/defining-the-color-characteristics-of-white-leds.

[1] Battino, R.; Seybold, P. G. "The O_2/N_2 Ratio Gas Solubility Mystery." *J. Chem. Eng. Data* **2011**, *56*, 5036.
[2] Li, H.; Mao, X.; Han, Y.; Luo, Y. "Wavelength Dependence of Colorimetric Properties of Lighting Sources Based on Multi-Color LEDs." *Opt. Express* **2013**, *21*, 3775.
[3] Favetta, V.; Colombo, R. C.; Mangili, J. F.; de Faria, R. T. "Light Sources and Culture Media in the in Vitro Growth of the Brazilian Orchid Microlaelia Lundii." *Semina: Ciências Agrárias, Londrina* **2017**, *38*(4), 1775.

The white LED (COB 40W, 6500K, E27) was tubular and fit through the center of the flow apparatus, similar to the white CFL (18W Feit-Electric, Model CE18/T/D6). When used, the red (infrared heat) spot lamp was placed on top of the apparatus.

WHITE LED:
https://www.amazon.com/Daylight-Workshop-Warehouse-Backyard-BestCircle/dp/B07GCH95B8/ref=sr_1_3_sspa?hvadid=190507955711&hvdev=c&hvlocphy=9005925&hvnetw=g&hvpos=1t1&hvqmt=b&hvrand=9748065246127574657&hvtargid=kwd-296268375769&ie=UTF8&keywords=e27+bulb+40w&qid=1547818280&sr=8-3-spons&tag=googhydr-20&psc=1

WHITE CFL:
https://www.amazon.com/Feit-Electric-Fluorescent-Daylight-Equivalent/dp/B002962SRG/ref=redir_mobile_desktop?_encoding=UTF8&%2AVersion%2A=1&%2Aentries%2A=0

When degassed MeOH (3x freeze-pump-thaw) was used according to the optimized conditions, with the end of the tubing open to air, full conversion was observed. In contrast, MeOH that was deoxygenated by sparging and sonication resulted in a diminished conversion. The MeOH was first argon sparged (30 min) under sonication, and the flow system was argon purged (1 h). When the photo-flow reaction was performed under the optimized conditions in this deoxygenated MeOH under an atmosphere of argon, carefully avoiding exposure to air of the open ends of the tubing, only 17% conversion by ^{1}H NMR was observed. See below for this reaction setup.

Left: Purging line with argon. Right: Flow reaction under argon atmosphere.

11. Figure S3. Concentration-PTP4A3 phosphatase inhibition response curves

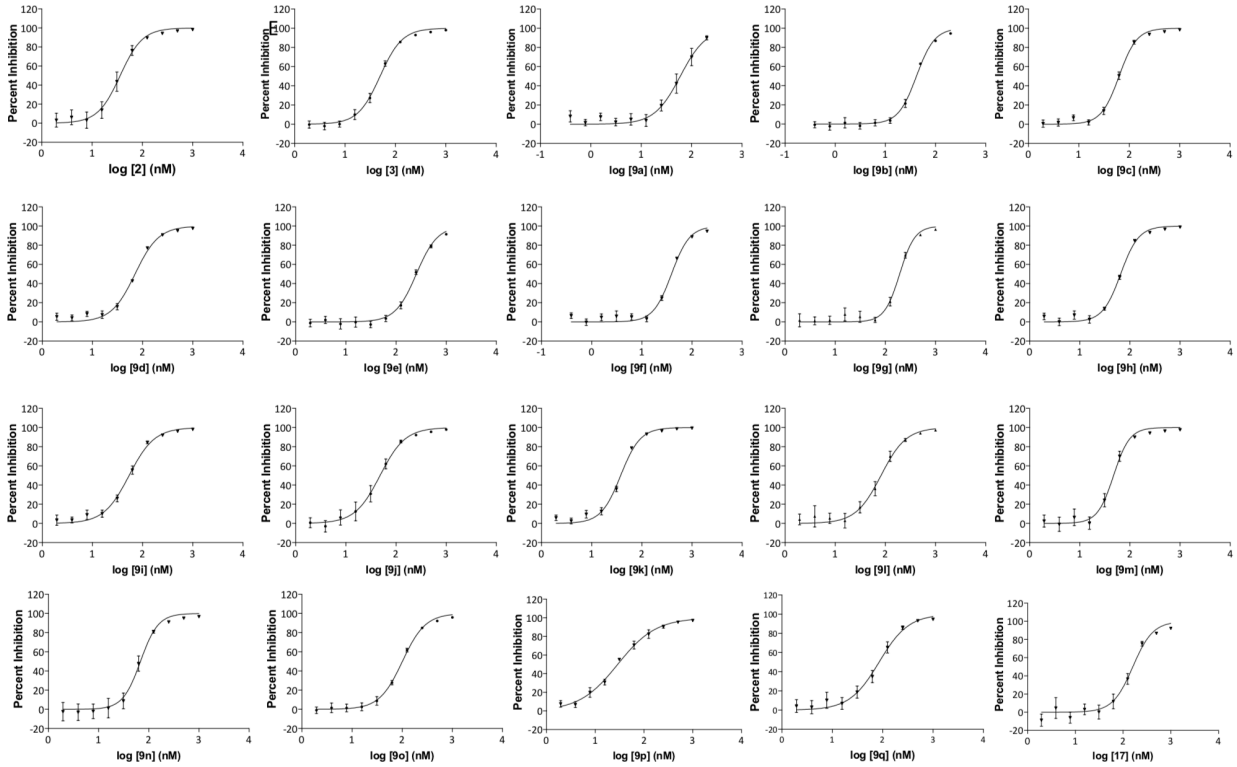

Inhibition of PTP4A3 was assayed in 3 independent experiments and the mean results ± SEM are indicated.

12. Table S1. General procedure and results for optimization of photooxygenation

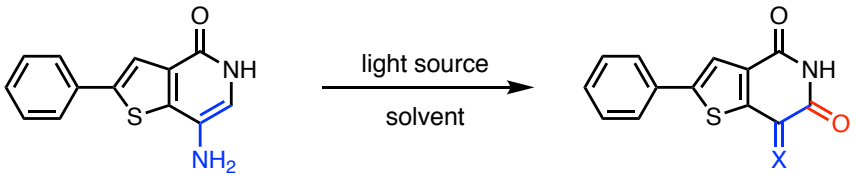

1

2 X = NH
3 X = O

The tubing was flushed with ~50 mL of MeOH. Immediately afterwards, a solution of thienopyridone **1** (10 mg) in MeOH (30 mL) was passed through the tubing at a rate of 1.9 mL/min using a peristaltic pump (5 RPM). The tubing was subsequently flushed again with MeOH (40 mL). The crude mixture was concentrated and analyzed by ^{1}H NMR.

Entry	Solvent	Additive	Flow rate (mL/min)	Light Source	Product Ratio (2:3)
1	1,2-DCE	-	0.1	CFL	0:1
2	1,2-DCE	-	0.8	CFL	1.5:1
3	$CHCl_3$	-	0.8	CFL	0:1
4	MeOH	-	0.8	CFL	8.7:1
5	MeOH	-	1.5	CFL	8:1
6	**MeOH**	**-**	**1.9**	**CFL**	**10:1**
7	MeOH	-	3.8	CFL	6.3:1
8	*i*-PrOH	-	1.9	CFL	7.5:1
9	HFIP	-	1.9	CFL	6:1
10	THF	-	1.9	CFL	6.3:1
11	MeOH	-	1.9	Red LED	NR
12	*i*-PrOH	-	1.9	Red LED	6.7:1
13	MeOH	(*i*-Pr)$_2$NEt (5 equiv)	1.5[a]	CFL	5.8:1
14	MeOH/AcOH (9:1)	-	1.9	CFL	5.7:1
15	MeOH/CF_3CH_2OH (1:1)	-	1.9	CFL	8.3:1
16	1,2-DCE	TPP (1 mol%)	0.1	CFL	0:1

[a]Starting material was still observed.

13. Table S2. Purification methods of **2**:**3** mixture.

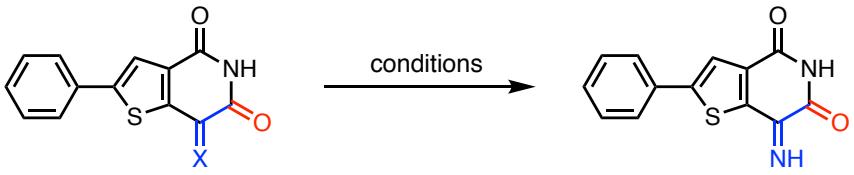

2 X = NH
3 X = O

2

Entry	Conditions	Result
1	**NH_4OAc, MeOH, 65 ºC,** ***homogeneous solution, sealed tube***	**>95% imine, quant., *no chromatography needed***
2	NH_4OAc, MeOH, reflux	decomposition
3	NH_3 in MeOH	decomposition
4	Ph_3P=NH, THF or MeCN	r.s.m.[a]
5	$BF_3{\cdot}OEt_2$, Et_2O	r.s.m.
6	NH_4Cl, MeOH, 65 ºC	r.s.m.
7	NH_4OH, 65 ºC	decomposition
8	HMDS,[b] 65 ºC	r.s.m.
9	HMDS, TBAF, THF, rt	>95% imine, but impurities present
10	HMDS, excess CsF, DMF, 80 ºC	>95% imine, but impurities present

[a]Recovered starting material. [b]Hexamethyldisilyazane.

14. Table S3. Computational drug-likeness estimates for derivatives of **2**[a]

Entry	Compound	Drug-likeness	cLogP	cLogS	Polar surface area	Mutagenic	Tumorigenic	Reproductive
1	JMS-053 (**2**)	4.393	1.545	-3.430	98.26	No	No	No
2	**3**	0.979	1.944	-4.250	91.48	No	No	No
3	**9a**	4.342	1.889	-3.774	98.26	No	No	No
4	**9b**	4.436	2.151	-4.166	98.26	No	No	No
5	**9c**	-2.797	2.393	-4.208	98.26	No	No	No
6	**9d**	3.053	1.646	-3.744	98.26	No	No	No
7	**9e**	2.441	2.700	-4.337	124.56	No	No	Yes
8	**9f**	3.053	1.646	-3.744	98.26	No	No	No
9	**9g**	-2.797	2.393	-4.208	98.26	No	No	No
10	**9h**	4.436	2.1507	-4.166	98.26	No	No	No
11	**9i**	4.342	1.889	-3.774	98.26	No	No	No
12	**9j**	4.400	1.4747	-3.448	107.49	No	No	No
13	**9k**	4.436	2.151	-4.166	98.26	No	No	No
14	**9l**	3.053	1.645	-3.744	189.1	No	No	No
15	**9m**	3.906	2.252	-4.480	98.26	No	No	No
16	**9n**	3.096	2.251	-4.48	204.5	No	No	No
17	**9o**	5.924	1.144	-2.938	119.96	No	No	Yes
18	**9p**	4.693	-3.068	1.798	89.47	No	No	No
19	**9q**	6.403	2.522	-3.884	221.85	No	No	No
20	**17**	1.198	1.9437	-4.25	91.48	No	No	No

[a] Computational results derived from Data Warrior (http://www.openmolecules.org/datawarrior/).

15. Single Crystal X-ray Diffraction Data

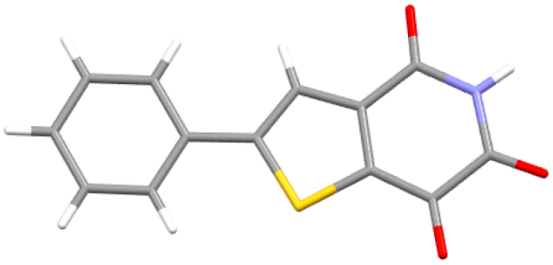

X-ray crystal structure of **3.**

Table S4. Crystal data and structure refinement for **3**.

CCDC	1880535
Empirical formula	$C_{13}H_7NO_3S$
Formula weight	257.26
Temperature	230(2) K
Wavelength	1.54178 Å
Crystal system, space group	Triclinic, P-1
Unit cell dimensions	a = 5.4276(4) Å α = 69.319(6)°
	b = 9.6873(7)Å β = 82.283(6)°
	c = 10.8442(8)Å γ = 83.399(5)°
Volume	527.20(7) A^3
Z, Calculated density	2, 1.621 Mg/m^3
Absorption coefficient	2.742 mm^{-1}
F(000)	264
Crystal color and shape	Light brown plate
Crystal size	0.03 x 0.02 x 0.005 mm
Theta range for data collection	4.380 to 68.418°
Limiting indices	-11<=h<=11, -12<=k<=11, 0<=l<=12
Reflections collected	6359
Absorption correction	Multi-scan
Max. and min. transmission	-
Goodness-of-fit on F^2	1.034
Largest diff. peak and hole	0.273 and -0.263 A^{-3}

16. Spectrofluorometry and UV-VIS data

Compounds **1**-**3** were excited at 380 nm, in accordance with the absorbance maxima in the UV-Vis spectra, using an HORIBA Jovin Yvon Fluoromax-3 spectrofluorometer in a quartz cuvette with a width of 1 cm. Emission spectra were also obtained at higher wavelengths. The experiments were performed at ambient temperature in methanol (3 mL). Approximately 1 mg of material was used for each experiment.

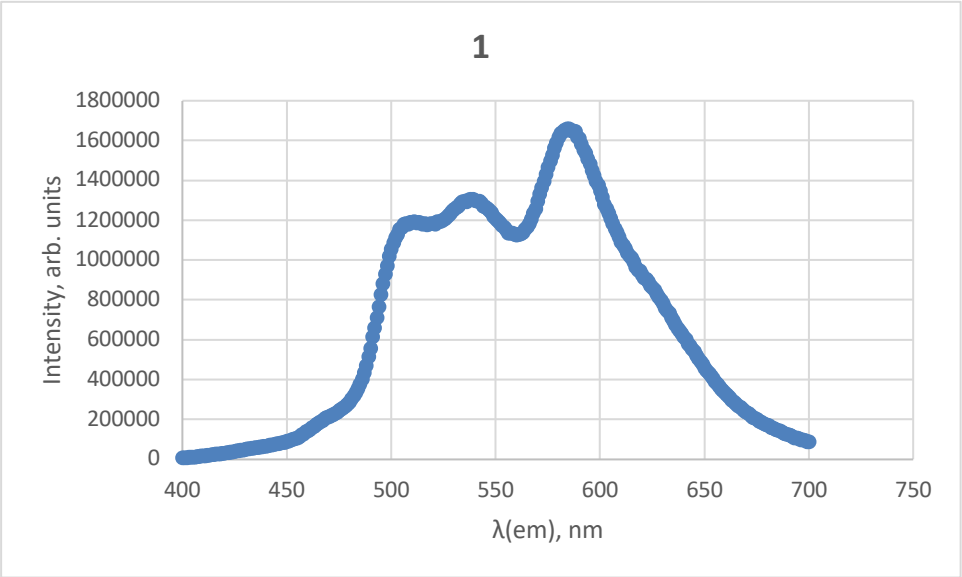

Figure S4. Emission spectrum of amine **1**.

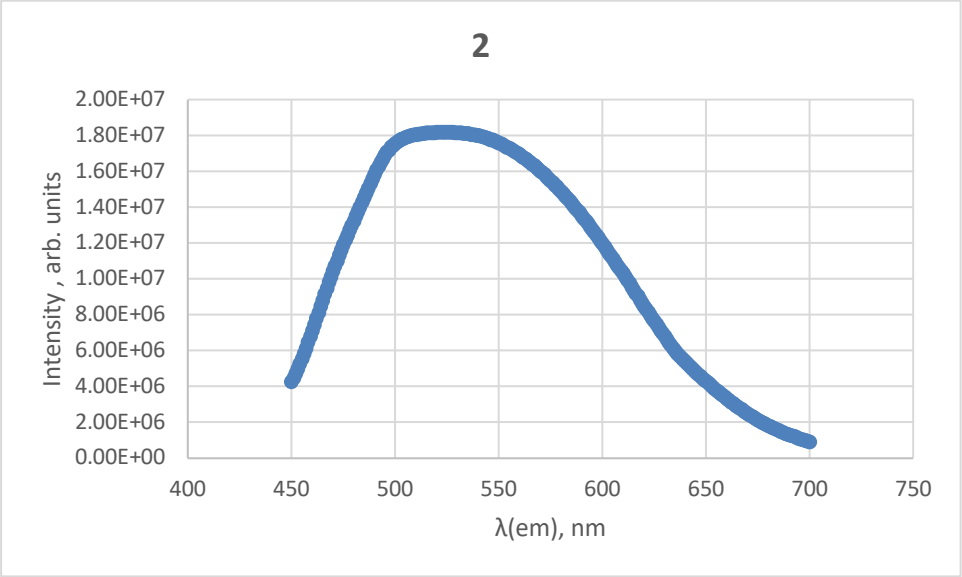

Figure S5. Emission spectrum of imine **2**.

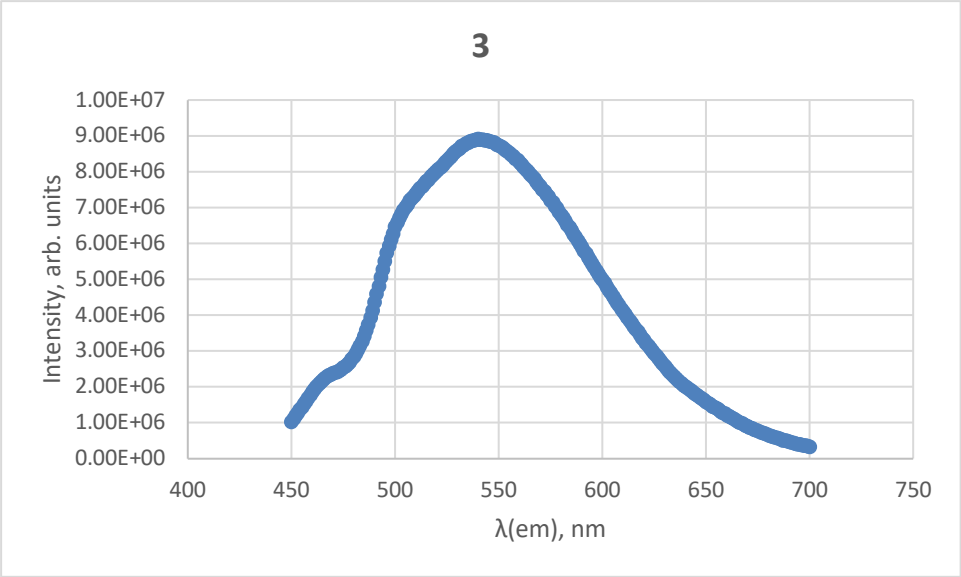

Figure S6. Emission spectrum of ketone **3**.

Report Date: 11:56:45, 02/05/2019

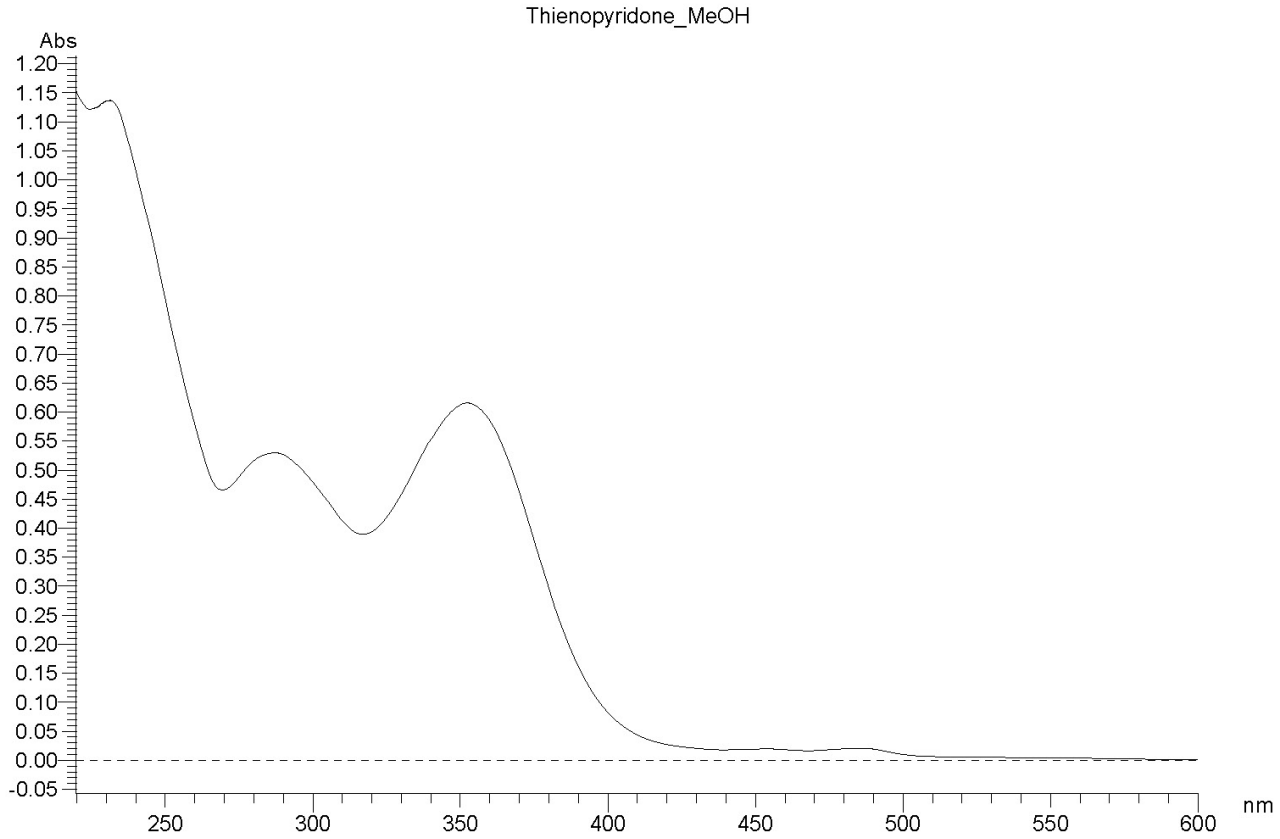

Sample: Thienopyridone_MeOH
Run Date: 11:54:12, 02/05/2019
Operator: All Users
Comment: Thienopyridone_MeOH

Instrument
Model: Lambda EZ210 Spectrophotometer
Serial Number:
ROM Version: 2550 02

Instrument Parameters
Measurement Type: Wavelength Scan
Data Mode: Abs
Starting Wavelength: 600.0 nm
Ending Wavelength: 220.0 nm
Scan Speed: 200 nm/min
Sampling Interval: 0.5 nm
Slit Width: 2 nm
Lamp Change: 340.0 nm
Baseline Correction: System
Response: Fast
Path Length: 10.0 mm

Processing Performed
Savitsky-Golay Smoothed
Smoothing Order: 3
Number of Points: 7
Number of Times: 1

Peak Integration
Method: Rectangular
Sensitivity: 1
Threshold: 0.0500

Peaks

Peak #	Start (nm)	Apex (nm)	End (nm)	Height (Abs)	Area (Abs*nm)	Valley (nm)	Valley (Abs)
1	600.0	352.5	316.5	0.616	38.102	316.5	0.389
2	316.5	286.5	269.5	0.530	22.731	269.5	0.466

Data Points

nm	Abs	nm	Abs
500.0	0.010	499.5	0.011
499.0	0.011	498.5	0.011
498.0	0.012	497.5	0.012
497.0	0.013	496.5	0.013
496.0	0.014	495.5	0.014
495.0	0.015	494.5	0.015
494.0	0.016	493.5	0.016
493.0	0.017	492.5	0.017
492.0	0.018	491.5	0.018
491.0	0.019	490.5	0.019
490.0	0.019	489.5	0.020
489.0	0.020	488.5	0.020
488.0	0.020	487.5	0.020
487.0	0.020	486.5	0.021
486.0	0.021	485.5	0.021
485.0	0.021	484.5	0.021
484.0	0.021	483.5	0.021
483.0	0.020	482.5	0.020
482.0	0.020	481.5	0.020
481.0	0.020	480.5	0.020
480.0	0.020	479.5	0.019
479.0	0.019	478.5	0.019
478.0	0.019	477.5	0.019
477.0	0.019	476.5	0.019
476.0	0.018	475.5	0.018
475.0	0.018	474.5	0.018
474.0	0.018	473.5	0.018
473.0	0.018	472.5	0.018
472.0	0.017	471.5	0.017
471.0	0.017	470.5	0.017
470.0	0.017	469.5	0.017
469.0	0.016	468.5	0.016
468.0	0.016	467.5	0.016
467.0	0.016	466.5	0.016
466.0	0.016	465.5	0.017
465.0	0.017	464.5	0.017
464.0	0.017	463.5	0.017
463.0	0.017	462.5	0.017
462.0	0.018	461.5	0.018
461.0	0.018	460.5	0.018
460.0	0.018	459.5	0.019
459.0	0.019	458.5	0.019
458.0	0.019	457.5	0.019
457.0	0.019	456.5	0.019
456.0	0.019	455.5	0.019
455.0	0.019	454.5	0.020
454.0	0.020	453.5	0.020
453.0	0.020	452.5	0.020
452.0	0.020	451.5	0.020
451.0	0.019	450.5	0.019
450.0	0.019	449.5	0.019
449.0	0.019	448.5	0.019
448.0	0.019	447.5	0.019
447.0	0.019	446.5	0.019
446.0	0.019	445.5	0.019
445.0	0.019	444.5	0.019
444.0	0.018	443.5	0.018
443.0	0.018	442.5	0.018
442.0	0.018	441.5	0.018
441.0	0.018	440.5	0.018
440.0	0.018	439.5	0.018
439.0	0.018	438.5	0.018
438.0	0.018	437.5	0.018
437.0	0.018	436.5	0.018
436.0	0.018	435.5	0.018
435.0	0.018	434.5	0.018
434.0	0.019	433.5	0.019
433.0	0.019	432.5	0.019
432.0	0.019	431.5	0.020
431.0	0.020	430.5	0.020
430.0	0.021	429.5	0.021
429.0	0.021	428.5	0.021

nm	Abs	nm	Abs
428.0	0.022	427.5	0.022
427.0	0.022	426.5	0.022
426.0	0.023	425.5	0.023
425.0	0.023	424.5	0.024
424.0	0.024	423.5	0.025
423.0	0.025	422.5	0.025
422.0	0.025	421.5	0.026
421.0	0.026	420.5	0.027
420.0	0.027	419.5	0.028
419.0	0.028	418.5	0.029
418.0	0.029	417.5	0.030
417.0	0.031	416.5	0.031
416.0	0.032	415.5	0.033
415.0	0.034	414.5	0.034
414.0	0.035	413.5	0.036
413.0	0.037	412.5	0.038
412.0	0.039	411.5	0.040
411.0	0.041	410.5	0.043
410.0	0.044	409.5	0.045
409.0	0.047	408.5	0.048
408.0	0.050	407.5	0.051
407.0	0.053	406.5	0.054
406.0	0.056	405.5	0.058
405.0	0.060	404.5	0.062
404.0	0.064	403.5	0.066
403.0	0.068	402.5	0.071
402.0	0.073	401.5	0.075
401.0	0.078	400.5	0.080
400.0	0.083	399.5	0.086
399.0	0.089	398.5	0.092
398.0	0.095	397.5	0.098
397.0	0.101	396.5	0.105
396.0	0.109	395.5	0.112
395.0	0.116	394.5	0.120
394.0	0.124	393.5	0.128
393.0	0.133	392.5	0.137
392.0	0.142	391.5	0.147
391.0	0.152	390.5	0.157
390.0	0.162	389.5	0.168
389.0	0.173	388.5	0.178
388.0	0.184	387.5	0.190
387.0	0.196	386.5	0.202
386.0	0.209	385.5	0.215
385.0	0.222	384.5	0.229
384.0	0.236	383.5	0.243
383.0	0.250	382.5	0.257
382.0	0.264	381.5	0.271
381.0	0.280	380.5	0.289
380.0	0.298	379.5	0.306
379.0	0.314	378.5	0.321
378.0	0.329	377.5	0.338
377.0	0.346	376.5	0.354
376.0	0.362	375.5	0.371
375.0	0.379	374.5	0.388
374.0	0.396	373.5	0.405
373.0	0.413	372.5	0.421
372.0	0.430	371.5	0.438
371.0	0.446	370.5	0.454
370.0	0.462	369.5	0.470
369.0	0.478	368.5	0.485
368.0	0.493	367.5	0.500
367.0	0.507	366.5	0.514
366.0	0.521	365.5	0.527
365.0	0.534	364.5	0.540
364.0	0.546	363.5	0.552
363.0	0.557	362.5	0.563
362.0	0.568	361.5	0.573
361.0	0.577	360.5	0.582
360.0	0.586	359.5	0.590
359.0	0.593	358.5	0.596
358.0	0.599	357.5	0.602
357.0	0.604	356.5	0.606
356.0	0.609	355.5	0.611
355.0	0.612	354.5	0.613
354.0	0.614	353.5	0.615
353.0	0.615	352.5	0.616
352.0	0.615	351.5	0.615

nm	Abs	nm	Abs
351.0	0.256	350.5	0.253
350.0	0.249	349.5	0.246
349.0	0.243	348.5	0.239
348.0	0.236	347.5	0.234
347.0	0.231	346.5	0.228
346.0	0.225	345.5	0.222
345.0	0.219	344.5	0.216
344.0	0.214	343.5	0.211
343.0	0.209	342.5	0.208
342.0	0.206	341.5	0.204
341.0	0.202	340.5	0.200
340.0	0.199	339.5	0.198
339.0	0.197	338.5	0.195
338.0	0.193	337.5	0.191
337.0	0.190	336.5	0.188
336.0	0.187	335.5	0.186
335.0	0.185	334.5	0.185
334.0	0.184	333.5	0.183
333.0	0.182	332.5	0.181
332.0	0.181	331.5	0.180
331.0	0.180	330.5	0.179
330.0	0.179	329.5	0.179
329.0	0.179	328.5	0.179
328.0	0.179	327.5	0.179
327.0	0.180	326.5	0.180
326.0	0.181	325.5	0.181
325.0	0.182	324.5	0.182
324.0	0.183	323.5	0.183
323.0	0.184	322.5	0.186
322.0	0.187	321.5	0.188
321.0	0.189	320.5	0.191
320.0	0.192	319.5	0.194
319.0	0.196	318.5	0.198
318.0	0.201	317.5	0.203
317.0	0.205	316.5	0.208
316.0	0.211	315.5	0.214
315.0	0.218	314.5	0.222
314.0	0.226	313.5	0.230
313.0	0.234	312.5	0.238
312.0	0.243	311.5	0.247
311.0	0.252	310.5	0.257
310.0	0.262	309.5	0.267
309.0	0.272	308.5	0.277
308.0	0.283	307.5	0.288
307.0	0.294	306.5	0.299
306.0	0.305	305.5	0.311
305.0	0.318	304.5	0.324
304.0	0.331	303.5	0.338
303.0	0.345	302.5	0.352
302.0	0.360	301.5	0.368
301.0	0.376	300.5	0.385
300.0	0.393	299.5	0.403
299.0	0.412	298.5	0.422
298.0	0.432	297.5	0.443
297.0	0.454	296.5	0.465
296.0	0.478	295.5	0.490
295.0	0.503	294.5	0.517
294.0	0.531	293.5	0.545
293.0	0.560	292.5	0.575
292.0	0.591	291.5	0.608
291.0	0.624	290.5	0.641
290.0	0.659	289.5	0.677
289.0	0.696	288.5	0.715
288.0	0.734	287.5	0.754
287.0	0.773	286.5	0.793
286.0	0.814	285.5	0.834
285.0	0.855	284.5	0.876
284.0	0.896	283.5	0.915
283.0	0.936	282.5	0.955
282.0	0.975	281.5	0.994
281.0	1.011	280.5	1.027
280.0	1.043	279.5	1.058
279.0	1.072	278.5	1.085
278.0	1.097	277.5	1.109
277.0	1.121	276.5	1.130
276.0	1.138	275.5	1.146
275.0	1.152	274.5	1.158

nm	Abs	nm	Abs
274.0	0.483	273.5	0.480
273.0	0.477	272.5	0.475
272.0	0.472	271.5	0.470
271.0	0.468	270.5	0.467
270.0	0.466	269.5	0.466
269.0	0.466	268.5	0.467
268.0	0.468	267.5	0.470
267.0	0.473	266.5	0.477
266.0	0.482	265.5	0.487
265.0	0.493	264.5	0.500
264.0	0.507	263.5	0.516
263.0	0.524	262.5	0.533
262.0	0.542	261.5	0.551
261.0	0.561	260.5	0.570
260.0	0.580	259.5	0.589
259.0	0.598	258.5	0.607
258.0	0.617	257.5	0.627
257.0	0.638	256.5	0.648
256.0	0.659	255.5	0.670
255.0	0.681	254.5	0.692
254.0	0.703	253.5	0.714
253.0	0.724	252.5	0.735
252.0	0.747	251.5	0.758
251.0	0.771	250.5	0.784
250.0	0.795	249.5	0.807
249.0	0.818	248.5	0.830
248.0	0.843	247.5	0.856
247.0	0.868	246.5	0.880
246.0	0.891	245.5	0.903
245.0	0.913	244.5	0.924
244.0	0.934	243.5	0.944
243.0	0.953	242.5	0.963
242.0	0.974	241.5	0.985
241.0	0.996	240.5	1.006
240.0	1.016	239.5	1.026
239.0	1.037	238.5	1.047
238.0	1.058	237.5	1.067
237.0	1.075	236.5	1.083
236.0	1.092	235.5	1.101
235.0	1.110	234.5	1.117
234.0	1.121	233.5	1.126
233.0	1.130	232.5	1.133
232.0	1.135	231.5	1.137
231.0	1.136	230.5	1.137
230.0	1.137	229.5	1.135
229.0	1.132	228.5	1.132
228.0	1.129	227.5	1.127
227.0	1.125	226.5	1.124
226.0	1.123	225.5	1.123
225.0	1.122	224.5	1.122
224.0	1.122	223.5	1.124
223.0	1.126	222.5	1.130
222.0	1.134	221.5	1.137
221.0	1.141	220.5	1.145
220.0	1.153		

Figure S7. Absorption spectrum of thienopyridone **1** in MeOH.

Report Date: 10:24:11, 02/05/2019

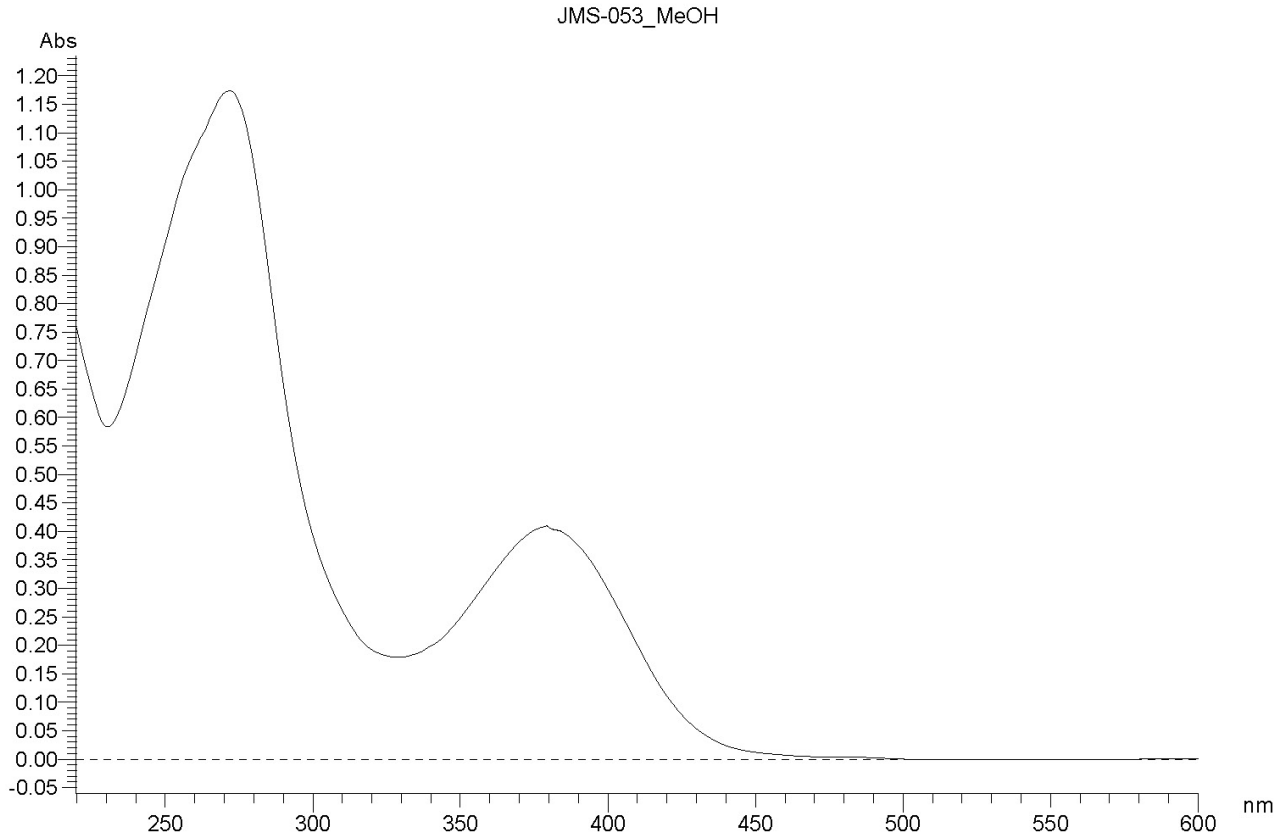

Sample: JMS-053 MeOH
Run Date: 10:19:00, 02/05/2019
Operator: All Users
Comment: JMS-053_MeOH

Instrument
Model: Lambda EZ210 Spectrophotometer
Serial Number:
ROM Version: 2550 02

Instrument Parameters
Measurement Type: Wavelength Scan
Data Mode: Abs
Starting Wavelength: 600.0 nm
Ending Wavelength: 220.0 nm
Scan Speed: 200 nm/min
Sampling Interval: 0.5 nm
Slit Width: 2 nm
Lamp Change: 340.0 nm
Baseline Correction: System
Response: Fast
Path Length: 10.0 mm

Processing Performed
Savitsky-Golay Smoothed
Smoothing Order: 3
Number of Points: 7
Number of Times: 1

Peak Integration
Method: Rectangular
Sensitivity: 1
Threshold: 0.0500

Peaks

Peak #	Start (nm)	Apex (nm)	End (nm)	Height (Abs)	Area (Abs*nm)	Valley (nm)	Valley (Abs)
1	600.0	379.0	329.0	0.410	27.584	329.0	0.179
2	329.0	271.5	230.5	1.173	67.556	230.5	0.584

Data Points

nm	Abs	nm	Abs
500.0	-0.000	499.5	0.000
499.0	0.000	498.5	0.000
498.0	0.000	497.5	0.001
497.0	0.000	496.5	0.001
496.0	0.001	495.5	0.001
495.0	0.001	494.5	0.001
494.0	0.002	493.5	0.002
493.0	0.002	492.5	0.002
492.0	0.002	491.5	0.002
491.0	0.002	490.5	0.002
490.0	0.002	489.5	0.003
489.0	0.003	488.5	0.003
488.0	0.003	487.5	0.003
487.0	0.003	486.5	0.003
486.0	0.003	485.5	0.003
485.0	0.003	484.5	0.003
484.0	0.003	483.5	0.004
483.0	0.004	482.5	0.004
482.0	0.004	481.5	0.004
481.0	0.004	480.5	0.004
480.0	0.004	479.5	0.004
479.0	0.004	478.5	0.004
478.0	0.004	477.5	0.004
477.0	0.004	476.5	0.004
476.0	0.004	475.5	0.004
475.0	0.004	474.5	0.004
474.0	0.004	473.5	0.004
473.0	0.004	472.5	0.004
472.0	0.004	471.5	0.004
471.0	0.004	470.5	0.004
470.0	0.004	469.5	0.004
469.0	0.004	468.5	0.004
468.0	0.004	467.5	0.005
467.0	0.005	466.5	0.005
466.0	0.005	465.5	0.005
465.0	0.005	464.5	0.005
464.0	0.005	463.5	0.006
463.0	0.006	462.5	0.006
462.0	0.006	461.5	0.007
461.0	0.007	460.5	0.007
460.0	0.007	459.5	0.007
459.0	0.008	458.5	0.008
458.0	0.008	457.5	0.008
457.0	0.008	456.5	0.008
456.0	0.009	455.5	0.009
455.0	0.009	454.5	0.009
454.0	0.010	453.5	0.010
453.0	0.010	452.5	0.011
452.0	0.011	451.5	0.011
451.0	0.011	450.5	0.012
450.0	0.012	449.5	0.012
449.0	0.013	448.5	0.013
448.0	0.013	447.5	0.014
447.0	0.014	446.5	0.015
446.0	0.015	445.5	0.016
445.0	0.016	444.5	0.017
444.0	0.018	443.5	0.018
443.0	0.019	442.5	0.020
442.0	0.021	441.5	0.021
441.0	0.022	440.5	0.023
440.0	0.024	439.5	0.025
439.0	0.026	438.5	0.027
438.0	0.028	437.5	0.029
437.0	0.031	436.5	0.032
436.0	0.034	435.5	0.035
435.0	0.036	434.5	0.038
434.0	0.039	433.5	0.041
433.0	0.042	432.5	0.044
432.0	0.046	431.5	0.048
431.0	0.050	430.5	0.052
430.0	0.054	429.5	0.056
429.0	0.058	428.5	0.061

nm	Abs	nm	Abs
428.0	0.063	427.5	0.065
427.0	0.068	426.5	0.071
426.0	0.073	425.5	0.076
425.0	0.079	424.5	0.081
424.0	0.084	423.5	0.088
423.0	0.091	422.5	0.094
422.0	0.097	421.5	0.101
421.0	0.104	420.5	0.108
420.0	0.111	419.5	0.115
419.0	0.119	418.5	0.123
418.0	0.127	417.5	0.131
417.0	0.135	416.5	0.139
416.0	0.143	415.5	0.148
415.0	0.153	414.5	0.157
414.0	0.162	413.5	0.167
413.0	0.171	412.5	0.176
412.0	0.181	411.5	0.186
411.0	0.191	410.5	0.196
410.0	0.201	409.5	0.206
409.0	0.211	408.5	0.216
408.0	0.221	407.5	0.226
407.0	0.231	406.5	0.236
406.0	0.241	405.5	0.246
405.0	0.251	404.5	0.255
404.0	0.260	403.5	0.265
403.0	0.270	402.5	0.275
402.0	0.280	401.5	0.285
401.0	0.289	400.5	0.294
400.0	0.299	399.5	0.303
399.0	0.308	398.5	0.312
398.0	0.317	397.5	0.321
397.0	0.326	396.5	0.330
396.0	0.334	395.5	0.338
395.0	0.342	394.5	0.346
394.0	0.350	393.5	0.353
393.0	0.357	392.5	0.360
392.0	0.364	391.5	0.367
391.0	0.370	390.5	0.373
390.0	0.376	389.5	0.379
389.0	0.381	388.5	0.384
388.0	0.386	387.5	0.388
387.0	0.391	386.5	0.393
386.0	0.394	385.5	0.396
385.0	0.398	384.5	0.399
384.0	0.400	383.5	0.401
383.0	0.402	382.5	0.402
382.0	0.403	381.5	0.403
381.0	0.404	380.5	0.406
380.0	0.407	379.5	0.409
379.0	0.410	378.5	0.409
378.0	0.408	377.5	0.407
377.0	0.406	376.5	0.406
376.0	0.405	375.5	0.404
375.0	0.402	374.5	0.401
374.0	0.399	373.5	0.398
373.0	0.396	372.5	0.394
372.0	0.391	371.5	0.389
371.0	0.387	370.5	0.385
370.0	0.382	369.5	0.380
369.0	0.377	368.5	0.375
368.0	0.372	367.5	0.369
367.0	0.366	366.5	0.363
366.0	0.360	365.5	0.357
365.0	0.353	364.5	0.350
364.0	0.347	363.5	0.343
363.0	0.340	362.5	0.337
362.0	0.333	361.5	0.330
361.0	0.326	360.5	0.323
360.0	0.319	359.5	0.316
359.0	0.312	358.5	0.309
358.0	0.305	357.5	0.301
357.0	0.298	356.5	0.294
356.0	0.291	355.5	0.287
355.0	0.284	354.5	0.280
354.0	0.277	353.5	0.273
353.0	0.269	352.5	0.266
352.0	0.263	351.5	0.259

nm	Abs	nm	Abs
351.0	0.256	350.5	0.253
350.0	0.249	349.5	0.246
349.0	0.243	348.5	0.239
348.0	0.236	347.5	0.234
347.0	0.231	346.5	0.228
346.0	0.225	345.5	0.222
345.0	0.219	344.5	0.216
344.0	0.214	343.5	0.211
343.0	0.209	342.5	0.208
342.0	0.206	341.5	0.204
341.0	0.202	340.5	0.200
340.0	0.199	339.5	0.198
339.0	0.197	338.5	0.195
338.0	0.193	337.5	0.191
337.0	0.190	336.5	0.188
336.0	0.187	335.5	0.186
335.0	0.185	334.5	0.185
334.0	0.184	333.5	0.183
333.0	0.182	332.5	0.181
332.0	0.181	331.5	0.180
331.0	0.180	330.5	0.179
330.0	0.179	329.5	0.179
329.0	0.179	328.5	0.179
328.0	0.179	327.5	0.179
327.0	0.180	326.5	0.180
326.0	0.181	325.5	0.181
325.0	0.182	324.5	0.182
324.0	0.183	323.5	0.183
323.0	0.184	322.5	0.186
322.0	0.187	321.5	0.188
321.0	0.189	320.5	0.191
320.0	0.192	319.5	0.194
319.0	0.196	318.5	0.198
318.0	0.201	317.5	0.203
317.0	0.205	316.5	0.208
316.0	0.211	315.5	0.214
315.0	0.218	314.5	0.222
314.0	0.226	313.5	0.230
313.0	0.234	312.5	0.238
312.0	0.243	311.5	0.247
311.0	0.252	310.5	0.257
310.0	0.262	309.5	0.267
309.0	0.272	308.5	0.277
308.0	0.283	307.5	0.288
307.0	0.294	306.5	0.299
306.0	0.305	305.5	0.311
305.0	0.318	304.5	0.324
304.0	0.331	303.5	0.338
303.0	0.345	302.5	0.352
302.0	0.360	301.5	0.368
301.0	0.376	300.5	0.385
300.0	0.393	299.5	0.403
299.0	0.412	298.5	0.422
298.0	0.432	297.5	0.443
297.0	0.454	296.5	0.465
296.0	0.478	295.5	0.490
295.0	0.503	294.5	0.517
294.0	0.531	293.5	0.545
293.0	0.560	292.5	0.575
292.0	0.591	291.5	0.608
291.0	0.624	290.5	0.641
290.0	0.659	289.5	0.677
289.0	0.696	288.5	0.715
288.0	0.734	287.5	0.754
287.0	0.773	286.5	0.793
286.0	0.814	285.5	0.834
285.0	0.855	284.5	0.876
284.0	0.896	283.5	0.915
283.0	0.936	282.5	0.955
282.0	0.975	281.5	0.994
281.0	1.011	280.5	1.027
280.0	1.043	279.5	1.058
279.0	1.072	278.5	1.085
278.0	1.097	277.5	1.109
277.0	1.121	276.5	1.130
276.0	1.138	275.5	1.146
275.0	1.152	274.5	1.158

nm	Abs	nm	Abs
274.0	1.164	273.5	1.169
273.0	1.171	272.5	1.172
272.0	1.173	271.5	1.173
271.0	1.172	270.5	1.171
270.0	1.169	269.5	1.167
269.0	1.164	268.5	1.160
268.0	1.156	267.5	1.150
267.0	1.145	266.5	1.139
266.0	1.134	265.5	1.128
265.0	1.123	264.5	1.117
264.0	1.110	263.5	1.104
263.0	1.100	262.5	1.095
262.0	1.090	261.5	1.085
261.0	1.080	260.5	1.074
260.0	1.069	259.5	1.063
259.0	1.058	258.5	1.052
258.0	1.046	257.5	1.040
257.0	1.033	256.5	1.026
256.0	1.019	255.5	1.011
255.0	1.003	254.5	0.994
254.0	0.985	253.5	0.975
253.0	0.964	252.5	0.954
252.0	0.944	251.5	0.934
251.0	0.925	250.5	0.915
250.0	0.906	249.5	0.897
249.0	0.887	248.5	0.877
248.0	0.867	247.5	0.857
247.0	0.847	246.5	0.838
246.0	0.828	245.5	0.819
245.0	0.810	244.5	0.800
244.0	0.790	243.5	0.781
243.0	0.771	242.5	0.760
242.0	0.750	241.5	0.740
241.0	0.730	240.5	0.719
240.0	0.709	239.5	0.699
239.0	0.689	238.5	0.680
238.0	0.670	237.5	0.661
237.0	0.652	236.5	0.644
236.0	0.636	235.5	0.628
235.0	0.621	234.5	0.614
234.0	0.608	233.5	0.602
233.0	0.597	232.5	0.592
232.0	0.589	231.5	0.586
231.0	0.585	230.5	0.584
230.0	0.585	229.5	0.586
229.0	0.589	228.5	0.594
228.0	0.599	227.5	0.606
227.0	0.614	226.5	0.623
226.0	0.632	225.5	0.641
225.0	0.651	224.5	0.661
224.0	0.670	223.5	0.680
223.0	0.690	222.5	0.701
222.0	0.711	221.5	0.722
221.0	0.734	220.5	0.746
220.0	0.757		

Figure S8. Absorption spectrum of imine **2** in MeOH.

17. PTP4A3 Phosphatase Activity Assay

All compounds were evaluated *in vitro* with 1 µg full-length recombinant human His_6-PTP4A3, as previously described.[20] The assay was fully automated using an Agilent Bravo Liquid Handling Platform and miniaturized to 15 µL total volume. The liquid handler performed a two-fold serial dilution of each compound to achieve a 10-point concentration curve. Assays were performed in 40 mM Tris-HCl (pH 7.0), 75 mM NaCl, 2 mM EDTA, 0.099% BSA and 4 mM DTT; the reaction was initiated upon the addition of 12 µM 6,8-difluoro-4-methylumbelliferyl phosphate (DiFMUP) and incubated at 25 °C for 25 min before measuring fluorescence at Ex = 358 nm/Em = 455 nm using a SpectraMax M5 plate reader. Each component was prepared at 3x the final concentration and dispensed 5 µL at a time into the wells of black 384-well low volume plates using the liquid handler; compound was dispensed first, followed by PTP4A3, then DiFMUP. Percent inhibition of enzyme activity was calculated using PTP4A3 in the absence of inhibitor as maximal activity and PTP4A3 with 2 mM Na_3VO_4 as minimal activity. The IC_{50} value for each compound was determined using GraphPad and was reported as the mean of three to six independent assays, with six replicates each.

18. Molecular modeling methods

Four PTP4A3 structures are available in the RCSB Protein Data Bank (PDB) (https://www.rcsb.org/). Three are NMR structures, and include PDB entries 1R6H (**Ref**: G., Kozlov, J., Cheng, E., Ziomek, D., Banville, K., Gehring, and I, Ekiel, *J. Biol. Chem.*, 2004, **279**, 11882), 1V3A (**Ref**: K.A., Kim, J.S., Song, J., Jee, M.R., Sheen, C., Lee, T.G., Lee, S., Ro, J.M., Cho, W., Lee, T., Yamazaki, Y.H., Jeon, and C. Cheong, *FEBS Lett*., 2004, **565**,181), and 2MBC (**Ref**: K.W., Jeong, D.I., Kang, E., Lee, A., Shin, B., Jin, Y.G., Park, C.K., Lee, E.H., Kim, Y.H., Jeon, E.E., Kim, and Y., Kim, *Biochemistry*, 2014, **53**, 4814), and the fourth, and most recently deposited PDB entry, 5TSR (**Ref**: H., Zhang, G., Kozlov, X., Li, H., Wu, I., Gulerez, and K., Gehring, *Sci. Rep.*, 2017, **7**, 48), is an X-Ray structure (3.19 Å resolution). Entries 1R6H and 1V3A are 'open' WPD-loop conformations of the enzyme; entries 2MBC and 5TSR are 'closed' WPD-loop conformations. **Figure S9**, shows representative/general conformational differences in the 'opened' versus the 'closed' WPD-loop structures based on a comparison between 1V3A and 5TSR. The loop colors and residues shown in **Figure S9** parallel those shown in **Figure 1** (in the main manuscript). Structural comparison of the opened and closed conformations of the enzyme formed the basis for the compound binding hypothesis presented in the manuscript. Specifically, the open WPD-loop conformation of the enzyme, which also has a less compact P-loop orientation, provides a sterically unimpeded approach for inhibitor binding. Therefore, it was hypothesized that, as the iminopyridinedione-based compounds approach the enzyme, and the WPD-loop and P-loop are concomitantly reorienting to adopt the closed conformation to impede access to the enzyme's catalytic Cys104, the inhibitor engages these loops in such a way that key, favorable intermolecular contacts are formed, thereby locking the enzyme in the inactive state. Following, as we hypothesize in the main text of the manuscript, it is possible that such a binding mode places the inhibitors in a position that can potentially result in a covalent bond with Cys104 (**Figure 1, Panel (b)** in the main manuscript).

Based on this binding hypothesis, the representative inhibitor **2** was docked into the closed conformation of the enzyme. X-ray crystal structure 5TSR (A chain) was chosen as the starting structure for the docking study, *i.e*., over that of NMR structure 2MBC, as its architecture is more well defined. For example, as seen in **Figure S10**, α-helix residues Thr56 – Glu59, and residues in β-sheets: Ala42 – Arg47 and Thr64 – Asp67, respectively, are more well defined in 5TSR versus 2MBC. Moreover, the Ramachandran plot of 5TSR indicates a strikingly better distribution of data points in favored regions versus PDB entry 2MBC. Note, the Ramachandran plots were generated using Maestro v2016 software (Schrödinger, LLC, New York, NY)).

PTP4A3 structure refinement, and the docking and optimization of inhibitor **2**, followed a protocol that has been described in detail (**Refs**: **a)** J.C., Burnett, C., Lim, B.D., Peyser, L.P., Samankumara, M., Kovaliov, R., Colombo, S.L., Bulfer, M.G., LaPorte, A.R., Hermone, C.F., McGrath, M.R., R., Gussio, D.M., Huryn, and P. Wipf, *Org. Biomol. Chem*., 2017, **15**, 4096; **b)** M.G., LaPorte, J.C., Burnett, R., Colombo, S.L., Bulfer, C., Alverez, T.F., Chou, R.J., Neitz, N., Green, W.J., Moore, Z., Yue, S. Li, M.R., Arkin, P. Wipf, and D.M. Huryn, *ACS Med. Chem. Lett*., 2018,**18**, 1075). As indicated in the paragraph above, PDB entry 5TSR was used for enzyme coordinates (with the Ala 104 mutation in the original structure being replaced with the native Cys residue). Energy refinement of the enzyme only was first performed (due to its low resolution) using the Discovery module of the Insight 2005 program (Dassault Systèmes BIOVIA, San Diego, CA). The protocol was iterative, with the following settings being used: cff91 force field and distance dielectric = 1.0. First, hydrogens only were minimized via 200 cycles of steepest descents, followed by conjugate gradients until the RMS gradient was < 0.001 kcal/Å. Subsequently, a tethering algorithm was employed to energy refine the side chains. Specifically, with all backbone atom coordinates fixed, and a force constant of 100 kcal/Å applied, 100 steps of steepest descents, followed by 200 steps of conjugant gradients, was repeatedly cycled until the RMS gradient was < 0.001 kcal/Å. Next, all atoms of the enzyme, including backbone atoms, were energy refine using the same tethered minimization protocol indicated above, *i.e*., for side chain refinement. Finally, all tethers were removed, and all enzyme atoms were allowed to move freely. For this final step, 200 cycles of steepest descents minimization were performed, and were followed by conjugate gradients minimization until the RMS gradient was < 0.001 kcal/Å.

For inhibitor **2** docking, compound coordinates were obtained from the Cambridge Crystallographic Data Centre (entry code IPOLOQ) (**Ref**: J.M., Salamoun, K.E., McQueeney, K. Patil, S.J., Geib, E.R., Sharlo, J.S., Lazo, and P., Wipf, *Org. Biomol. Chem.*, 2016, 14, 6398), and energy refined using Discovery Studio 2018 software (Dassault Systèmes BIOVIA, San Diego, CA). Energy refinement of the small molecule was performed using the MMFF force field. Two hundred steps of steepest descent, followed by conjugate gradients minimization until the RMS gradient was < 0.001 kcal/Å. To identify a compatible binding site location on the enzyme that would both accommodate the polar iminopyridinedione component of inhibitor **2**, as well as the compound's hydrophobic phenyl component, the SiteMap application in Maestro v2016 was used to evaluate the open form of the enzyme (PDB entry 1V3A). **Figure S11** shows the site map, which indicated that polar compatibility for the iminopyridinedione component of the inhibitor chemotype could be sequestered from backbone atoms of residues composing the P-loop, while at the same time indicating that a distal, mainly hydrophobic pocket near Trp 68 of the WPD loop could accommodate the inhibitor's phenyl component. Using this information, the same residues composing this site were examined in their coordinate positions in the closed, energy refined model of the enzyme generated from 5TSR (*vide supra*), and it was determined that there was the necessary combination of location, and both polar and hydrophobic compatibility to warrant exploratory docking. Subsequently, due to the complexity of the binding site and the flexible loops associated with it, inhibitor **2** docking was performed manually using Insight 2005, as the graphical user interface of this program provides not only three-dimensional viewing capability, but also dial box control, thereby allowing for fine, well controlled small molecule movement/manipulation, as well as the ability to select, retain, and modify multiple torsions with a single F7 key stroke that allows for quick movement from one selected torsion to the next. Following, inhibitor **2** was oriented into the predicted binding location, and with the intermolecular van der Waals bump set to 0.25 Å,

small molecule adjustments (translational, rotational, and torsional) and side chain torsional adjustments were performed to remove unacceptably close intermolecular and unfavorable intermolecular contacts, as well as to optimize favorable intermolecular contacts. Subsequently, the same energy minimization protocol that was used for the initial enzyme-only energy refinement (*vide supra*) was subsequently performed a second time on the enzyme:inhibitor complex.

A final, exploratory inhibitor binding pose for inhibitor **2** was generated using a method employing the HINT scoring algorithm (eduSoft LLC, Richmond, VA); this method has been described in detail previously (**Ref**: J.C., Burnett, C., Lim, B.D., Peyser, L.P., Samankumara, M., Kovaliov, R., Colombo, S.L., Bulfer, M.G., LaPorte, A.R., Hermone, C.F., McGrath, M.R., R., Gussio, D.M., Huryn, and P. Wipf, *Org. Biomol. Chem*., 2017, **15**, 4096). It is notable that the HINT program is unique in that it quantitates intermolecular contacts categorically by classifying atom-atom contacts as either favorable and positive (hydrogen bonds, acid/base contacts, and hydrophobic/hydrophobic contacts) or unfavorable and negative (acid/acid, base/base, and importantly, hydrophobic polar). Hence, using HINT-based atom-atom interaction scores as guides, it is possible to generate small molecule:inhibitor binding modes, in this case inhibitor **2**:PTP4A3, with optimized favorable intermolecular contact scores and significantly assuaged unfavorable intermolecular contact scores. Finally, an optimized docking model of inhibitor **2** was prepared using iterative rounds of HINT scoring, tethered minimizations, manual adjustments to inhibitor coordinates (including translational, rotational, and torsional), and torsional adjustments to surrounding side chain residues, and HINT scoring. In this way, we were able to use SAR-directed modeling, which provided a biochemically feasible binding mode rationalizing the IC_{50} values shown in **Table 2** of the main text of the manuscript. For the final binding model versus the original 5TSR structure, the RMSD was 1.28 Å (based on the comparison of backbone atom α-helix, β-sheet, and loop coordinates). This RMSD is well within the 3.19 Å resolution of the original X-ray structure.

The Ramachandran plot for the inhibitor **2**:PTP4A3 structure is shown in Figure **S12**, and PDB coordinates for the exploratory docking model are provided as a separate Supporting Information file.

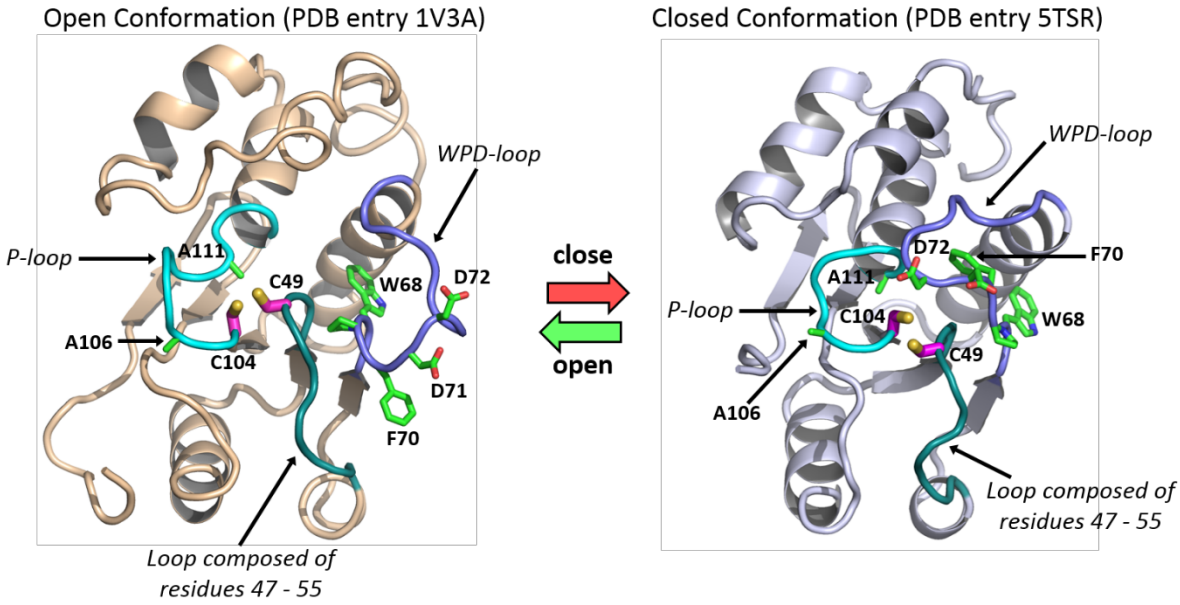

Figure S9. Conformational differences in the 'opened' versus the 'closed' WPD-loop structures based on a comparison between PDB entry 1V3A (light brown cartoon) and PDB entry 5TSR (light blue cartoon). In both structures, the WPD-loop, the P-loop, and a loop predicted to impact inhibitor **2** binding (and is composed of residues 47 – 55) are shown in slate, cyan, and teal cartoon, respectively. The open WPD-loop conformation of the enzyme, which also possesses a less compact P-loop orientation, provides a sterically unimpeded approach for inhibitor binding. The closed WPD-loop conformation of the enzyme, which also possesses a more compact P-loop conformation, impedes access to the enzyme's catalytic Cys104.

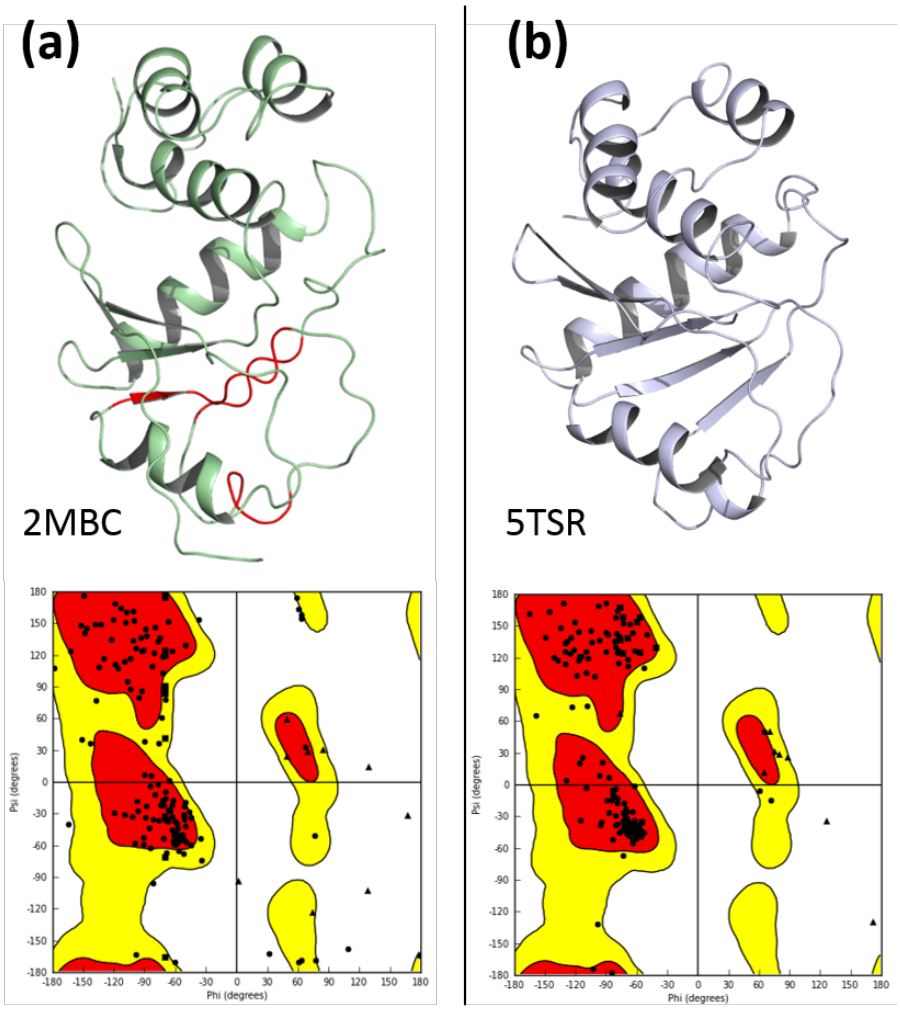

Figure S10. Comparison of closed WPD-loop structures 2MBC (solved by NMR) and 5TSR (solved using X-ray crystallography). Panel (a): PDB entry 2MBC is shown in pale green cartoon, and example residue stretches that are architecturally less well defined in this structure versus corresponding residues in PDB entry 5TSR are shown in red cartoon. The Ramachandran plot for 2MBC is shown underneath the cartoon. Panel (b): PDB entry 5TSR is shown in light blue cartoon, and its corresponding Ramachandran plot is shown underneath. The Ramachandran plot for 5TSR indicates a strikingly better distribution of data points in favored regions versus that of 2MBC.

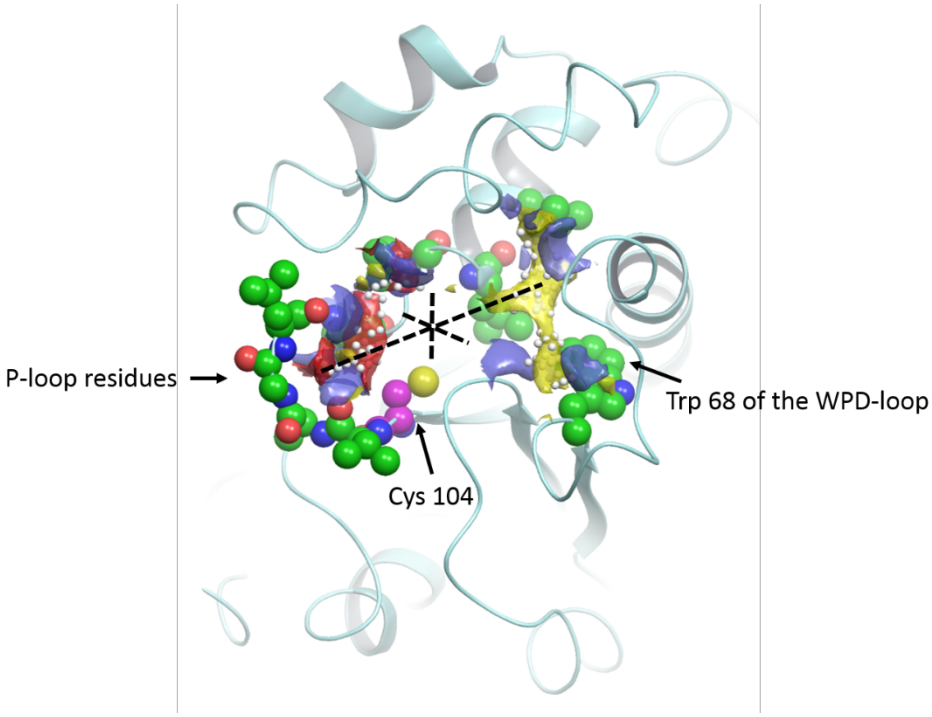

Figure S11. Site map was used to identify a potentially compatible binding location for inhibitor **2**. PTP4A3 (PDB entry code 1V3A) is shown in light blue cartoon. Select residues are shown in CPK with green carbons, while Cys104 is shown with magenta carbons. Site map points are represented by small white spheres. Red and blue contours indicate mapped hydrogen bond donor and acceptor sites, respectively. Yellow contours indicate mapped hydrophobic sites. The dashed black lines delineate the potential inhibitor **2** binding location that was identified by the SiteMap application in Maestro v2016.

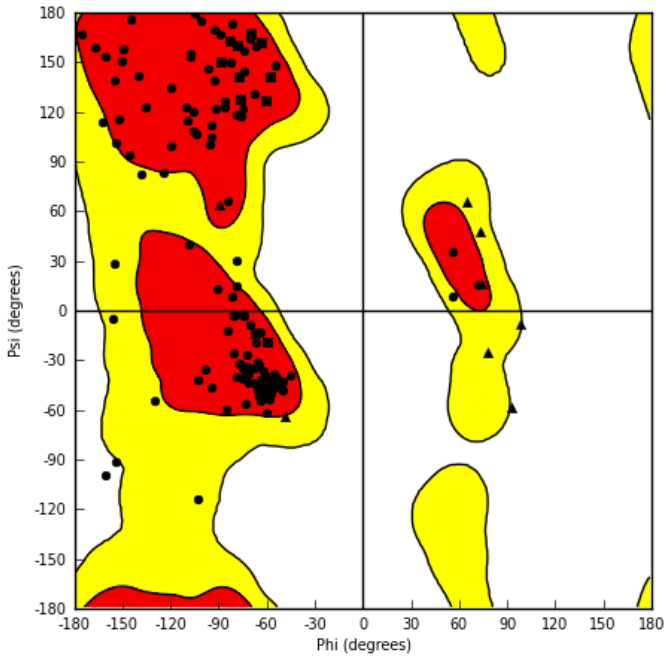

Figure S12. Ramachandran plot of the final PTP4A3 structure (*i.e.*, post energy minimization to obtain the final inhibitor **2** docking model).

19. Spectra (^{1}H NMR, ^{13}C NMR, ^{19}F NMR)

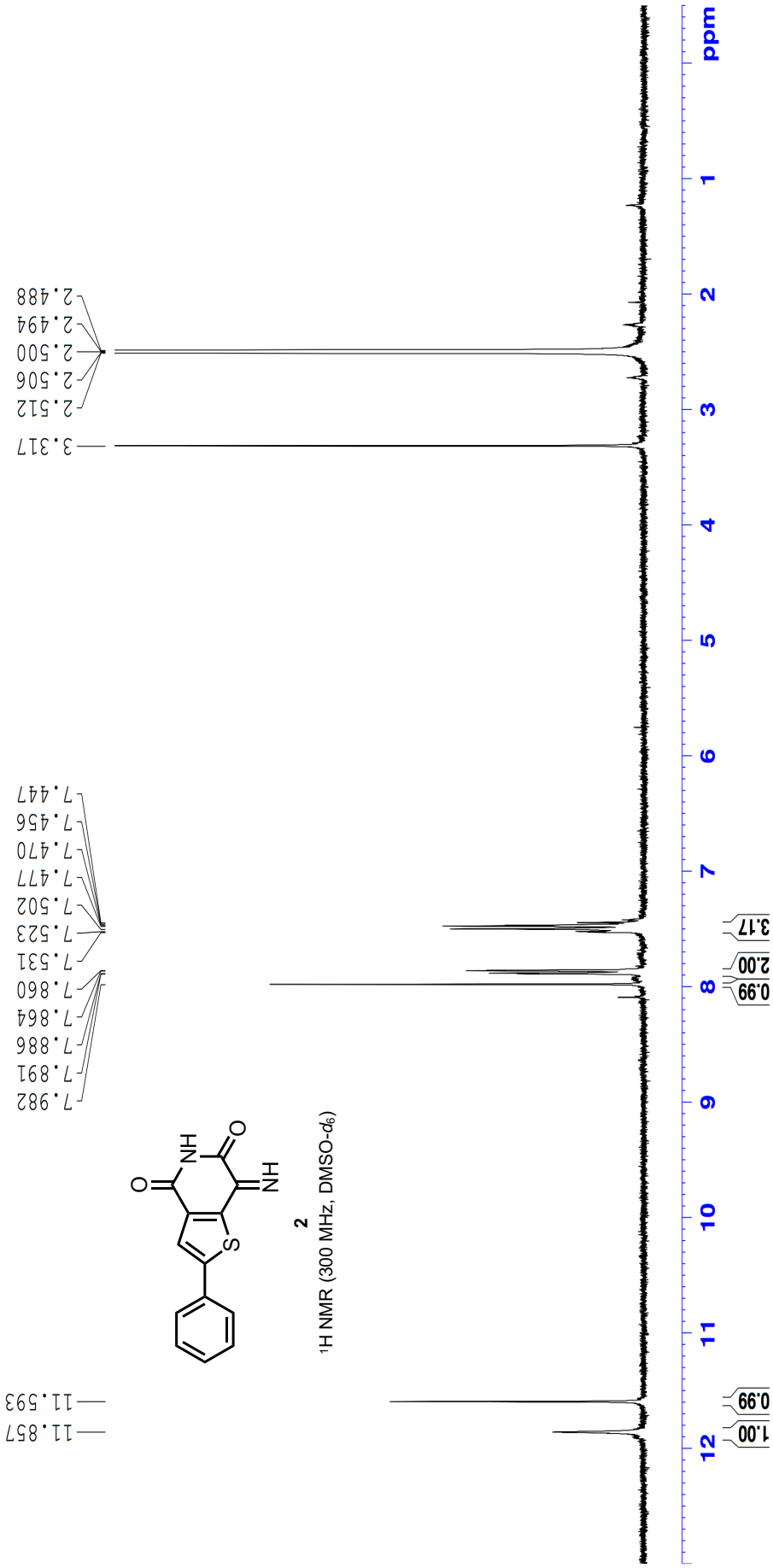
11.857
11.593
7.982
7.891
7.886
7.864
7.860
7.531
7.523
7.502
7.477
7.470
7.456
7.447
2.512
2.506
2.500
2.494
2.488
3.317
1.00
0.99
3.17
2.00
0.99
ppm
1
2
3
4
5
6
7
8
9
10
11
12
NH
O
O
NH
S
2
^{1}H NMR (300 MHz, DMSO-d_6)

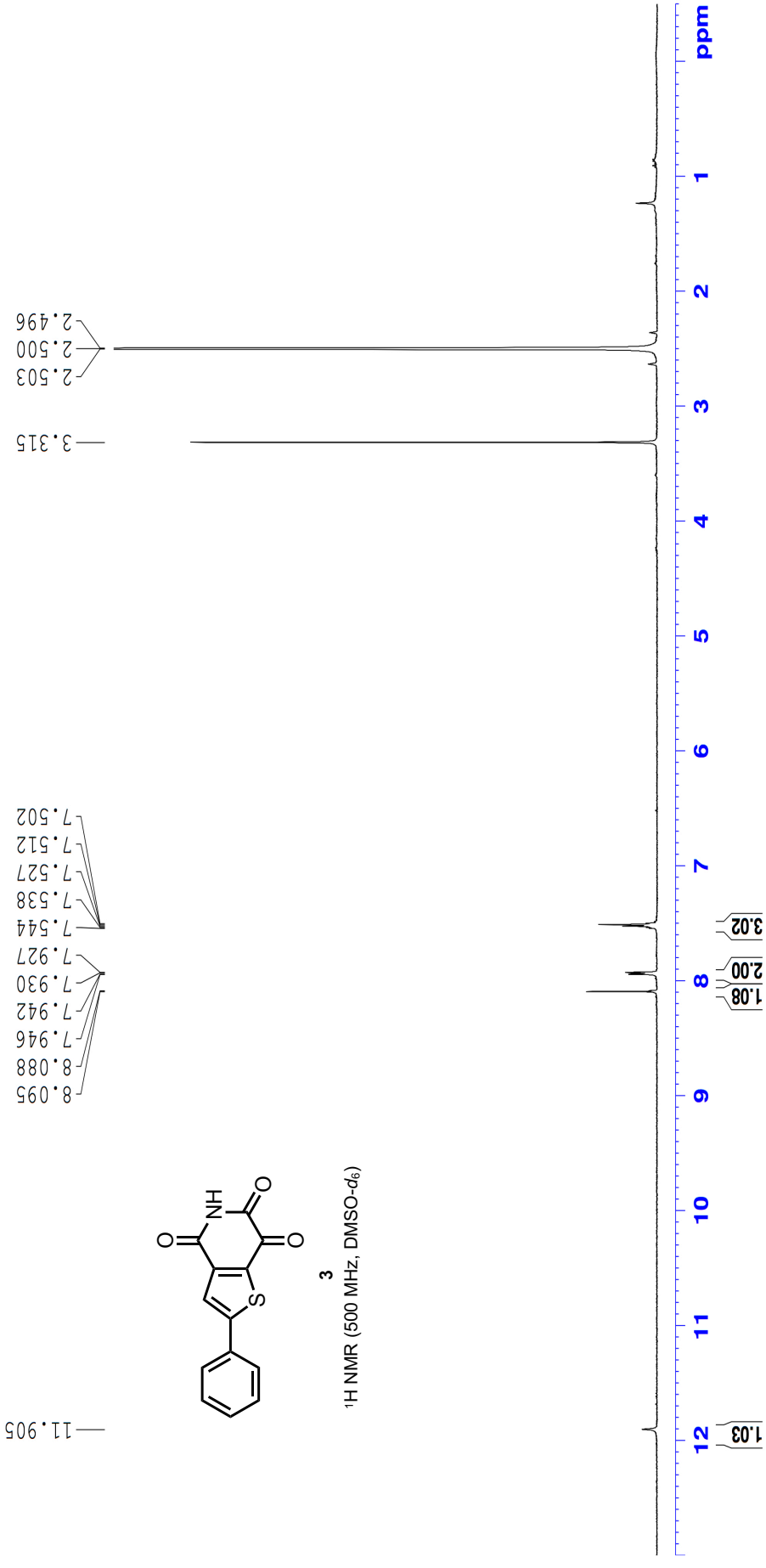

3

^{1}H NMR (500 MHz, DMSO-d_6)

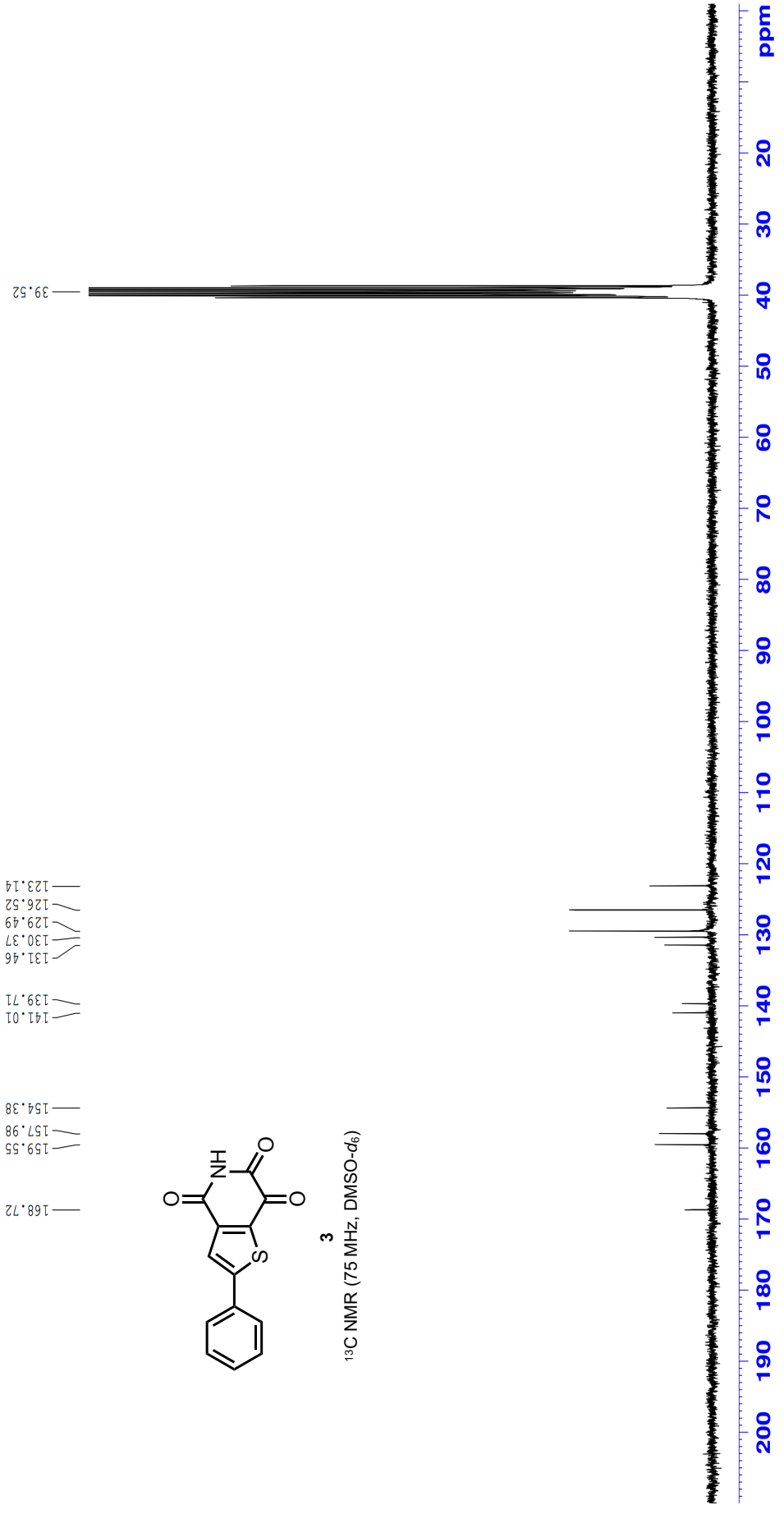
39.52
123.14
126.52
129.49
130.37
131.46
139.71
141.01
154.38
157.98
159.55
168.72
NH
O
O
O
S
3
^{13}C NMR (75 MHz, DMSO-d_6)
ppm
200
190
180
170
160
150
140
130
120
110
100
90
80
70
60
50
40
30
20

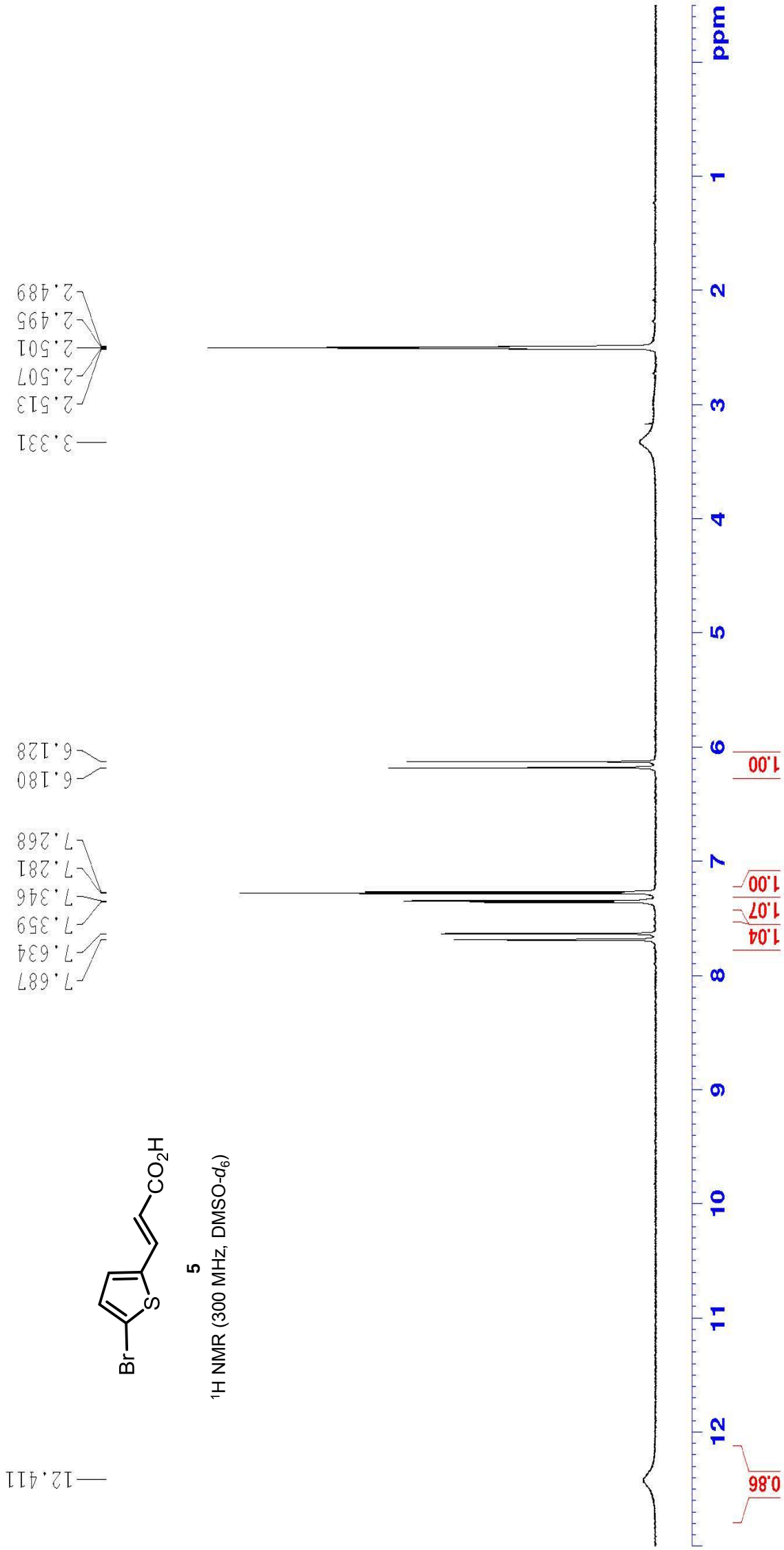

5

^{1}H NMR (300 MHz, DMSO-d_6)

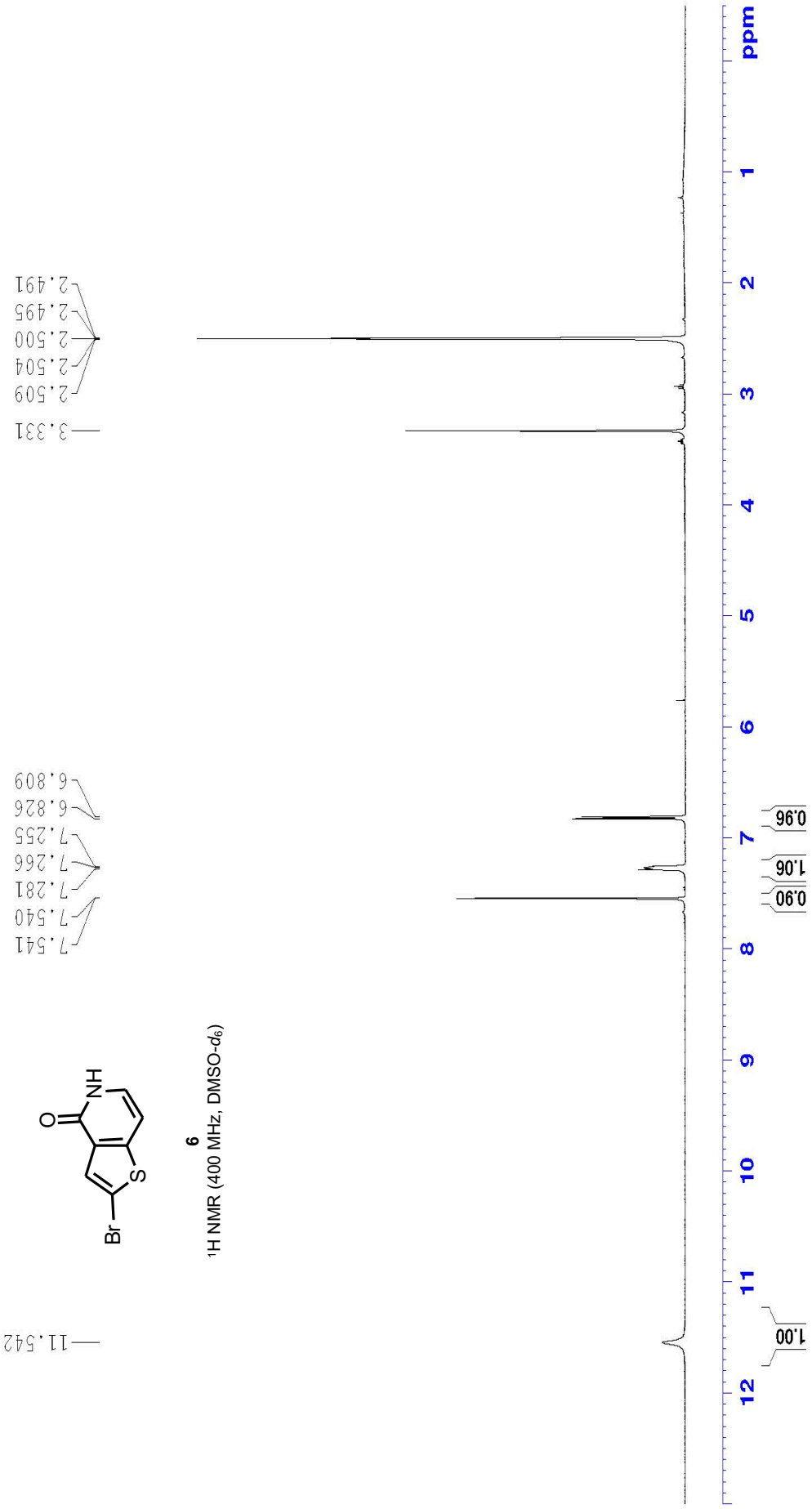

6

^{1}H NMR (400 MHz, DMSO-d_6)

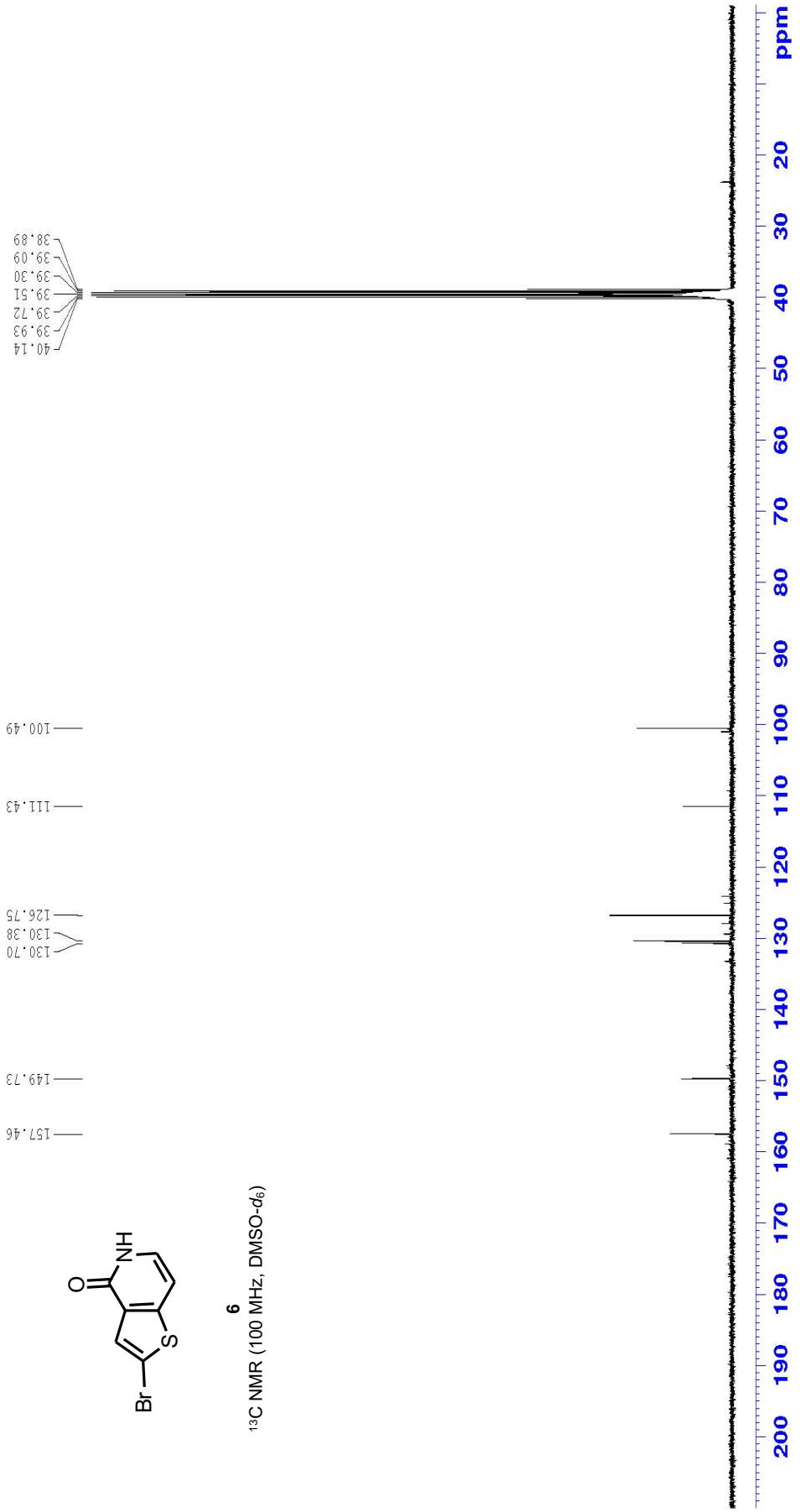

6

^{13}C NMR (100 MHz, DMSO-d_6)

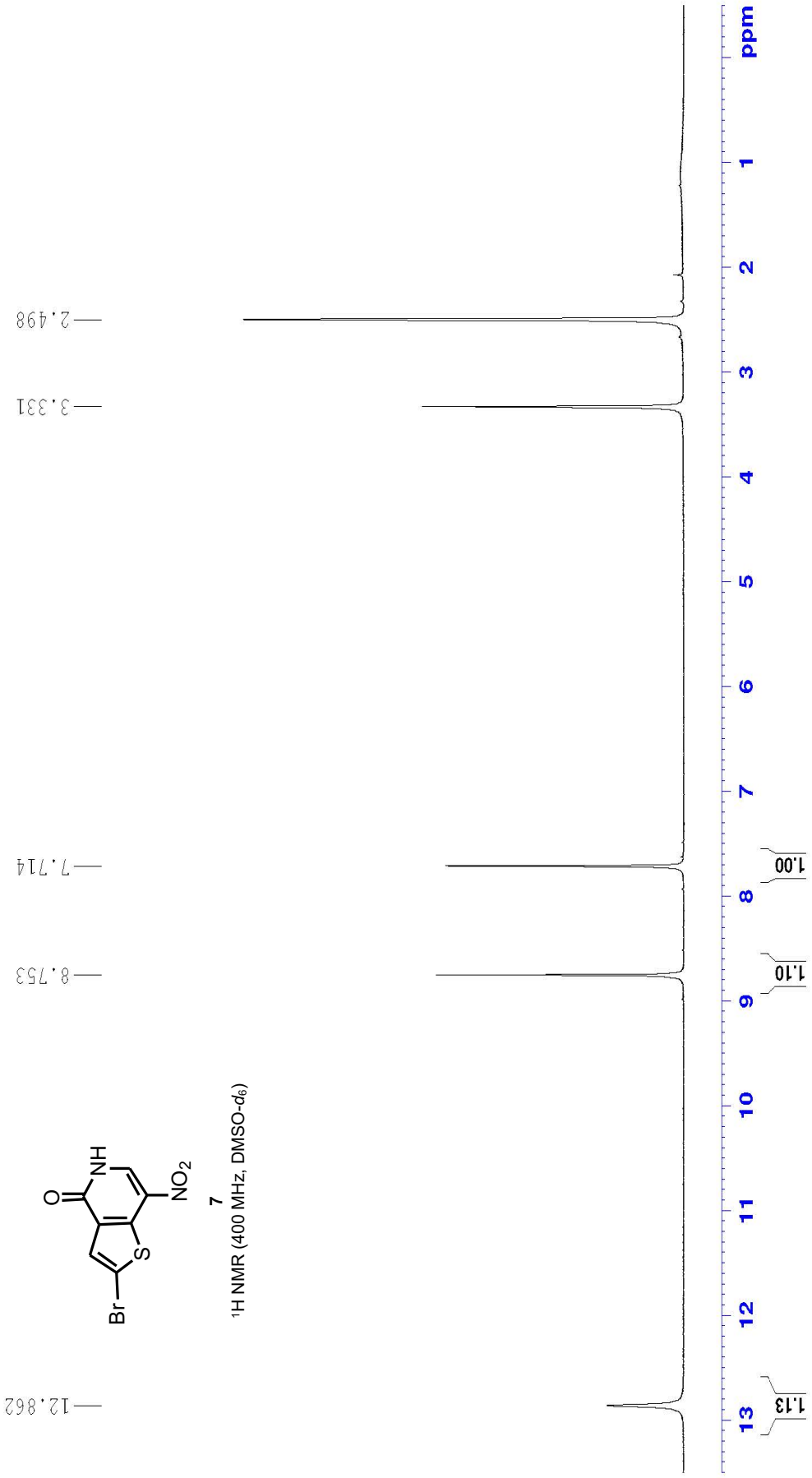

7

^{1}H NMR (400 MHz, DMSO-d_6)

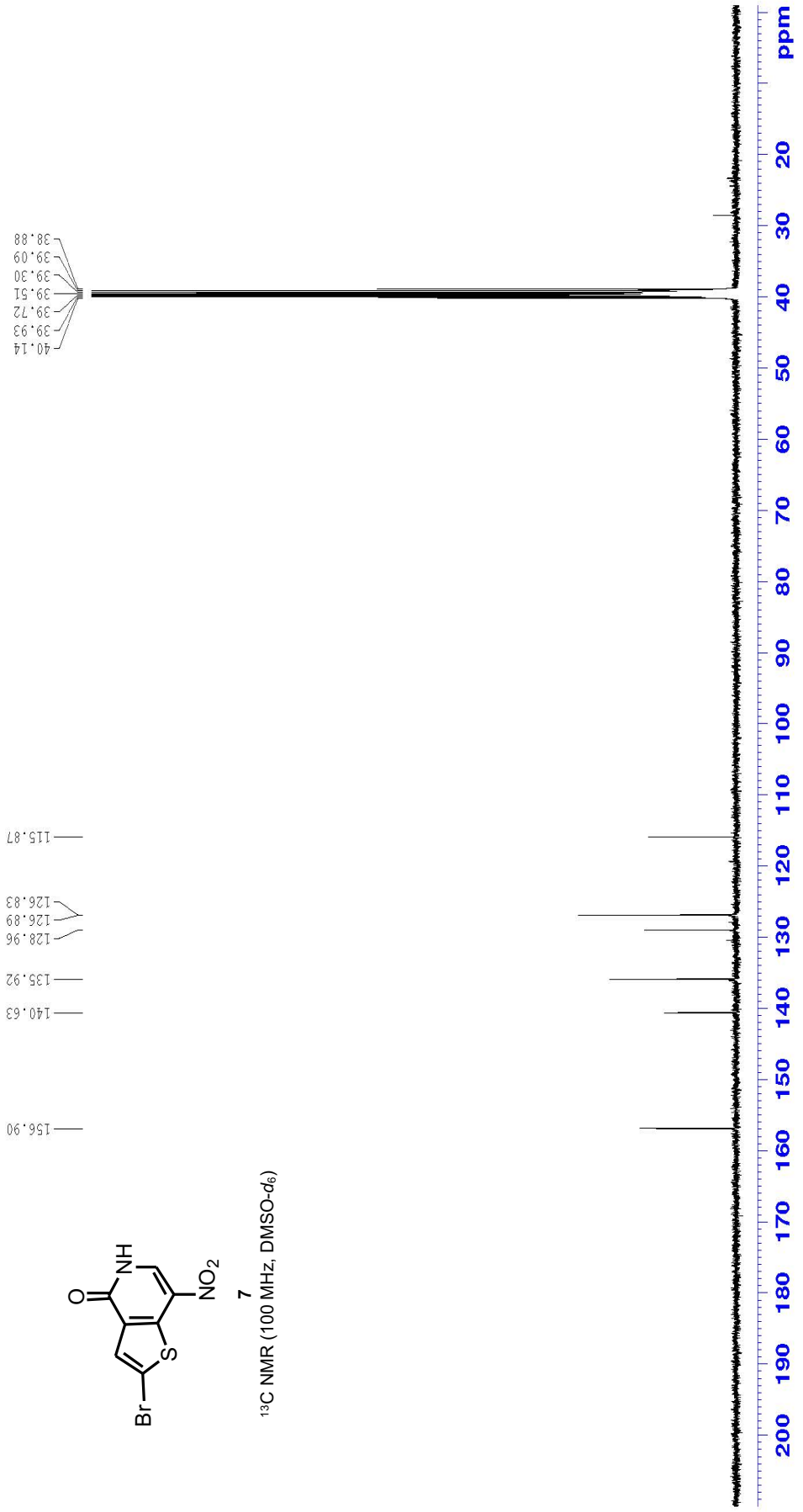

7

^{13}C NMR (100 MHz, DMSO-d_6)

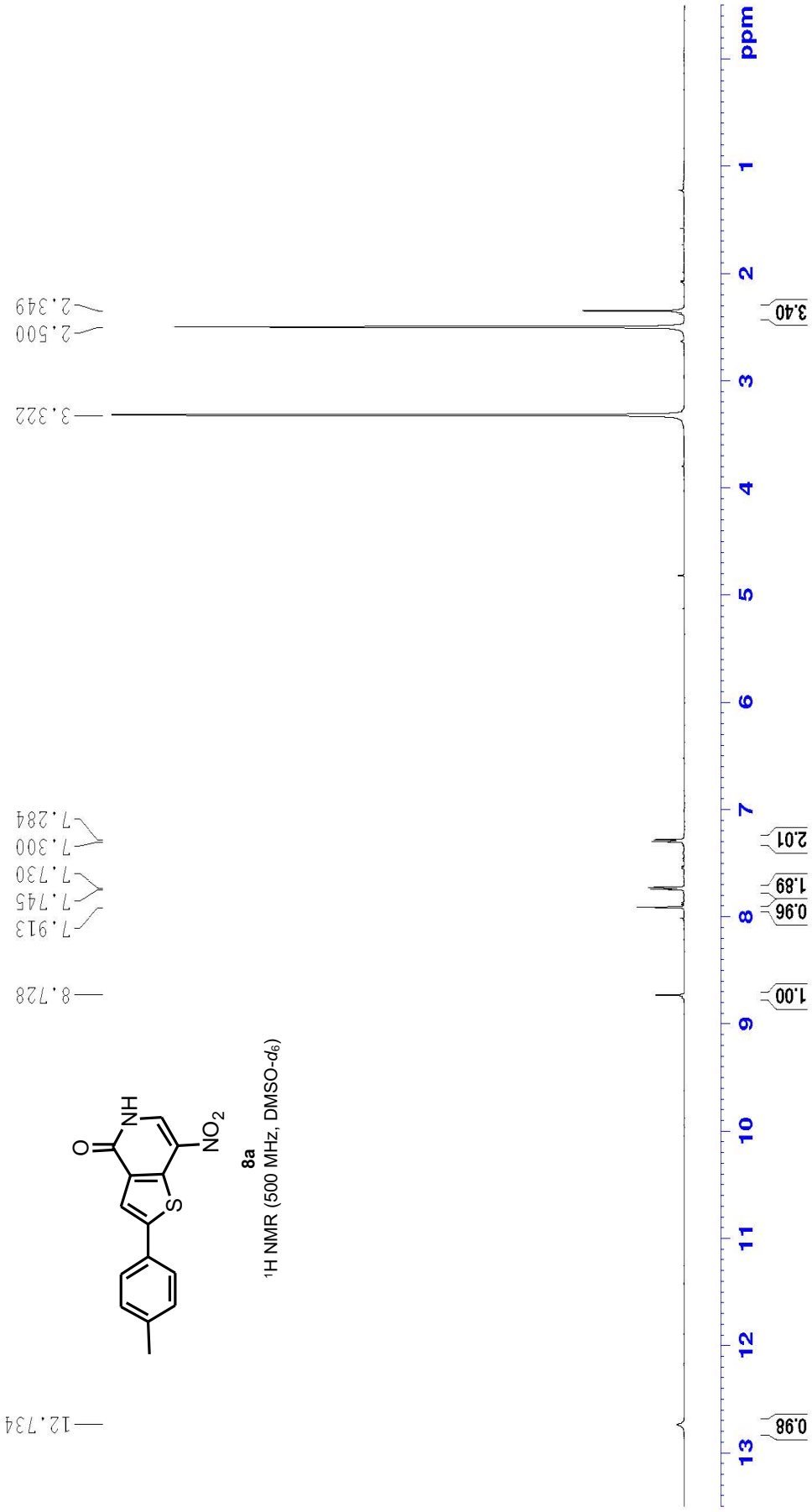

8a

^{1}H NMR (500 MHz, DMSO-d_6)

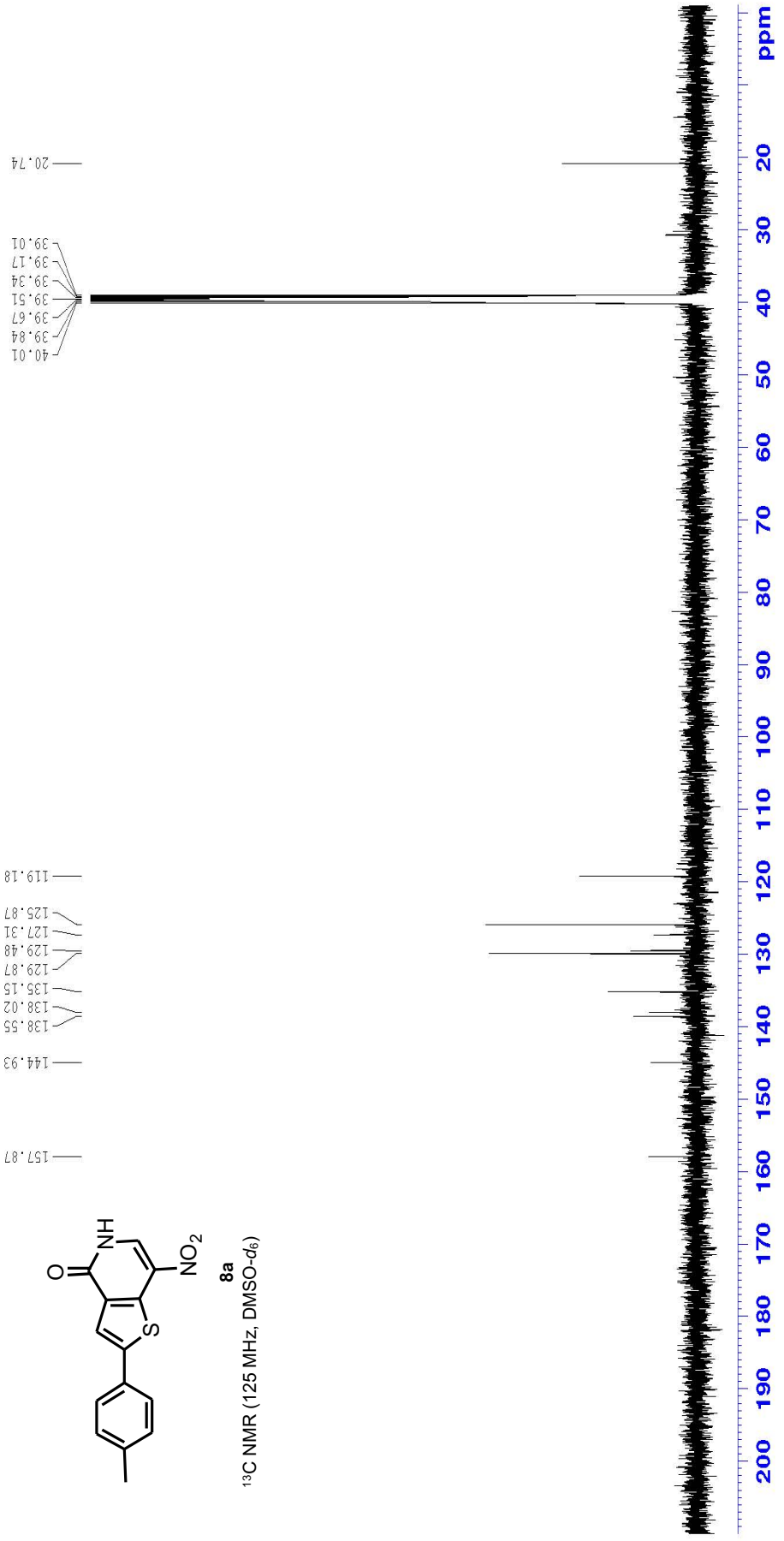

8a

^{13}C NMR (125 MHz, DMSO-d_6)

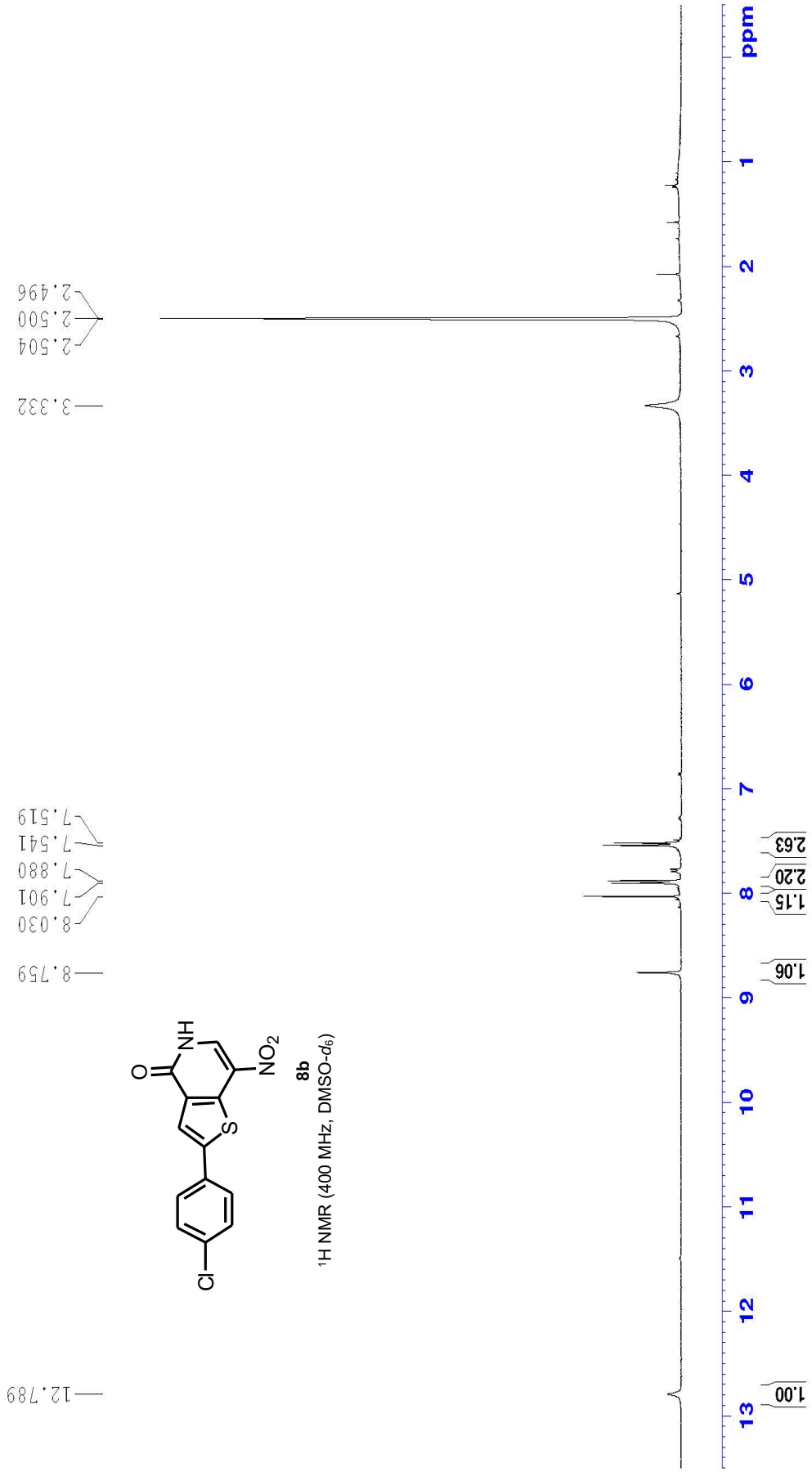

8b

^{1}H NMR (400 MHz, DMSO-d_6)

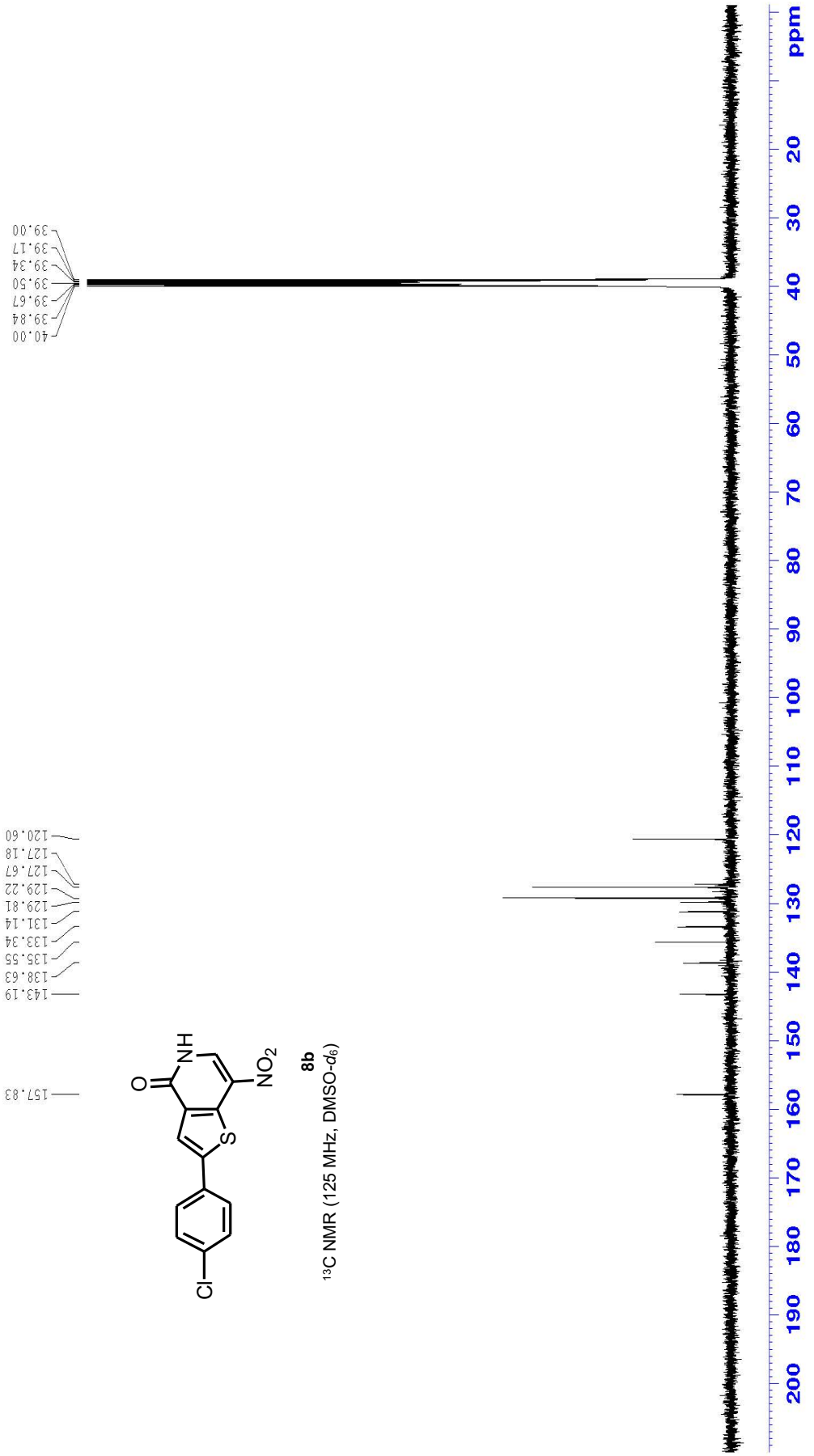

8b

^{13}C NMR (125 MHz, DMSO-d_6)

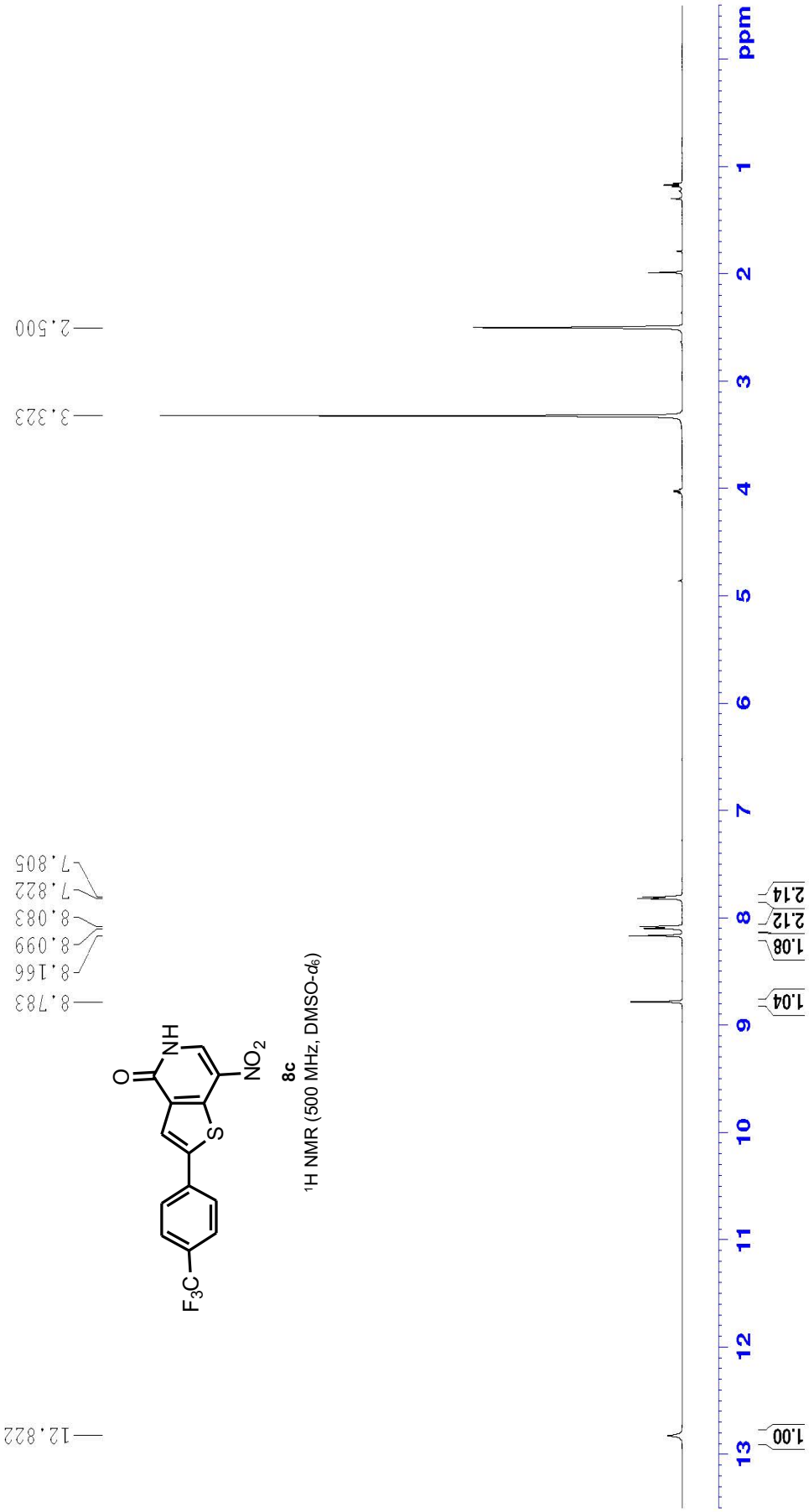

8c

^{1}H NMR (500 MHz, DMSO-d_6)

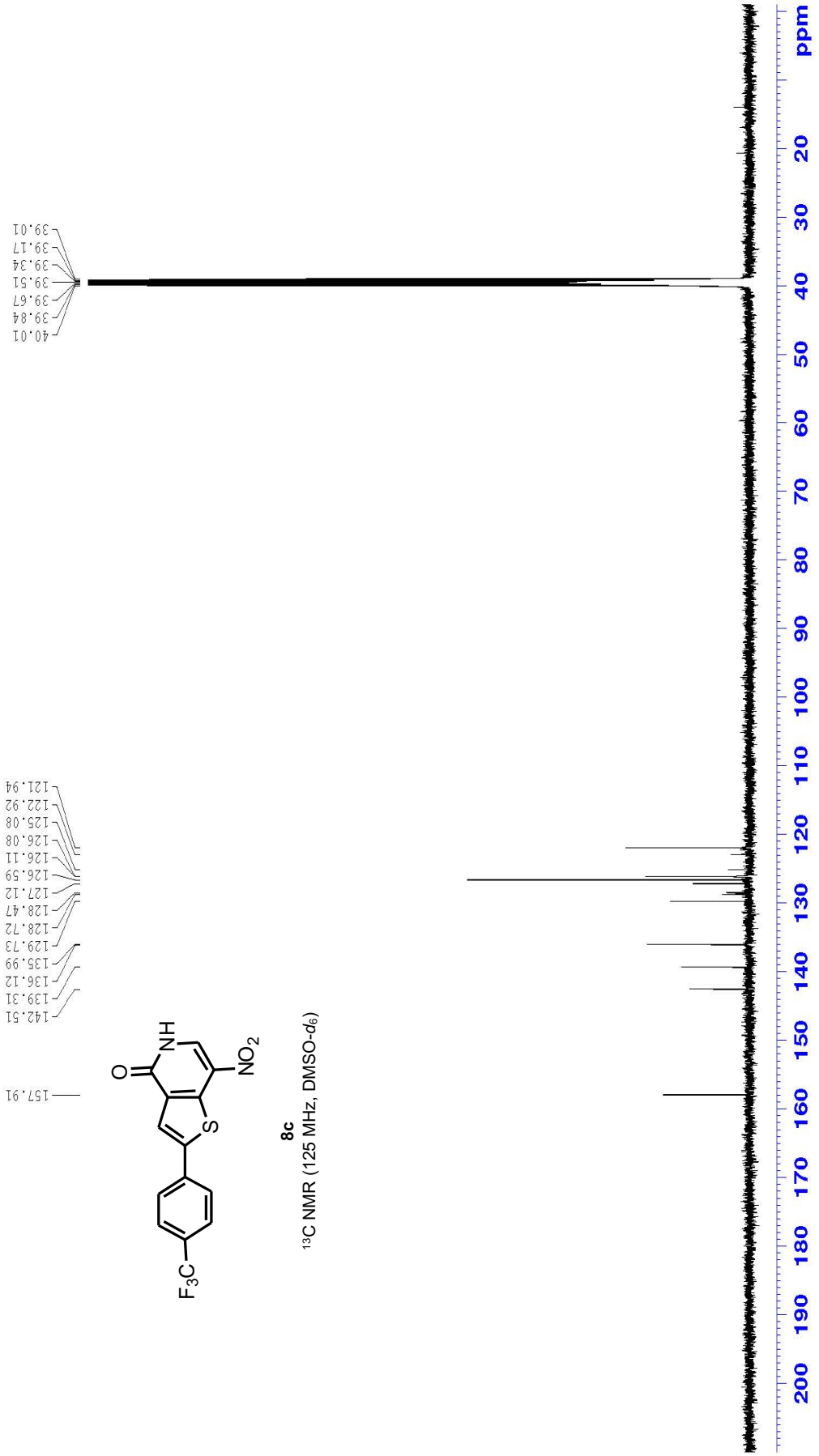

8c

^{13}C NMR (125 MHz, DMSO-d_6)

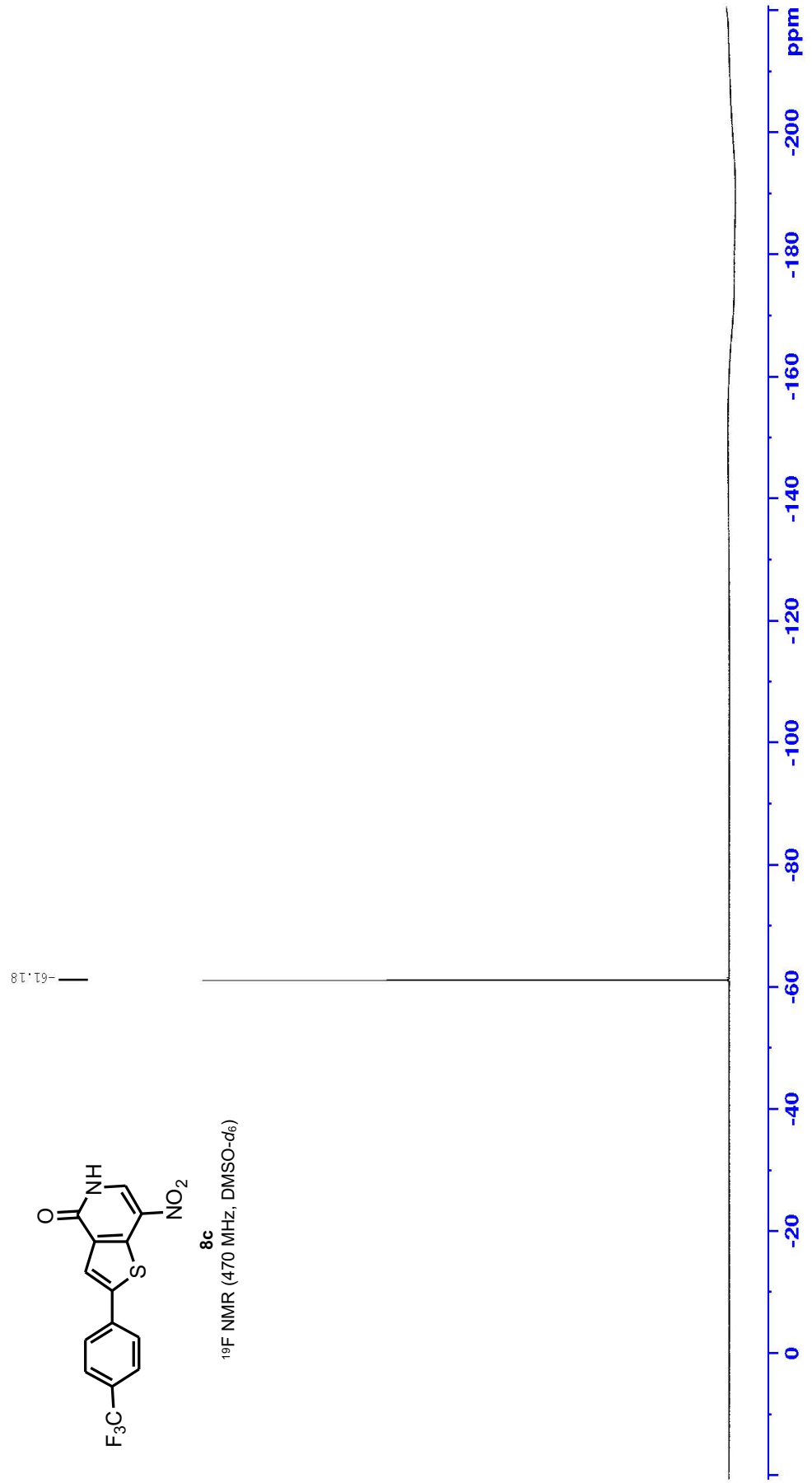

8c

^{19}F NMR (470 MHz, DMSO-d_6)

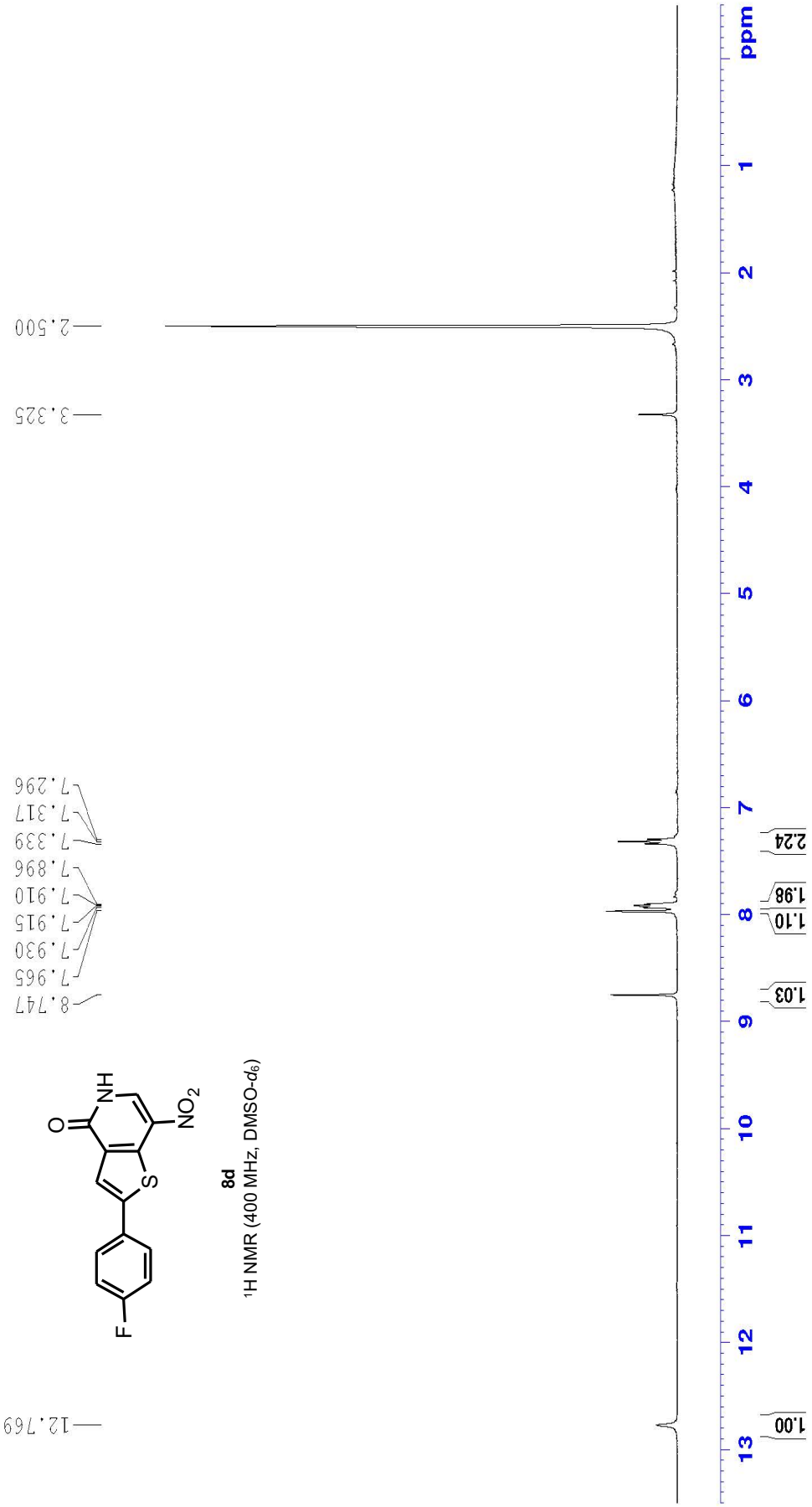

8d

^{1}H NMR (400 MHz, DMSO-d_6)

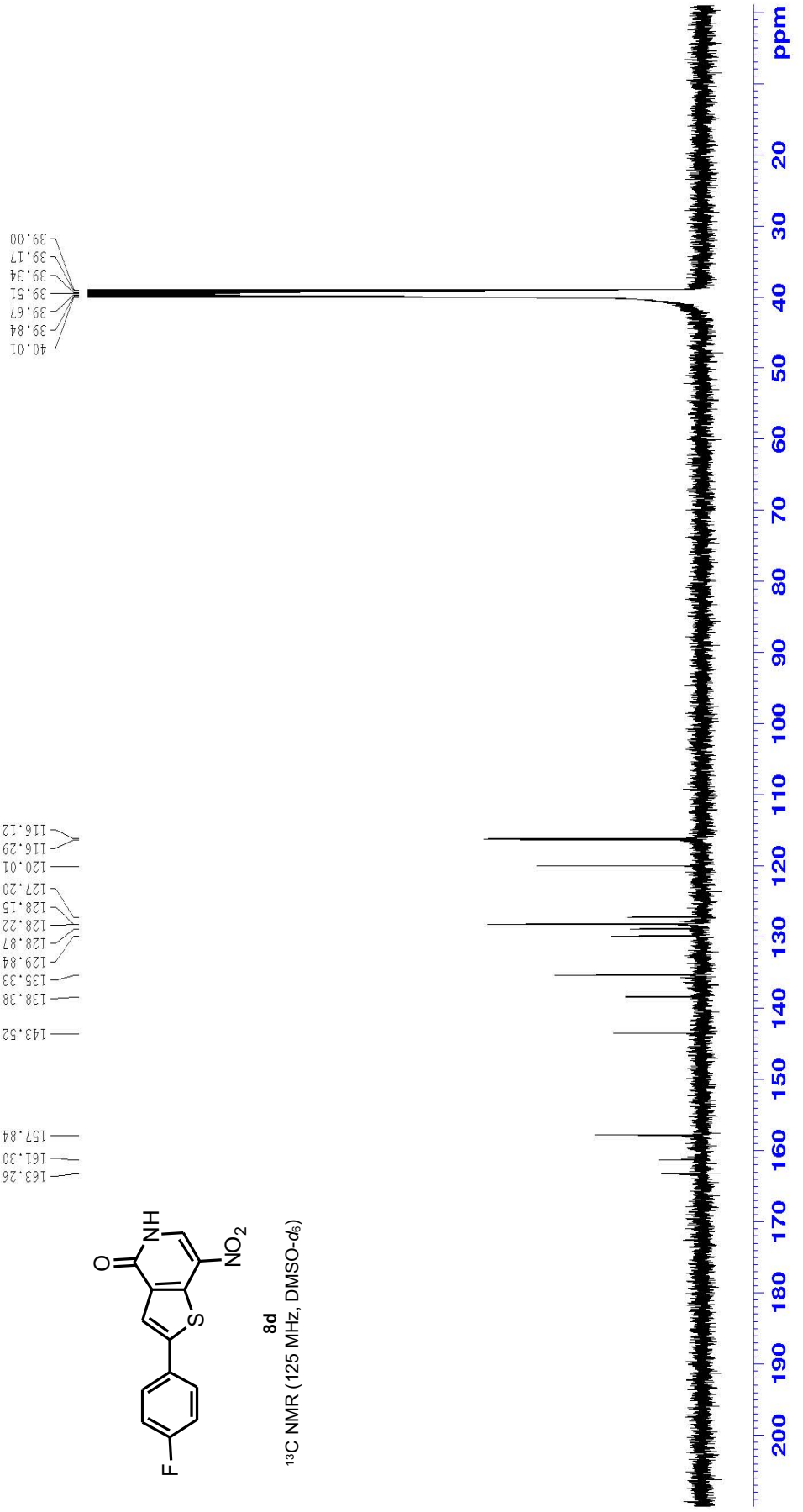
39.00
39.17
39.34
39.51
39.67
39.84
40.01
116.12
116.29
120.01
127.20
128.15
128.22
128.87
129.84
135.33
138.38
143.52
157.84
161.30
163.26
NH
O
NO2
S
F
8d
13C NMR (125 MHz, DMSO-d6)
ppm
200
190
180
170
160
150
140
130
120
110
100
90
80
70
60
50
40
30
20

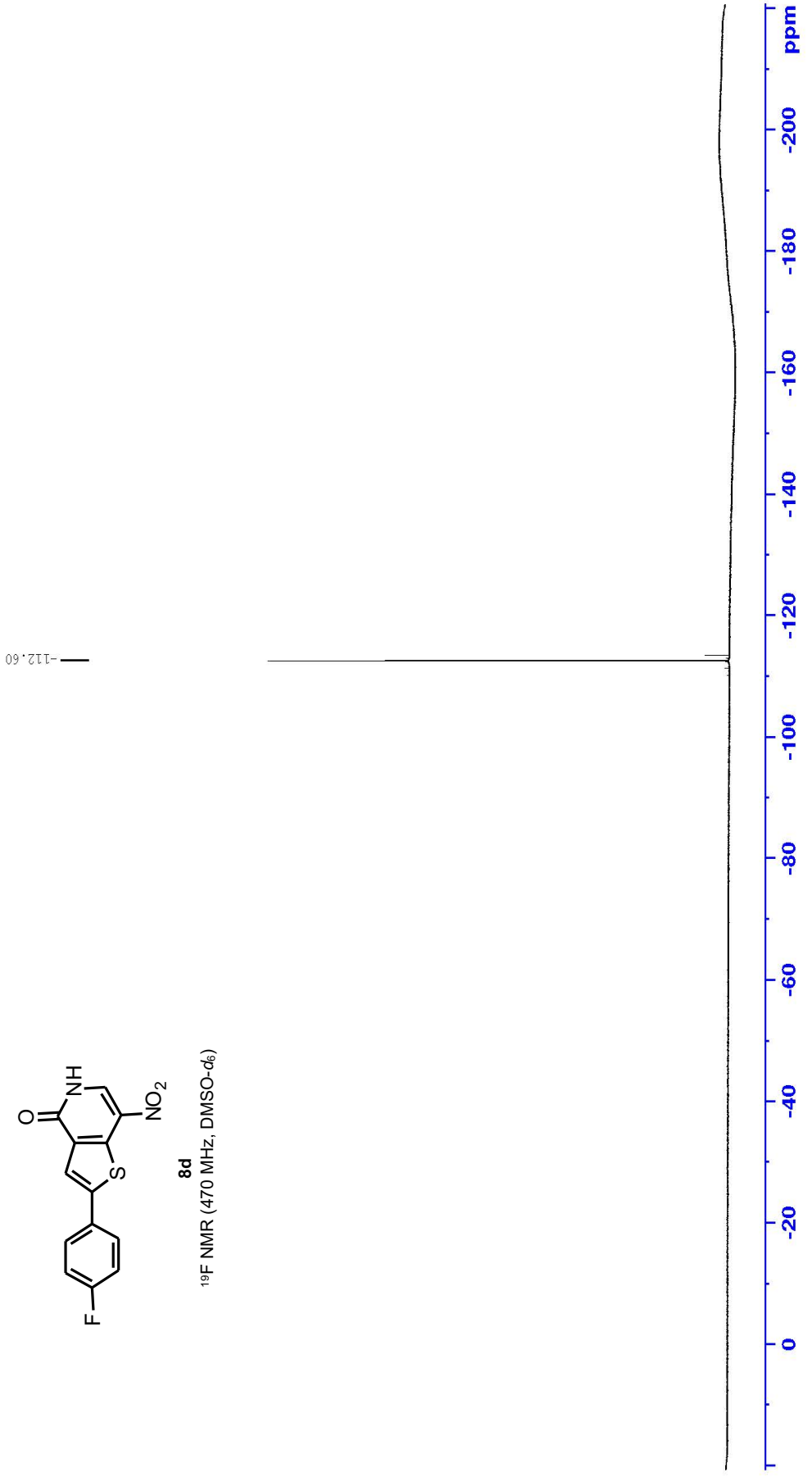

8d

^{19}F NMR (470 MHz, DMSO-d_6)

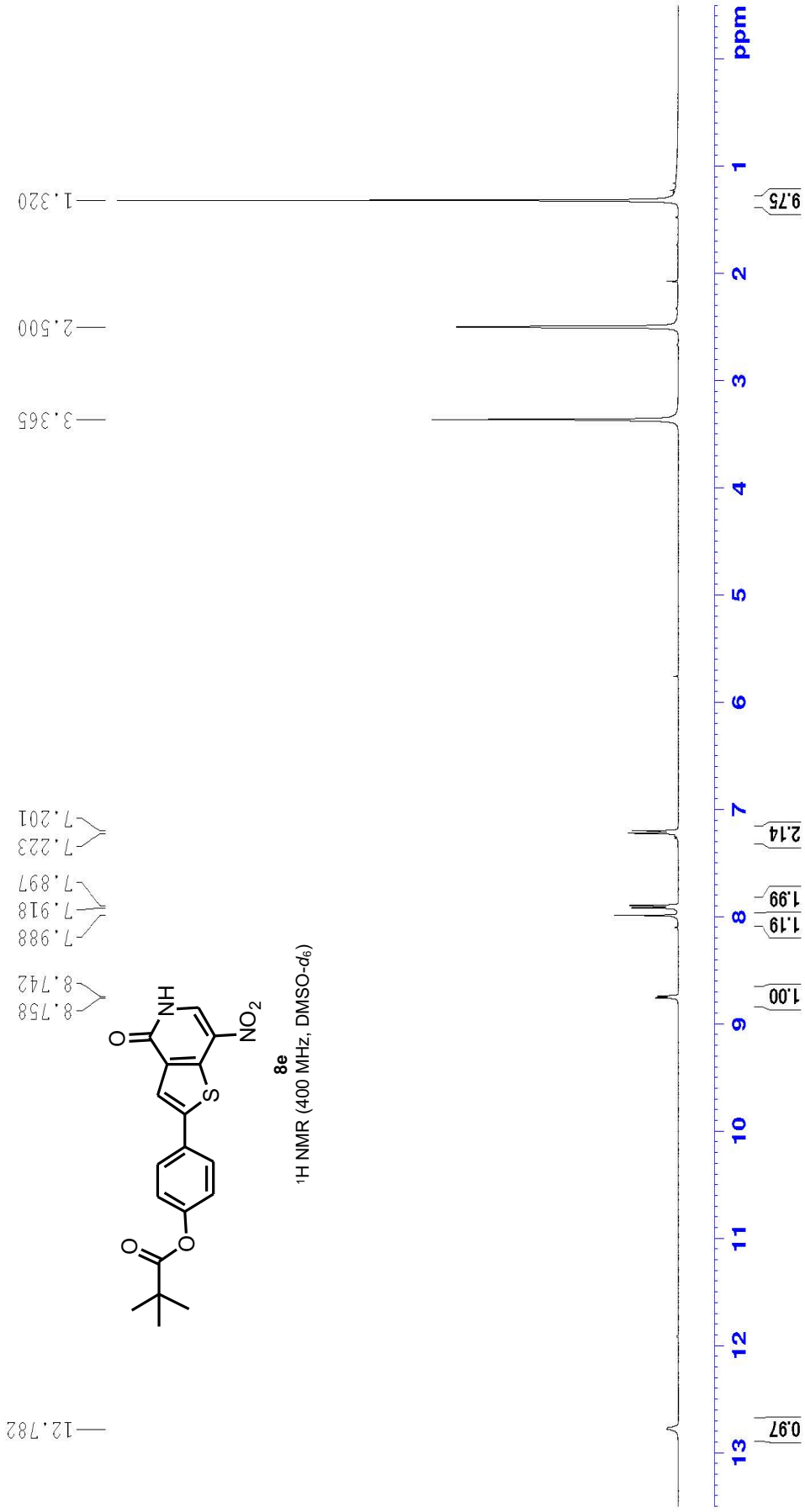
12.782
8.758
8.742
7.988
7.918
7.897
7.223
7.201
3.365
2.500
1.320
NH
O
NO2
S
O
O
8e
1H NMR (400 MHz, DMSO-d6)
ppm
0.97
1.00
1.19
1.99
2.14
9.75

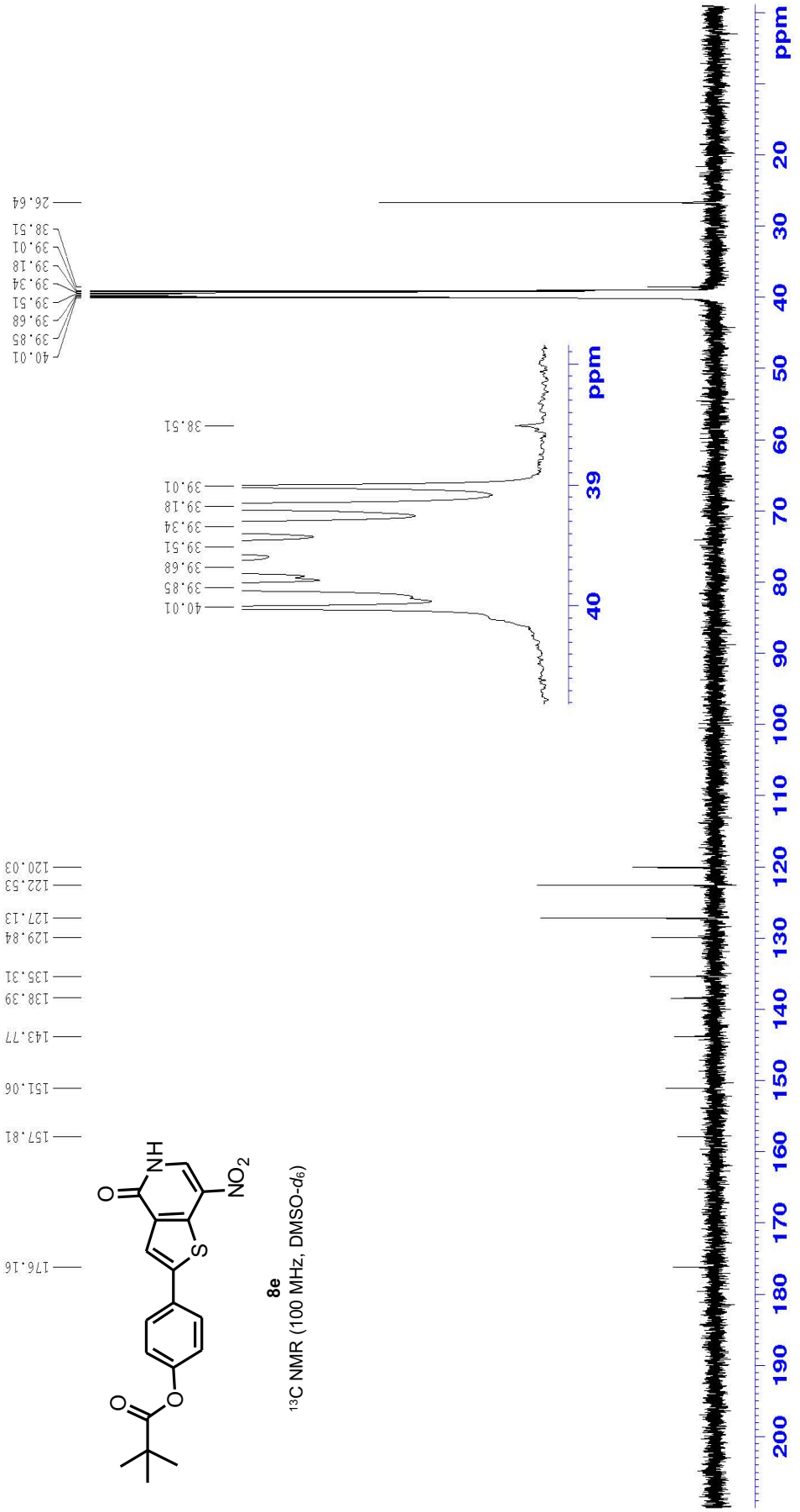

8e

^{13}C NMR (100 MHz, DMSO-d_6)

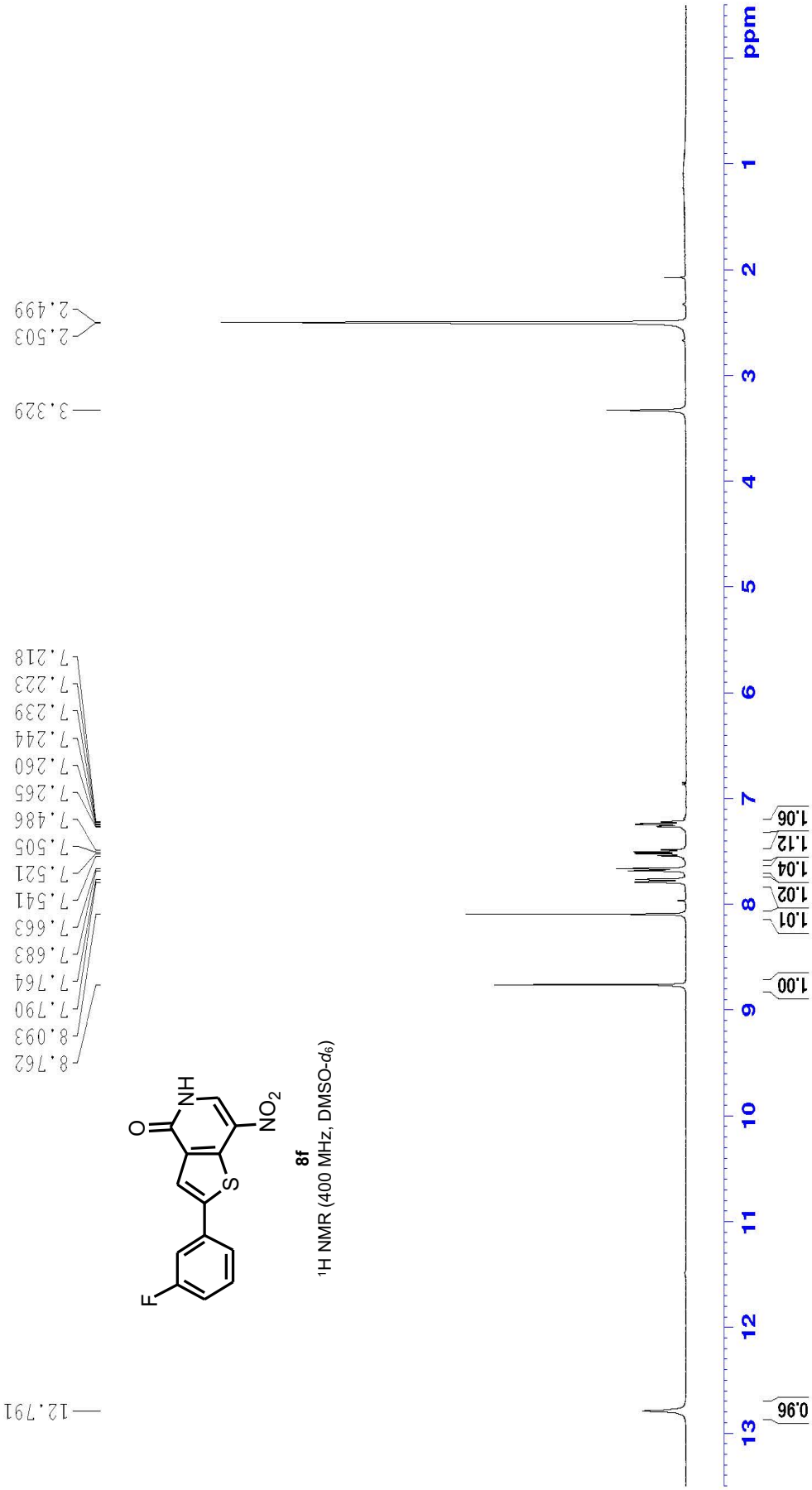

8f

^{1}H NMR (400 MHz, DMSO-d_6)

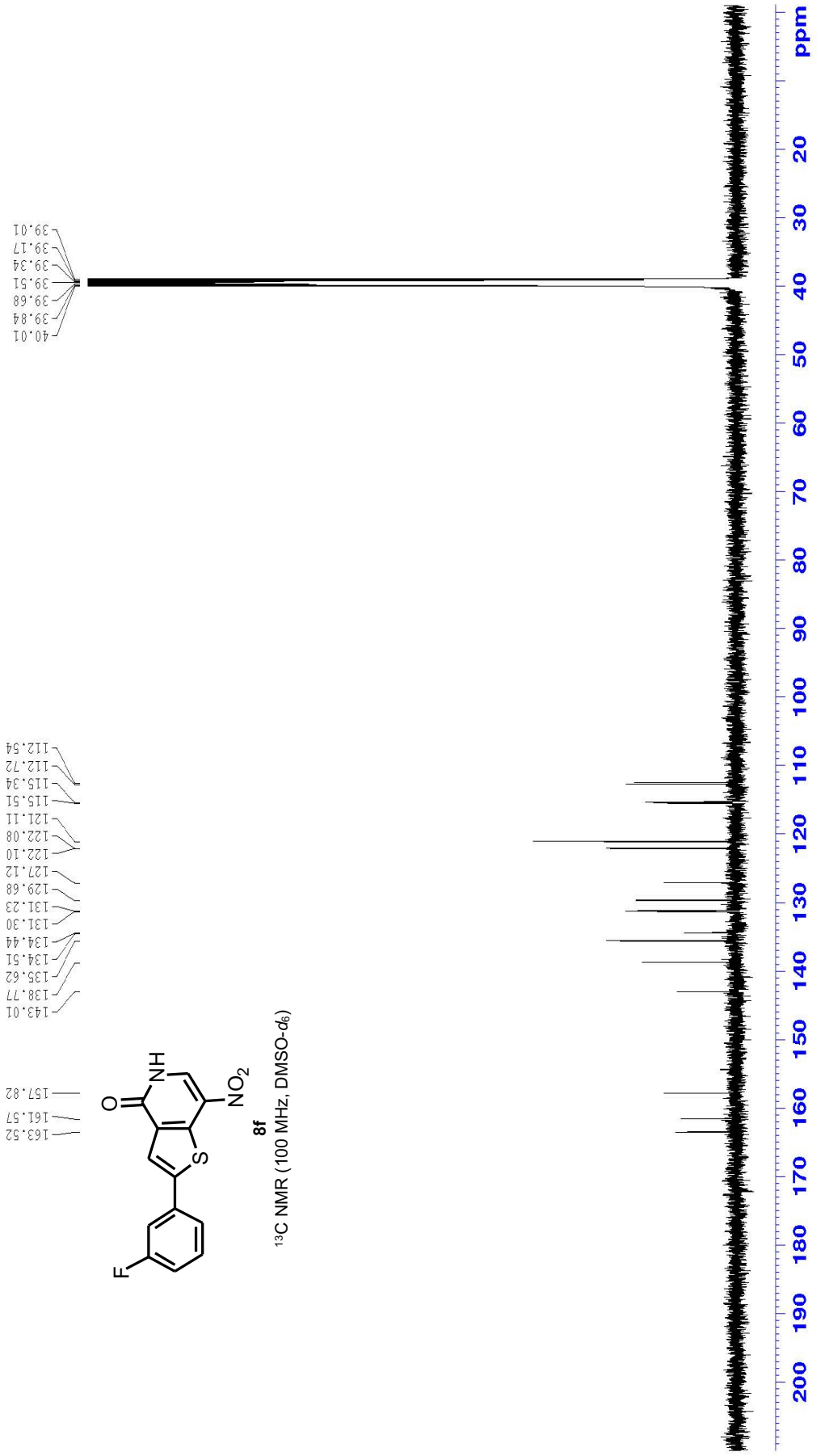
ppm
200
190
180
170
160
150
140
130
120
110
100
90
80
70
60
50
40
30
20
39.01
39.17
39.34
39.51
39.68
39.84
40.01
112.54
112.72
115.34
115.51
121.11
122.08
122.10
127.12
129.68
131.23
131.30
134.44
134.51
135.62
138.77
143.01
157.82
161.57
163.52
NH
O
NO2
S
F
8f
13C NMR (100 MHz, DMSO-d6)

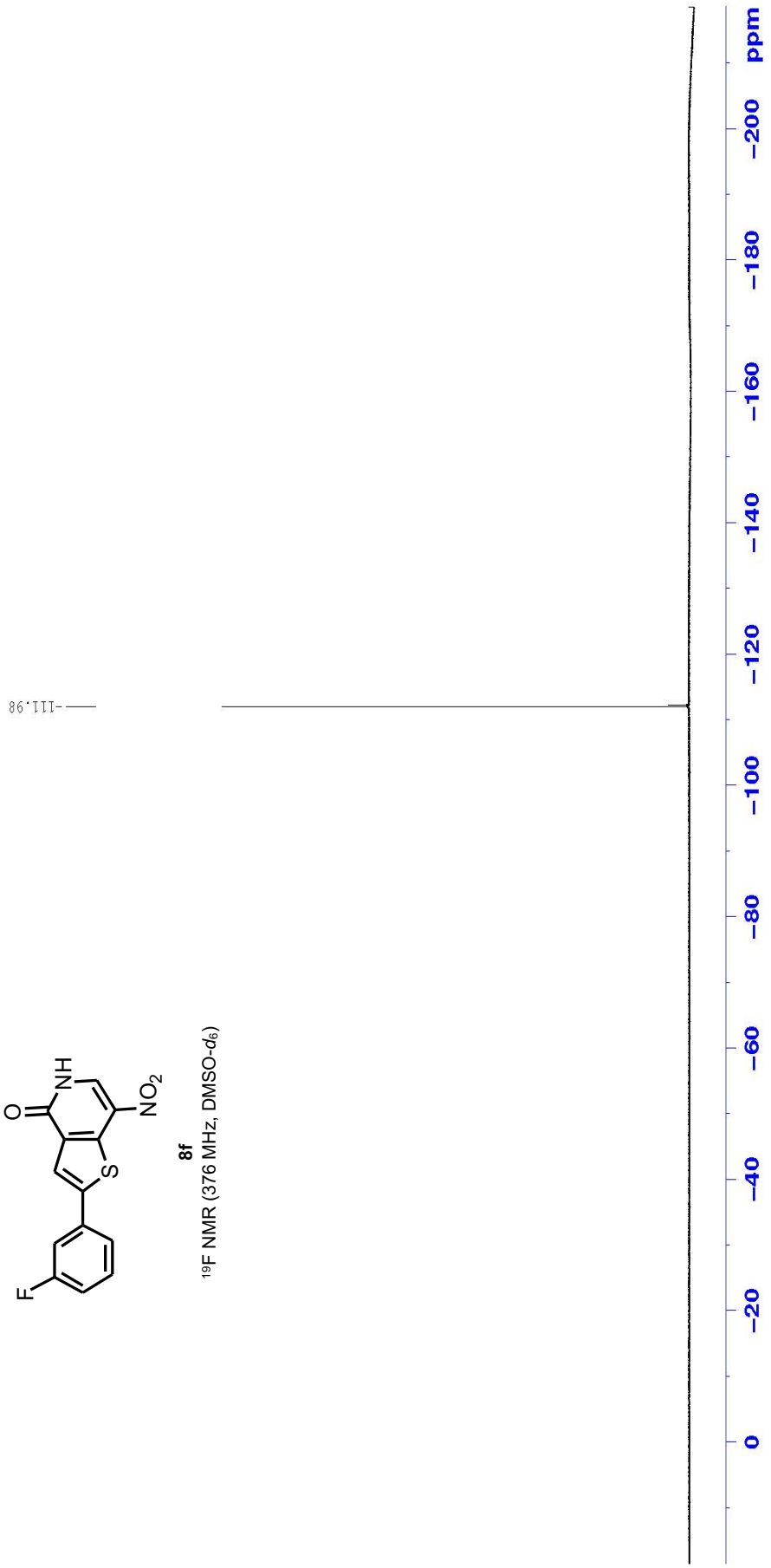

8f

^{19}F NMR (376 MHz, DMSO-d_6)

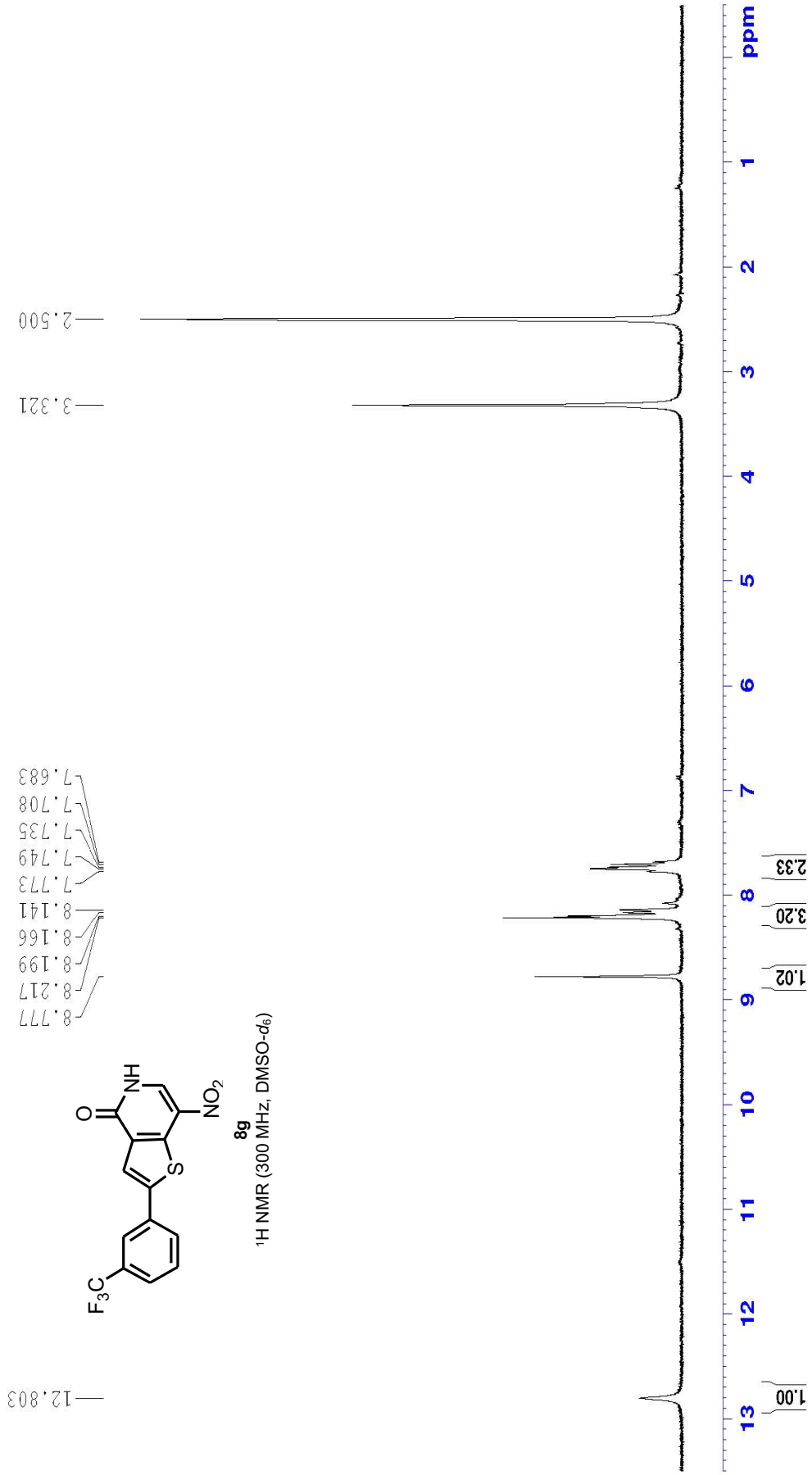

8g

^{1}H NMR (300 MHz, DMSO-d_6)

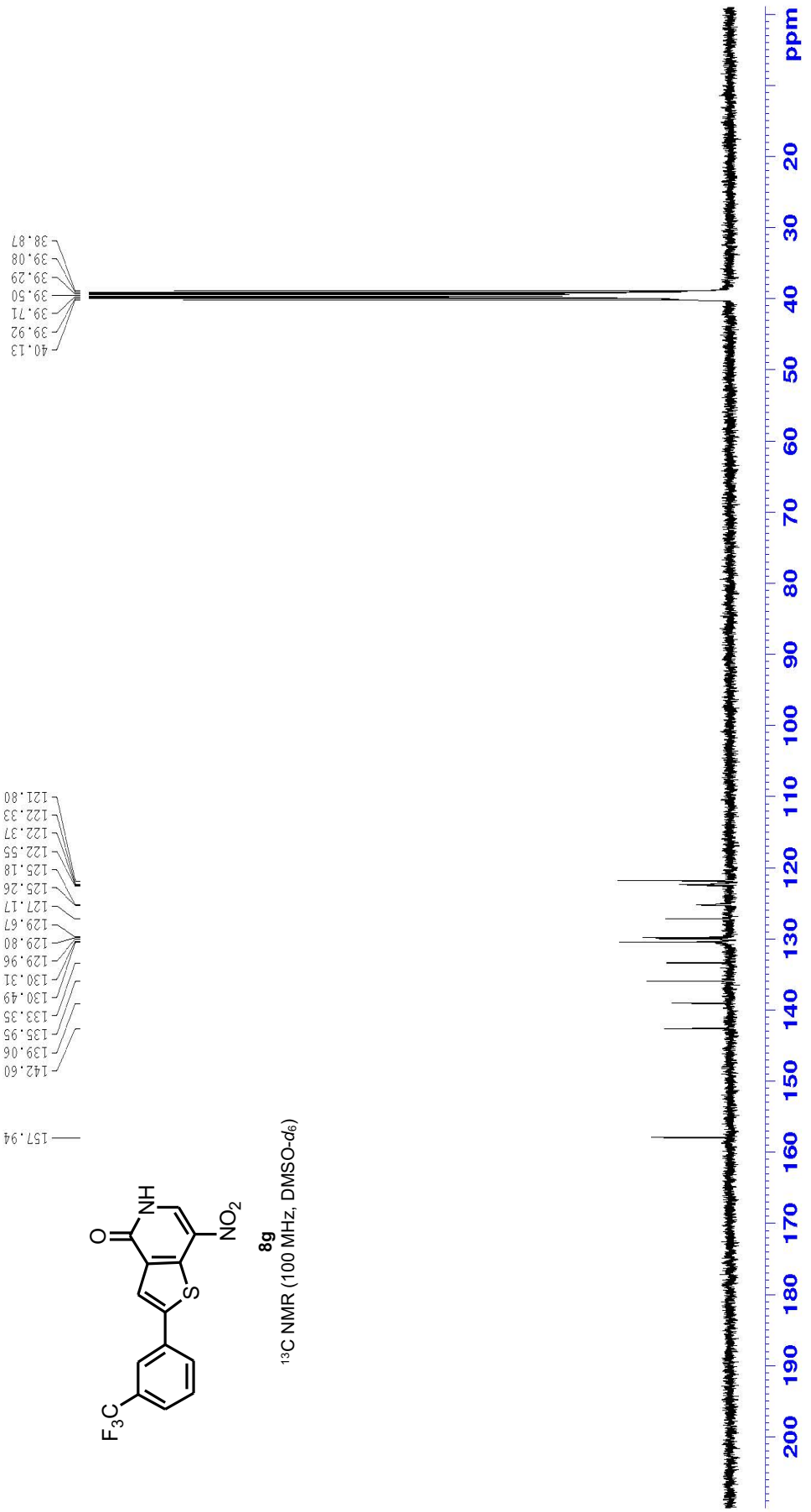

8g

^{13}C NMR (100 MHz, DMSO-d_6)

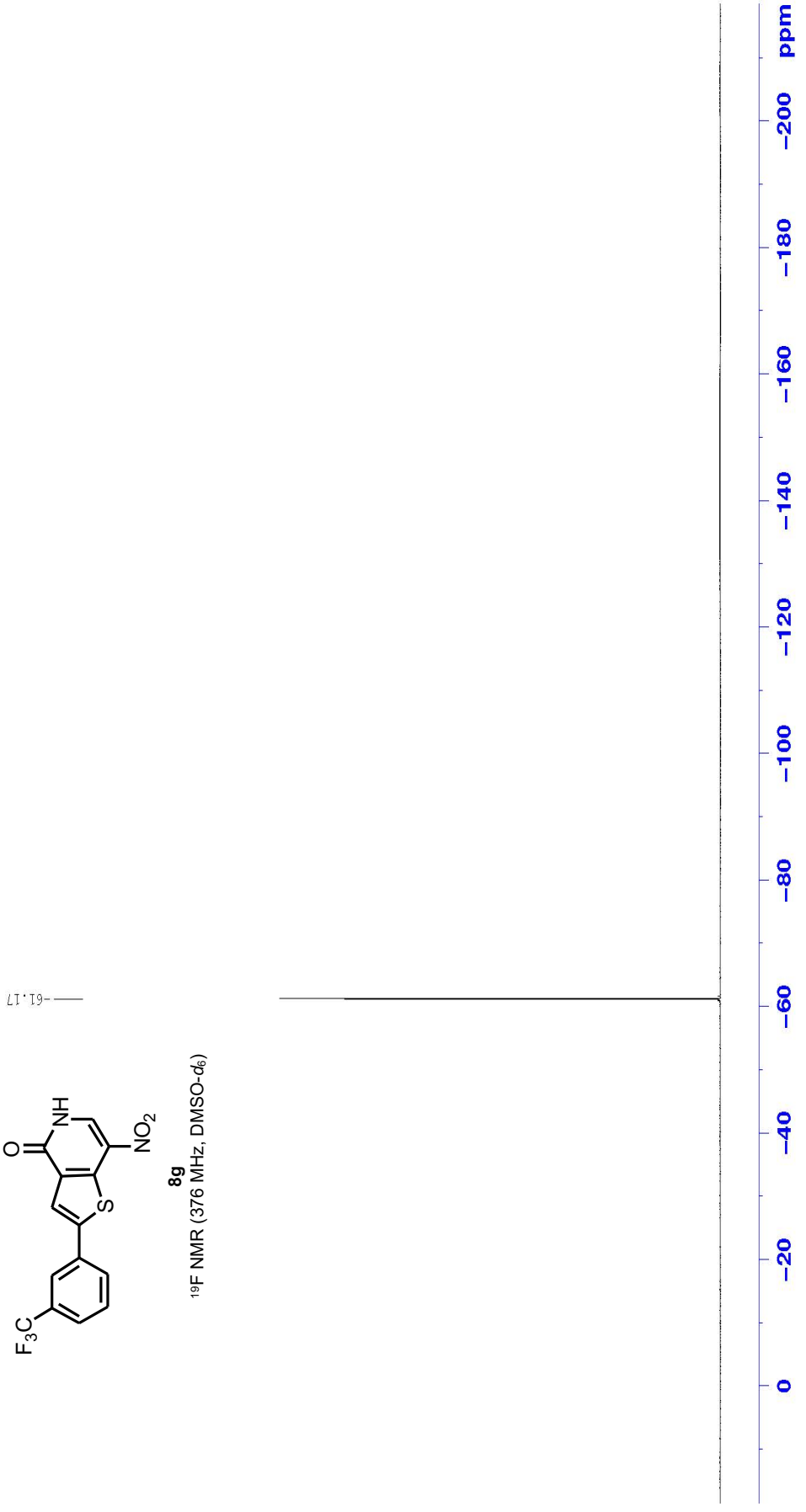

8g

^{19}F NMR (376 MHz, DMSO-d_6)

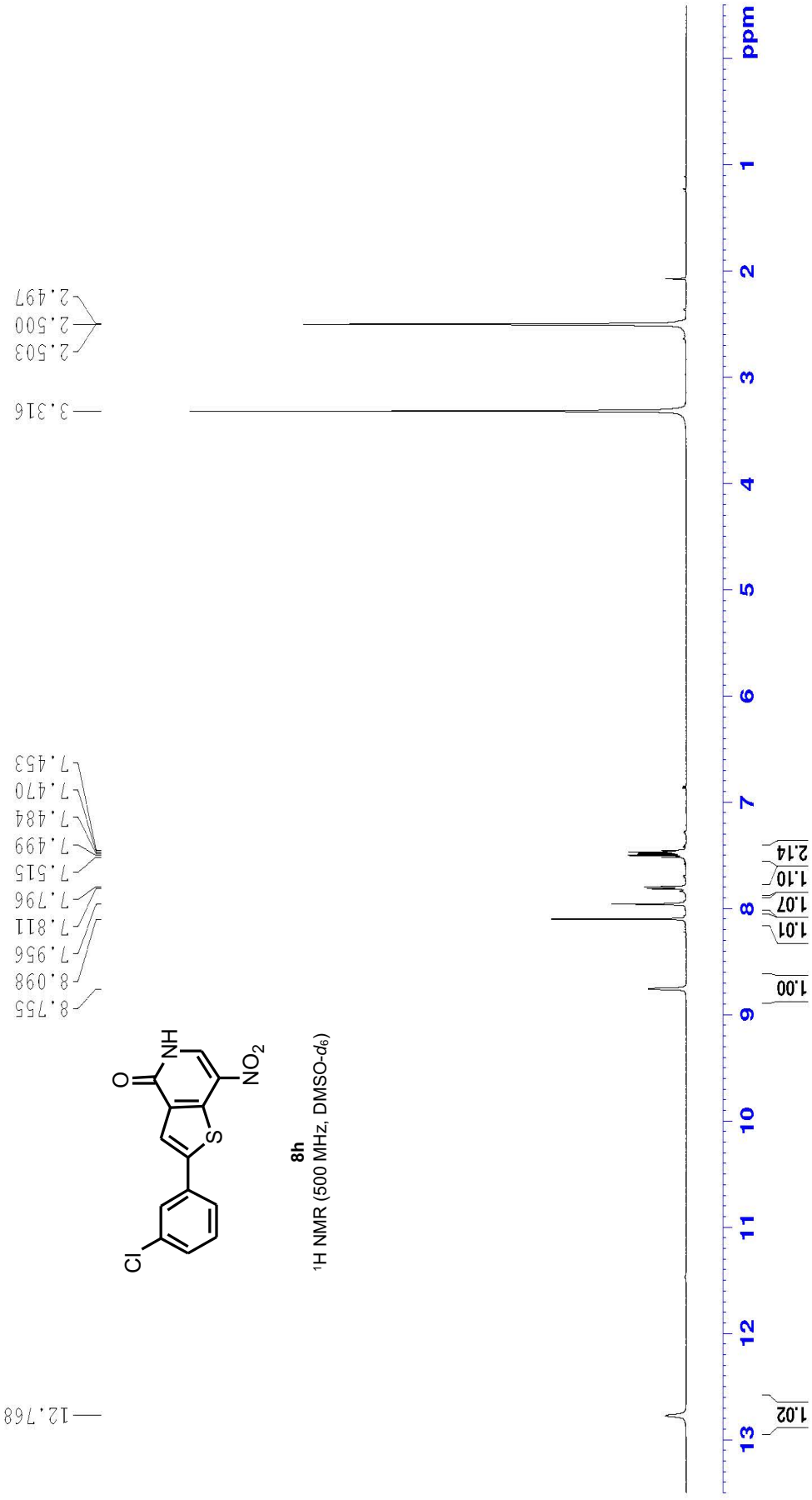

8h

^{1}H NMR (500 MHz, DMSO-d_6)

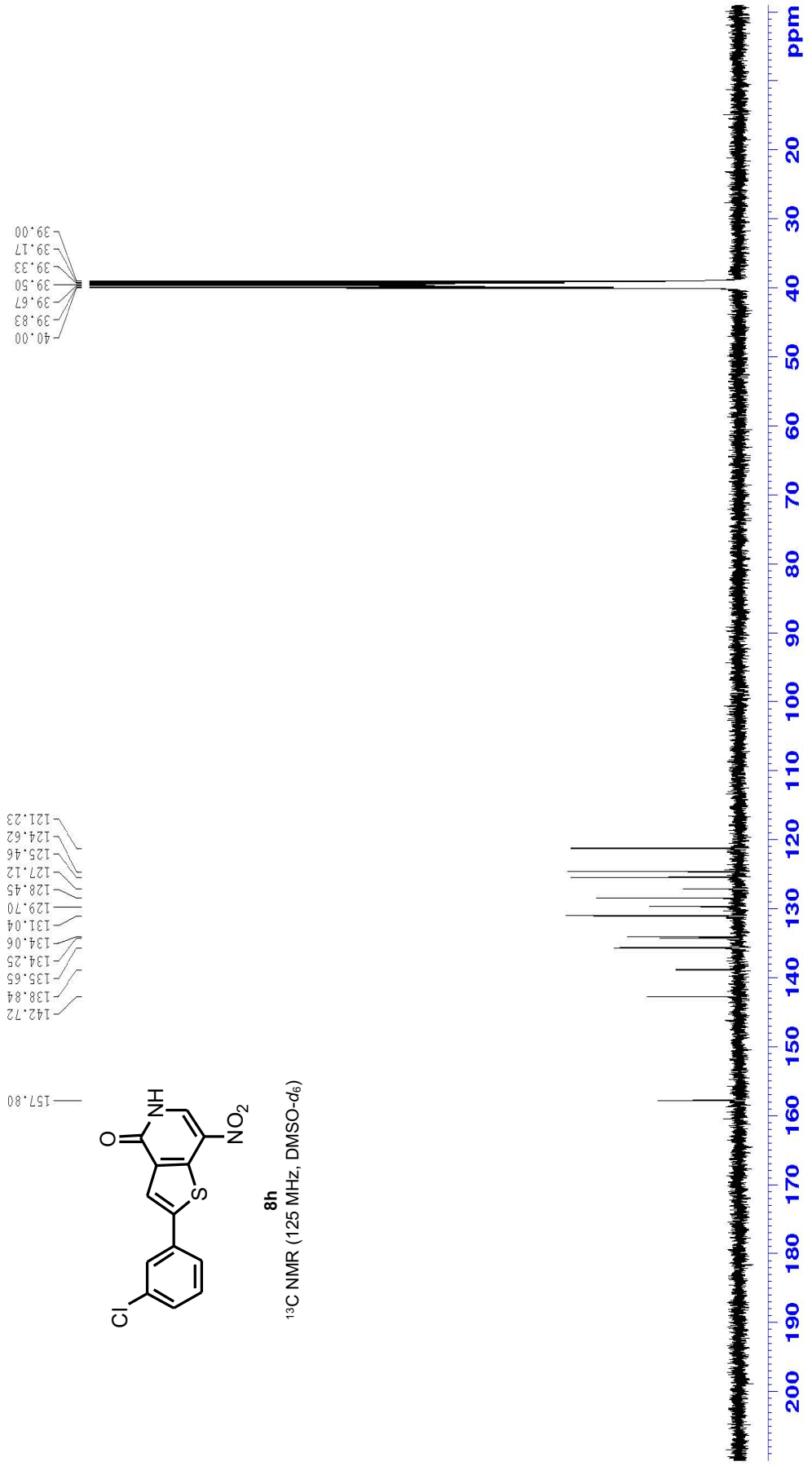

8h

^{13}C NMR (125 MHz, DMSO-d_6)

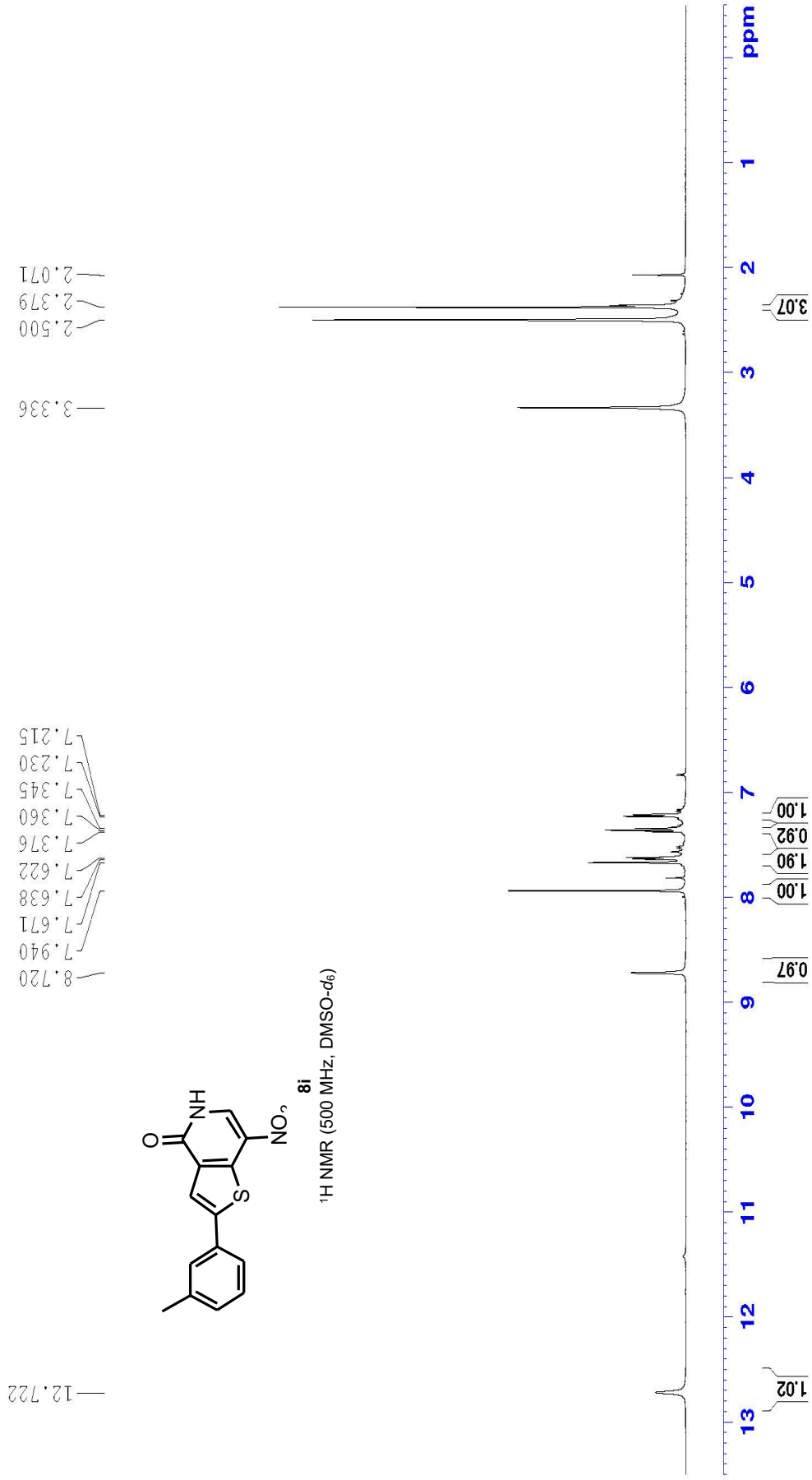

8i

^{1}H NMR (500 MHz, DMSO-d_6)

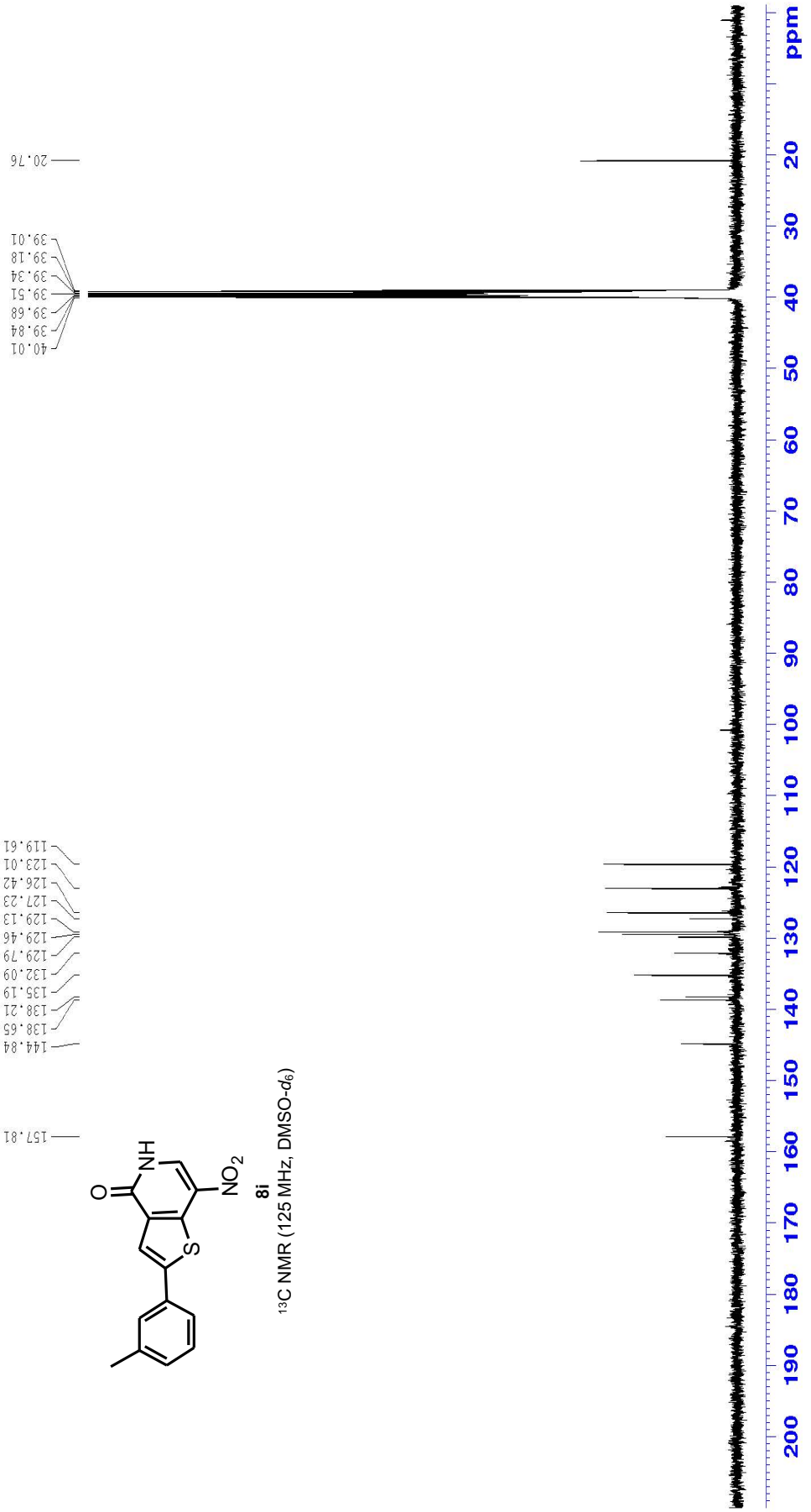

8i

^{13}C NMR (125 MHz, DMSO-d_6)

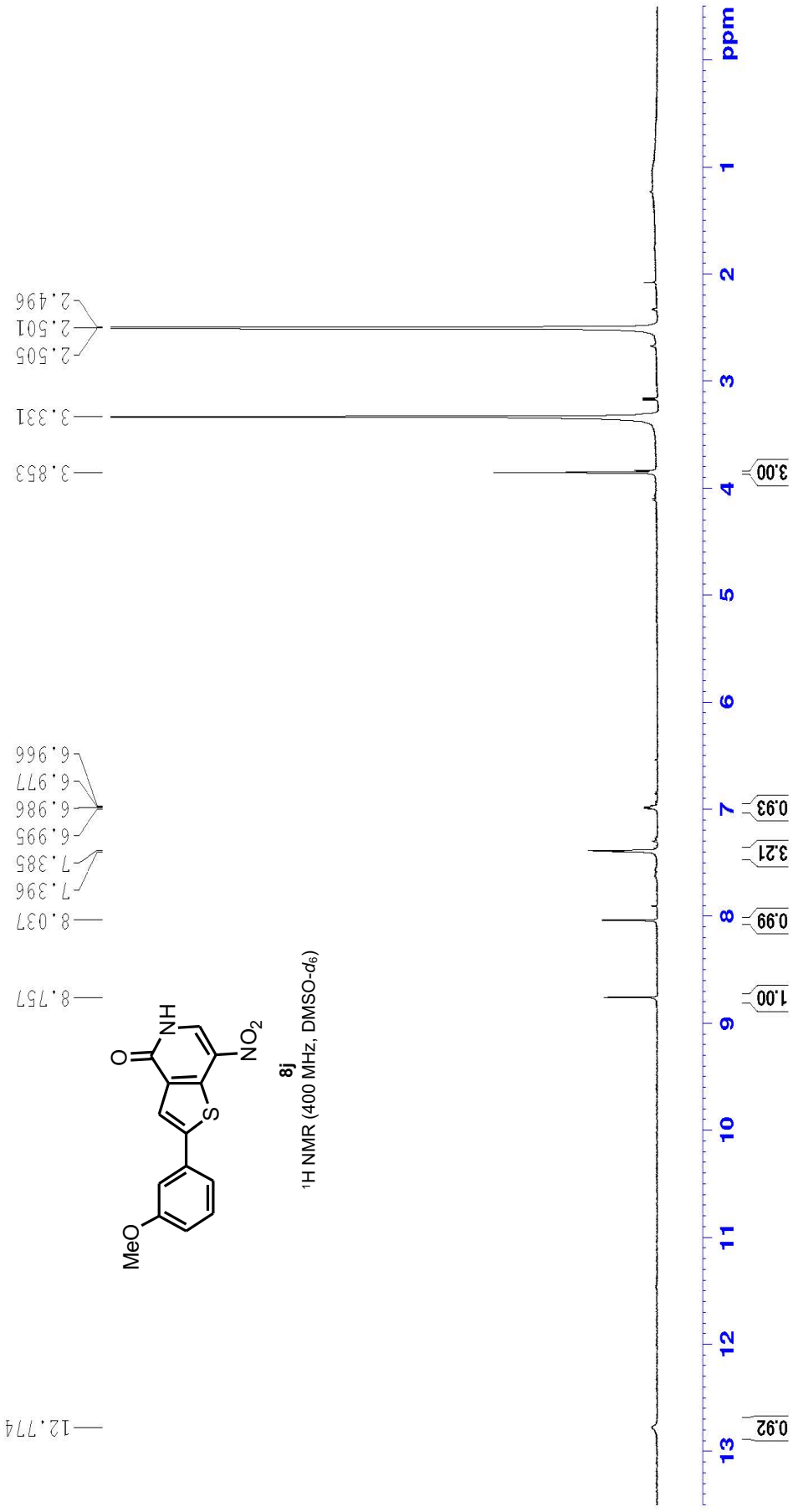

8j

^{1}H NMR (400 MHz, DMSO-d_6)

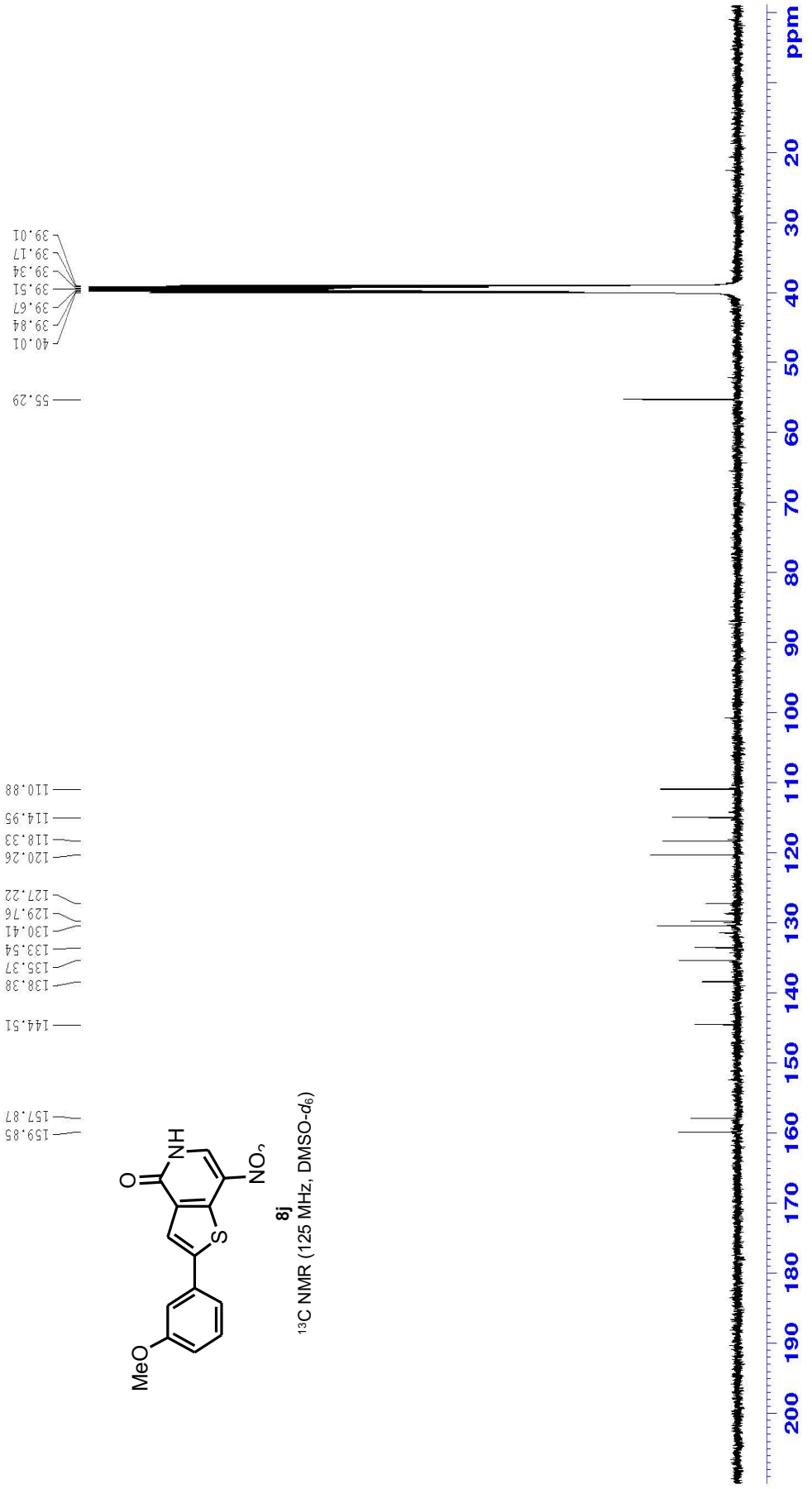

8j

^{13}C NMR (125 MHz, DMSO-d_6)

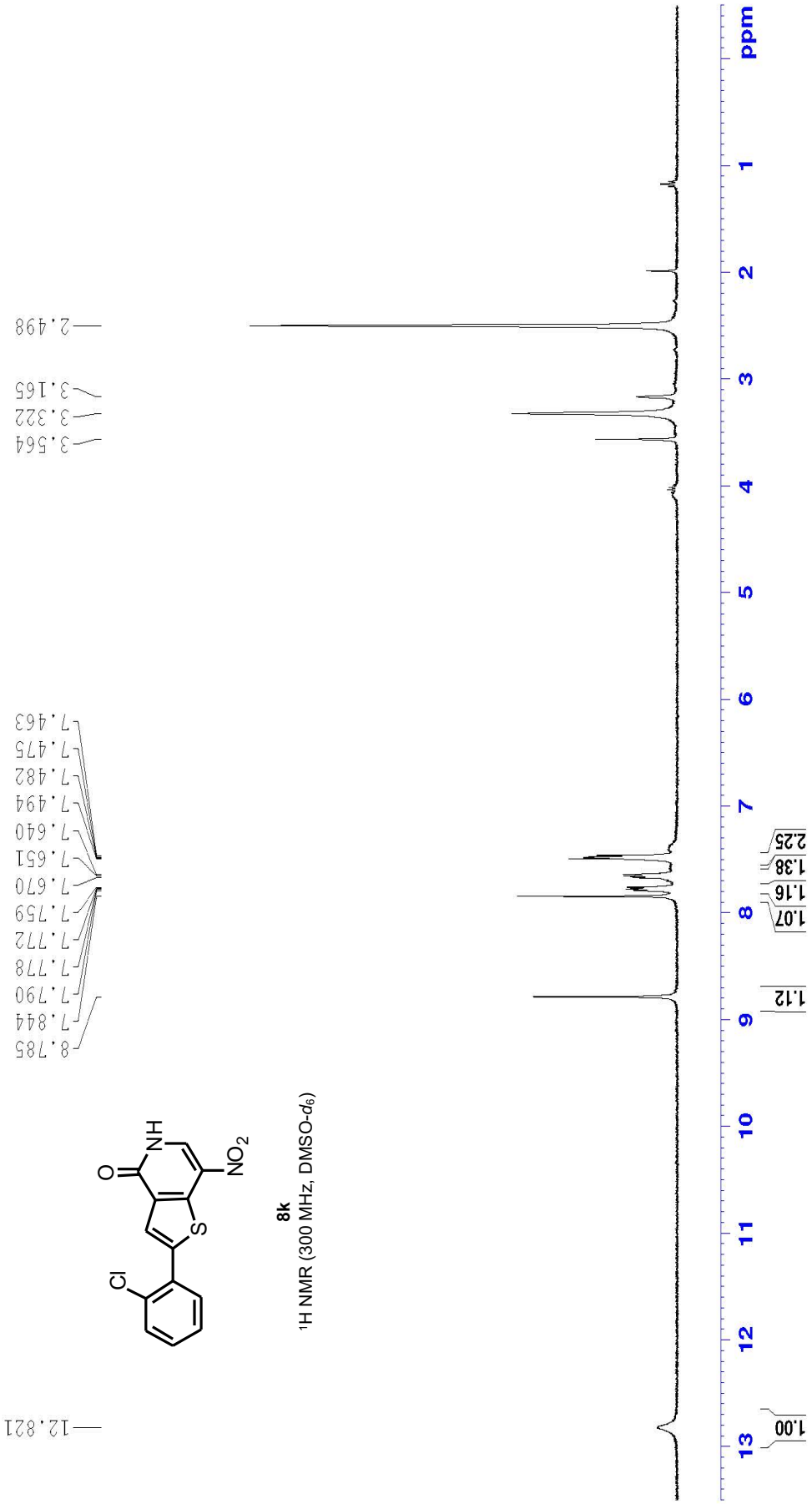
12.821
8.785
7.844
7.790
7.778
7.772
7.759
7.670
7.651
7.640
7.494
7.482
7.475
7.463
3.564
3.322
3.165
2.498
1.00
1.12
1.07
1.16
1.38
2.25
ppm
1 2 3 4 5 6 7 8 9 10 11 12 13
NH
O
NO2
S
Cl
8k
1H NMR (300 MHz, DMSO-d6)

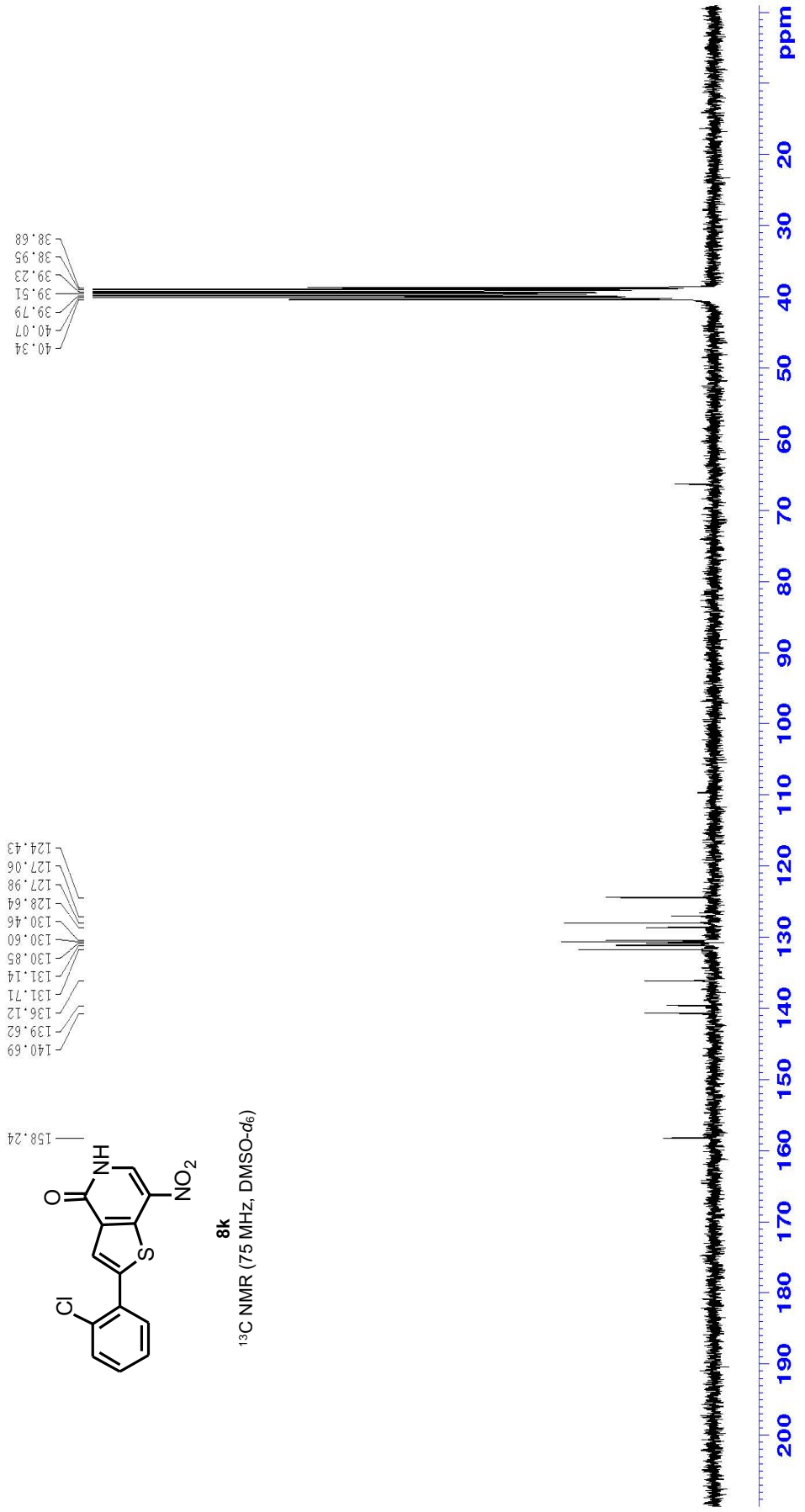

8k

^{13}C NMR (75 MHz, DMSO-d_6)

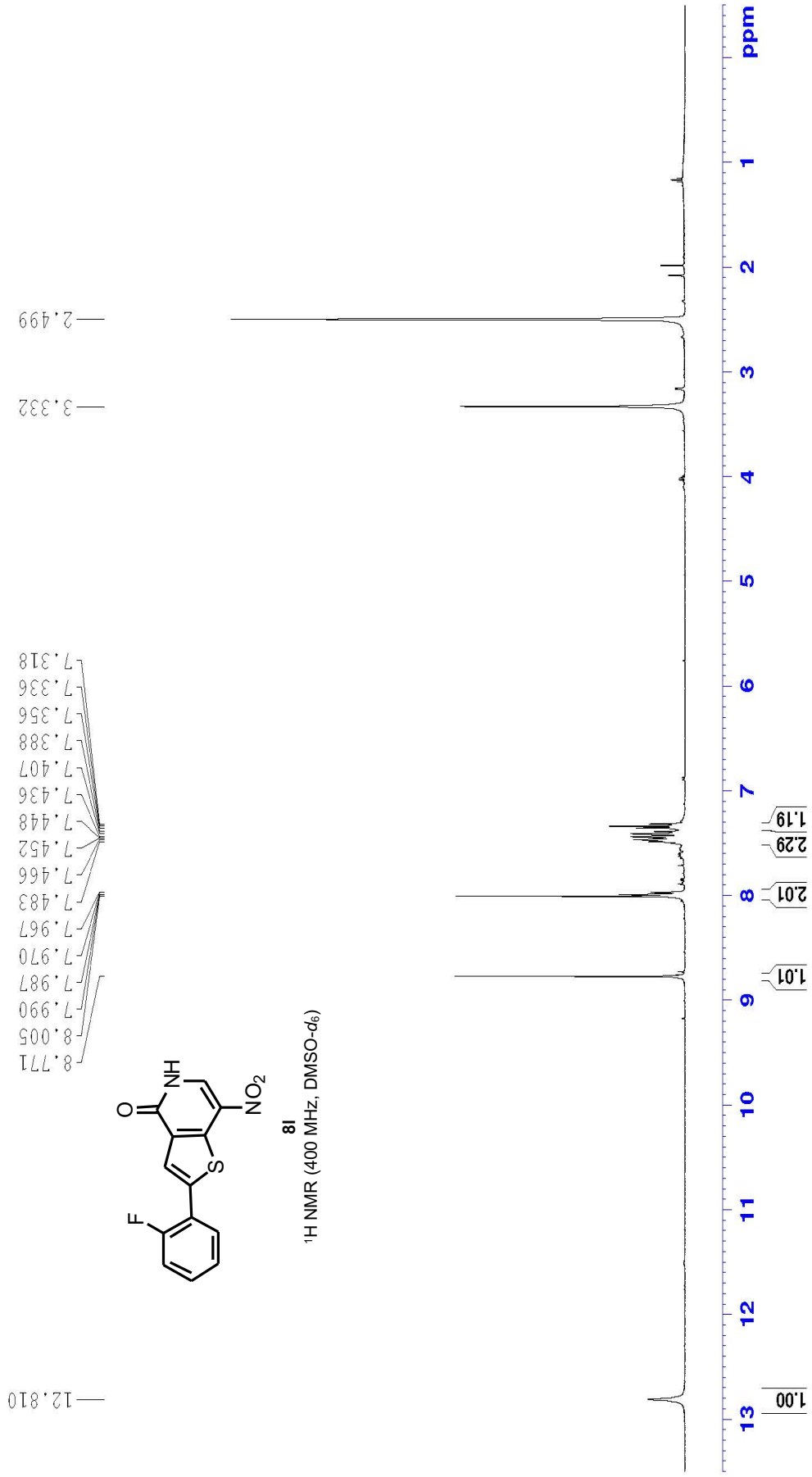

8l

^{1}H NMR (400 MHz, DMSO-d_6)

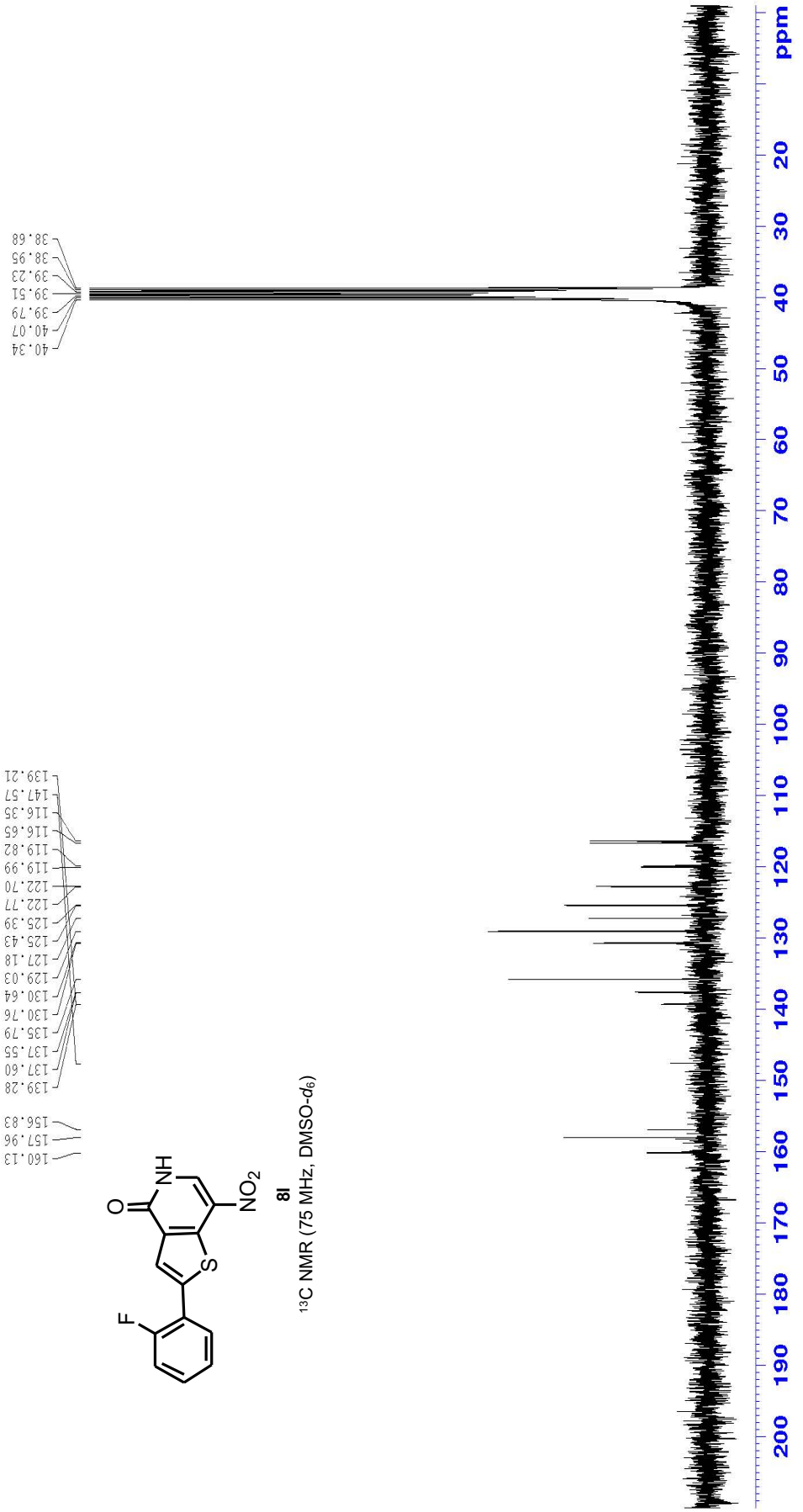
160.13
157.96
156.83
139.28
137.60
137.55
135.79
130.76
130.64
129.03
127.18
125.43
125.39
122.77
122.70
119.99
119.82
116.65
116.35
147.57
139.21
40.34
40.07
39.79
39.51
39.23
38.95
38.68
O
NH
NO2
S
F
8l
13C NMR (75 MHz, DMSO-d6)
ppm

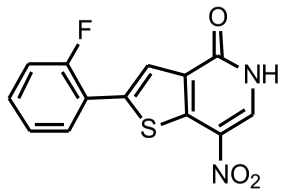

8l

^{19}F NMR (376 MHz, DMSO-d_6)

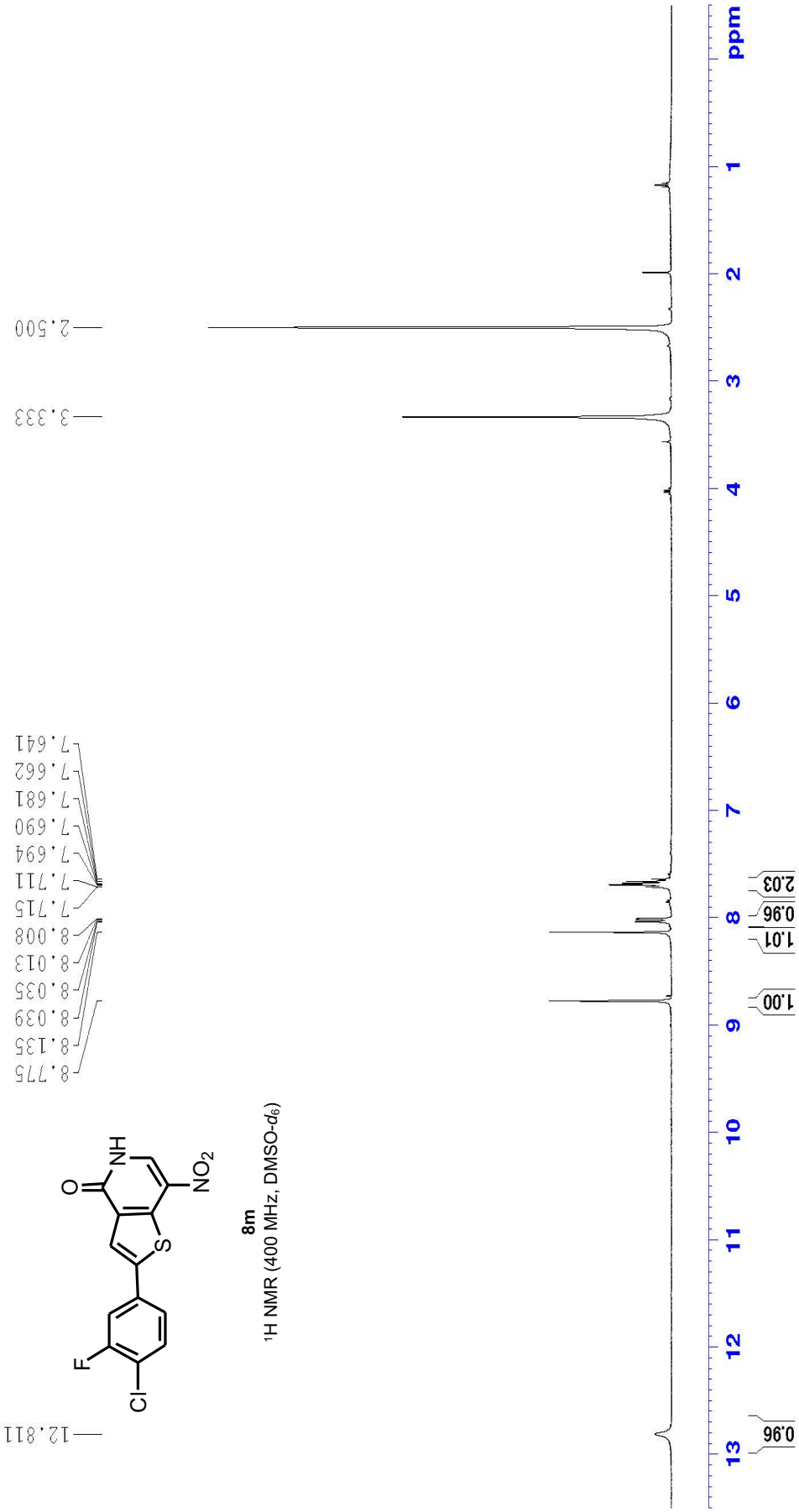
12.811
8.775
8.135
8.039
8.035
8.013
8.008
7.715
7.711
7.694
7.690
7.681
7.662
7.641
3.333
2.500
0.96
1.00
1.01
0.96
2.03
ppm
1 2 3 4 5 6 7 8 9 10 11 12 13
O
NH
NO2
S
F
Cl
8m
1H NMR (400 MHz, DMSO-d6)

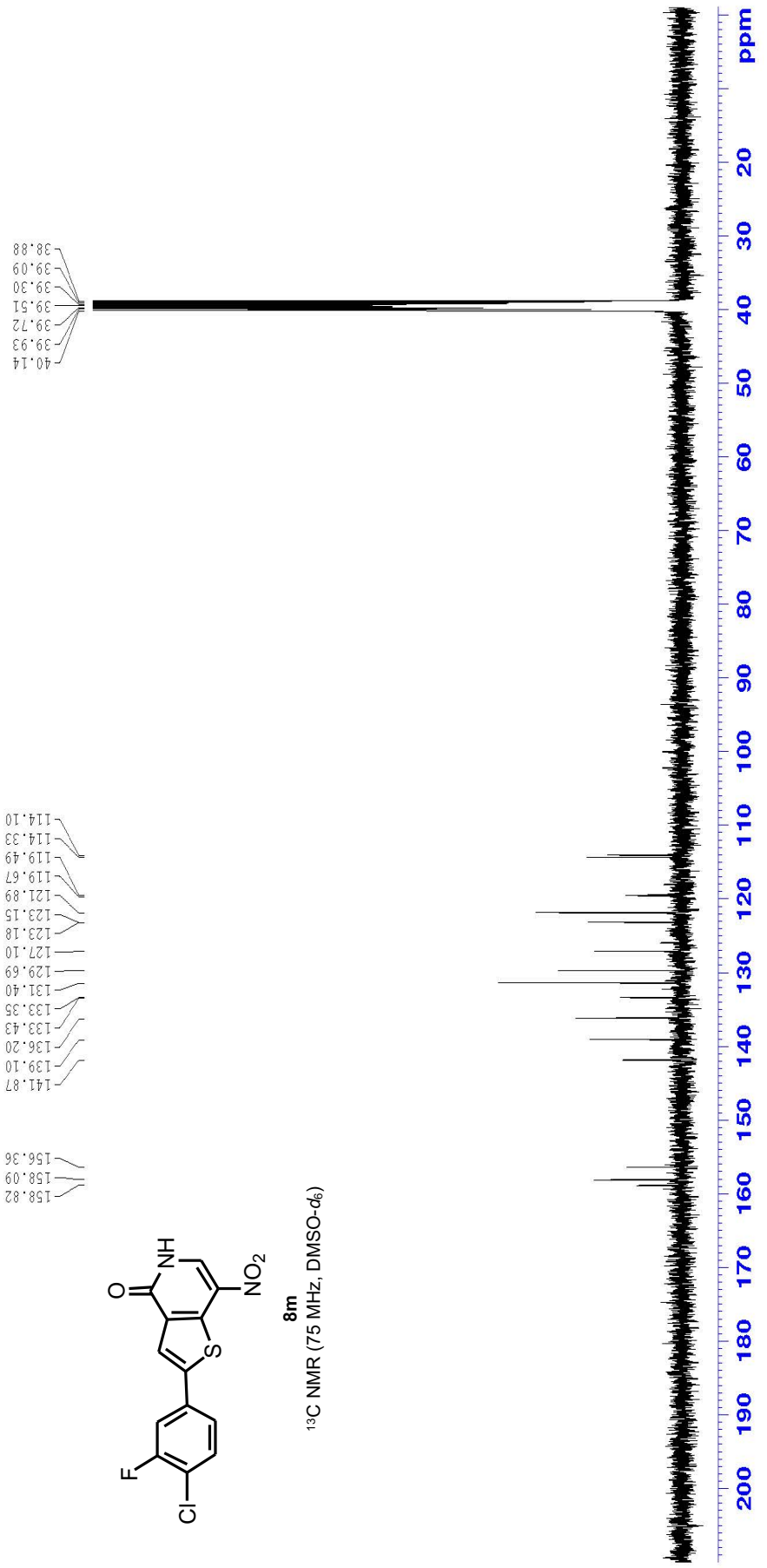
158.82
158.09
156.36
141.87
139.10
136.20
133.43
133.35
131.40
129.69
127.10
123.18
123.15
121.89
119.67
119.49
114.33
114.10
40.14
39.93
39.72
39.51
39.30
39.09
38.88
O
NH
NO2
S
F
Cl
8m
13C NMR (75 MHz, DMSO-d6)
ppm

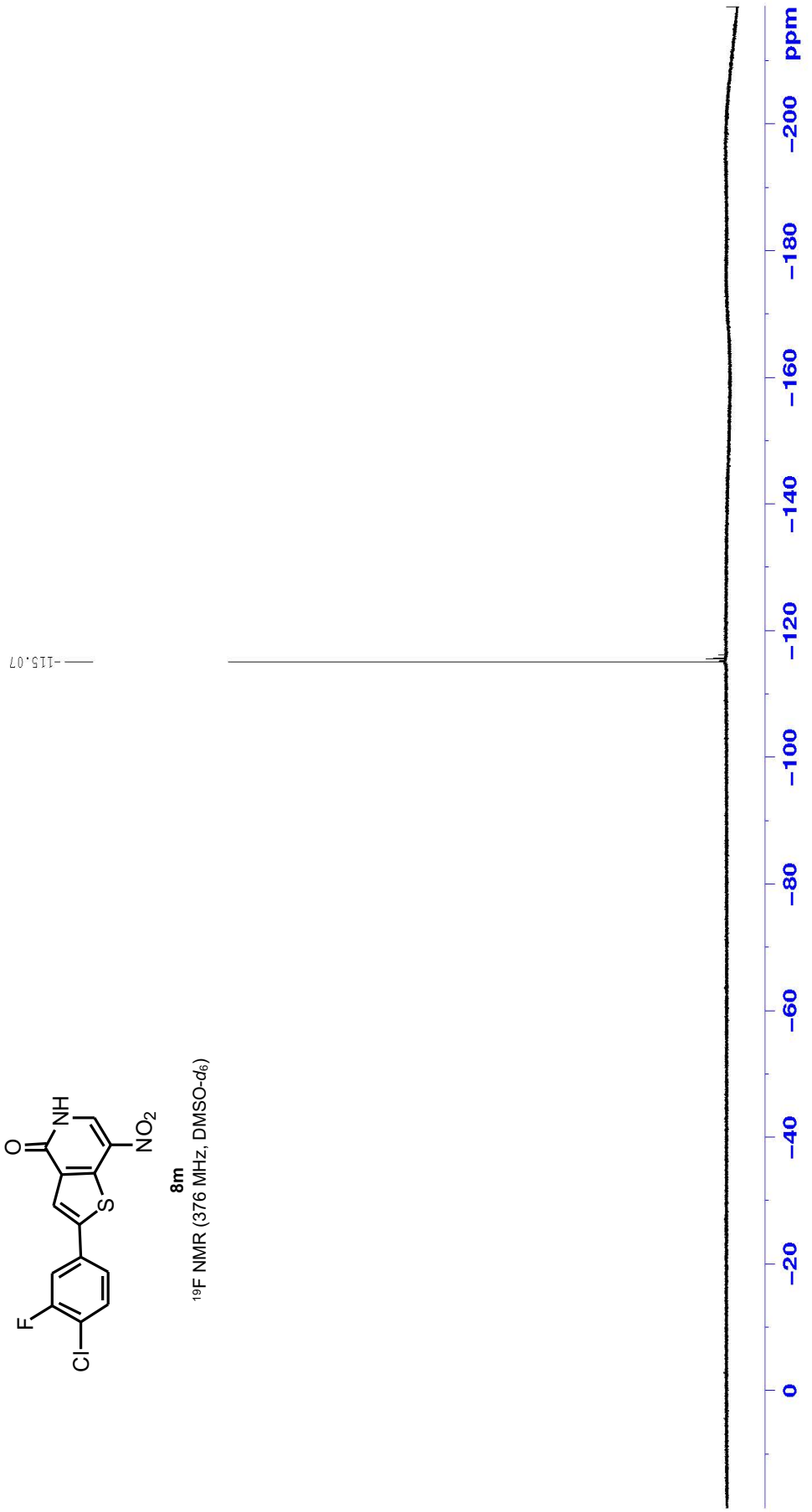

8m

^{19}F NMR (376 MHz, DMSO-d_6)

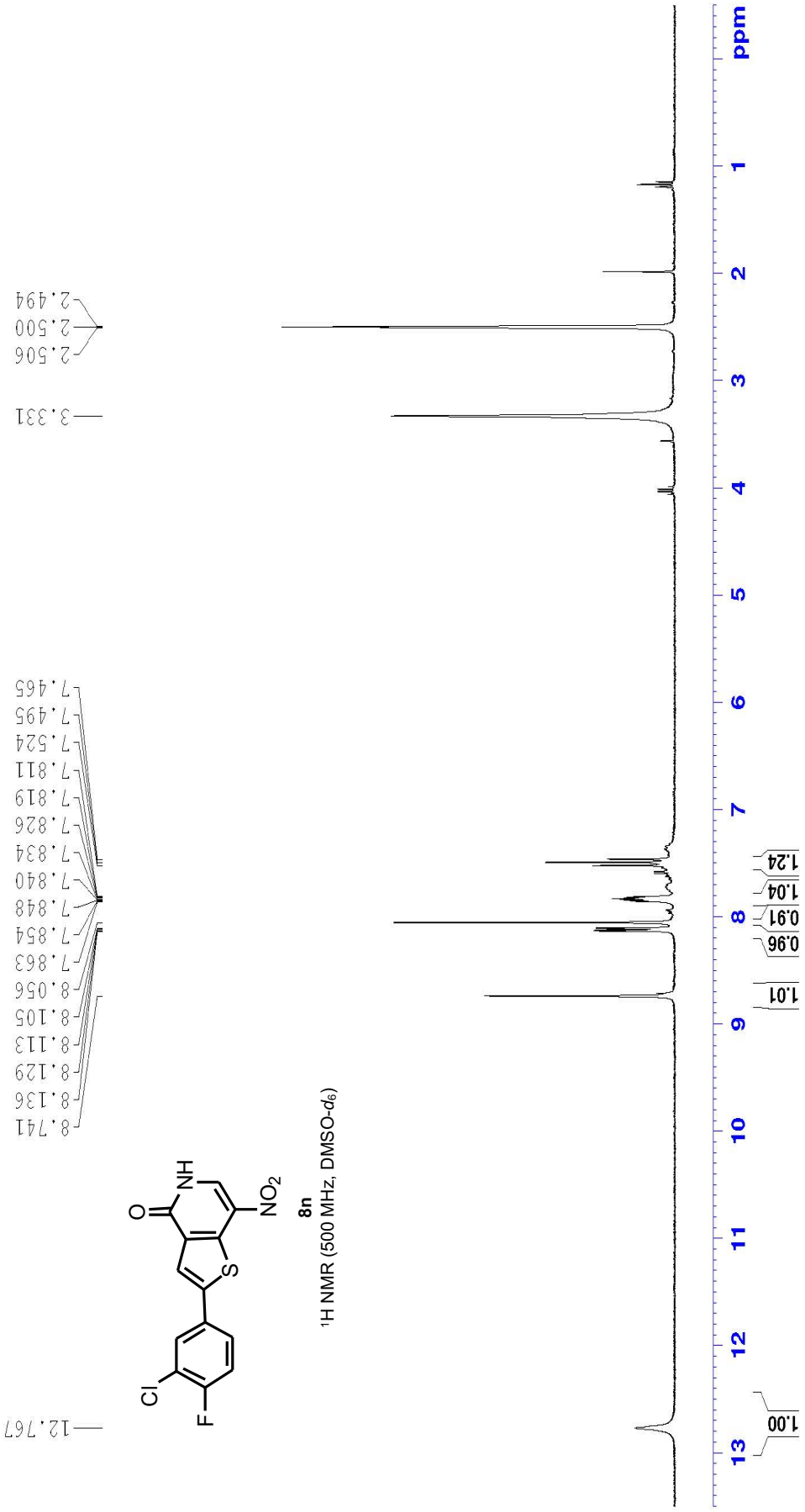

8n

^{1}H NMR (500 MHz, DMSO-d_6)

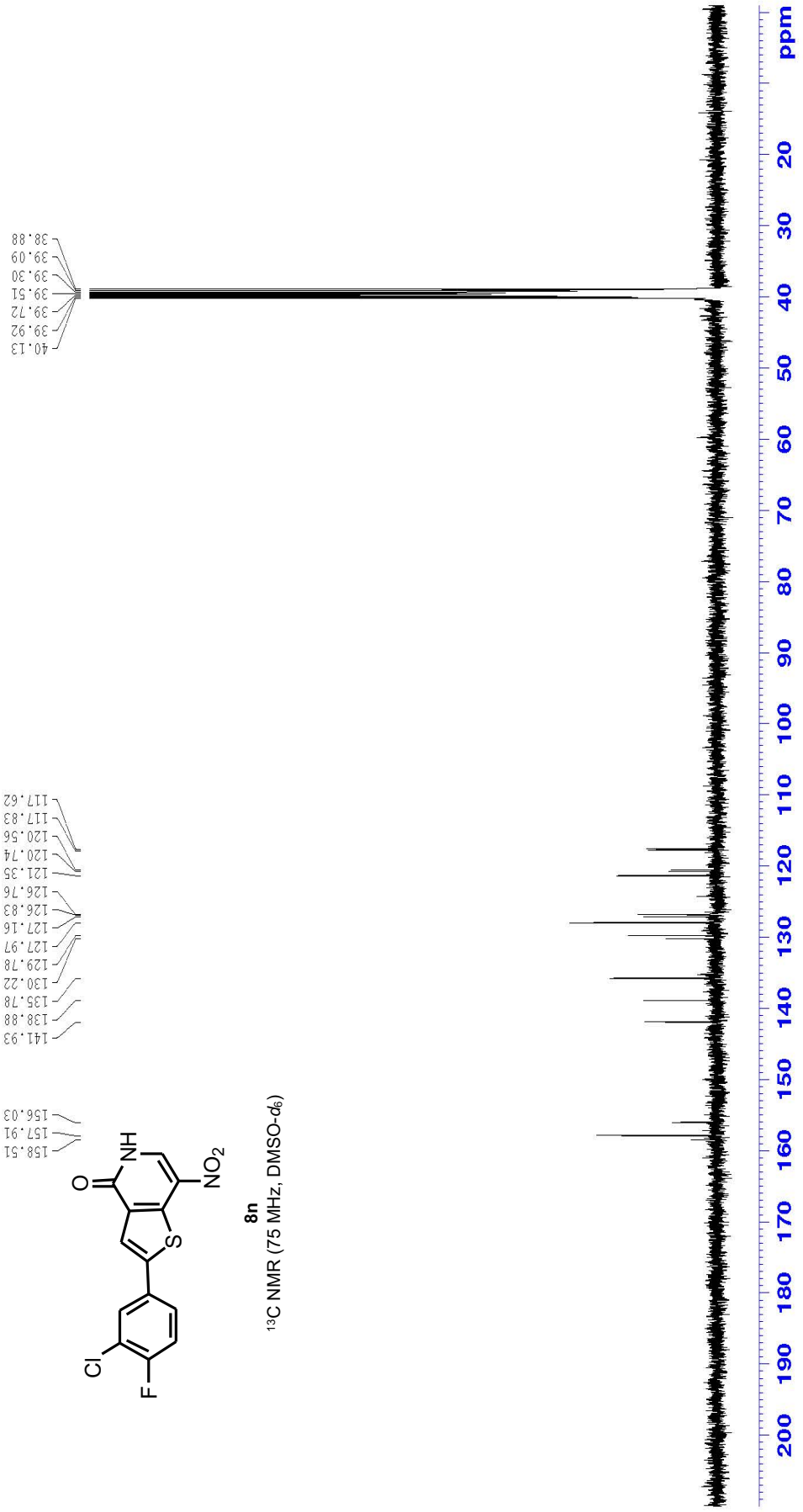
158.51
157.91
156.03
141.93
138.88
135.78
130.22
129.78
127.97
127.16
126.83
126.76
121.35
120.74
120.56
117.83
117.62
40.13
39.92
39.72
39.51
39.30
39.09
38.88
O
NH
NO2
S
Cl
F
8n
13C NMR (75 MHz, DMSO-d6)
ppm
200
190
180
170
160
150
140
130
120
110
100
90
80
70
60
50
40
30
20

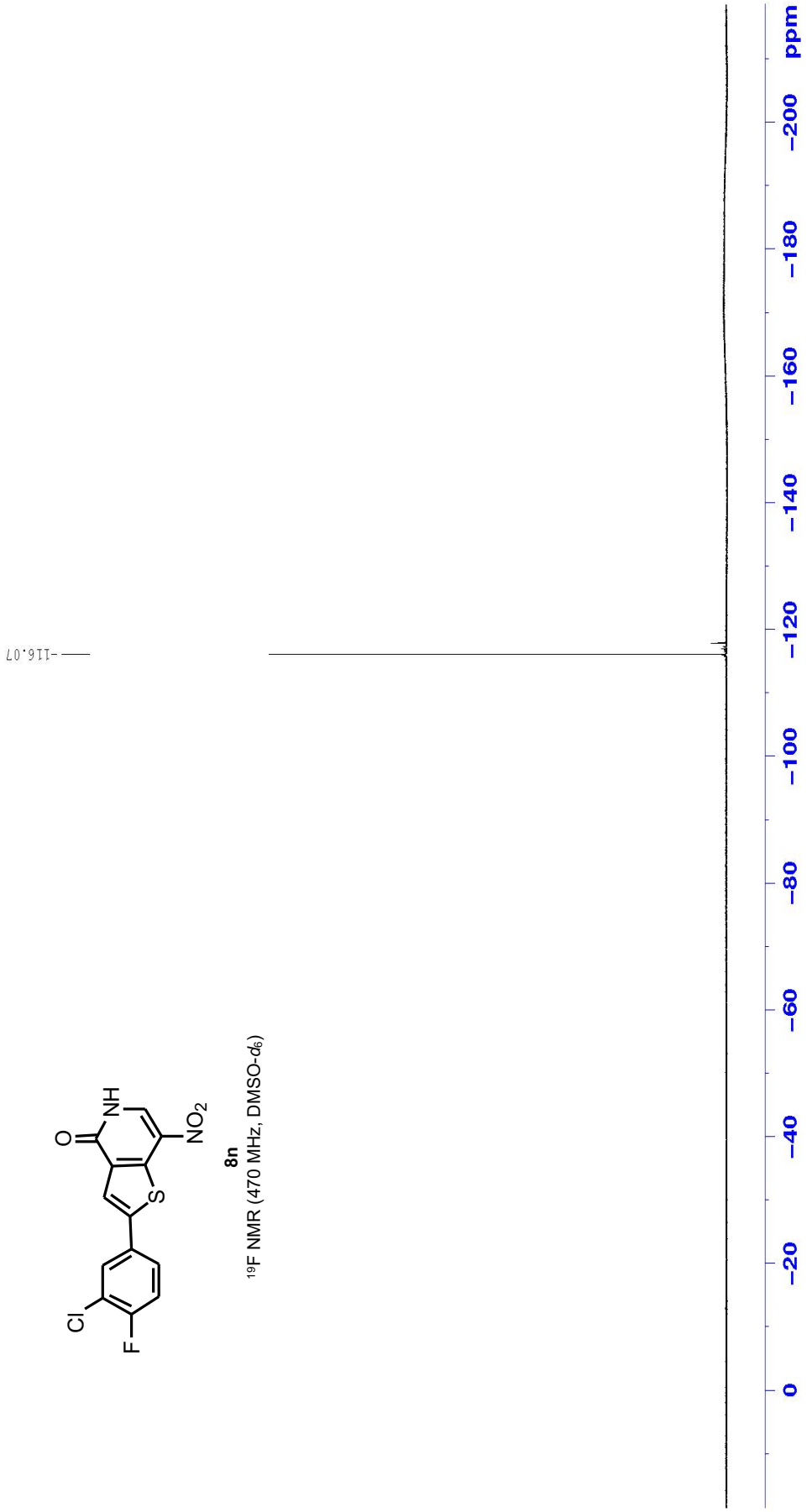

8n

^{19}F NMR (470 MHz, DMSO-d_6)

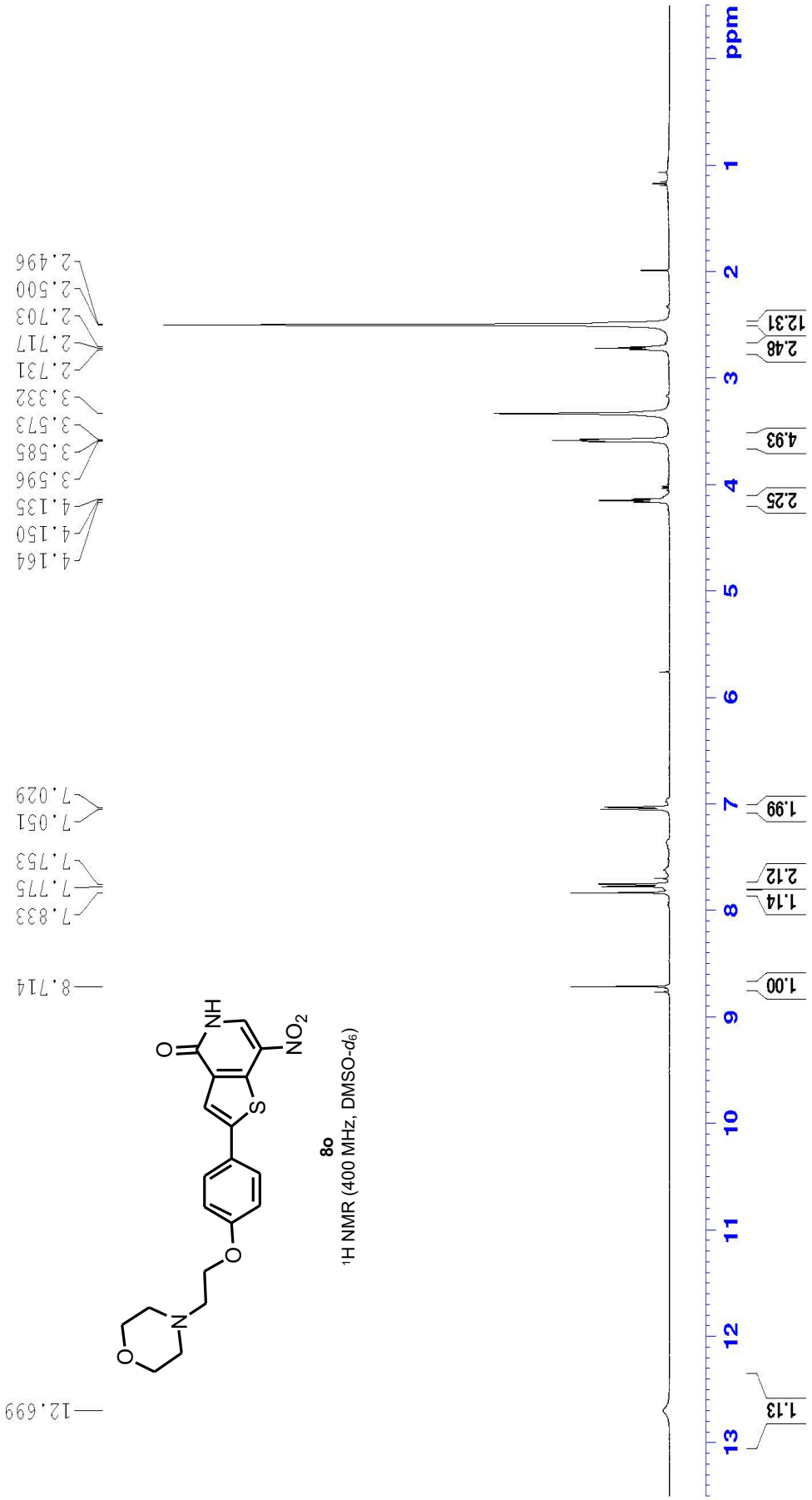
12.699
8.714
7.833
7.775
7.753
7.051
7.029
4.164
4.150
4.135
3.596
3.585
3.573
3.332
2.731
2.717
2.703
2.500
2.496
1.13
1.00
1.99
1.14
2.12
2.25
4.93
2.48
12.31
ppm
1 2 3 4 5 6 7 8 9 10 11 12 13
O
NH
NO2
S
O
N
O
8o
1H NMR (400 MHz, DMSO-d6)

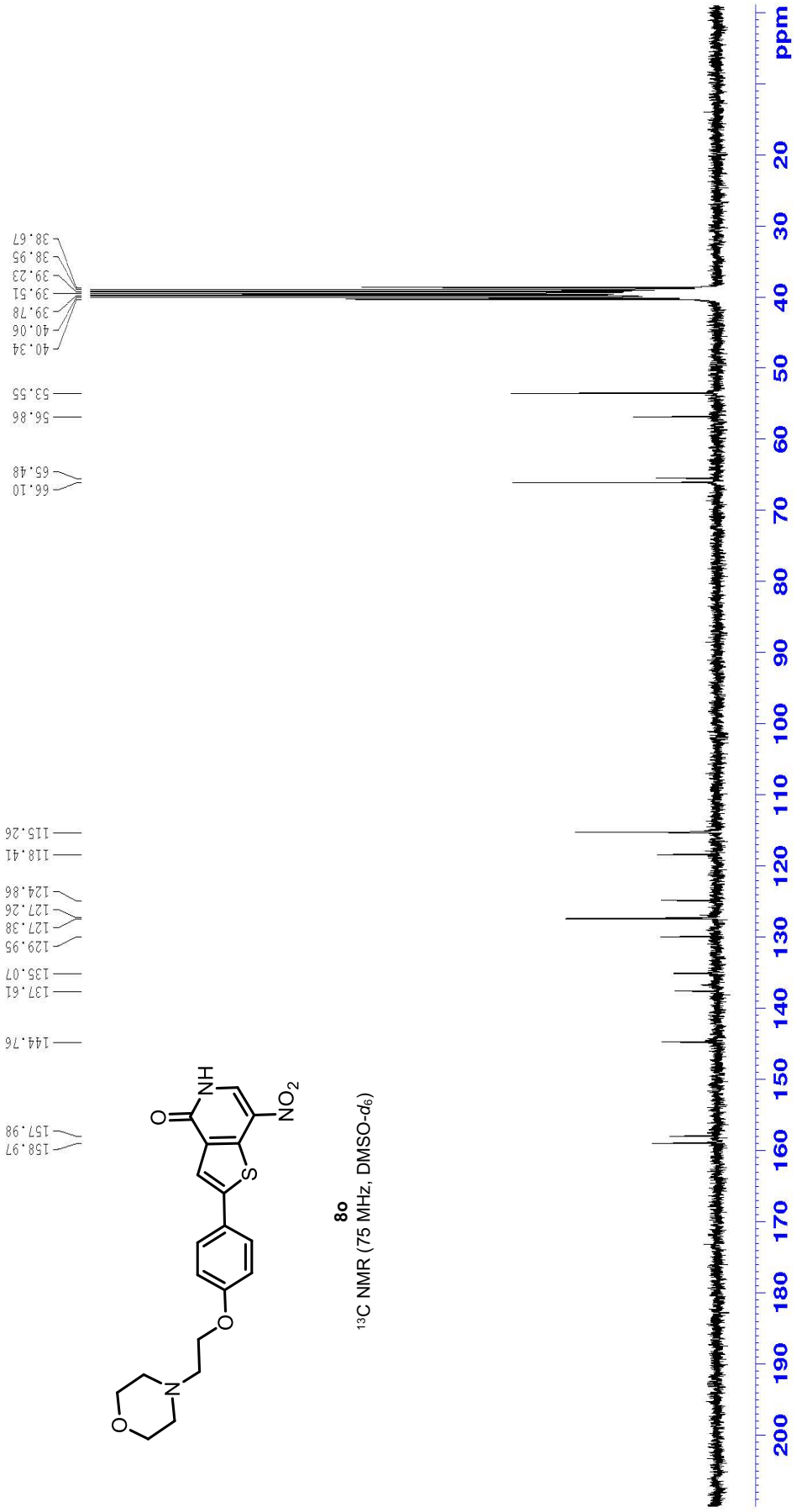

8o

^{13}C NMR (75 MHz, DMSO-d_6)

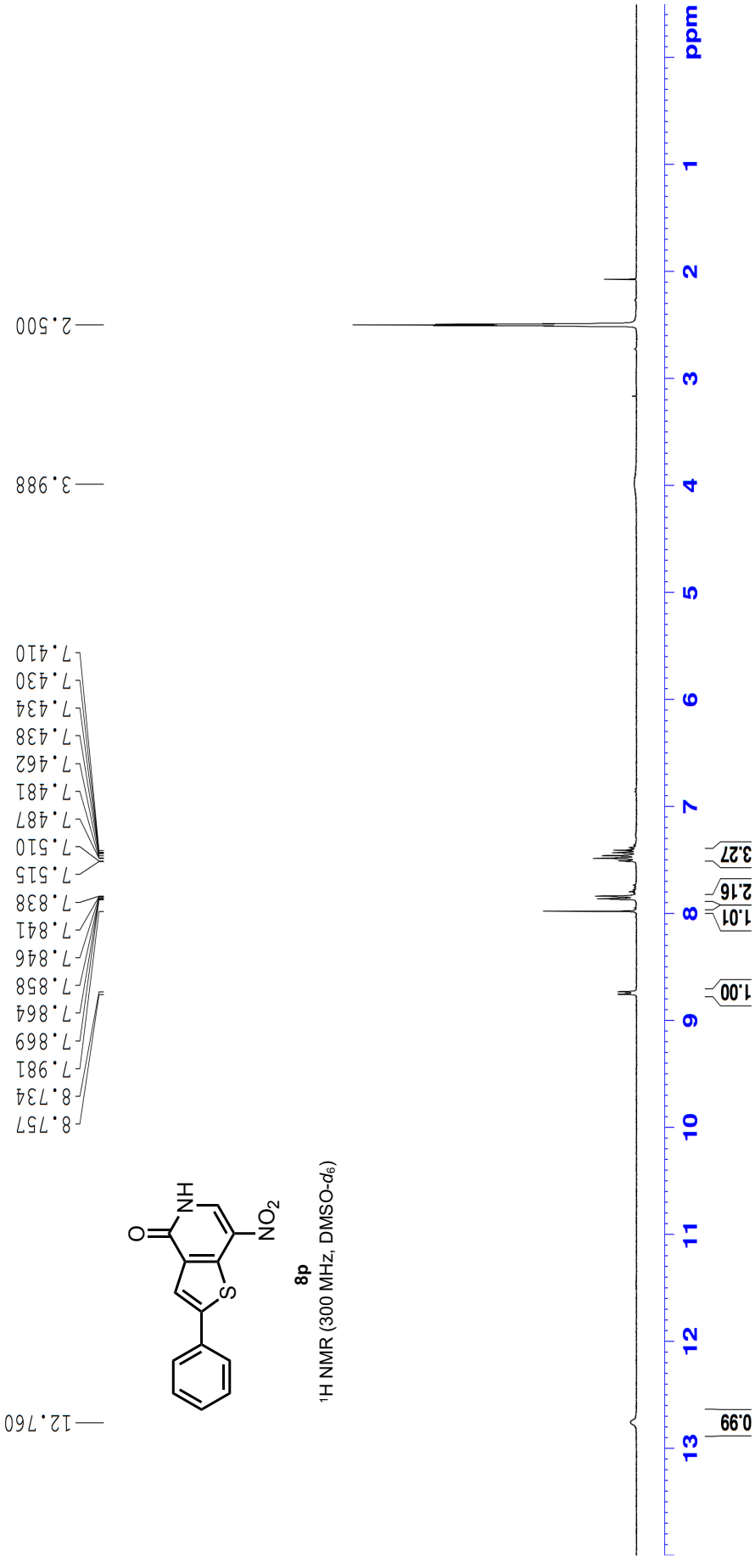

8p

^{1}H NMR (300 MHz, DMSO-d_6)

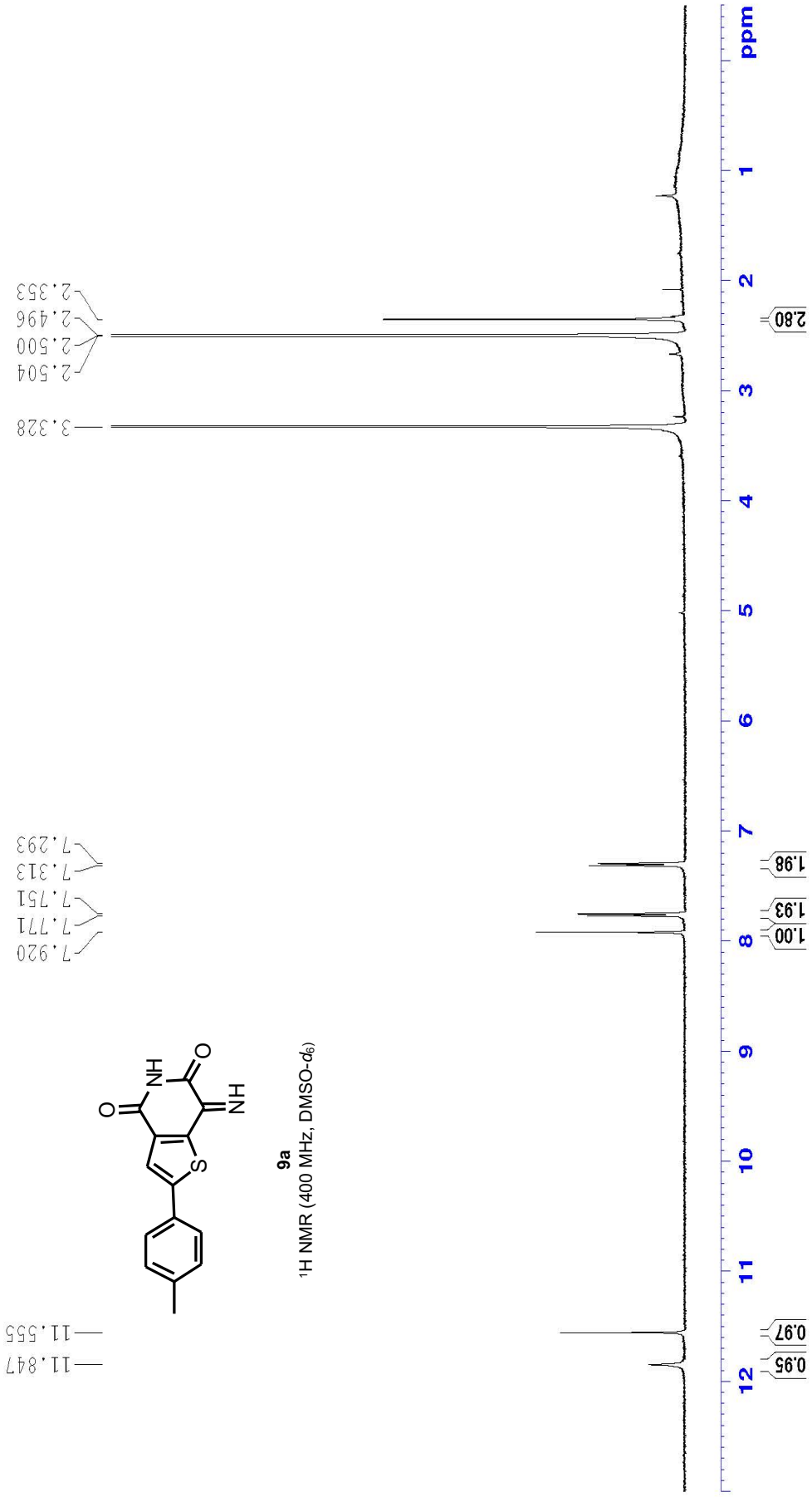

9a

^{1}H NMR (400 MHz, DMSO-d_6)

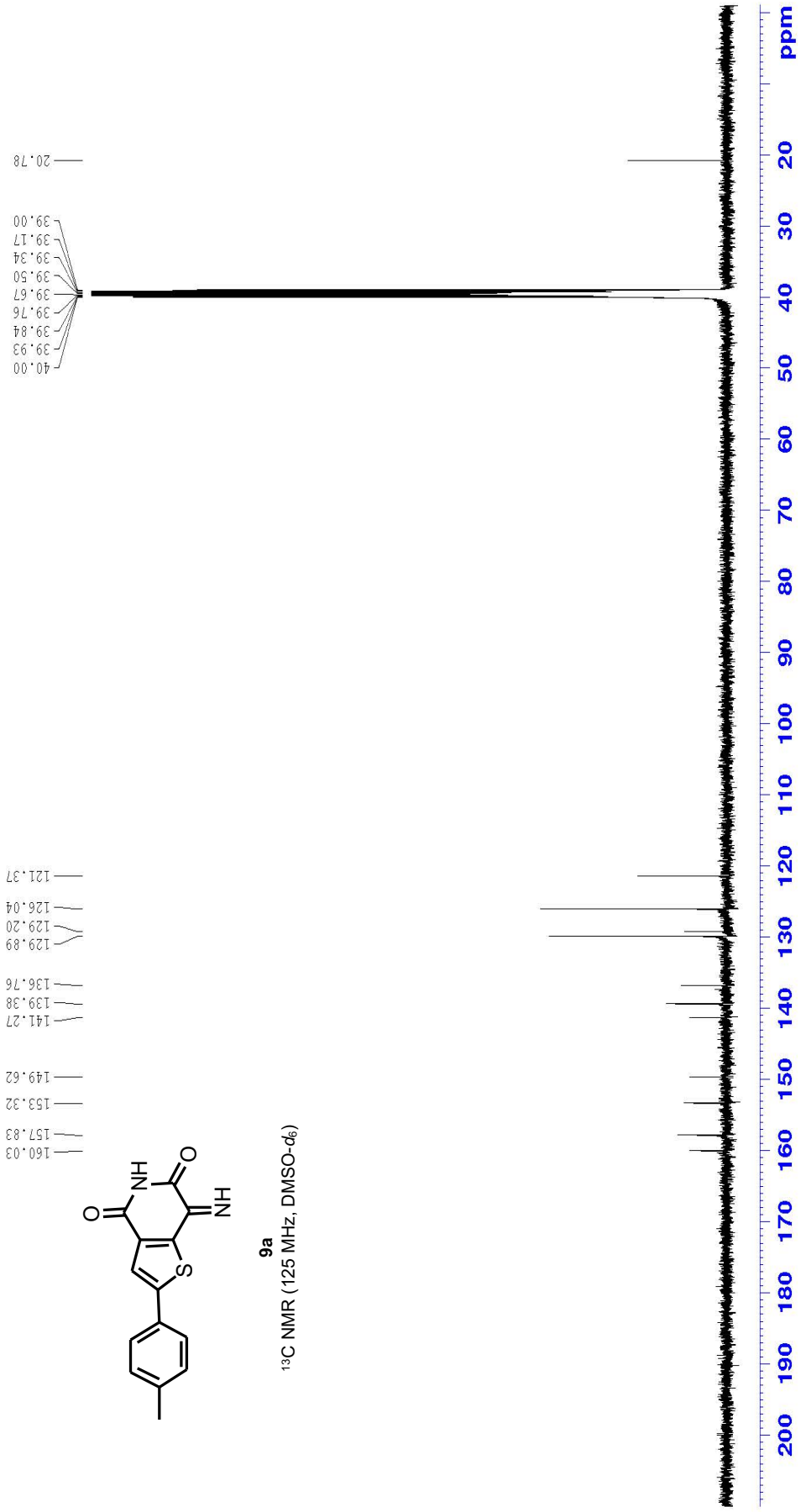

9a

^{13}C NMR (125 MHz, DMSO-d_6)

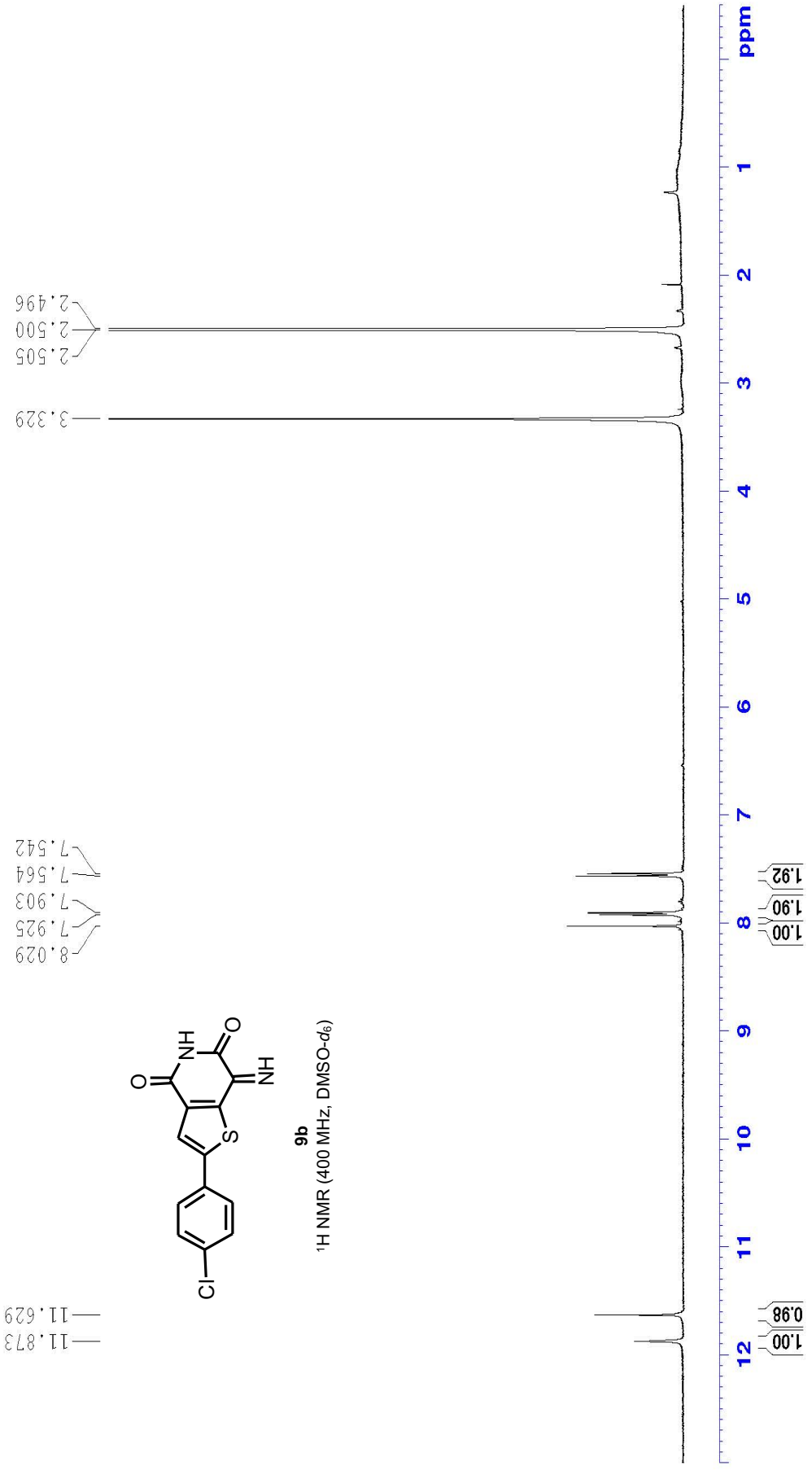

9b

^{1}H NMR (400 MHz, DMSO-d_6)

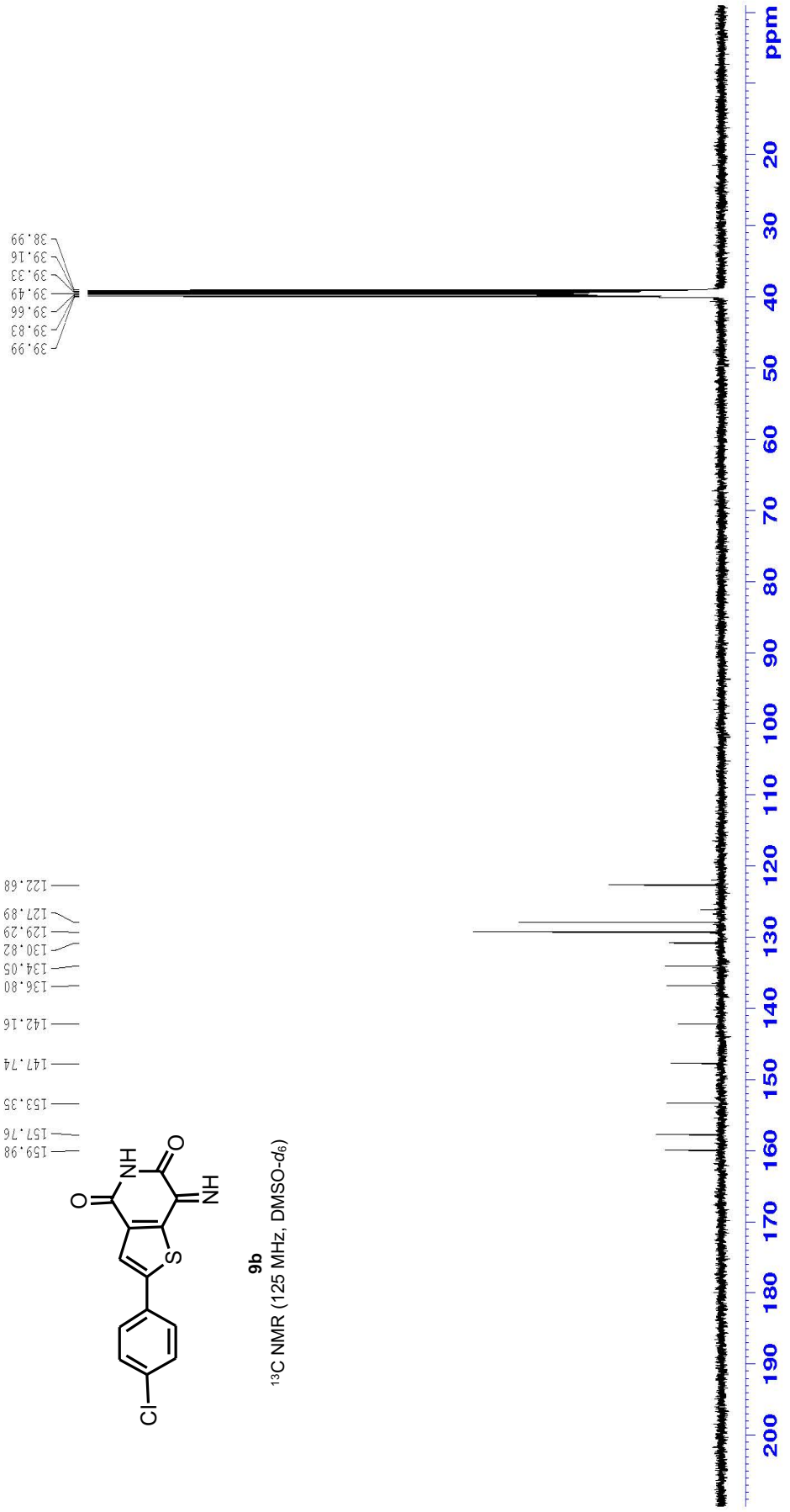

9b

^{13}C NMR (125 MHz, DMSO-d_6)

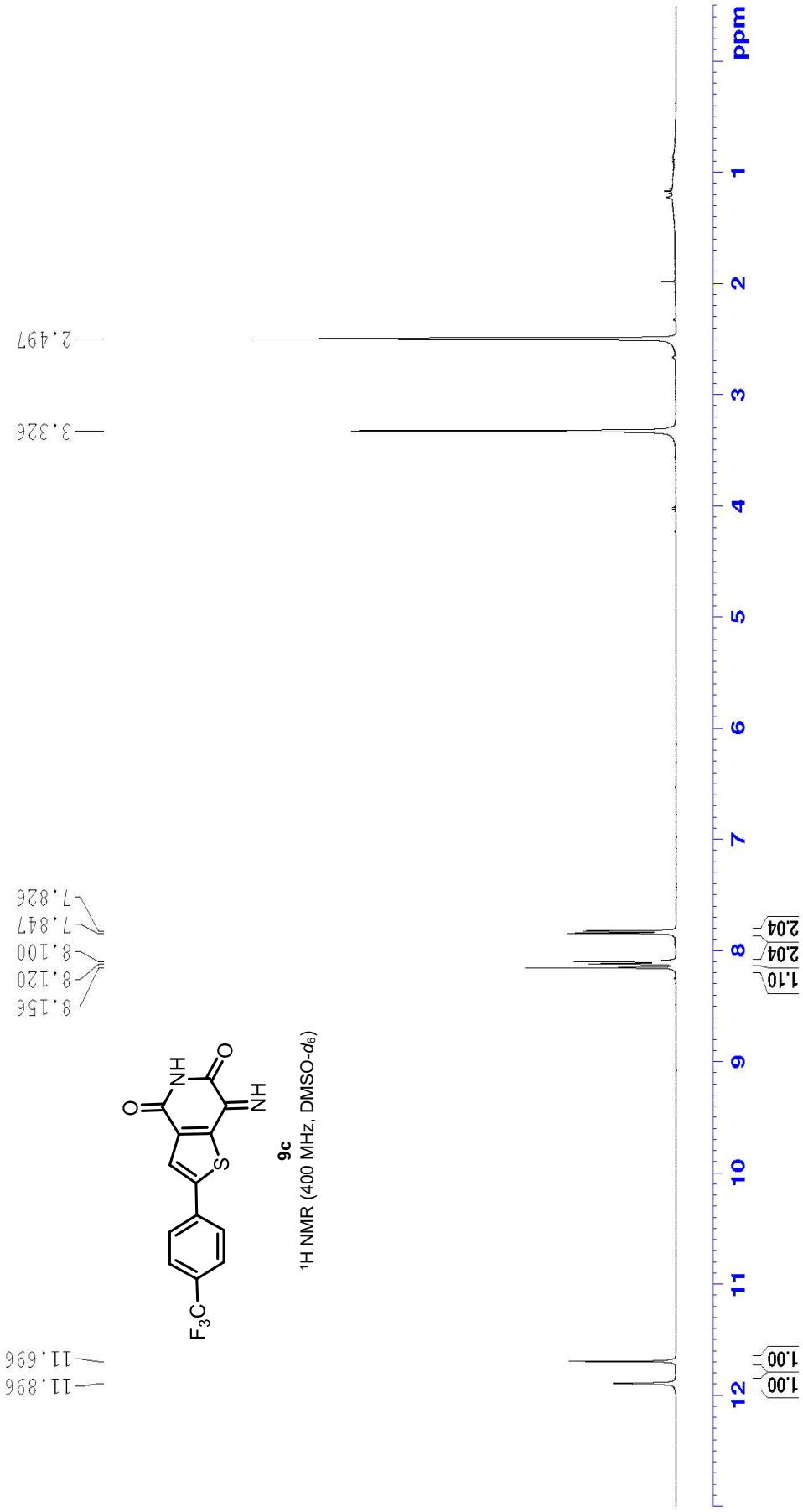

9c

^{1}H NMR (400 MHz, DMSO-d_6)

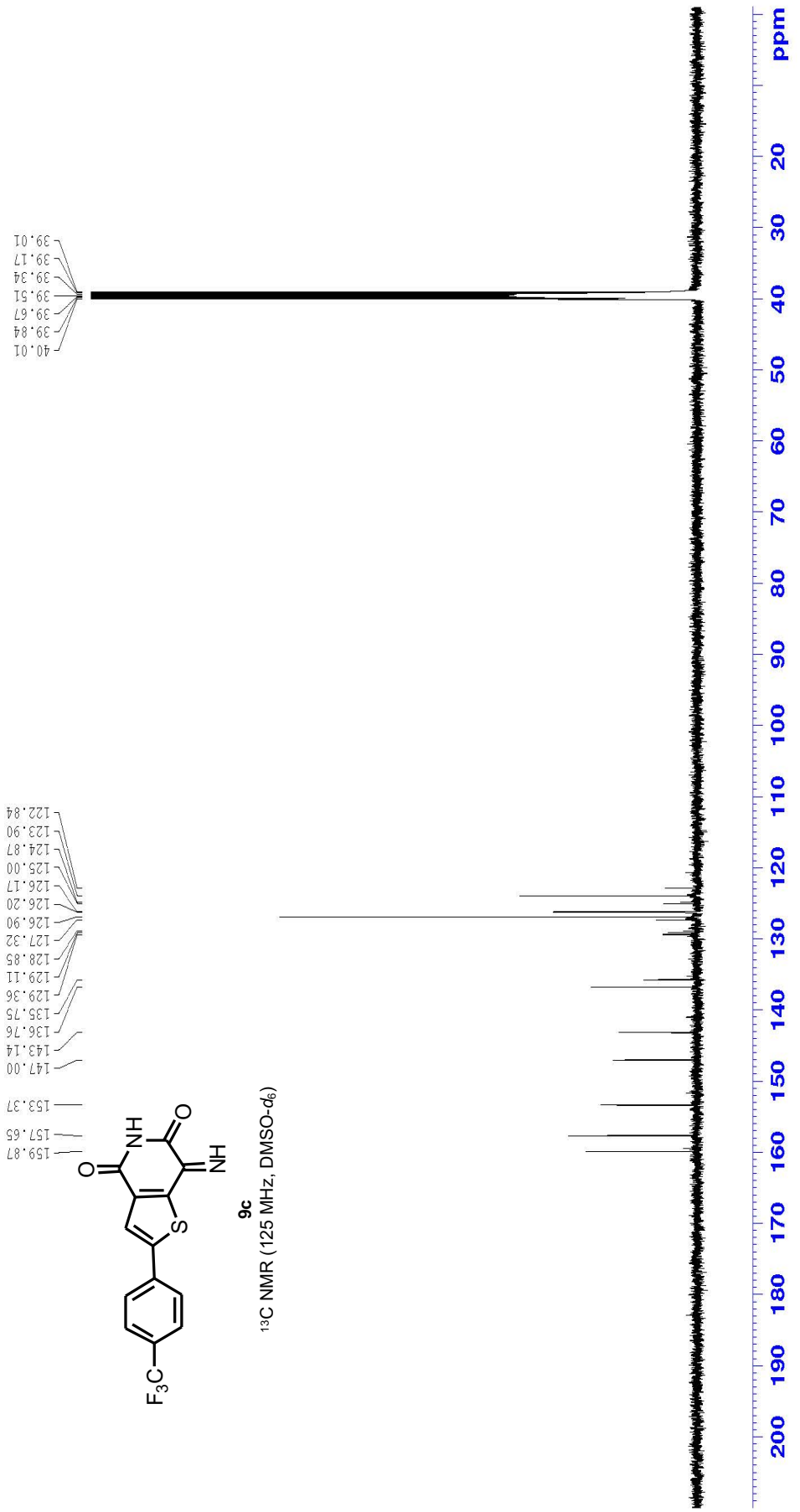

9c

^{13}C NMR (125 MHz, DMSO-d_6)

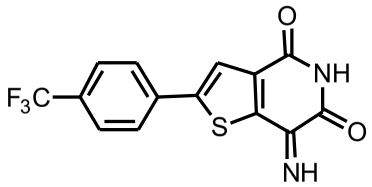

9c

^{19}F NMR (376 MHz, DMSO-d_6)

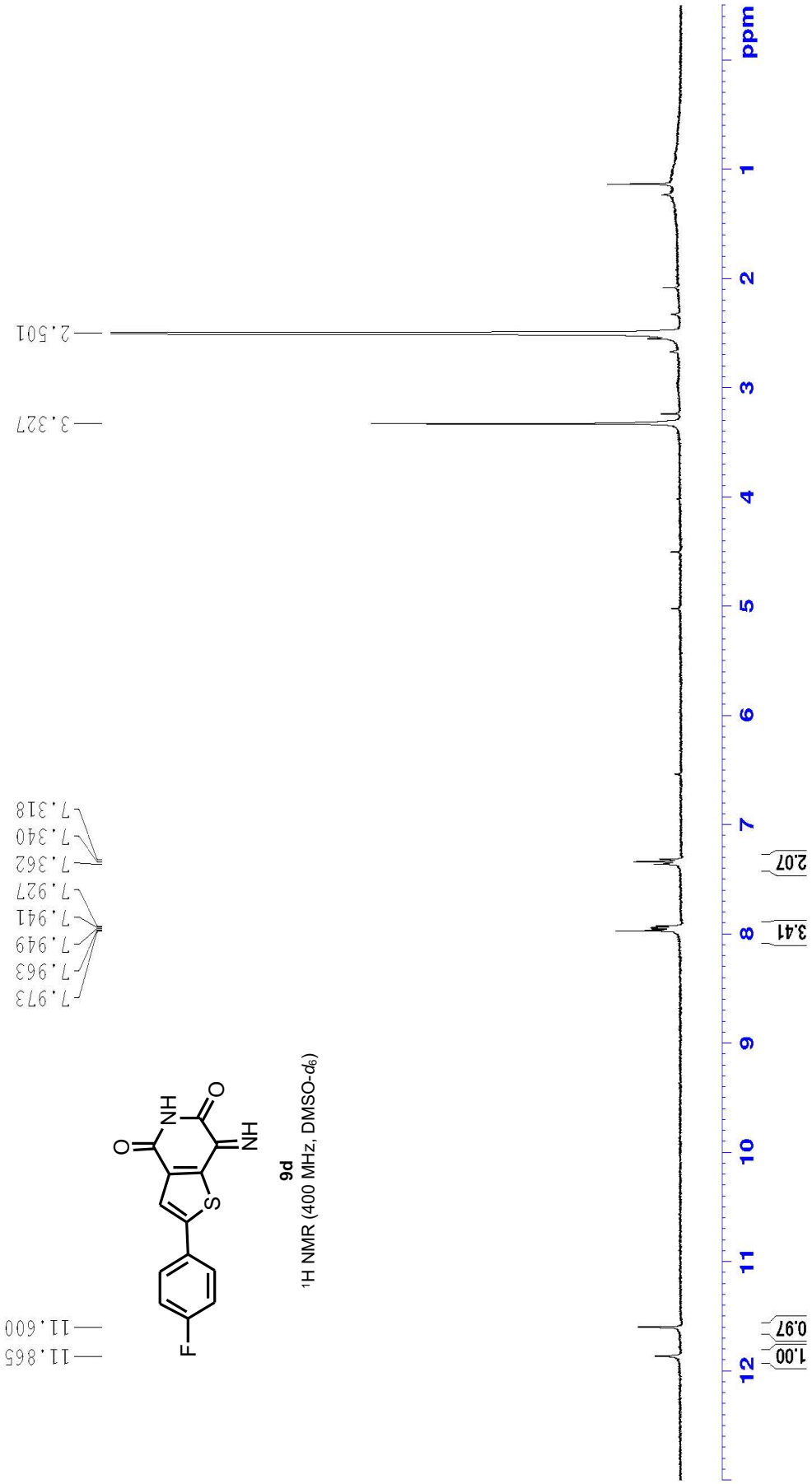

9d

^{1}H NMR (400 MHz, DMSO-d_6)

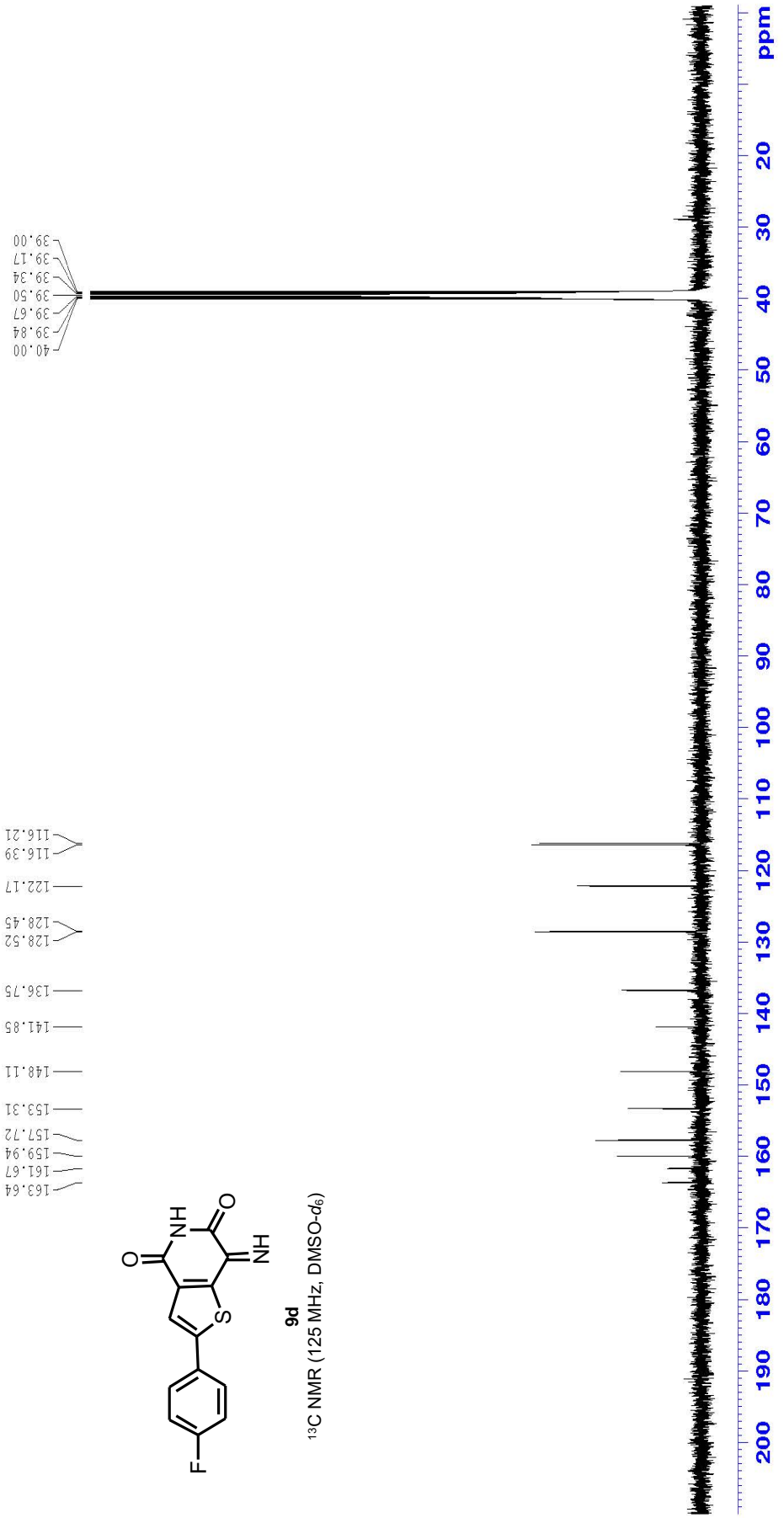

9d

^{13}C NMR (125 MHz, DMSO-d_6)

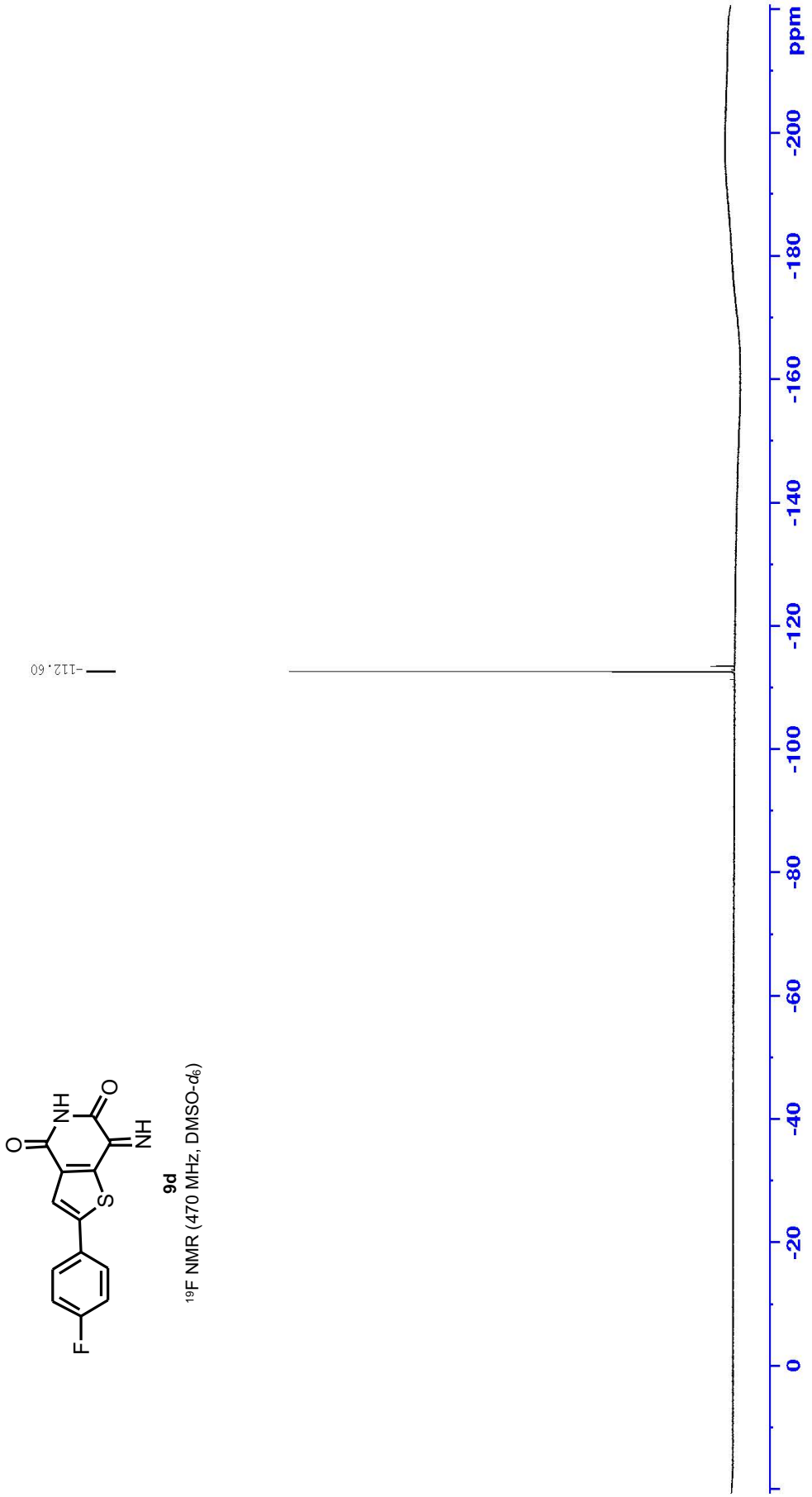

9d

^{19}F NMR (470 MHz, DMSO-d_6)

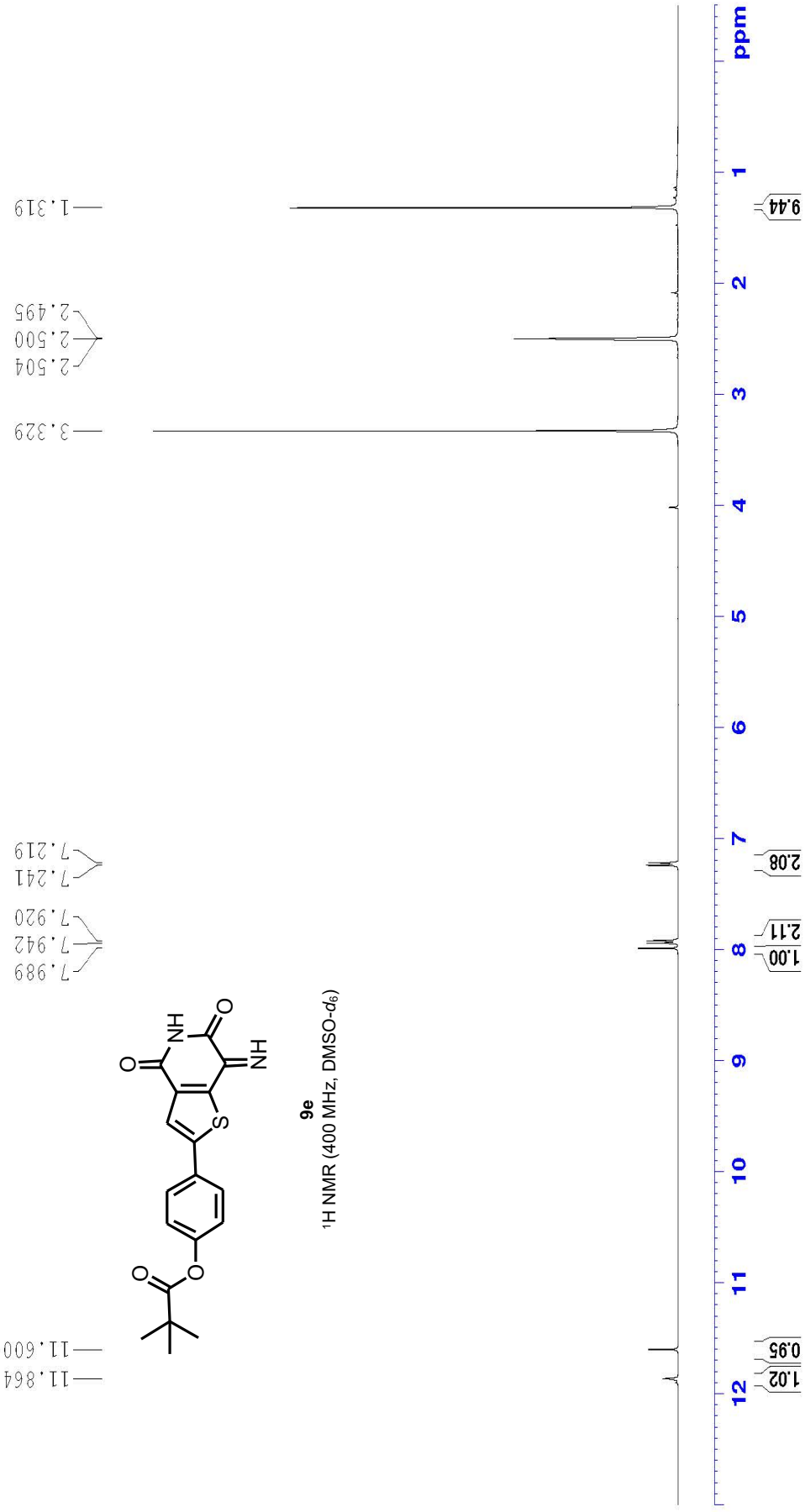
9e
^{1}H NMR (400 MHz, DMSO-d_6)
ppm
1
2
3
4
5
6
7
8
9
10
11
12
9.44
2.08
1.00
2.11
0.95
1.02
1.319
2.495
2.500
2.504
3.329
7.219
7.241
7.920
7.942
7.989
11.600
11.864
NH
O
NH
O
S
O
O

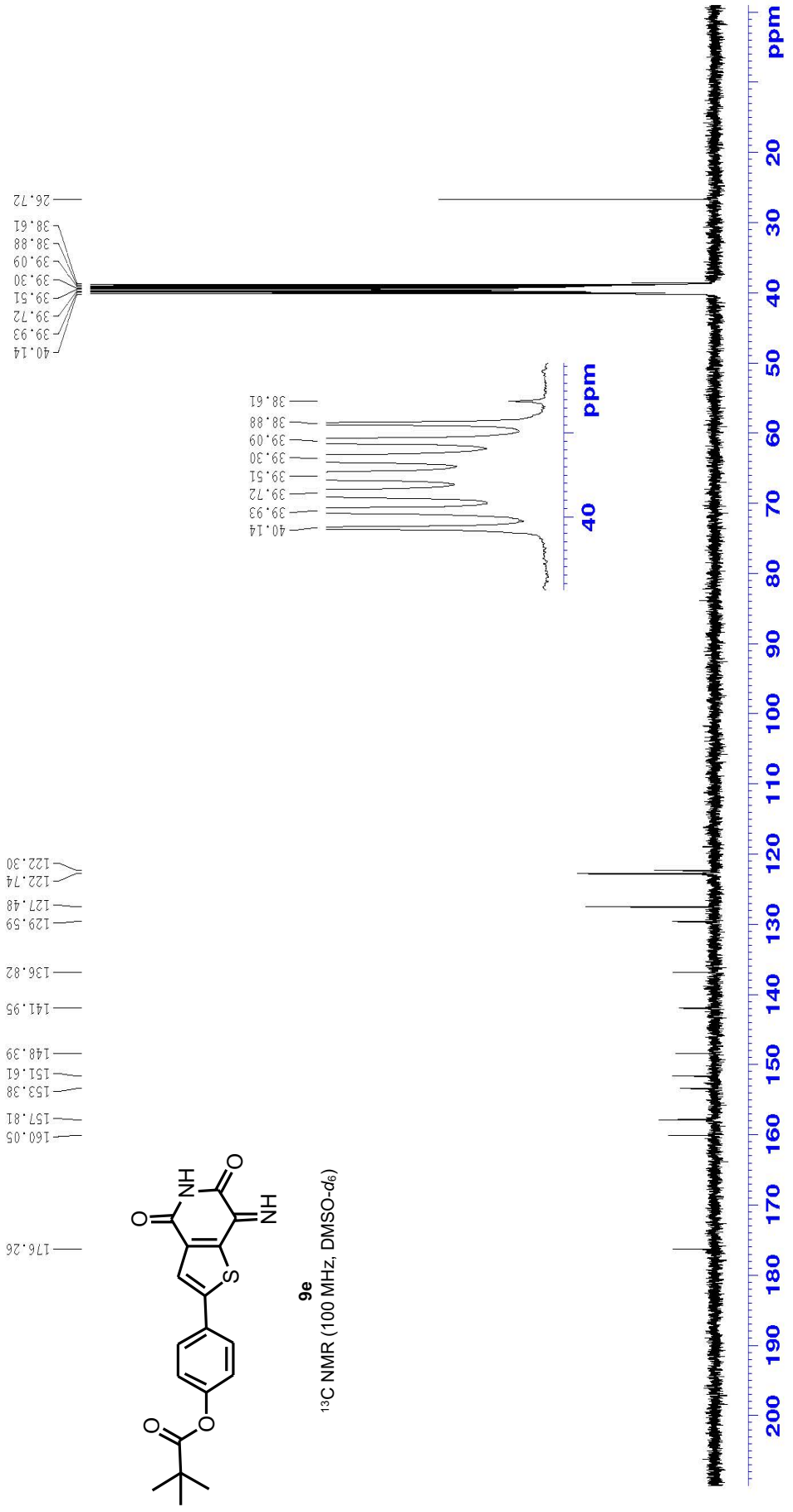
26.72
38.61
38.88
39.09
39.30
39.51
39.72
39.93
40.14
ppm
122.30
122.74
127.48
129.59
136.82
141.95
148.39
151.61
153.38
157.81
160.05
176.26
NH
HN
O
S
O
O
O
9e
^{13}C NMR (100 MHz, DMSO-d_6)

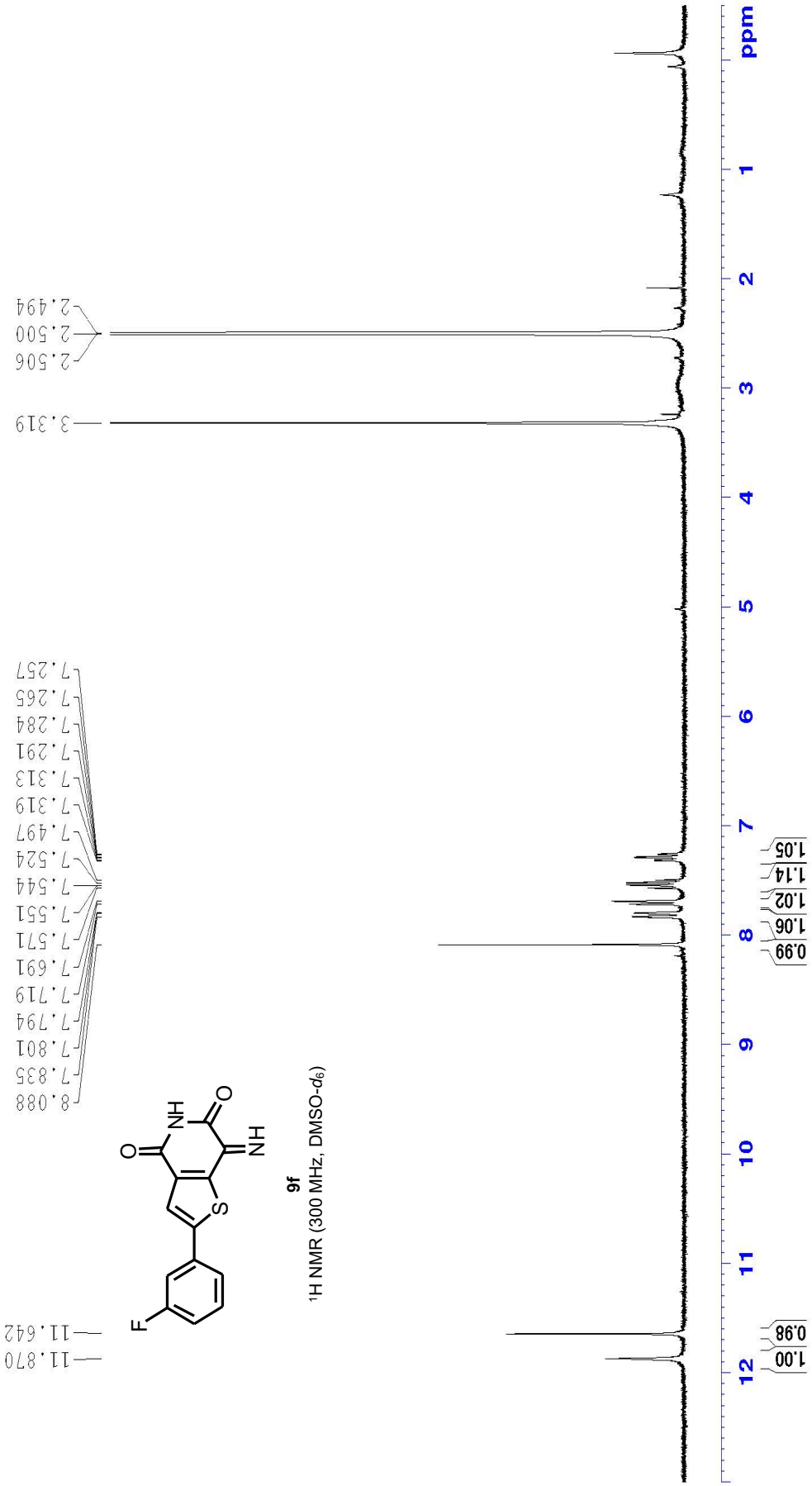

9f

^{1}H NMR (300 MHz, DMSO-d_6)

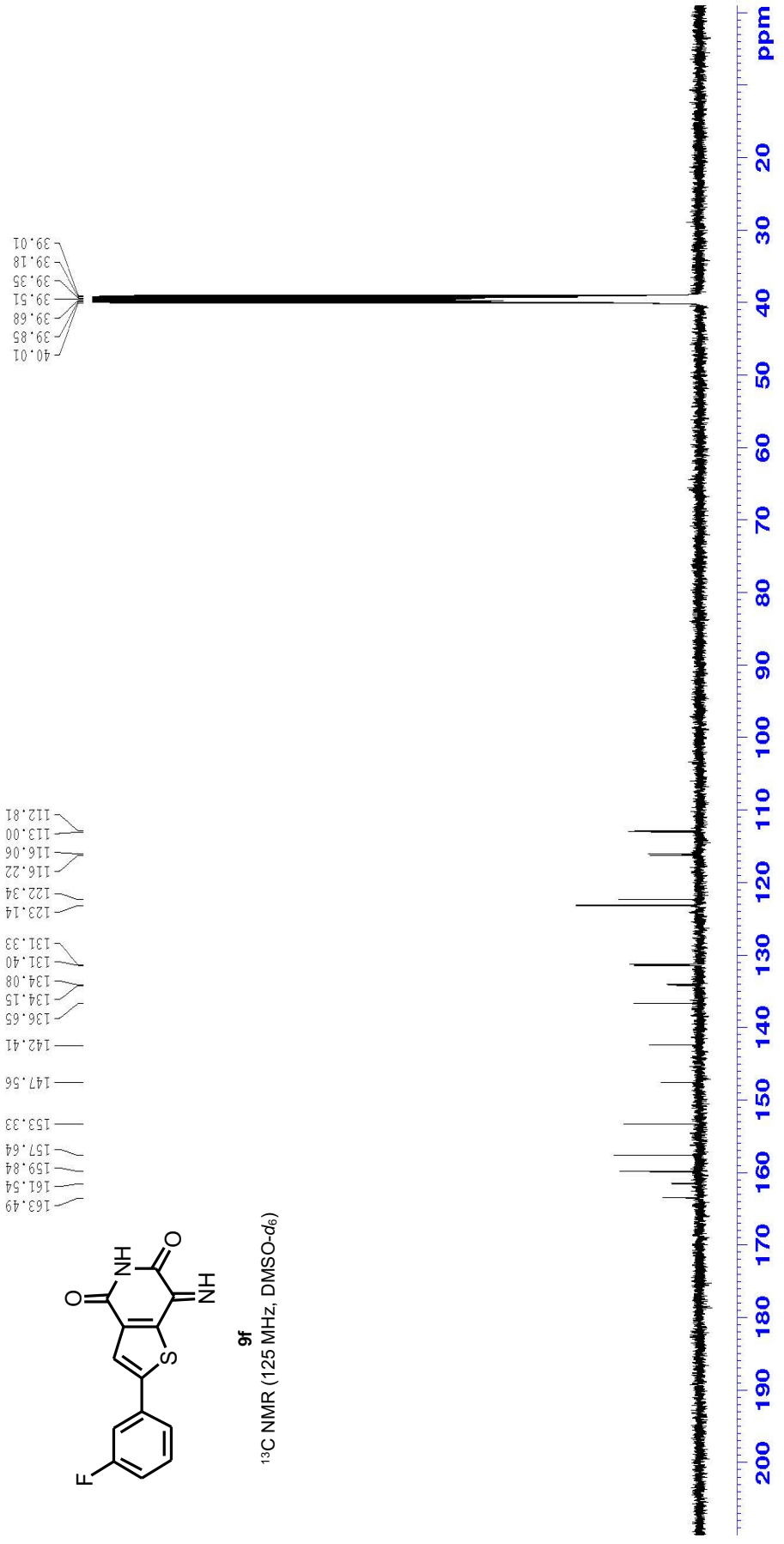

9f

^{13}C NMR (125 MHz, DMSO-d_6)

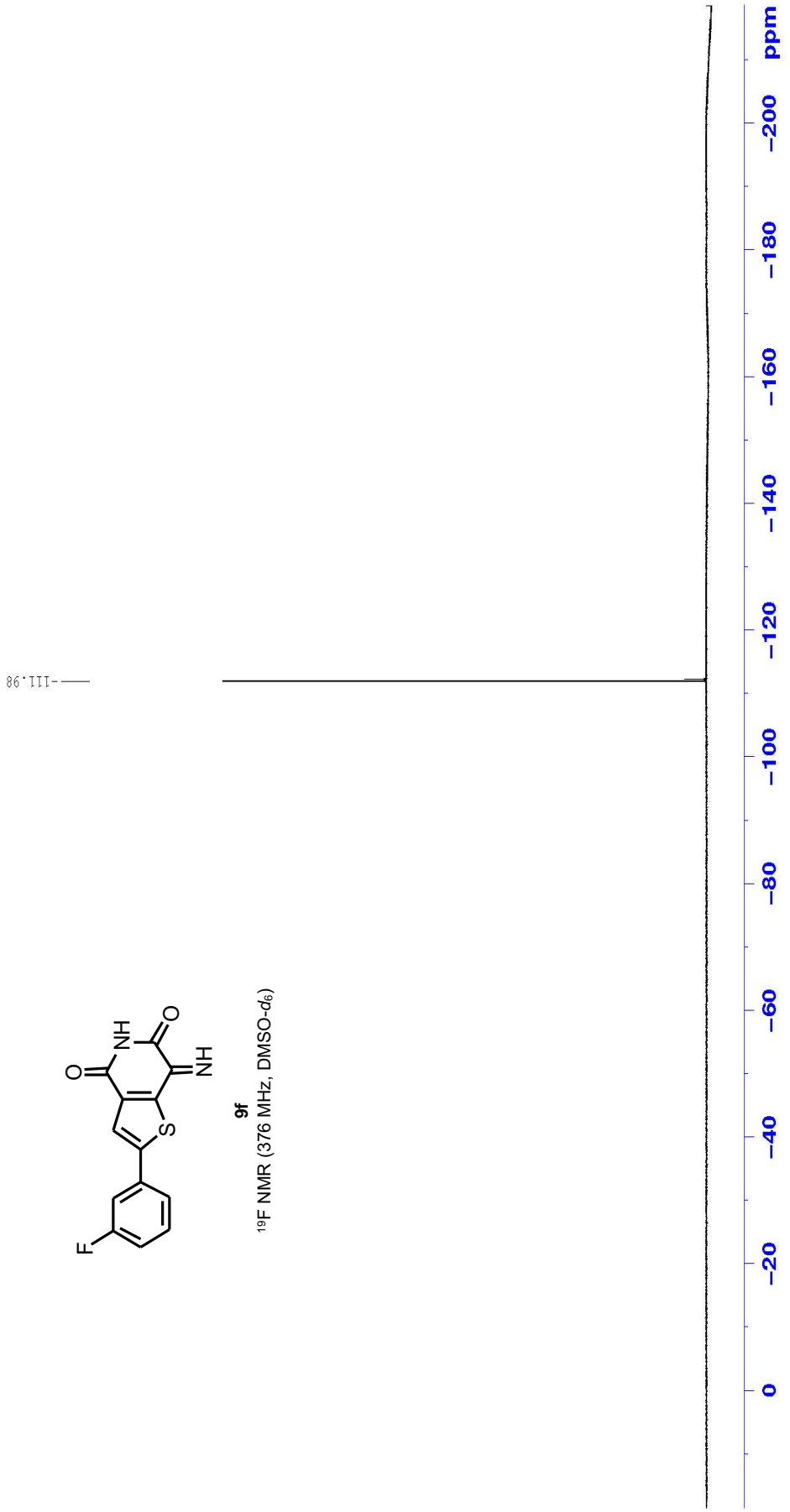

9f

^{19}F NMR (376 MHz, DMSO-d_6)

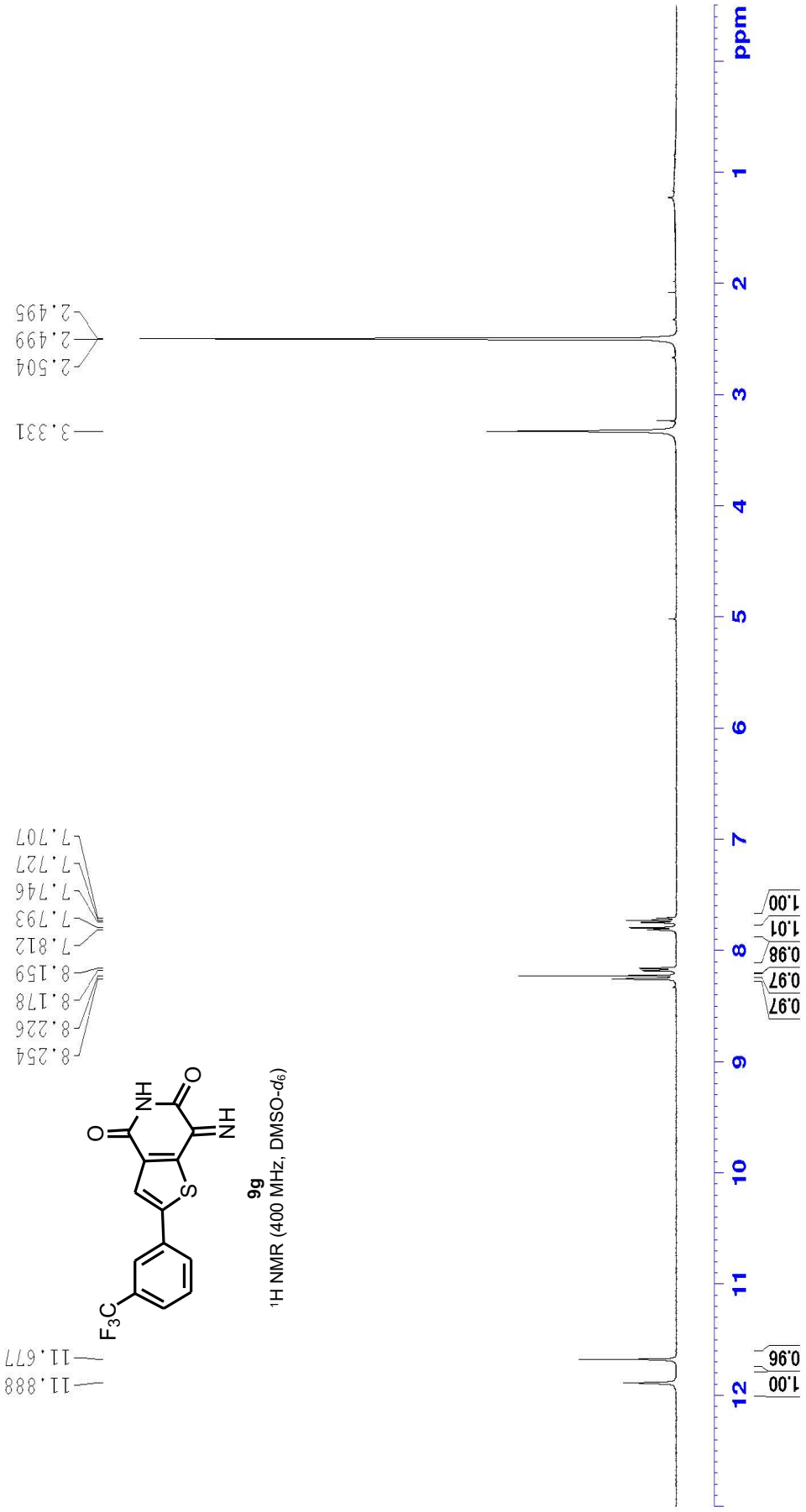
11.888
11.677
8.254
8.226
8.178
8.159
7.812
7.793
7.746
7.727
7.707
2.504
2.499
2.495
3.331
1.00
0.96
0.97
0.97
0.98
1.01
1.00
ppm
1 2 3 4 5 6 7 8 9 10 11 12
NH
O
O
NH
S
F3C
9g
1H NMR (400 MHz, DMSO-d6)

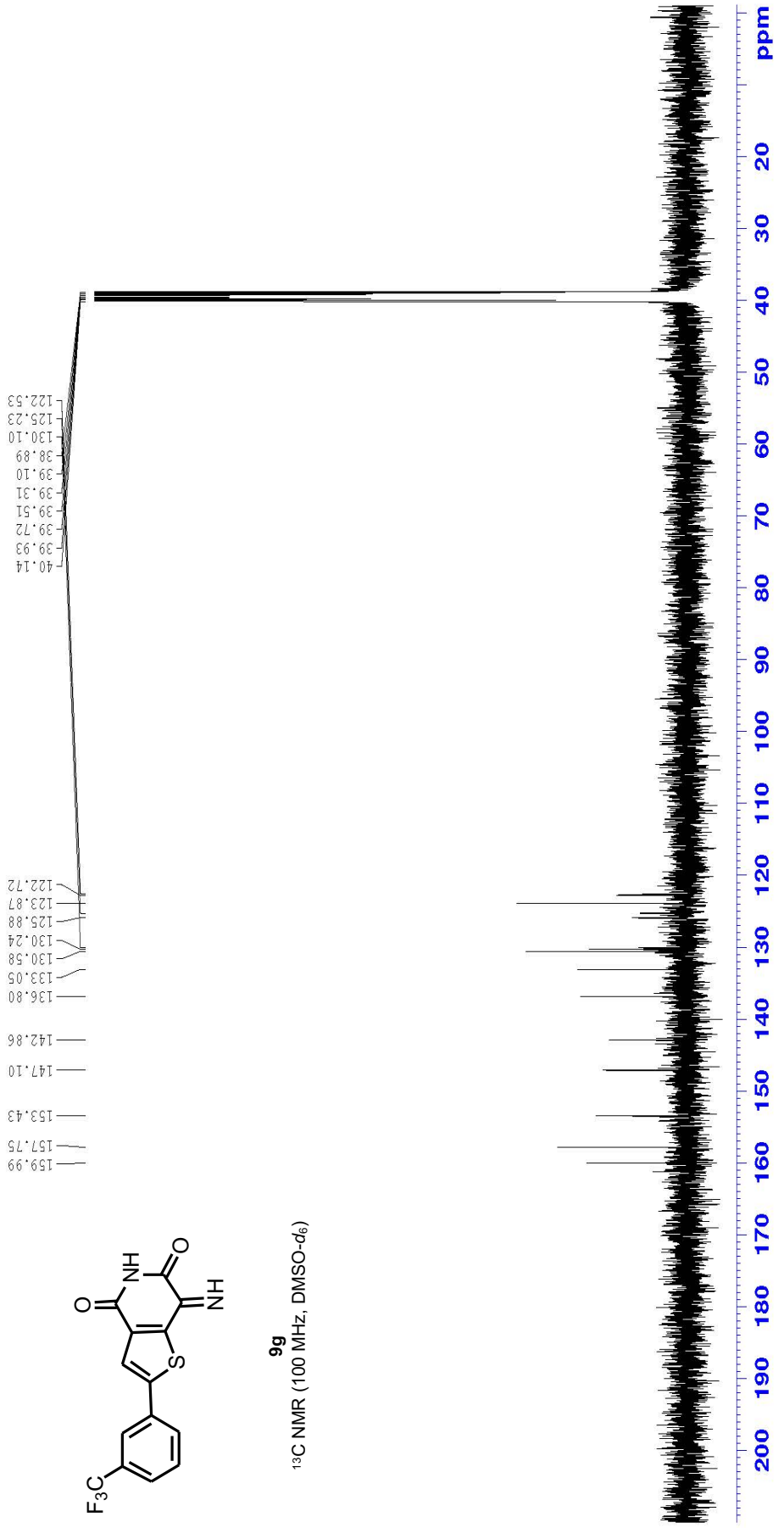

9g

^{13}C NMR (100 MHz, DMSO-d_6)

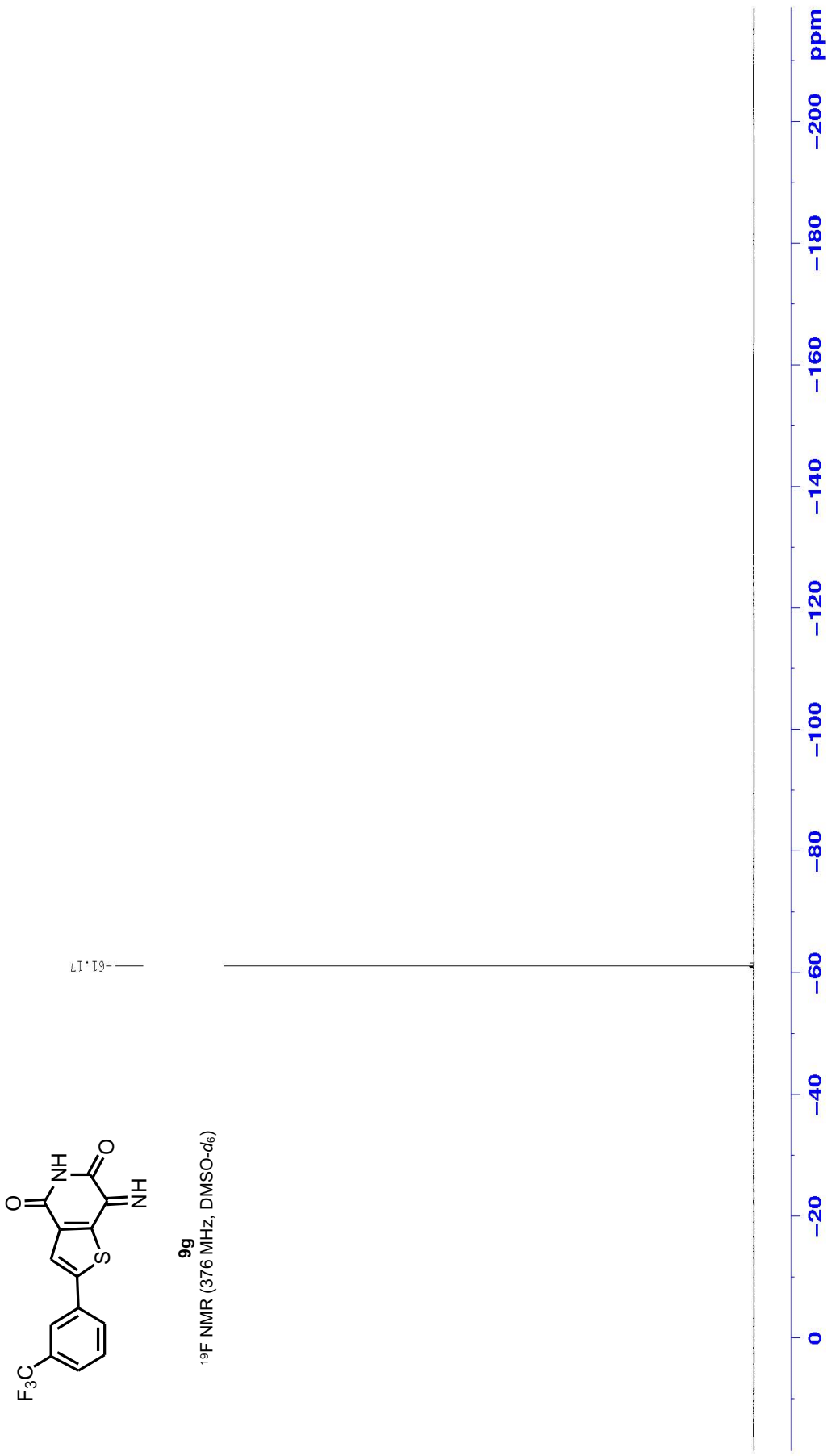

9g

^{19}F NMR (376 MHz, DMSO-d_6)

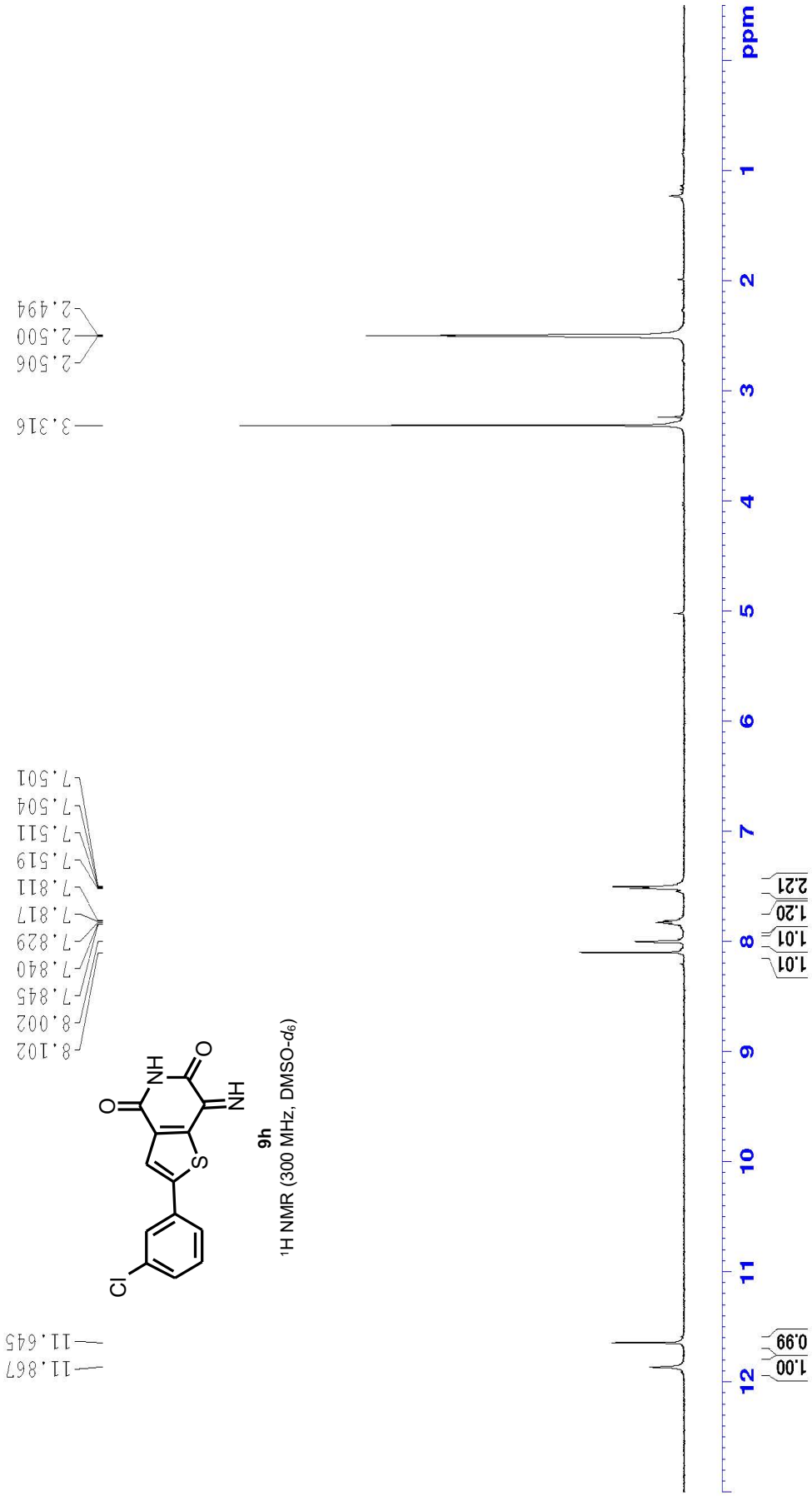
ppm
1
2
3
4
5
6
7
8
9
10
11
12
1.00
0.99
11.867
11.645
8.102
8.002
7.845
7.840
7.829
7.817
7.811
7.519
7.511
7.504
7.501
2.494
2.500
2.506
3.316
1.01
1.01
1.20
2.21
NH
O
O
NH
S
Cl
9h
1H NMR (300 MHz, DMSO-d6)

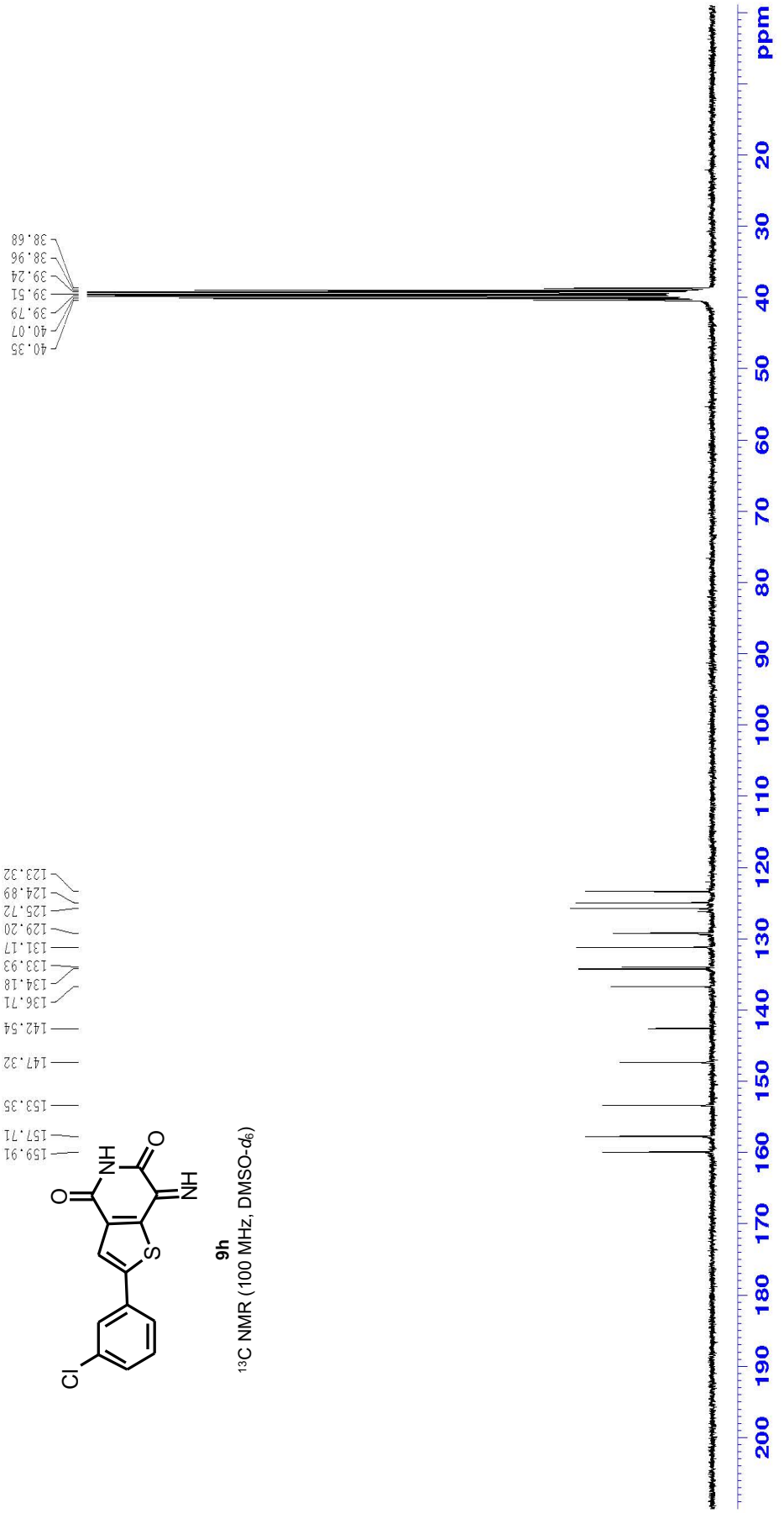

9h

^{13}C NMR (100 MHz, DMSO-d_6)

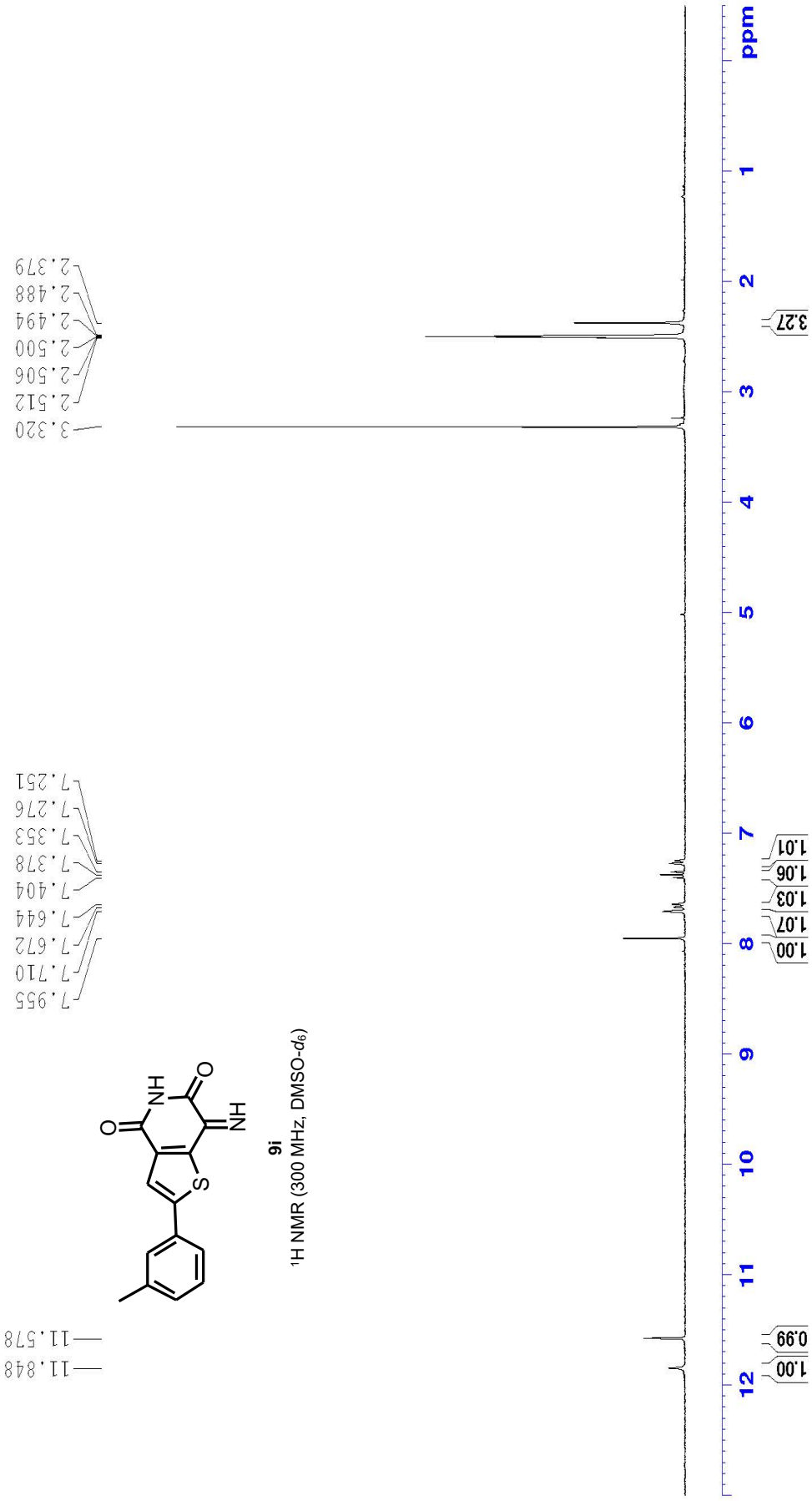

9i

^{1}H NMR (300 MHz, DMSO-d_6)

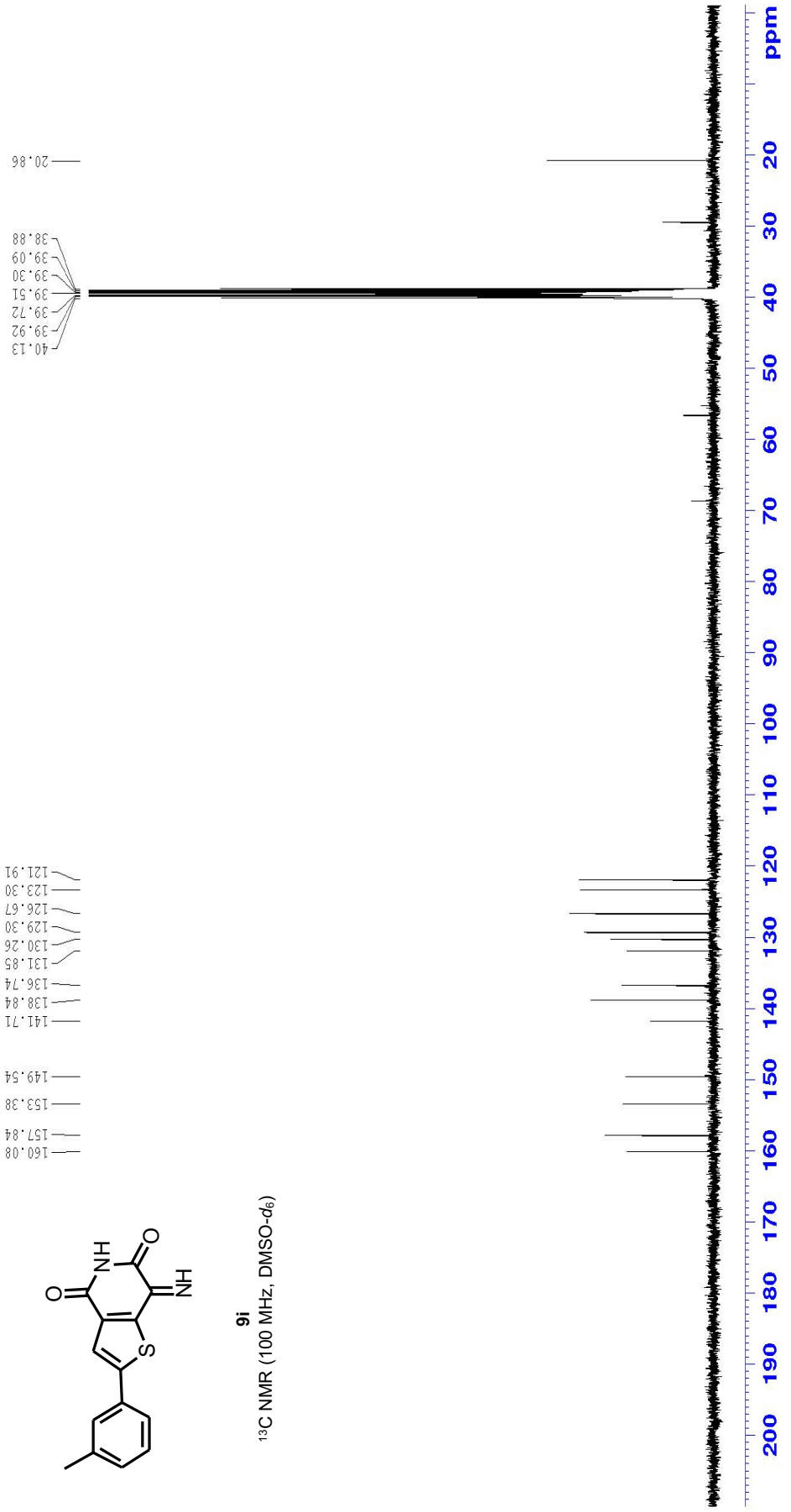

9i

^{13}C NMR (100 MHz, DMSO-d_6)

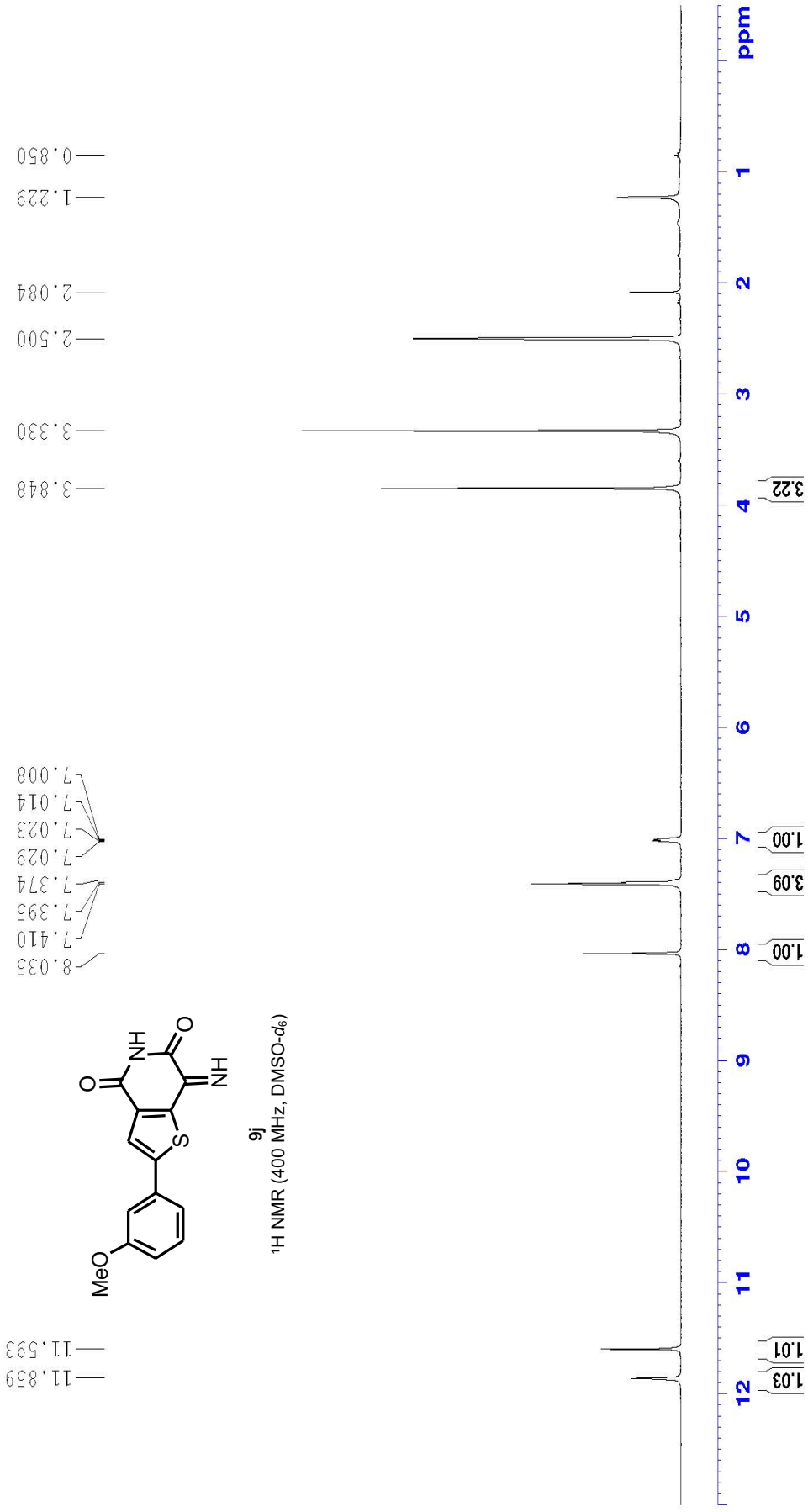

9j

^{1}H NMR (400 MHz, DMSO-d_6)

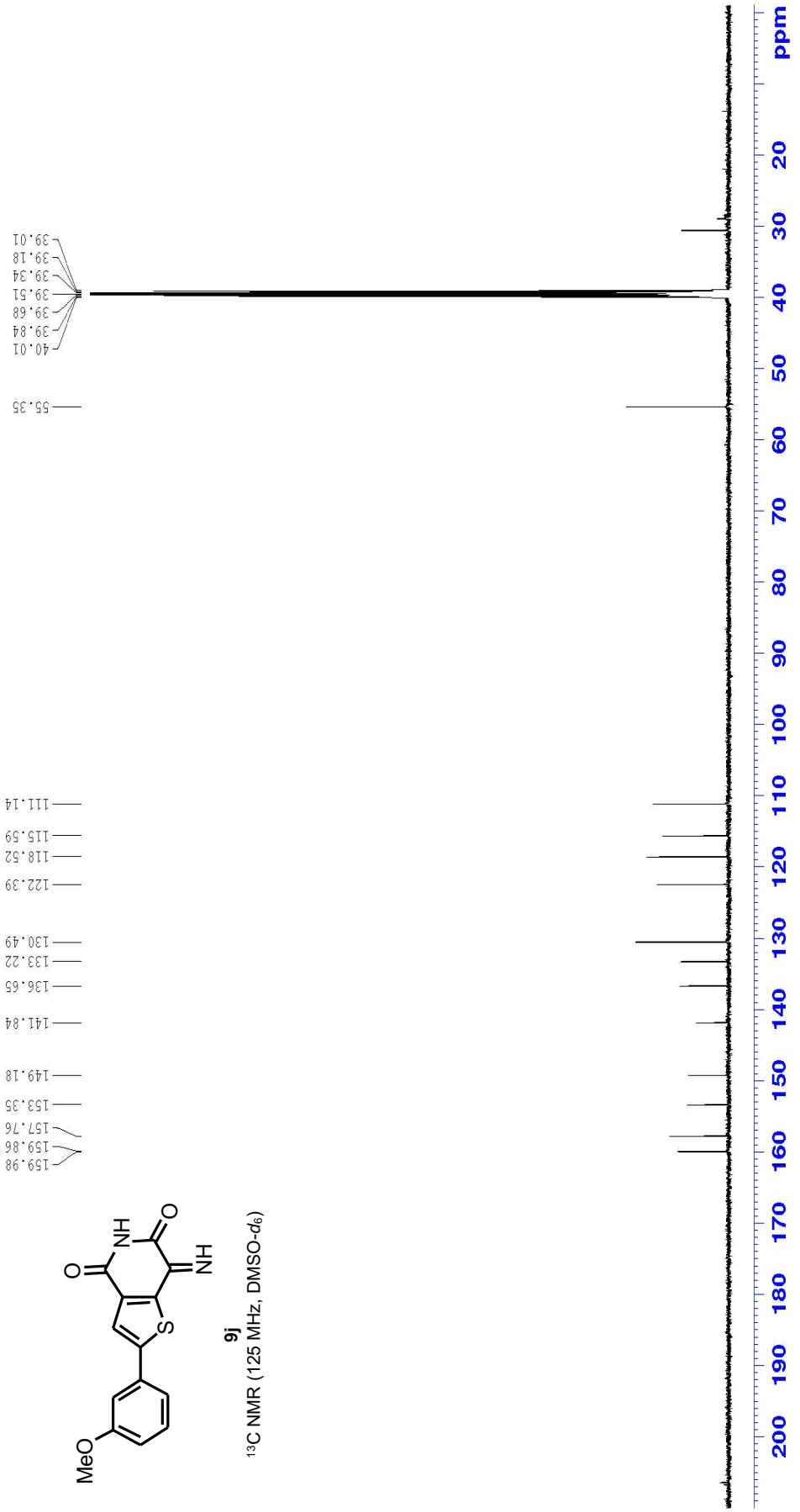

9j

^{13}C NMR (125 MHz, DMSO-d_6)

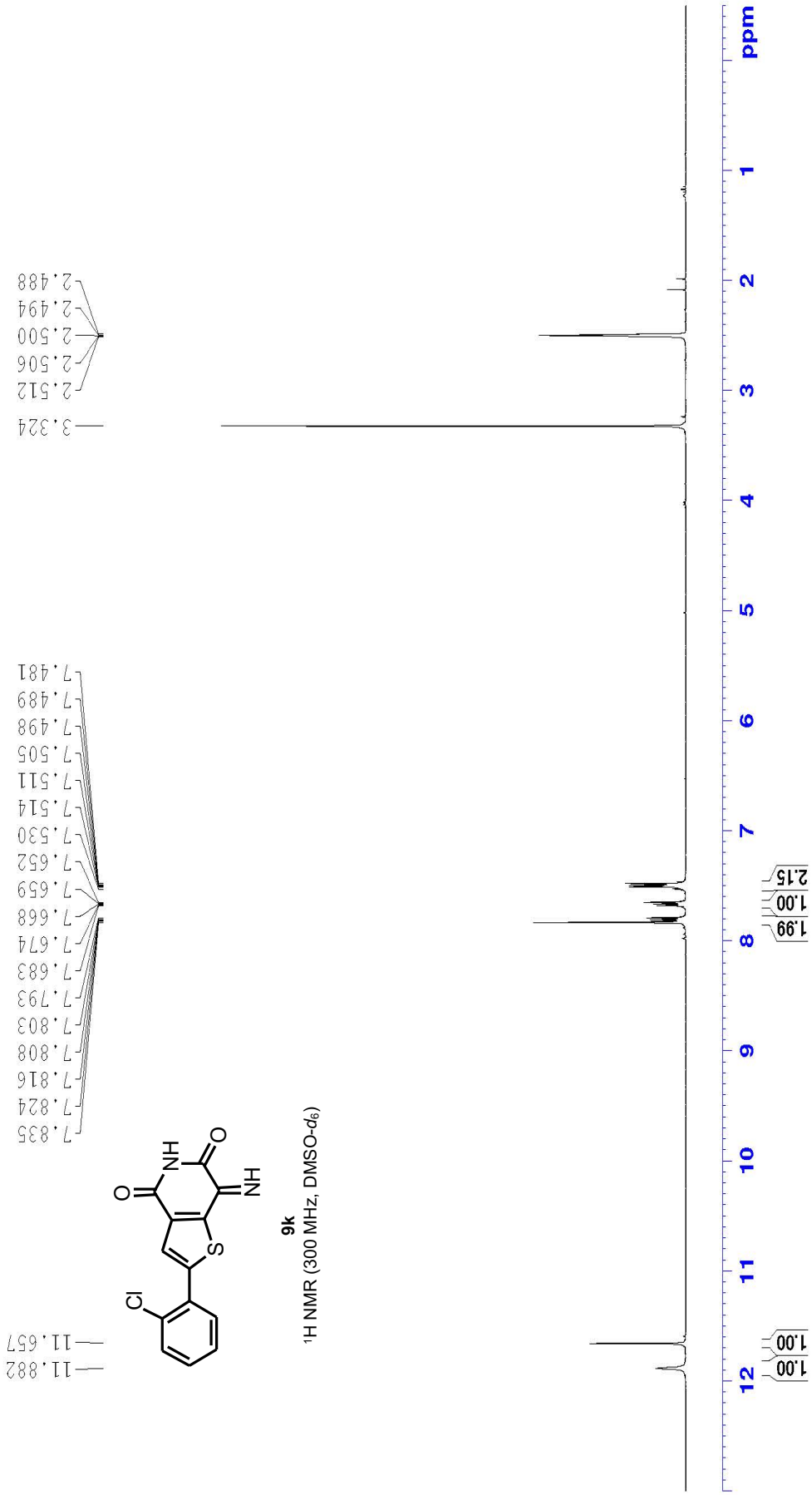

9k

^{1}H NMR (300 MHz, DMSO-d_6)

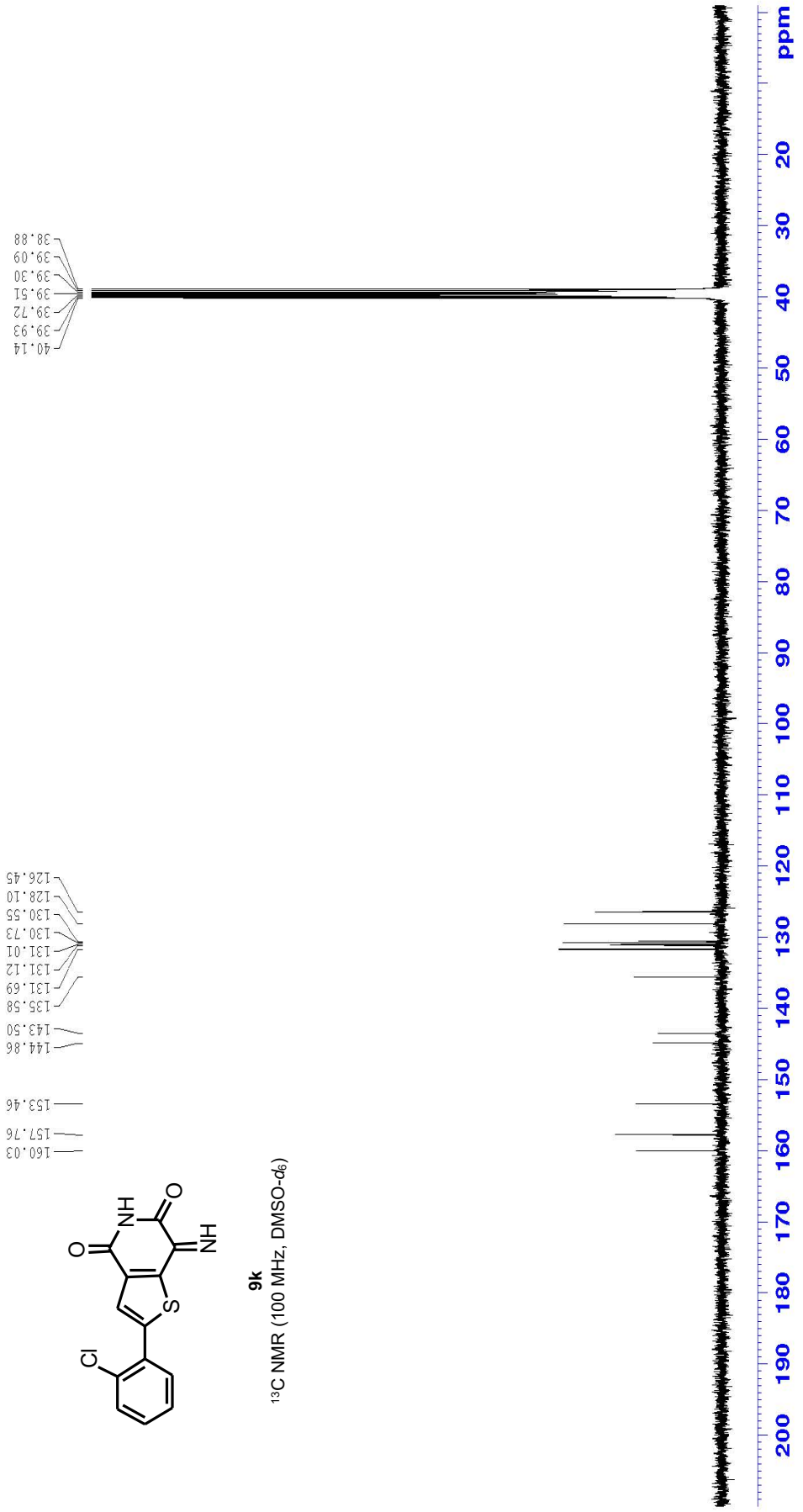

9k

^{13}C NMR (100 MHz, DMSO-d_6)

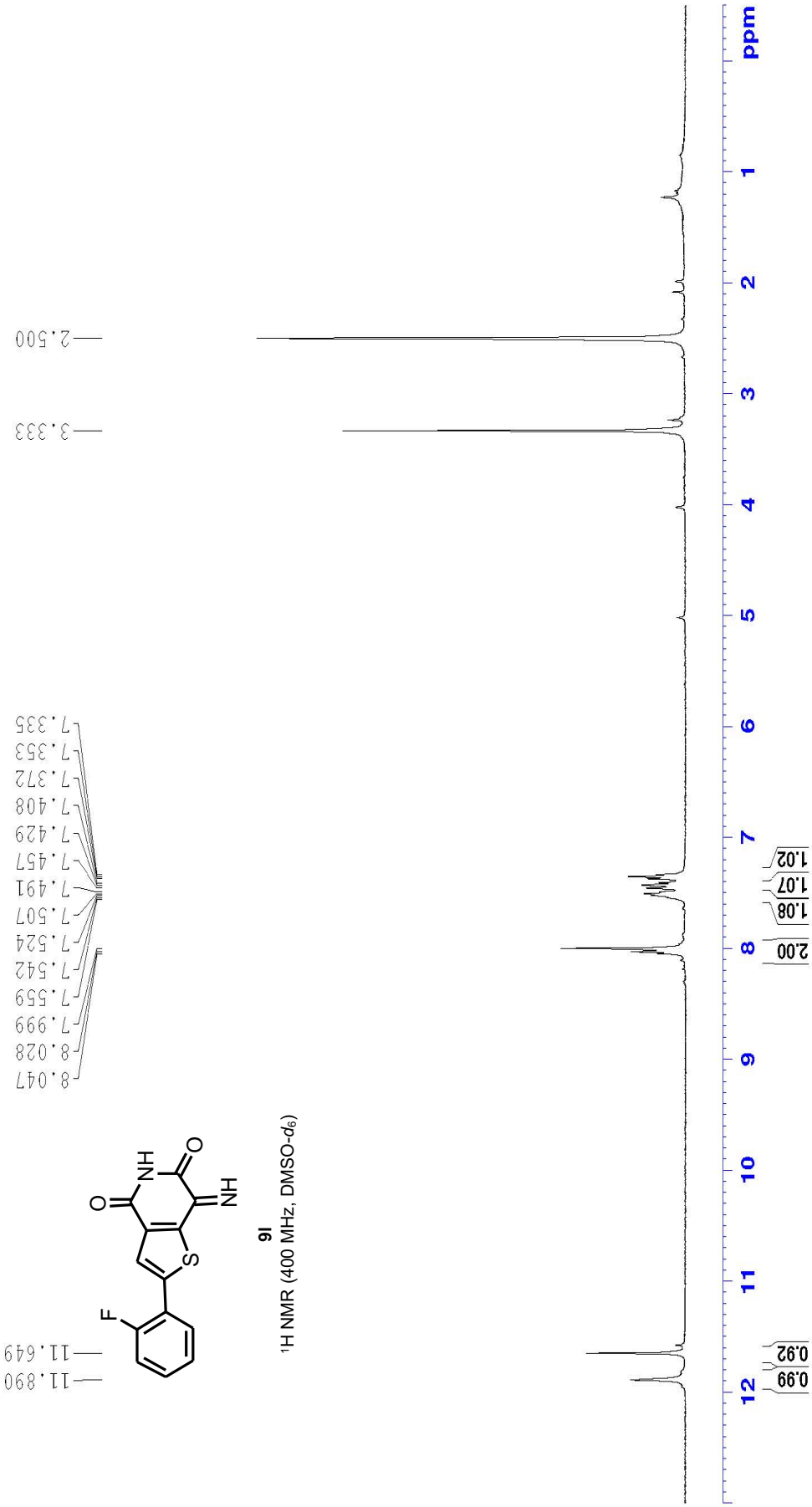

9l

^{1}H NMR (400 MHz, DMSO-d_6)

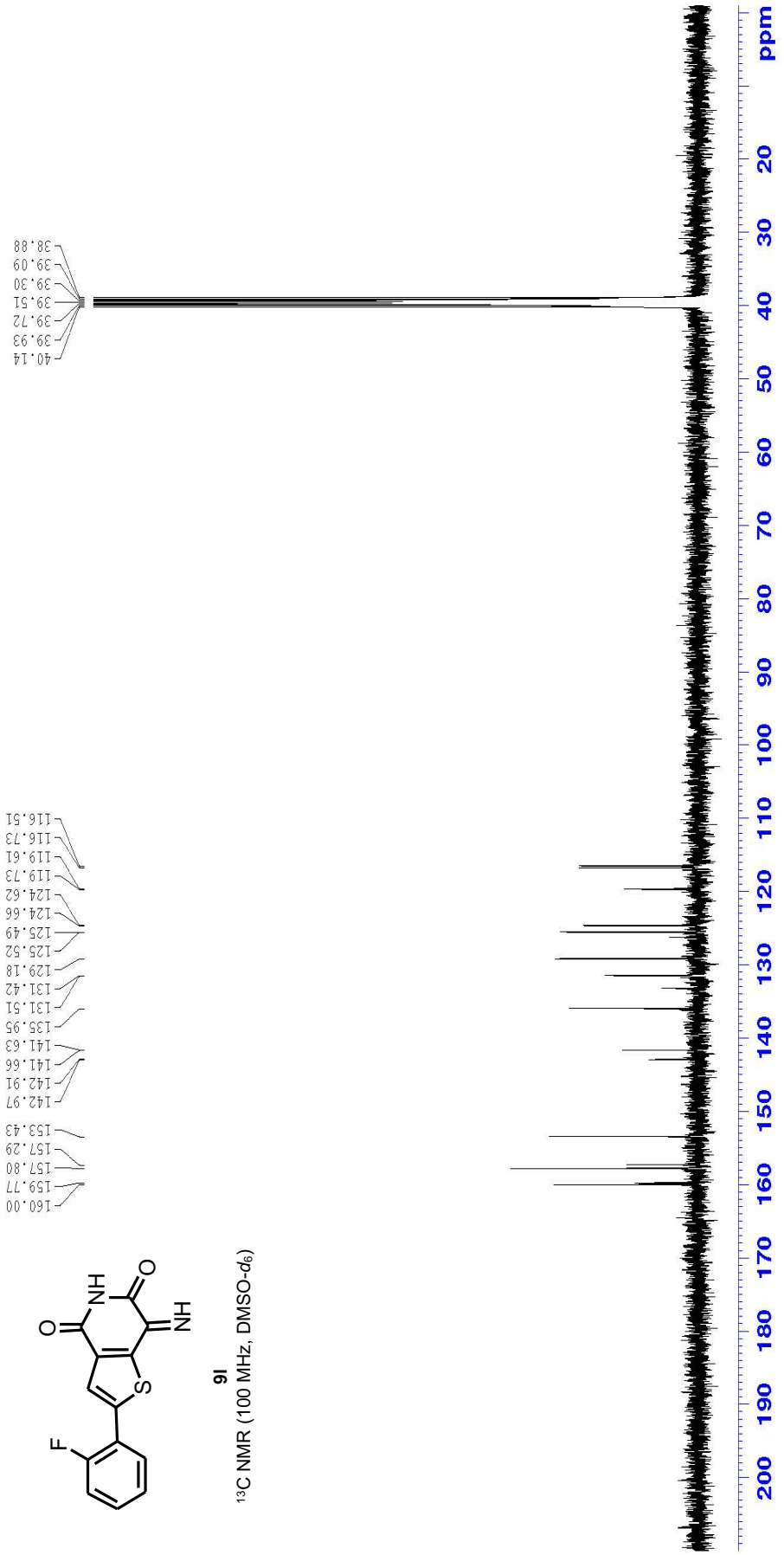

9l

^{13}C NMR (100 MHz, DMSO-d_6)

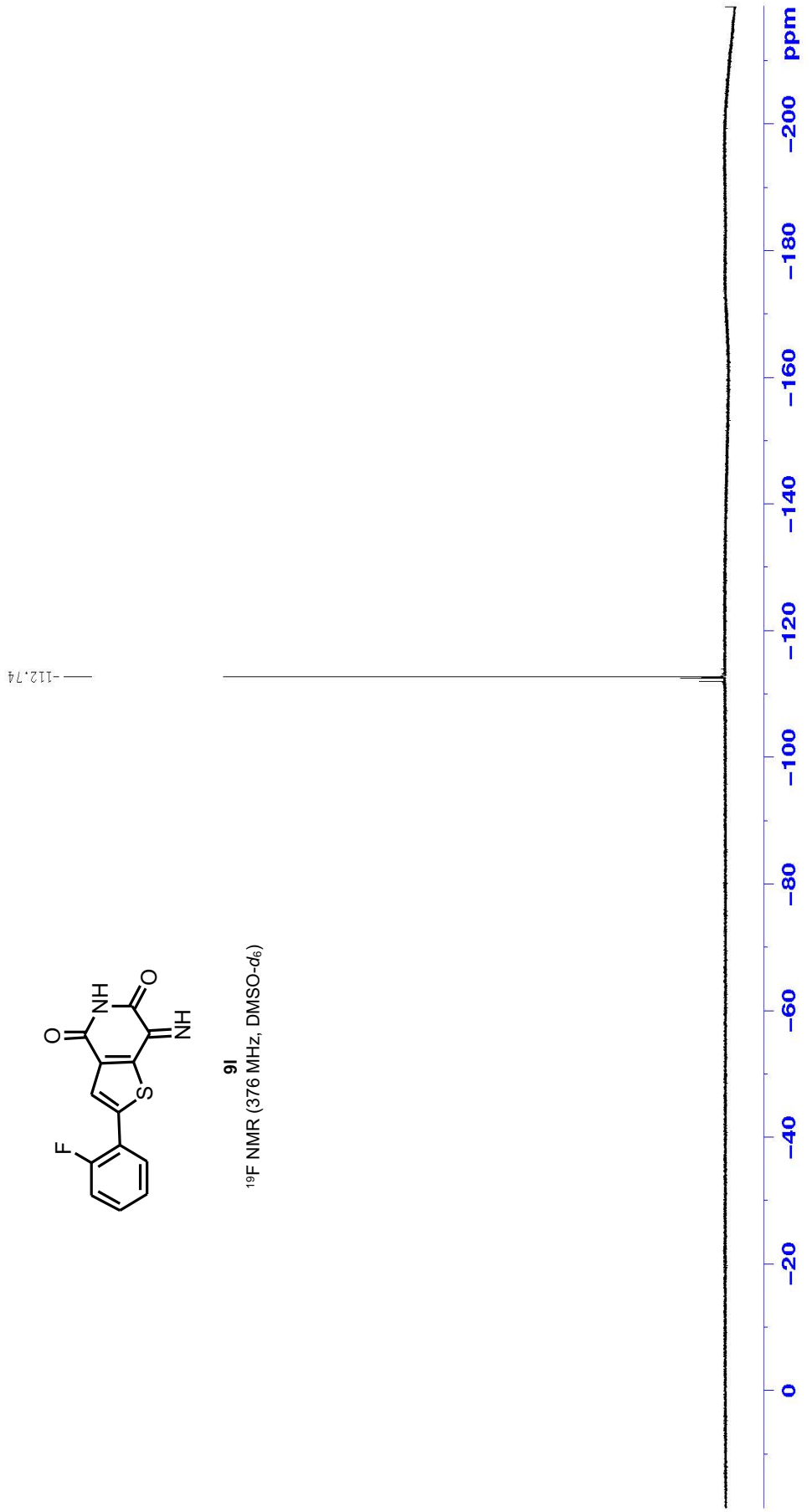

9l

^{19}F NMR (376 MHz, DMSO-d_6)

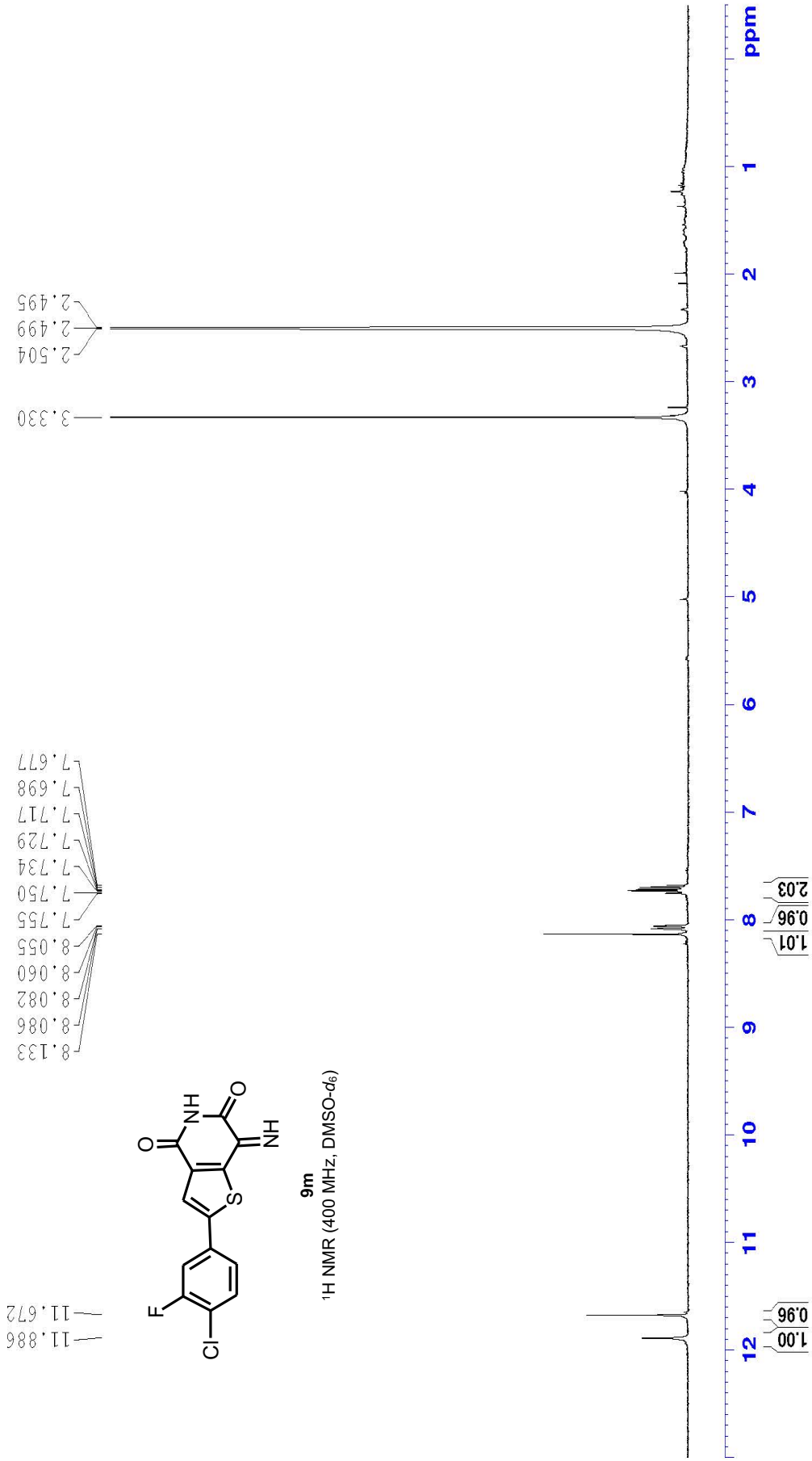

9m

^{1}H NMR (400 MHz, DMSO-d_6)

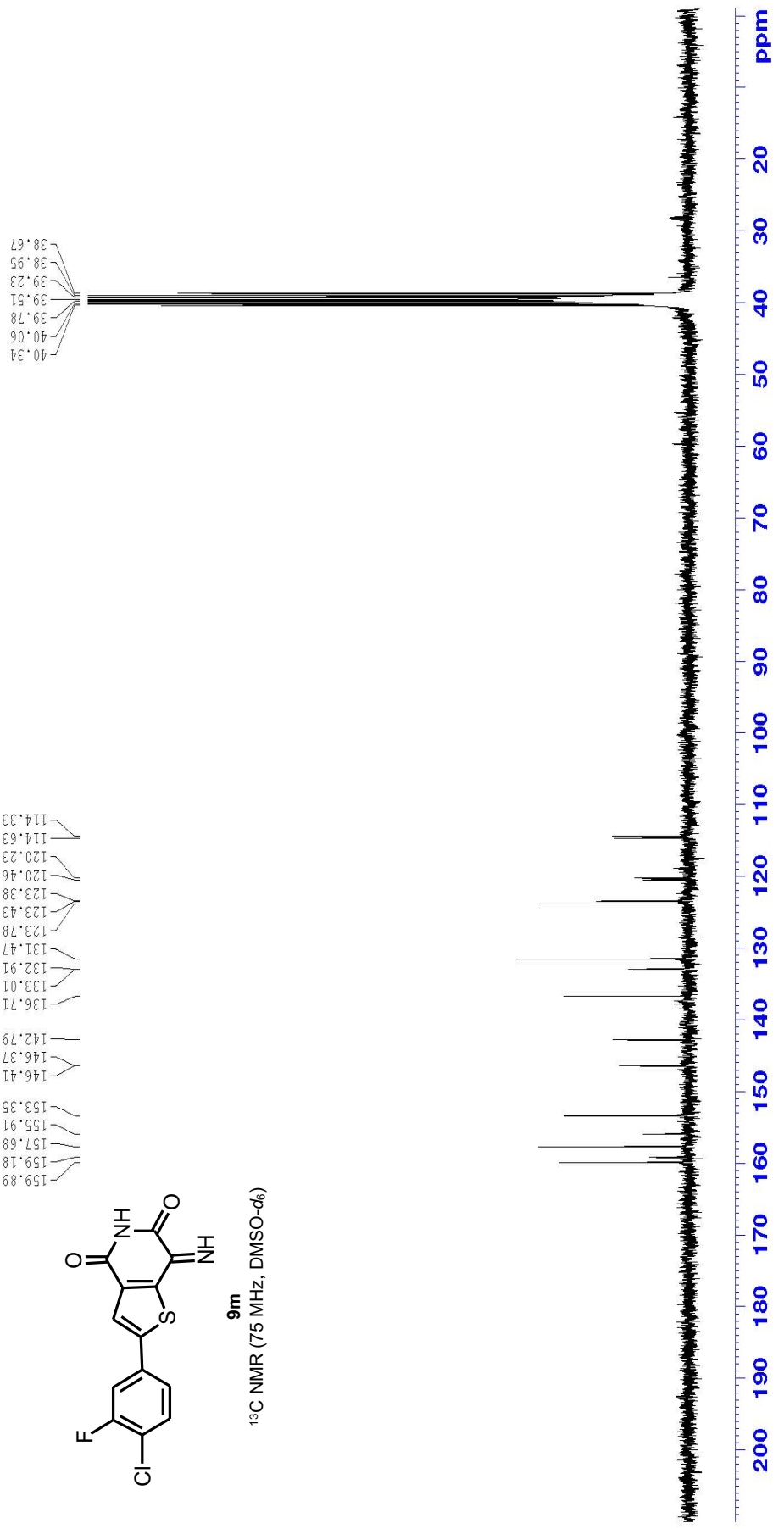
38.67
38.95
39.23
39.51
39.78
40.06
40.34
114.33
114.63
120.23
120.46
123.38
123.43
123.78
131.47
132.91
133.01
136.71
142.79
146.37
146.41
153.35
155.91
157.68
159.18
159.89
NH
O
O
NH
S
F
Cl
9m
^{13}C NMR (75 MHz, DMSO-d_6)
ppm
200
190
180
170
160
150
140
130
120
110
100
90
80
70
60
50
40
30
20

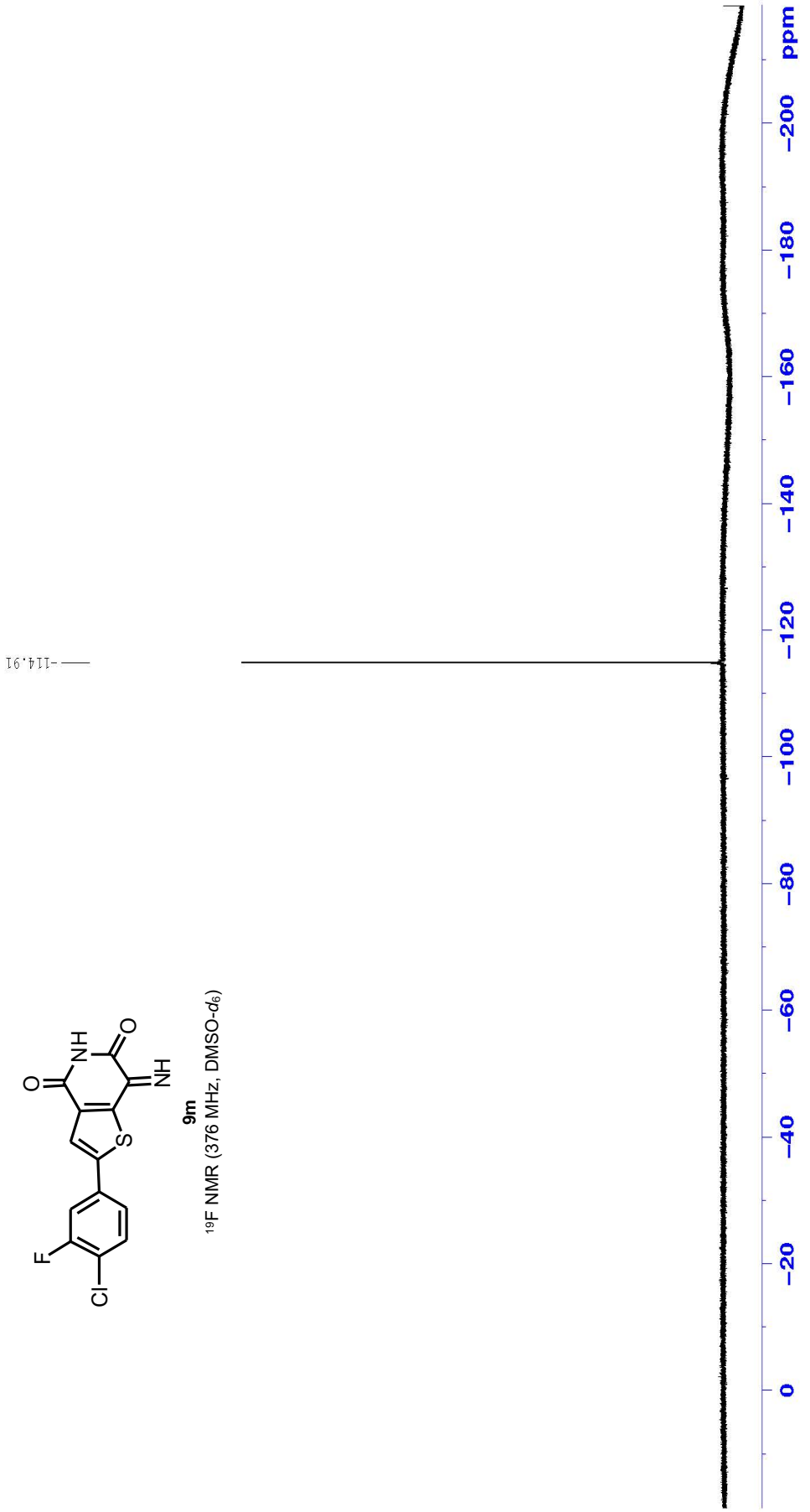

9m

^{19}F NMR (376 MHz, DMSO-d_6)

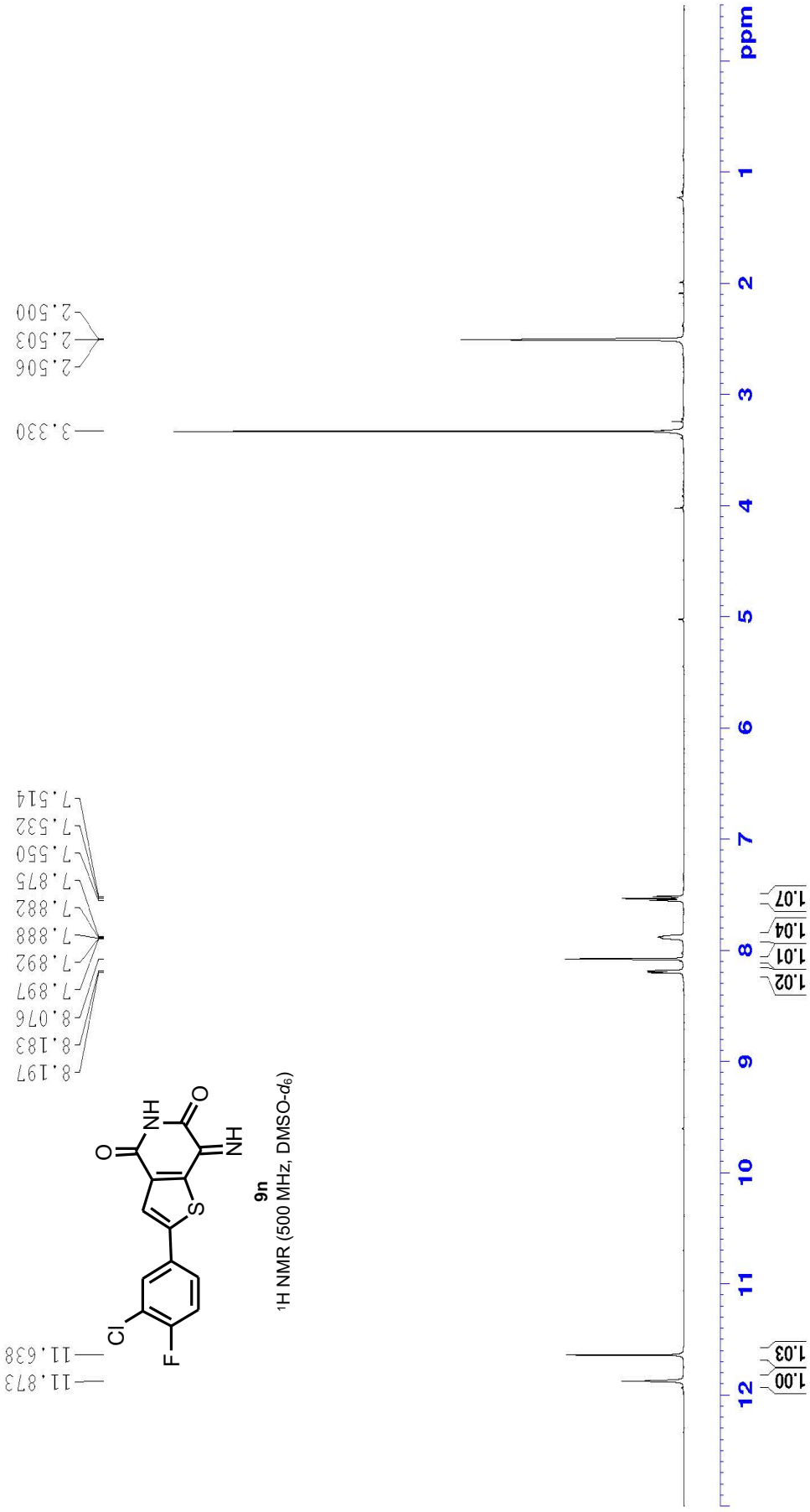

9n

^{1}H NMR (500 MHz, DMSO-d_6)

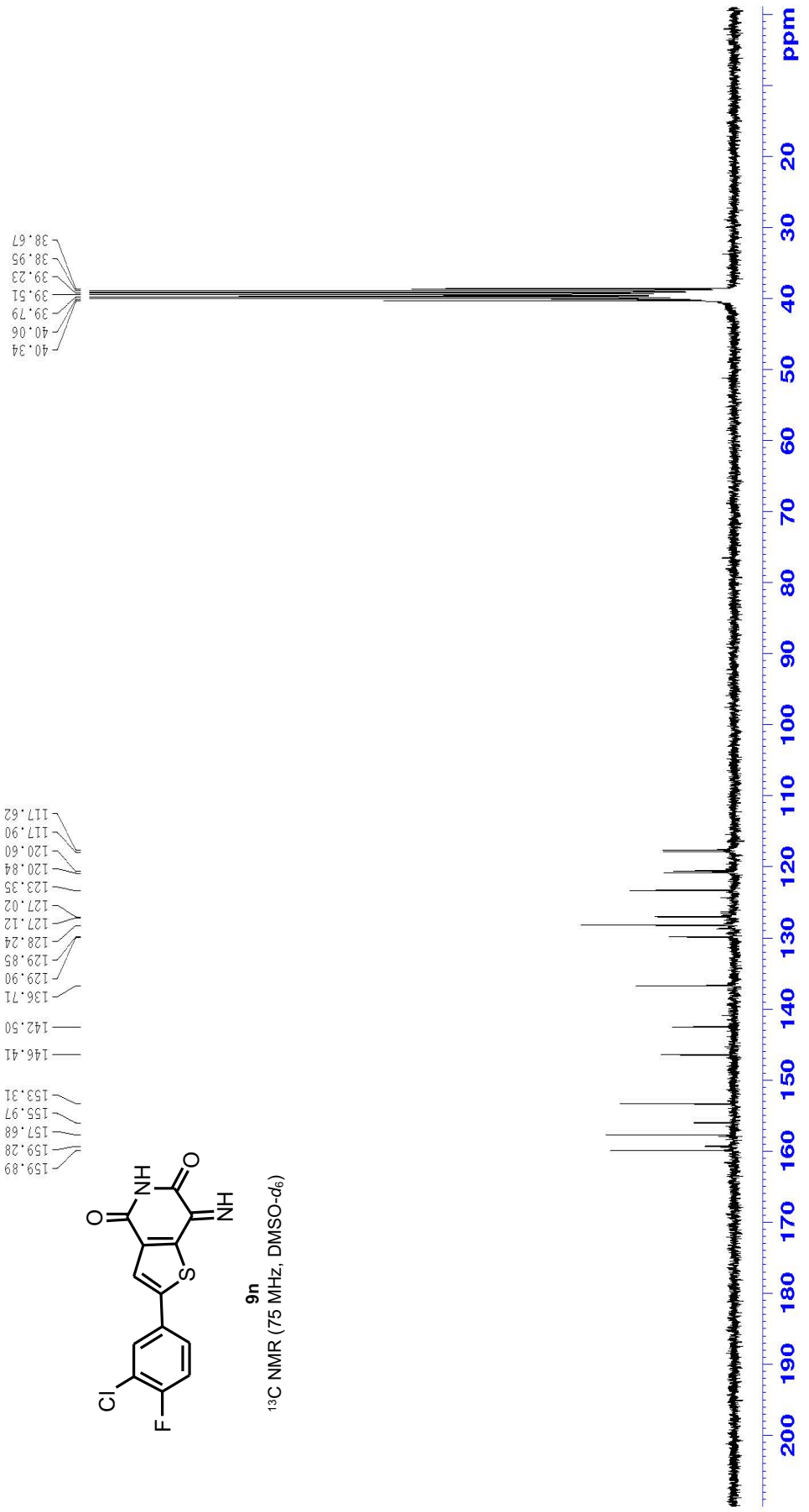

9n

^{13}C NMR (75 MHz, DMSO-d_6)

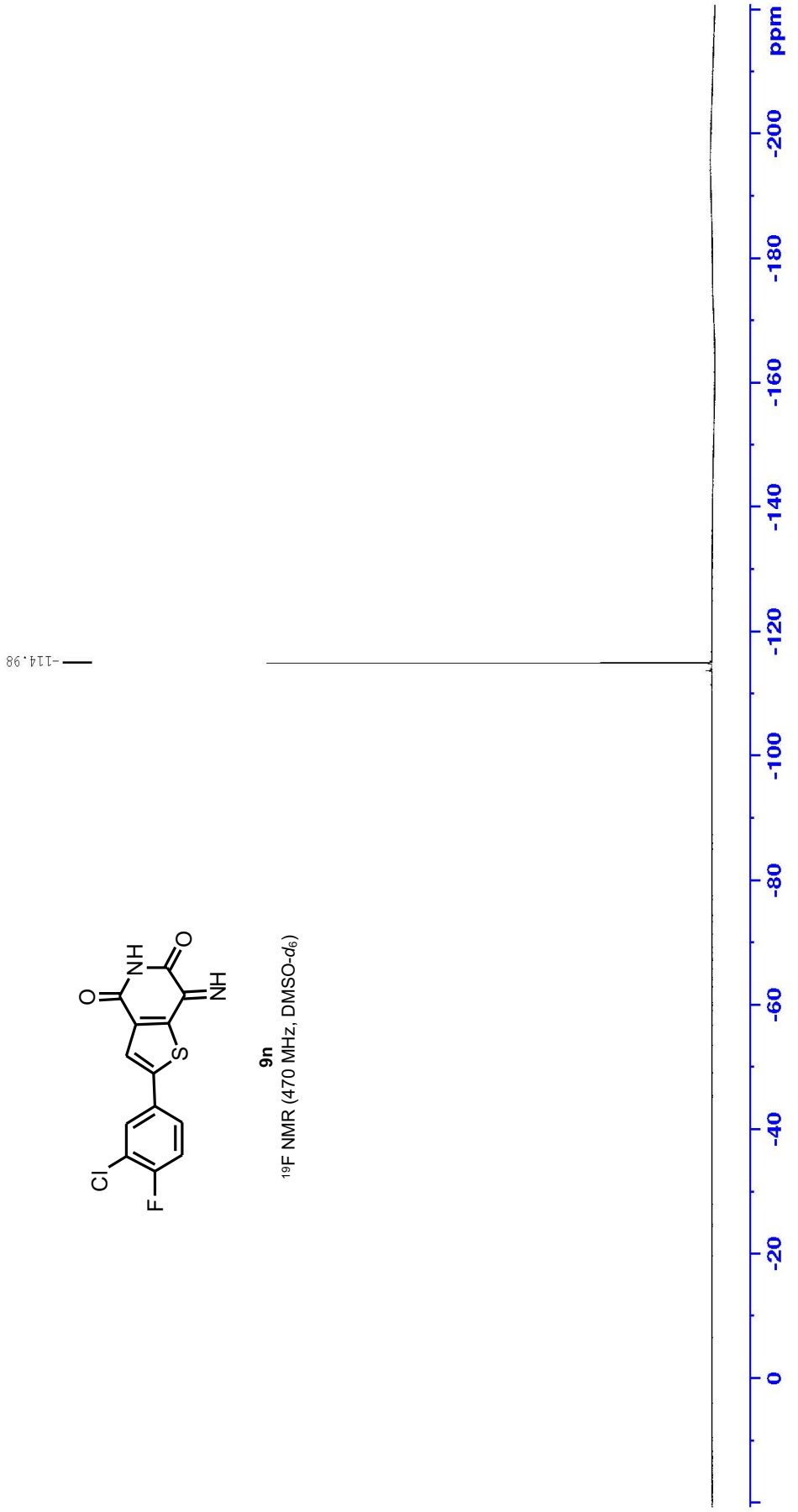

9n

^{19}F NMR (470 MHz, DMSO-d_6)

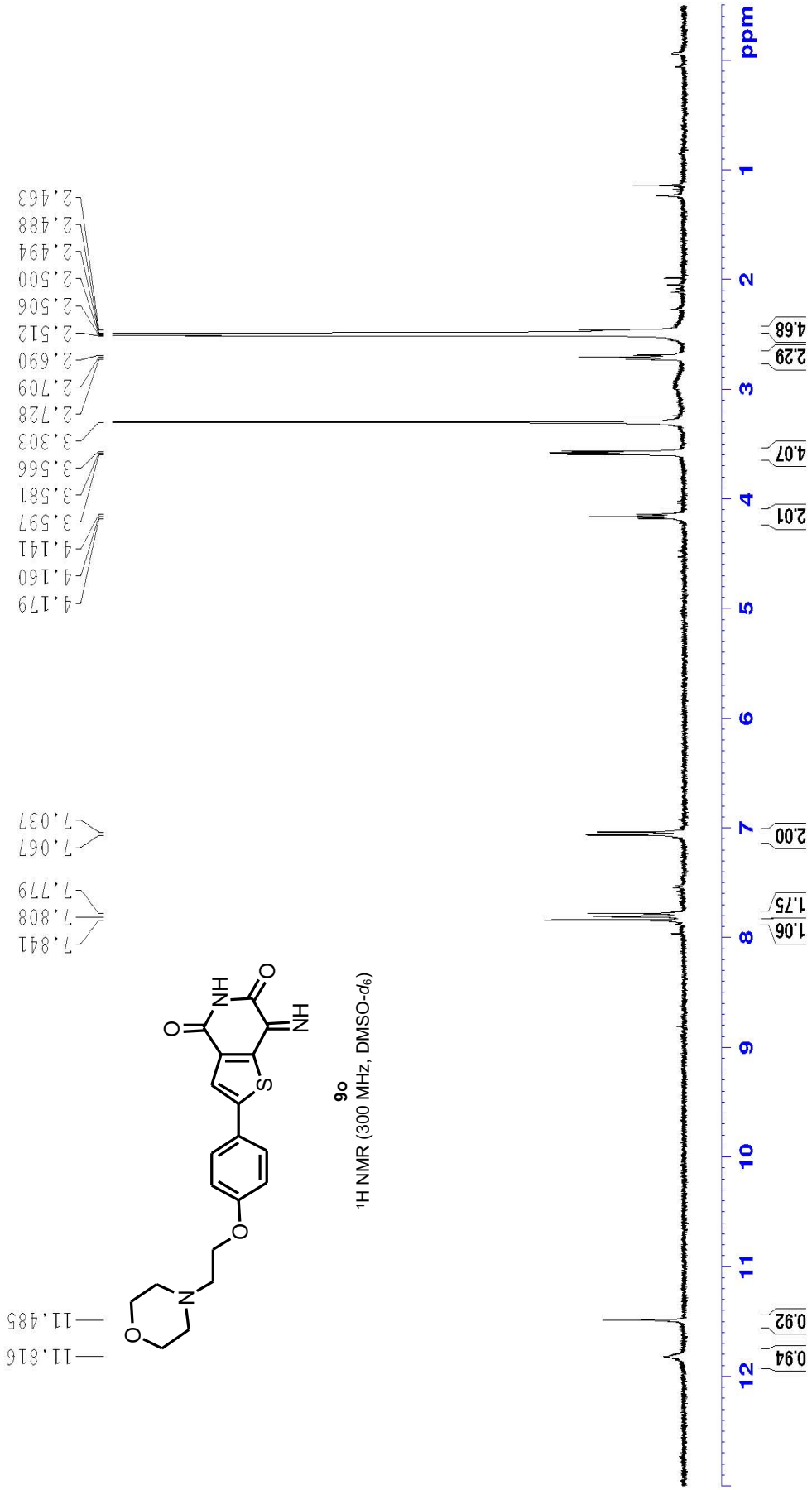

9o

^{1}H NMR (300 MHz, DMSO-d_6)

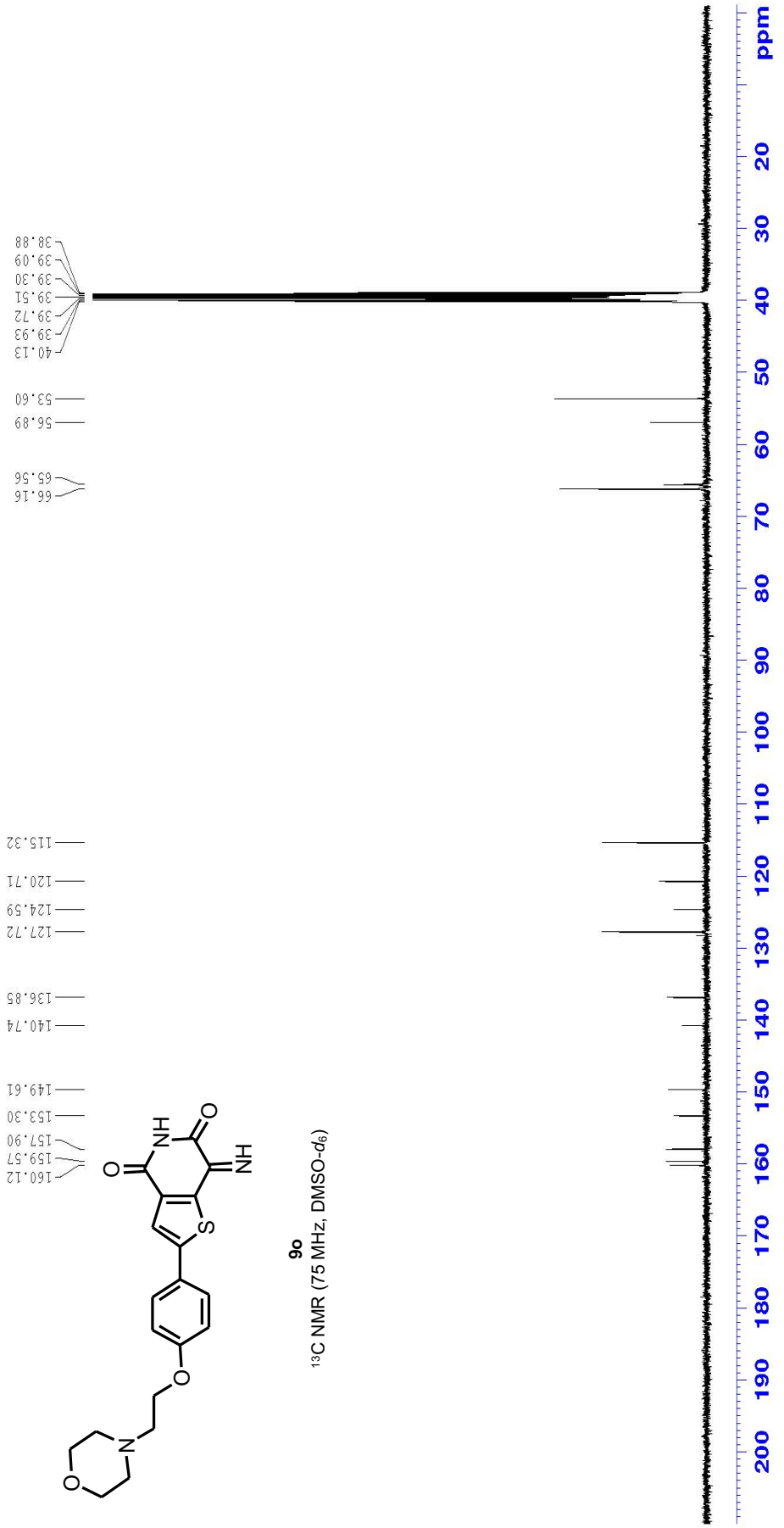

9o

^{13}C NMR (75 MHz, DMSO-d_6)

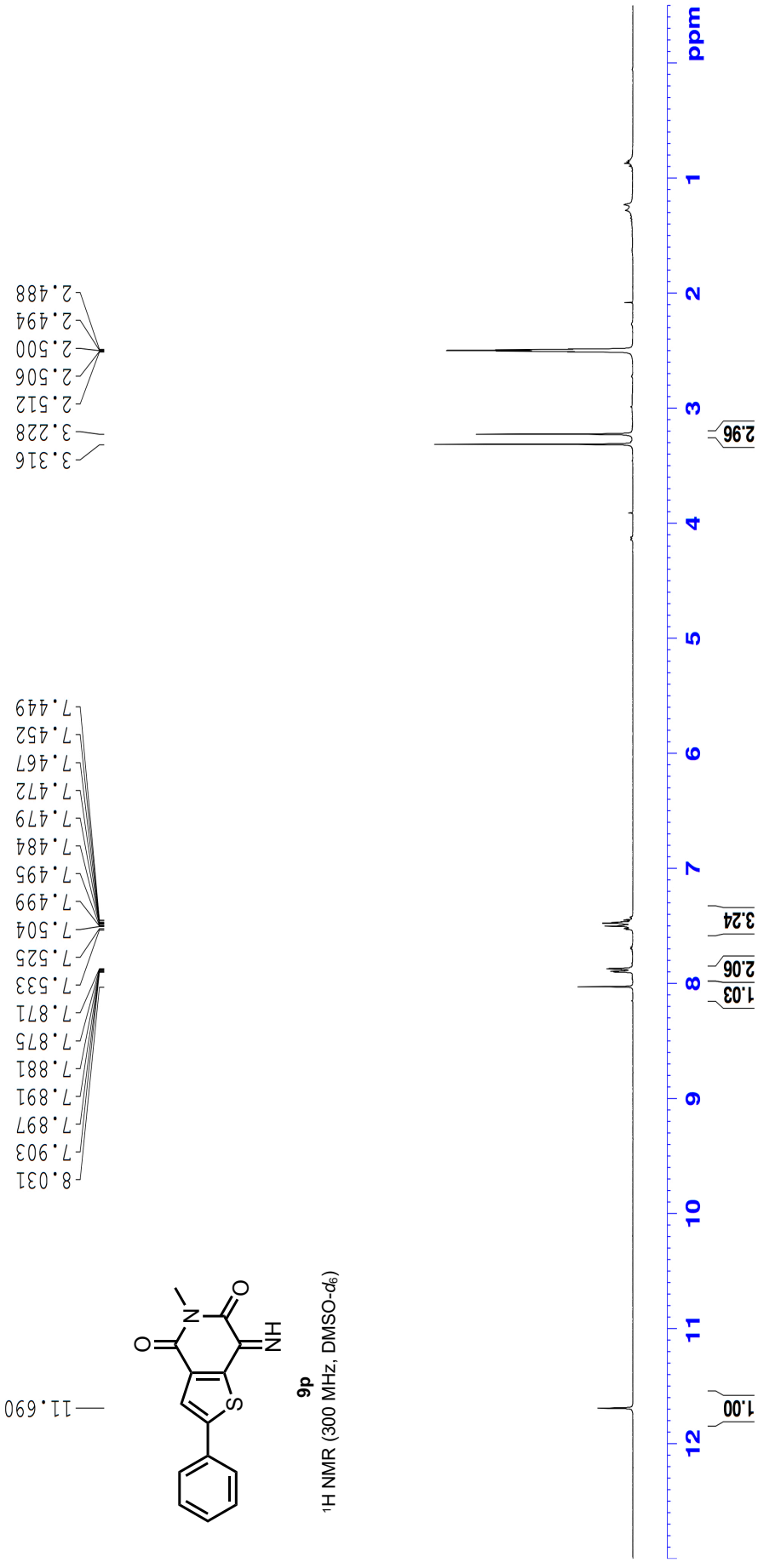
11.690
8.031
7.903
7.897
7.891
7.881
7.875
7.871
7.533
7.525
7.504
7.499
7.495
7.484
7.479
7.472
7.467
7.452
7.449
3.316
3.228
2.512
2.506
2.500
2.494
2.488
2.96
3.24
2.06
1.03
1.00
ppm
1 2 3 4 5 6 7 8 9 10 11 12
9p
^{1}H NMR (300 MHz, DMSO-d_6)

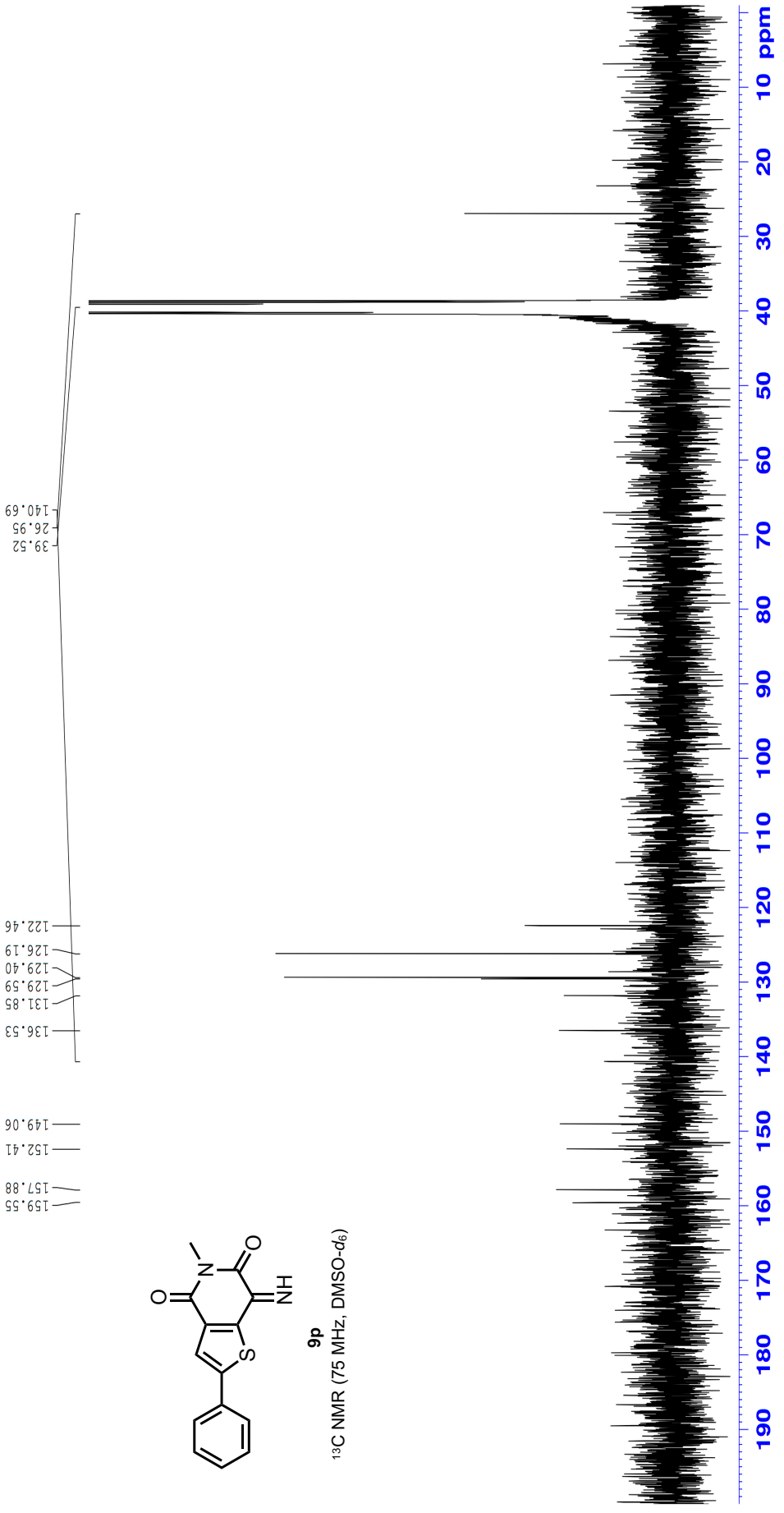
39.52
26.95
140.69
122.46
126.19
129.40
129.59
131.85
136.53
149.06
152.41
157.88
159.55
O
N
O
HN
S
9p
^{13}C NMR (75 MHz, DMSO-d_6)
190
180
170
160
150
140
130
120
110
100
90
80
70
60
50
40
30
20
10
ppm

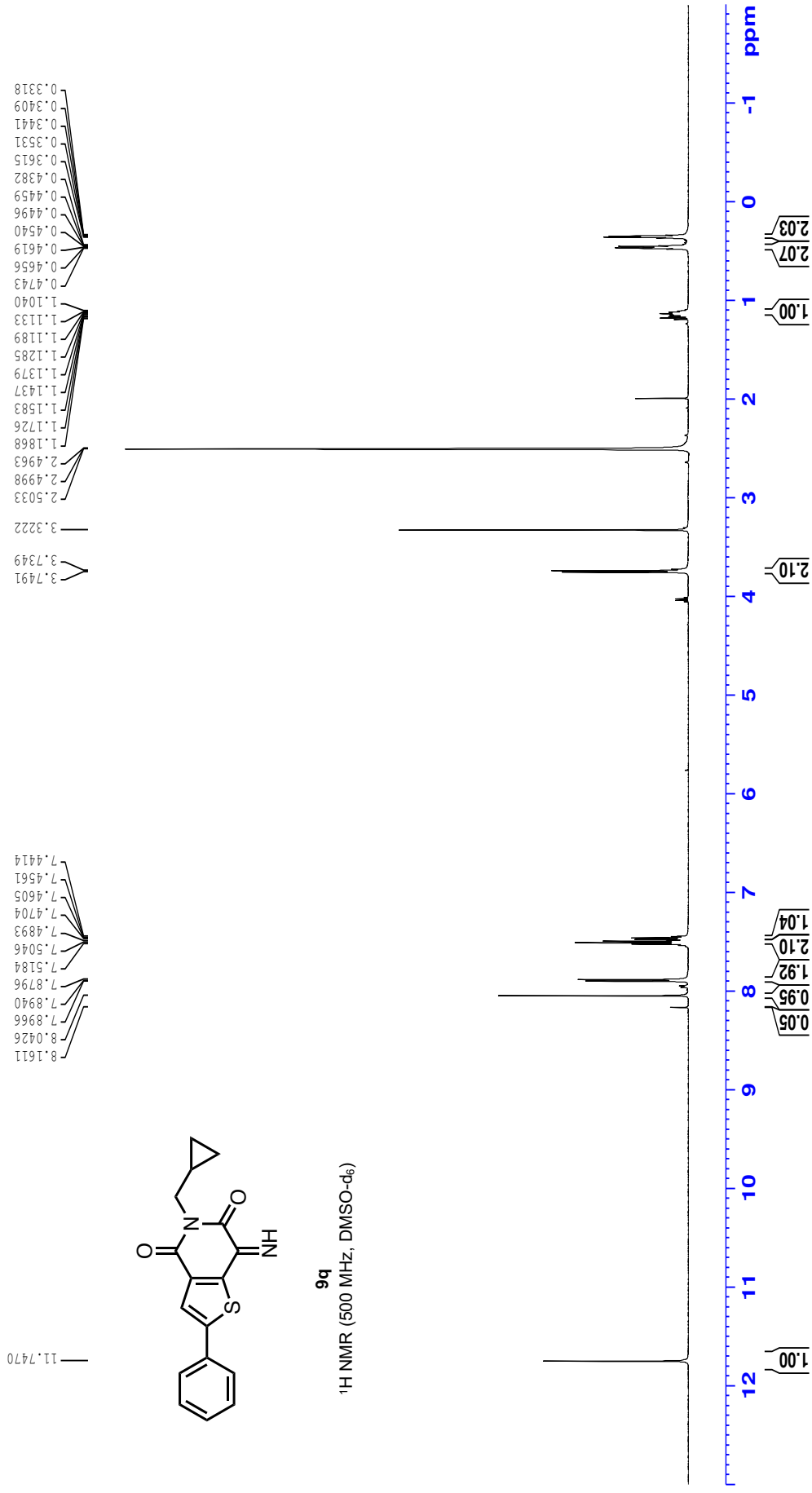

9q

^{1}H NMR (500 MHz, DMSO-d_6)

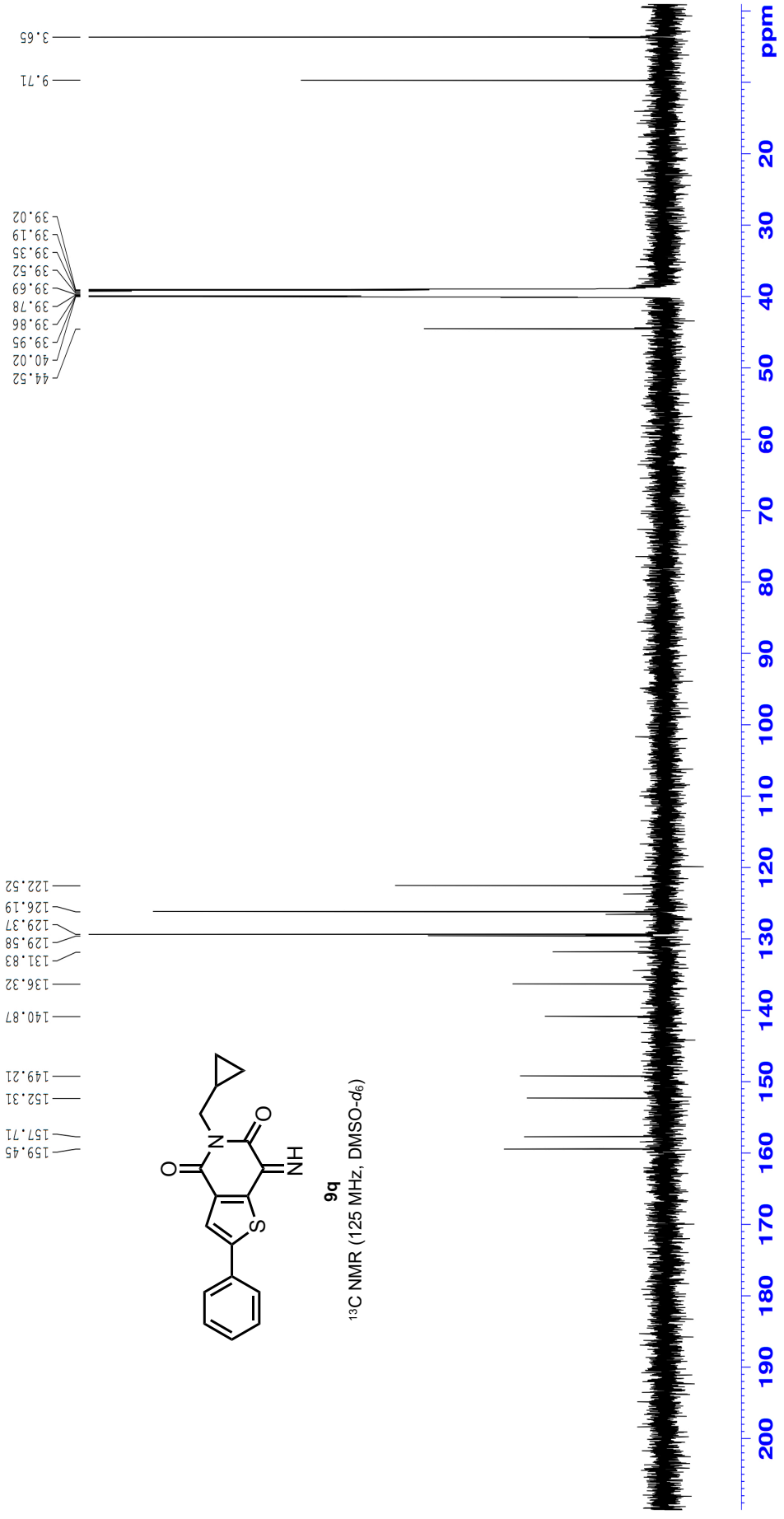
3.65
9.71
39.02
39.19
39.35
39.52
39.69
39.78
39.86
39.95
40.02
44.52
122.52
126.19
129.37
129.58
131.83
136.32
140.87
149.21
152.31
157.71
159.45
O
N
O
NH
S
9q
^{13}C NMR (125 MHz, DMSO-d_6)
ppm
200
190
180
170
160
150
140
130
120
110
100
90
80
70
60
50
40
30
20

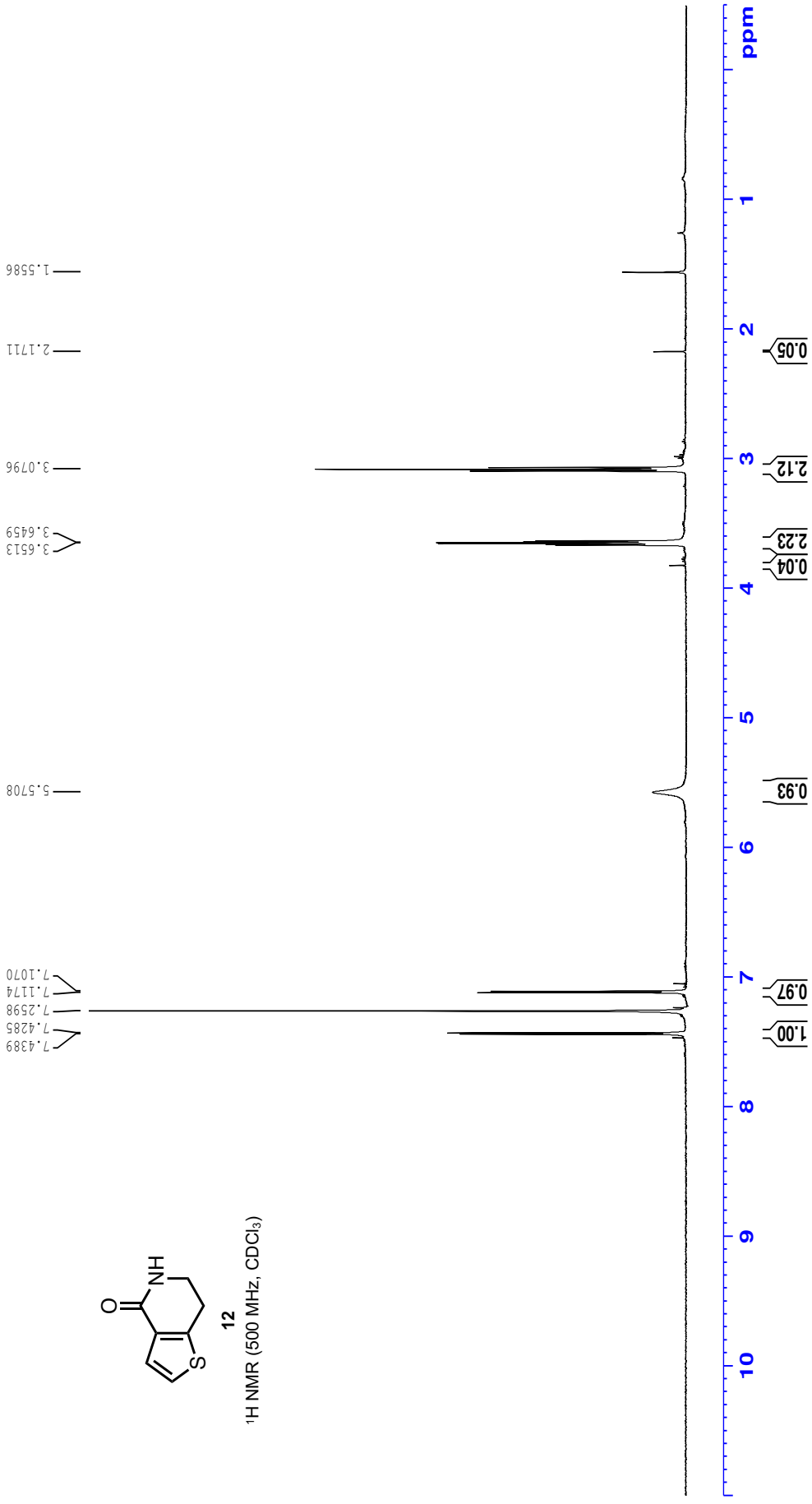

12

^{1}H NMR (500 MHz, $CDCl_3$)

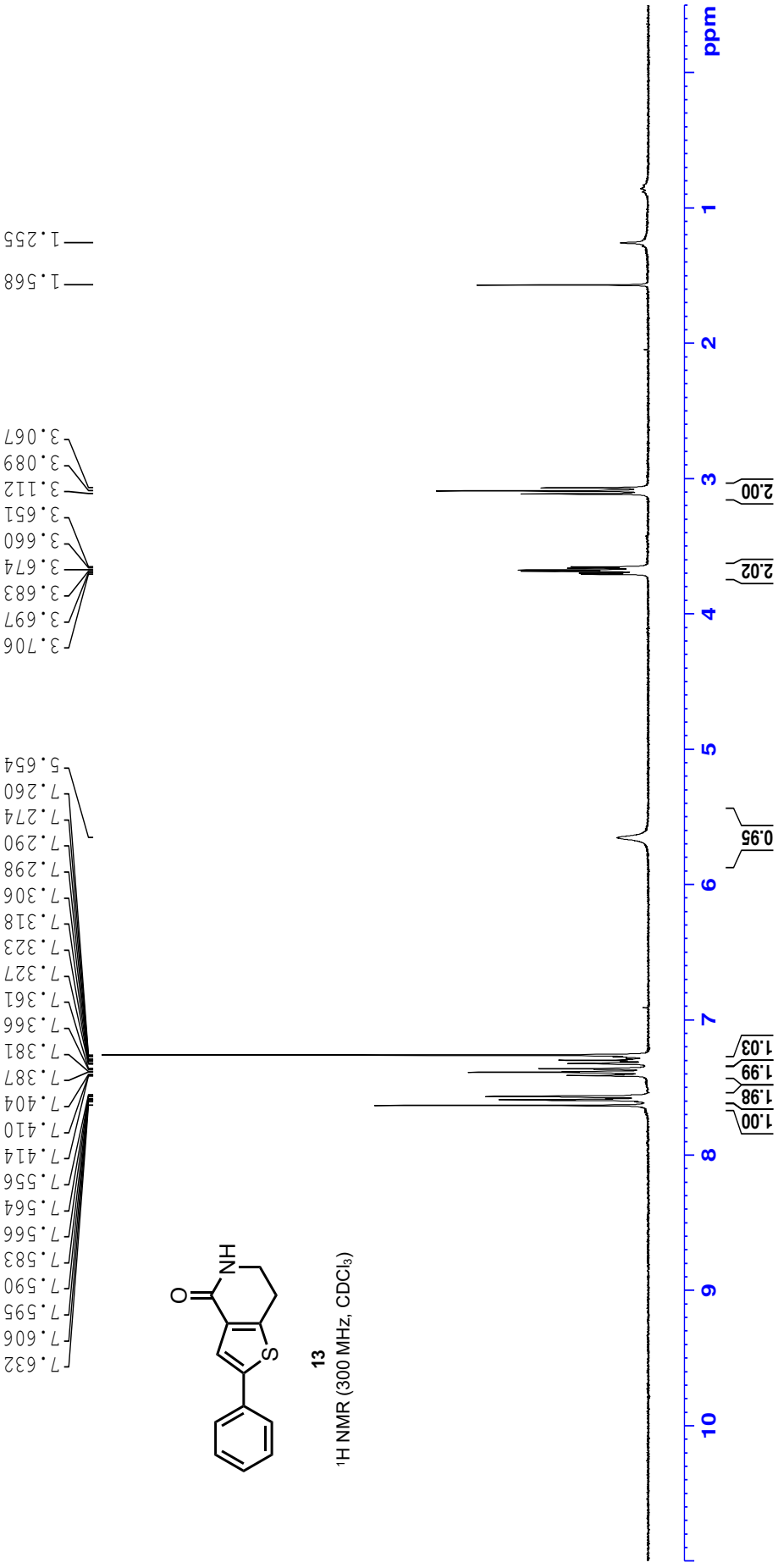
13
^{1}H NMR (300 MHz, CDCl$_3$)
ppm
1 2 3 4 5 6 7 8 9 10
2.00
2.02
0.95
1.03
1.99
1.98
1.00
1.255
1.568
3.067
3.089
3.112
3.651
3.660
3.674
3.683
3.697
3.706
5.654
7.260
7.274
7.290
7.298
7.306
7.318
7.323
7.327
7.361
7.366
7.381
7.387
7.404
7.410
7.414
7.556
7.564
7.566
7.583
7.590
7.595
7.606
7.632

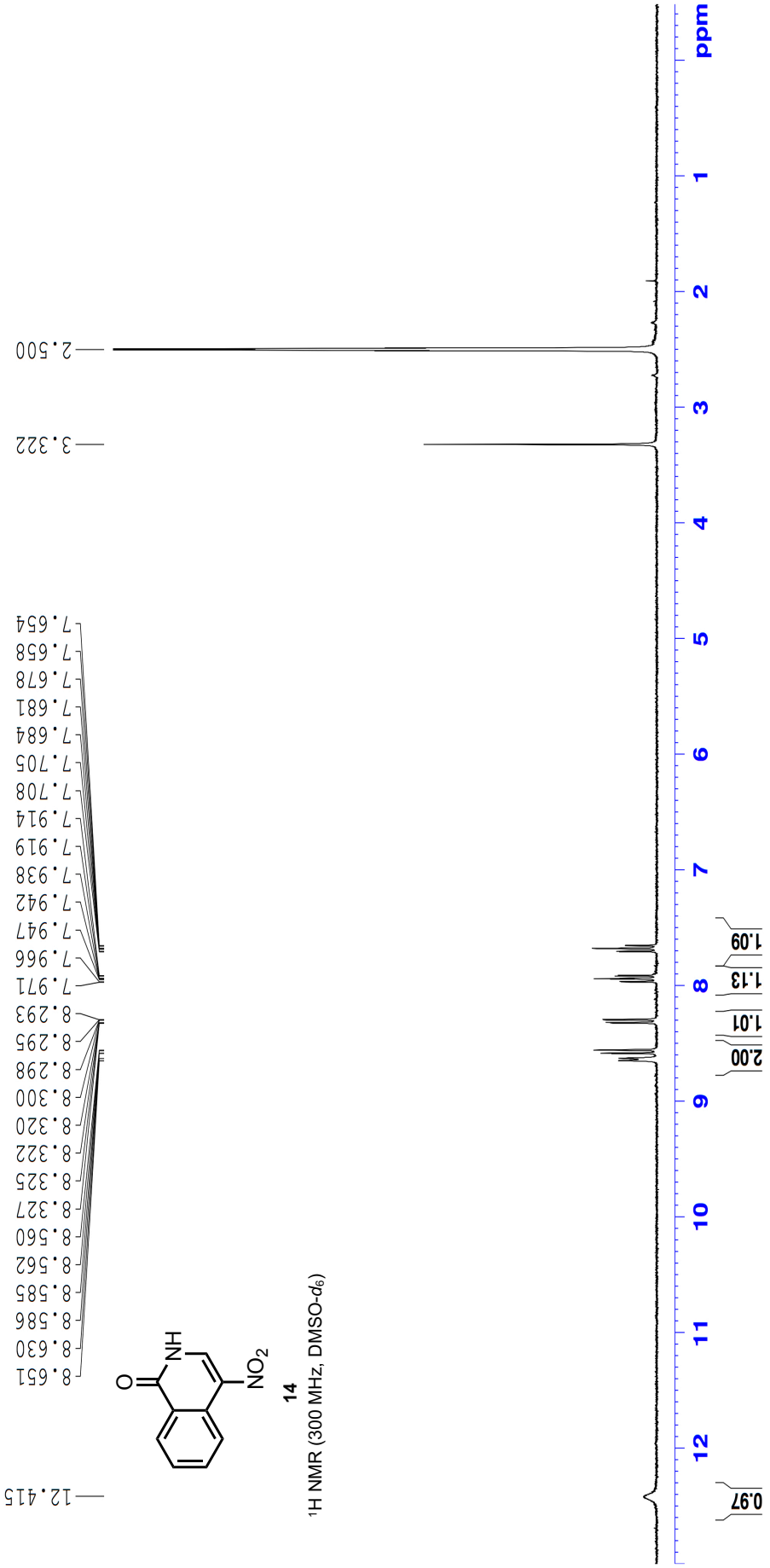

14

^{1}H NMR (300 MHz, DMSO-d_6)

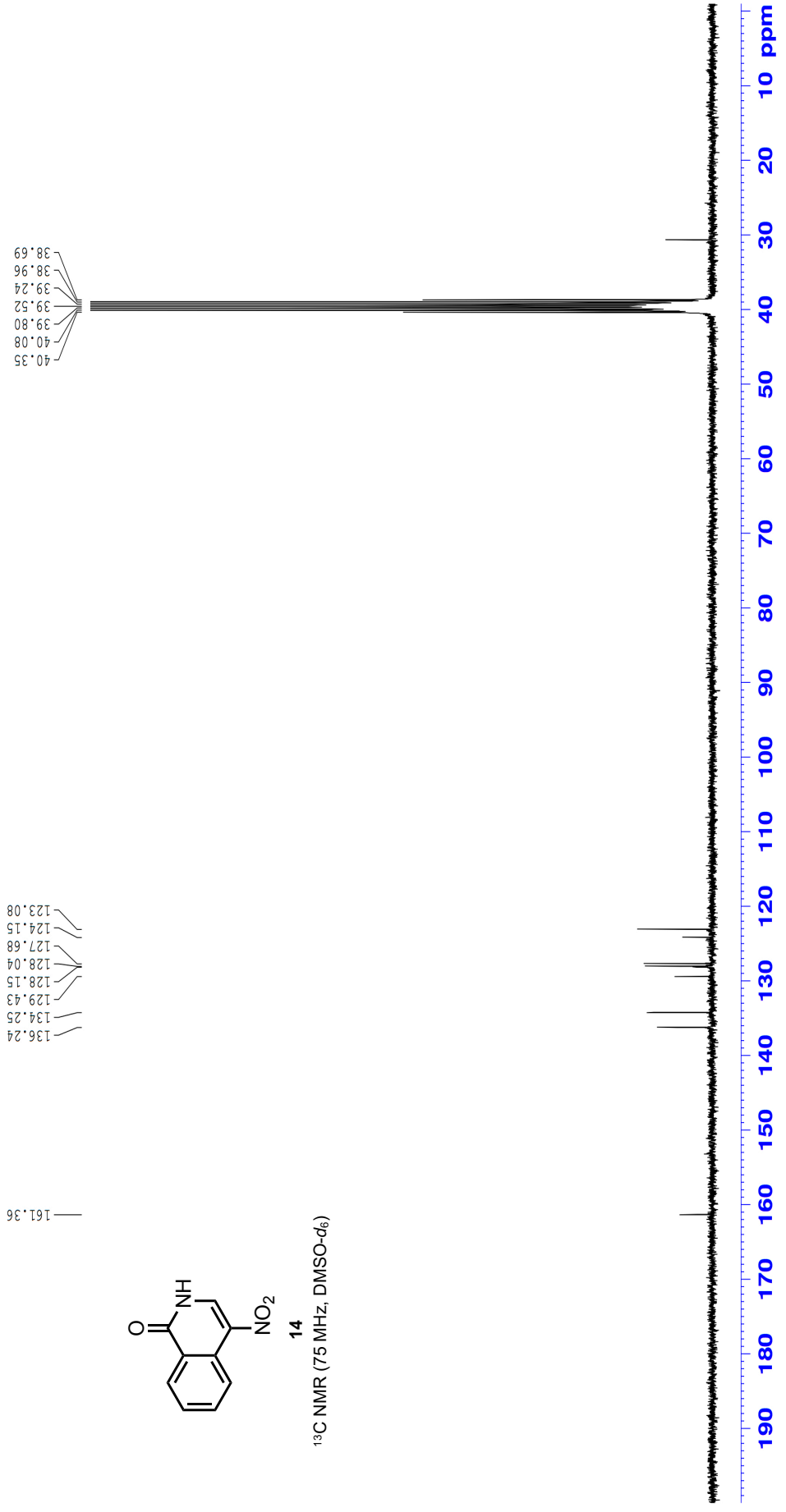

14

^{13}C NMR (75 MHz, DMSO-d_6)

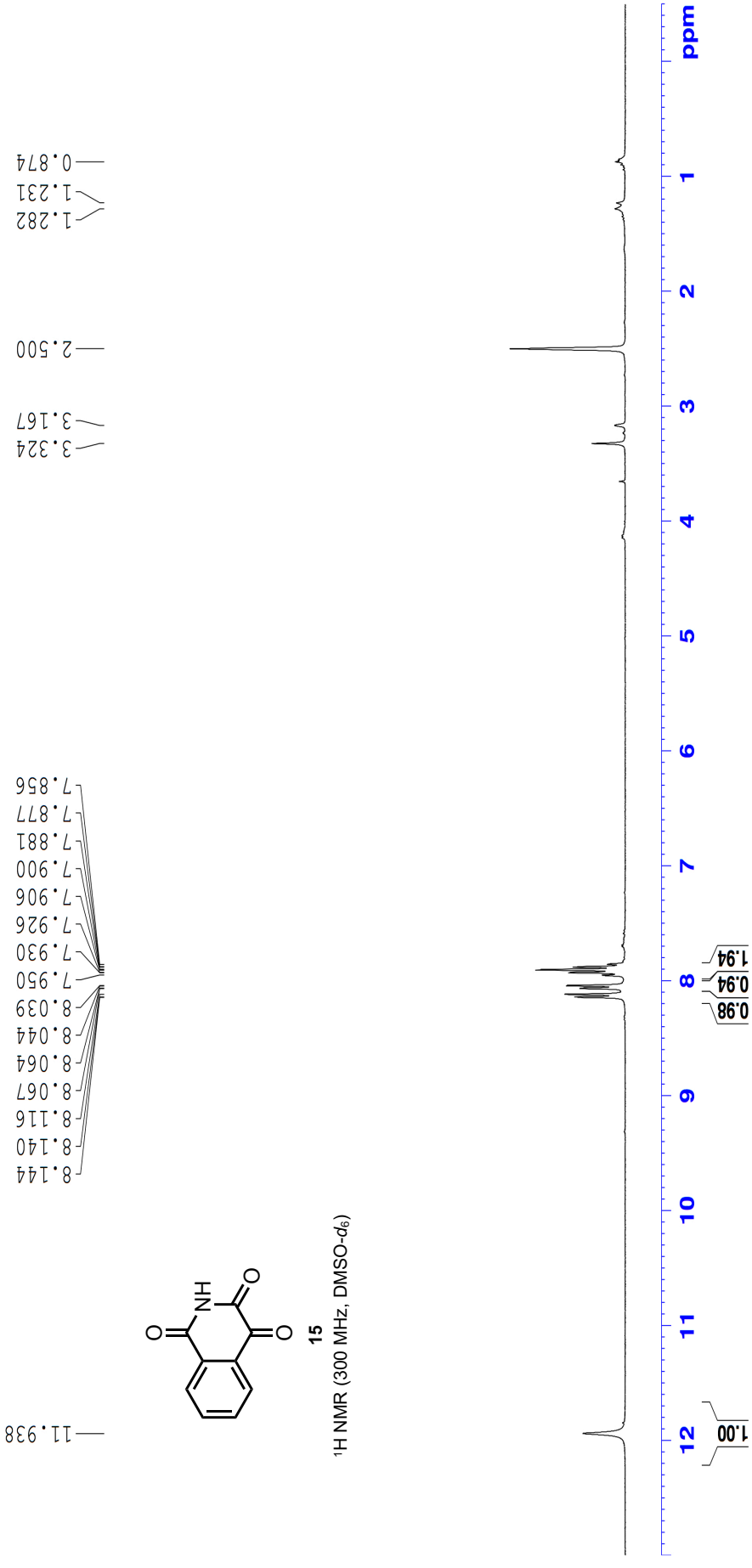

15

^{1}H NMR (300 MHz, DMSO-d_6)

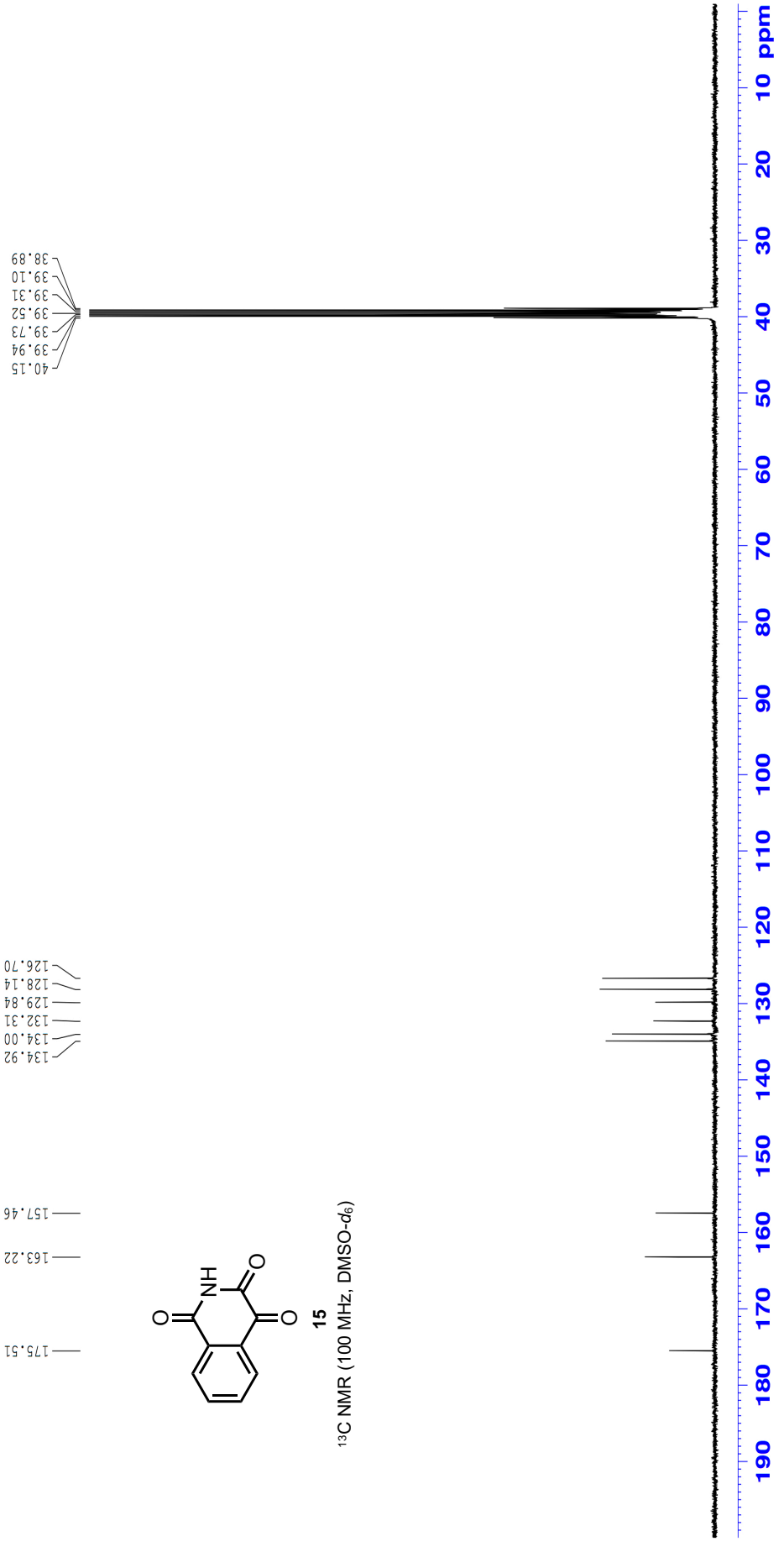

15

^{13}C NMR (100 MHz, DMSO-d_6)

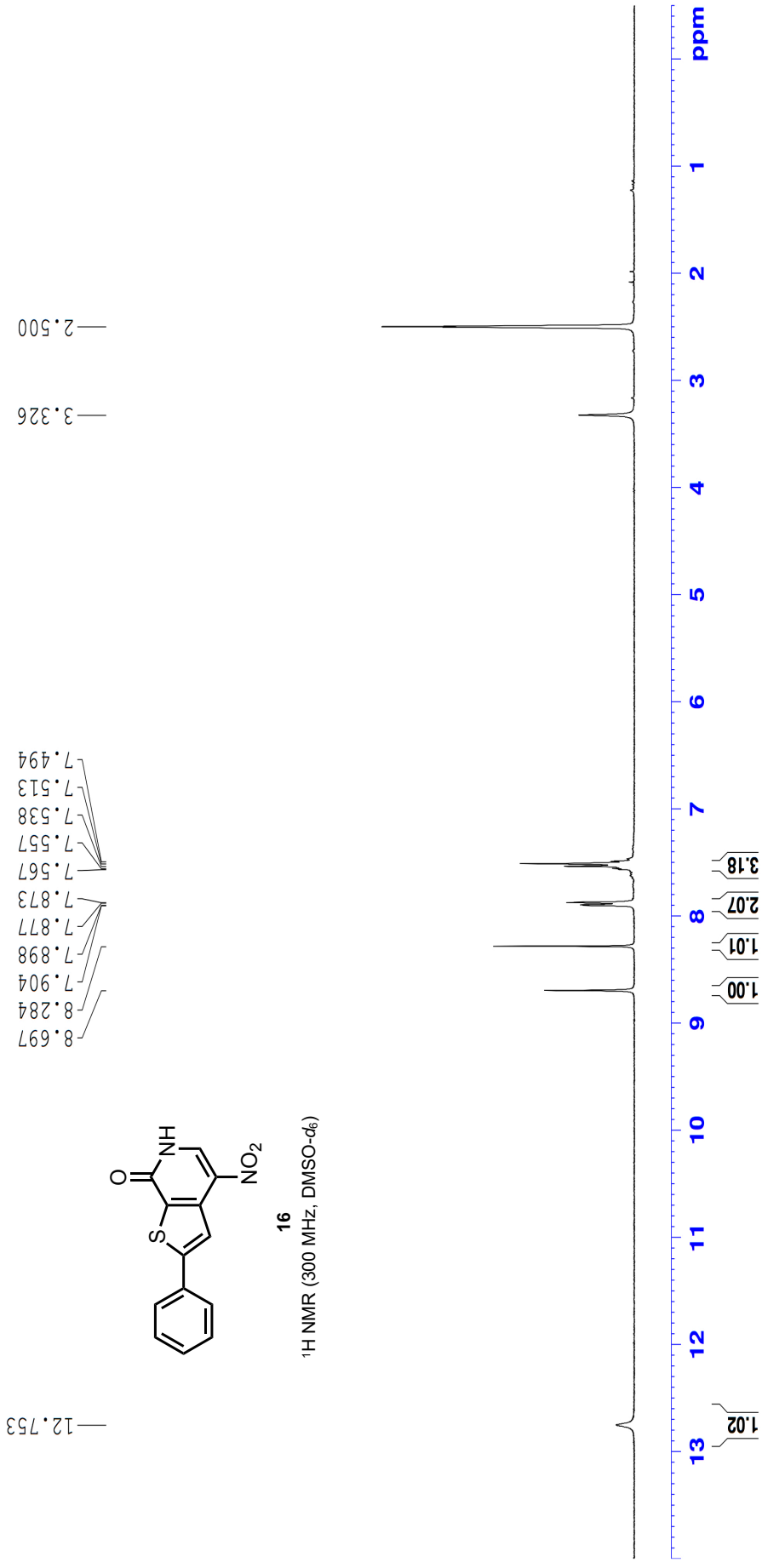

16

^{1}H NMR (300 MHz, DMSO-d_6)

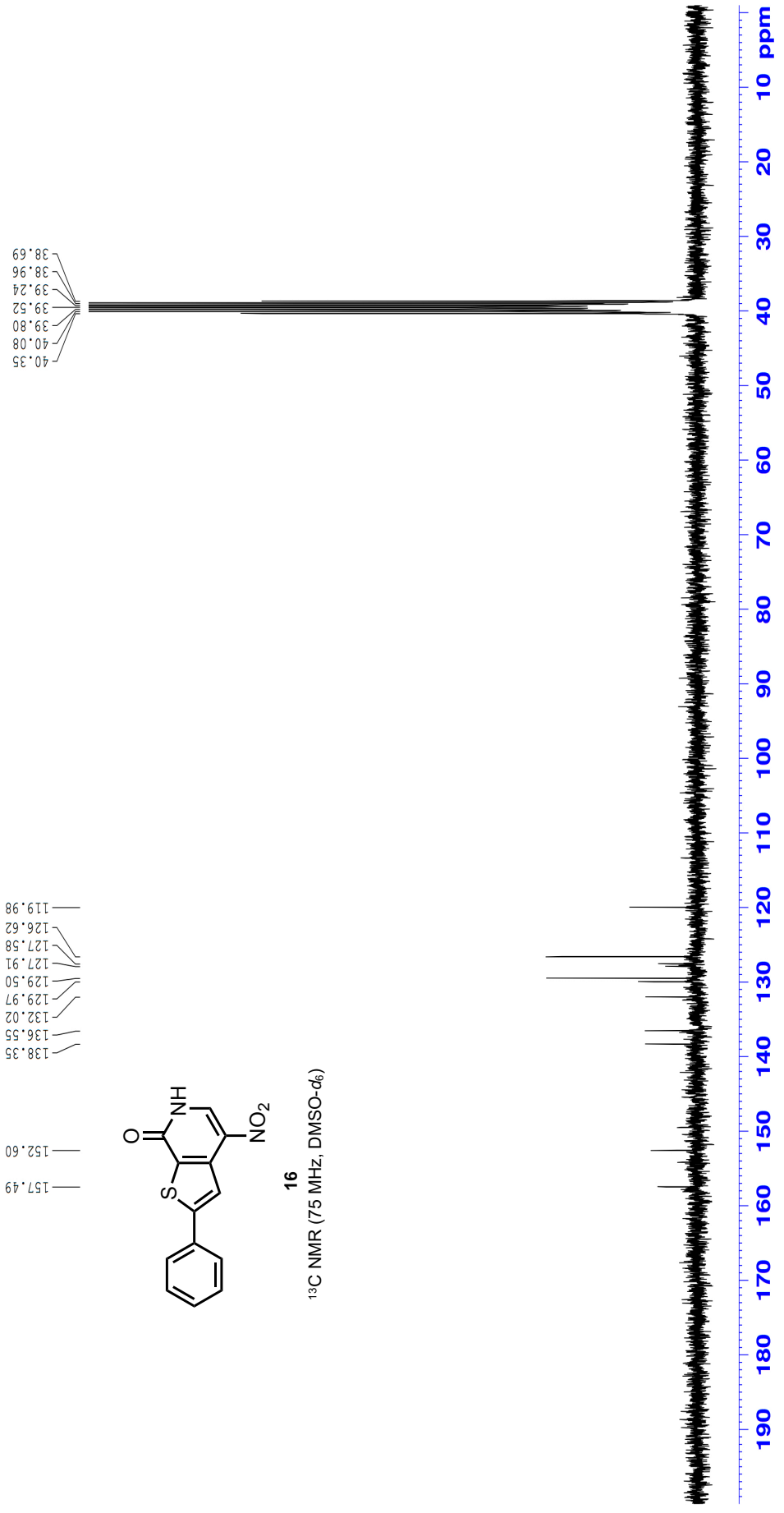
38.69
38.96
39.24
39.52
39.80
40.08
40.35
119.98
126.62
127.58
127.91
129.50
129.97
132.02
136.55
138.35
152.60
157.49
NH
O
S
NO2
16
13C NMR (75 MHz, DMSO-d6)
ppm
10
20
30
40
50
60
70
80
90
100
110
120
130
140
150
160
170
180
190

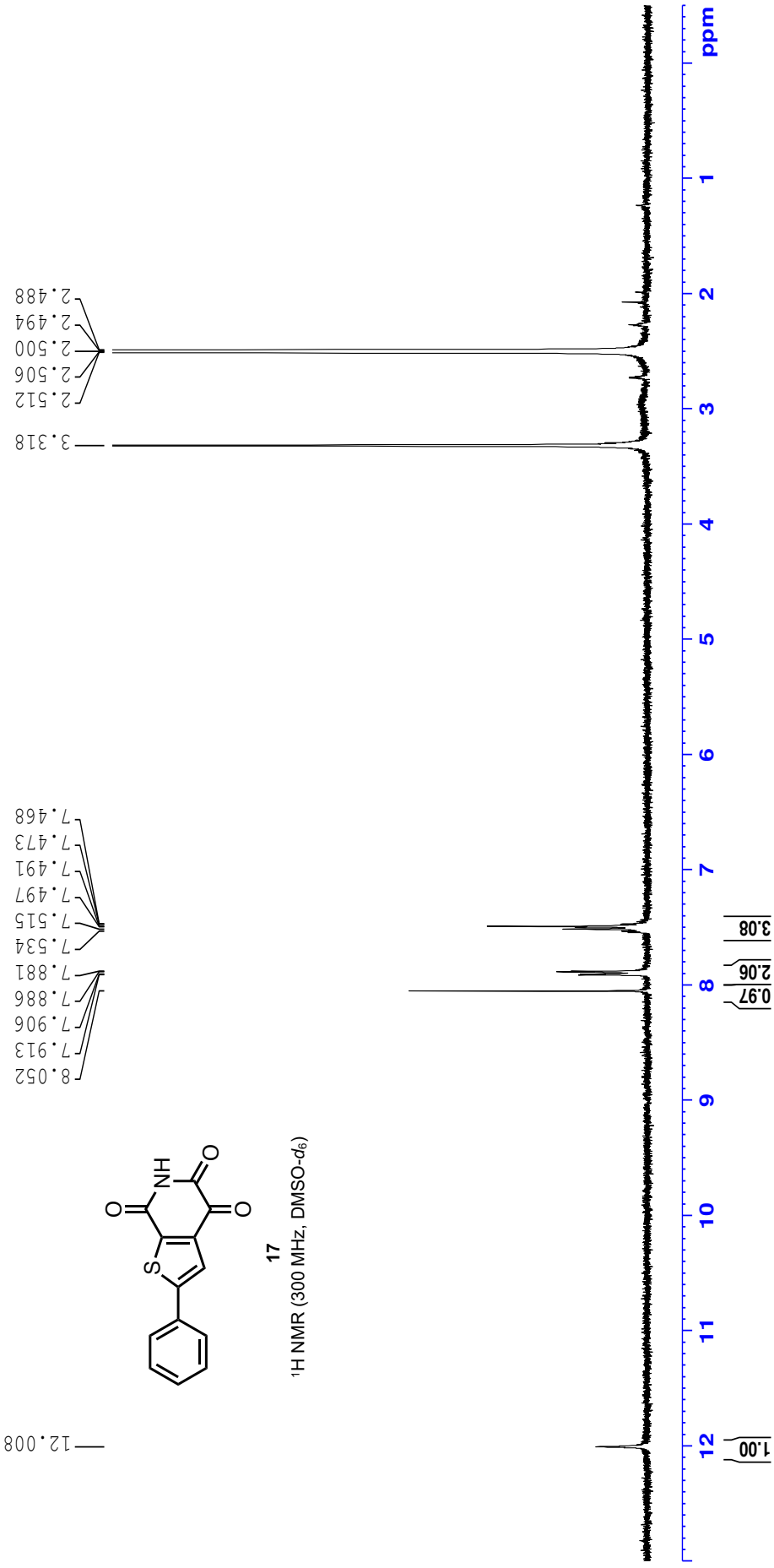

17

^{1}H NMR (300 MHz, DMSO-d_6)

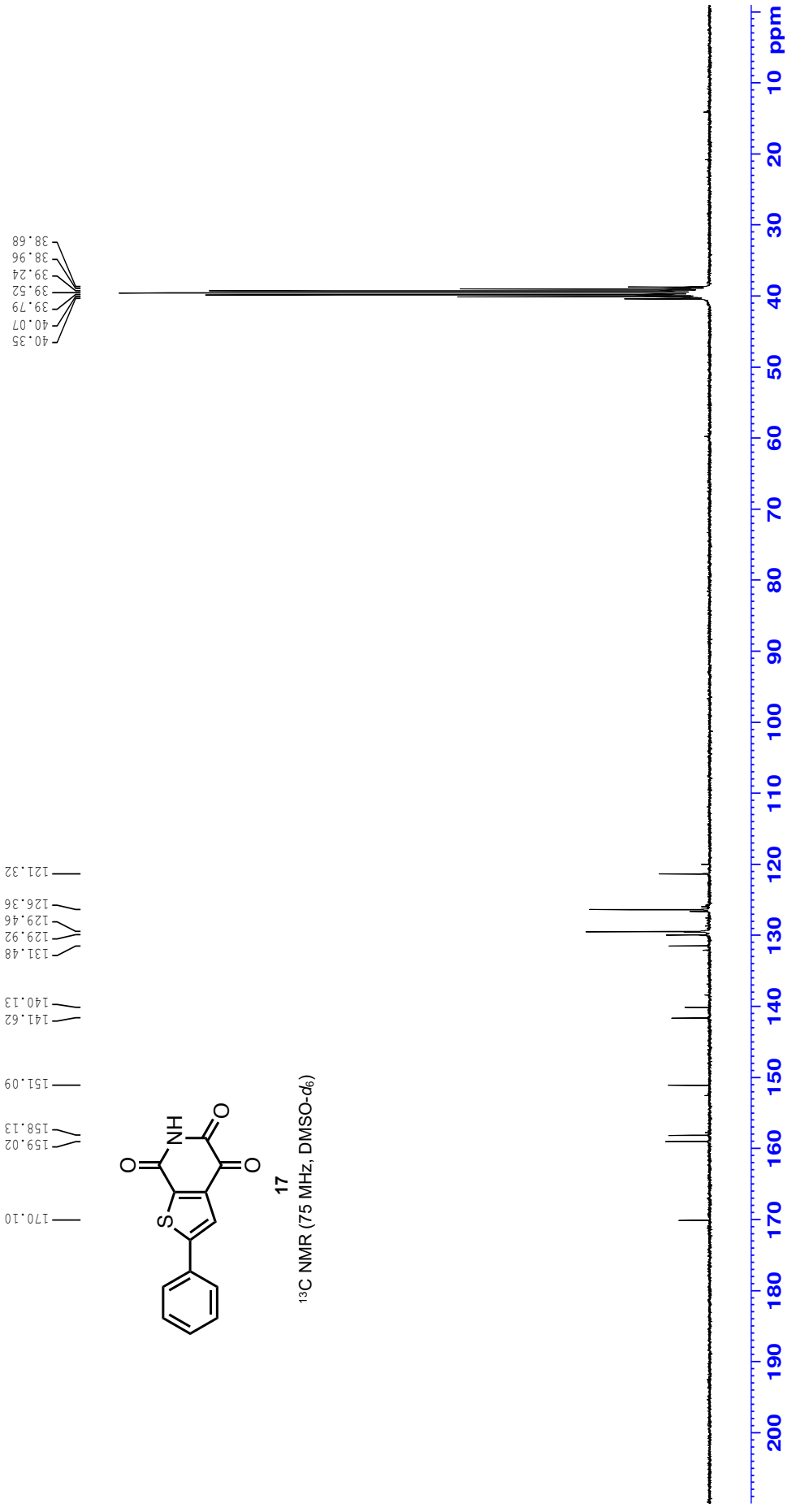
38.68
38.96
39.24
39.52
39.79
40.07
40.35
121.32
126.36
129.46
129.92
131.48
140.13
141.62
151.09
158.13
159.02
170.10
NH
O
O
O
S
17
^{13}C NMR (75 MHz, DMSO-d_6)
ppm

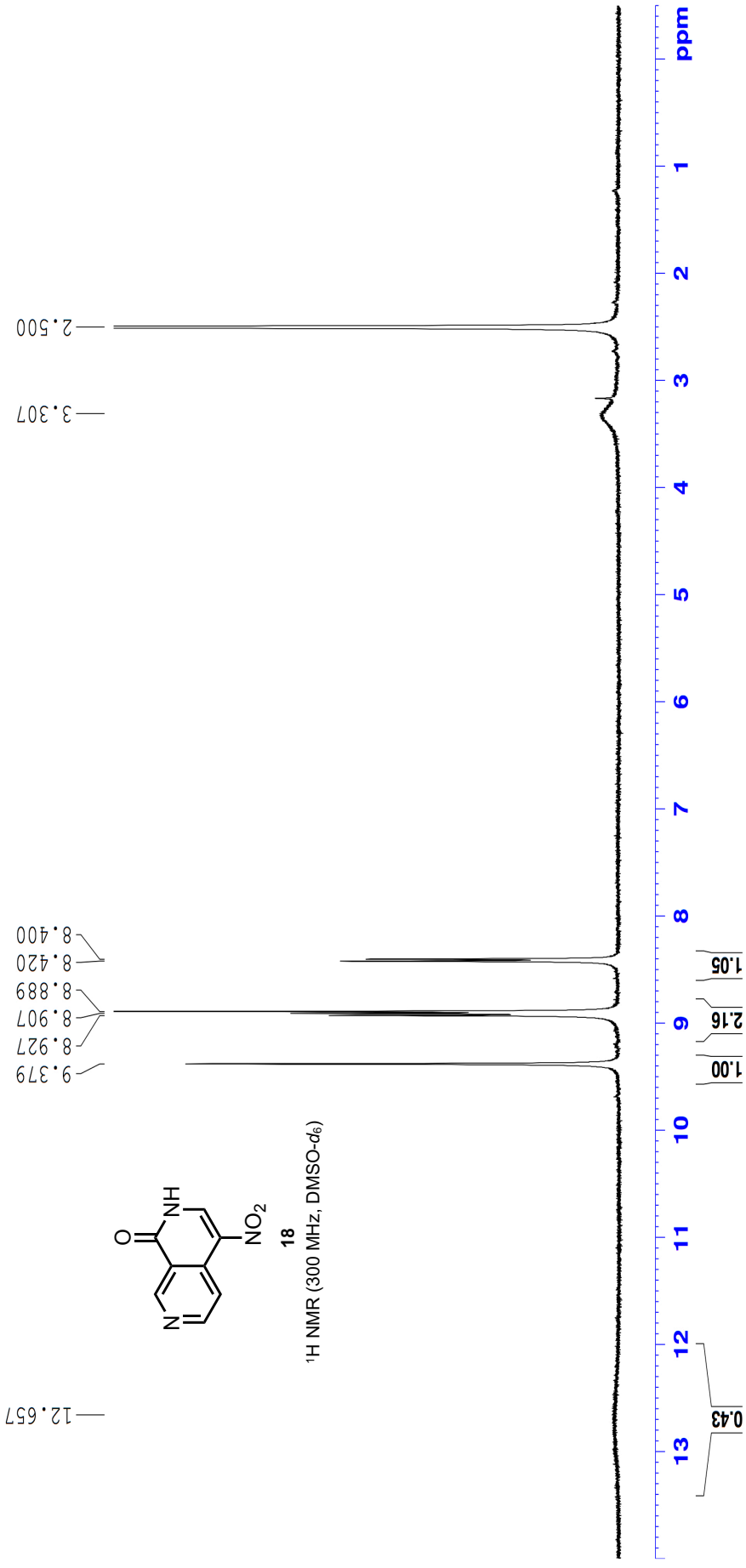
12.657
9.379
8.927
8.907
8.889
8.420
8.400
3.307
2.500
ppm
1
2
3
4
5
6
7
8
9
10
11
12
13
1.00
2.16
1.05
0.43
NH
O
NO2
N
18
1H NMR (300 MHz, DMSO-d6)

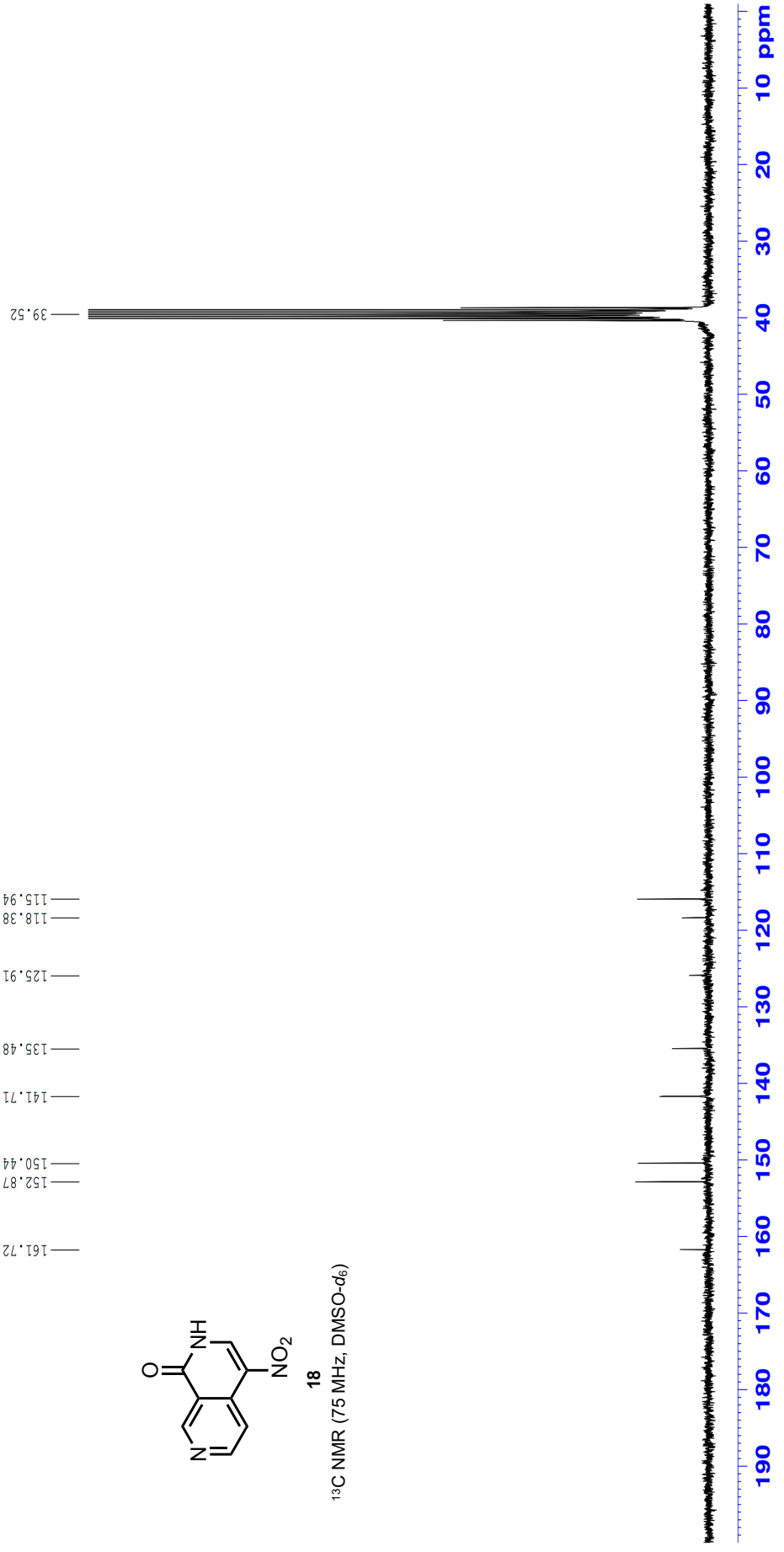

18

^{13}C NMR (75 MHz, DMSO-d_6)

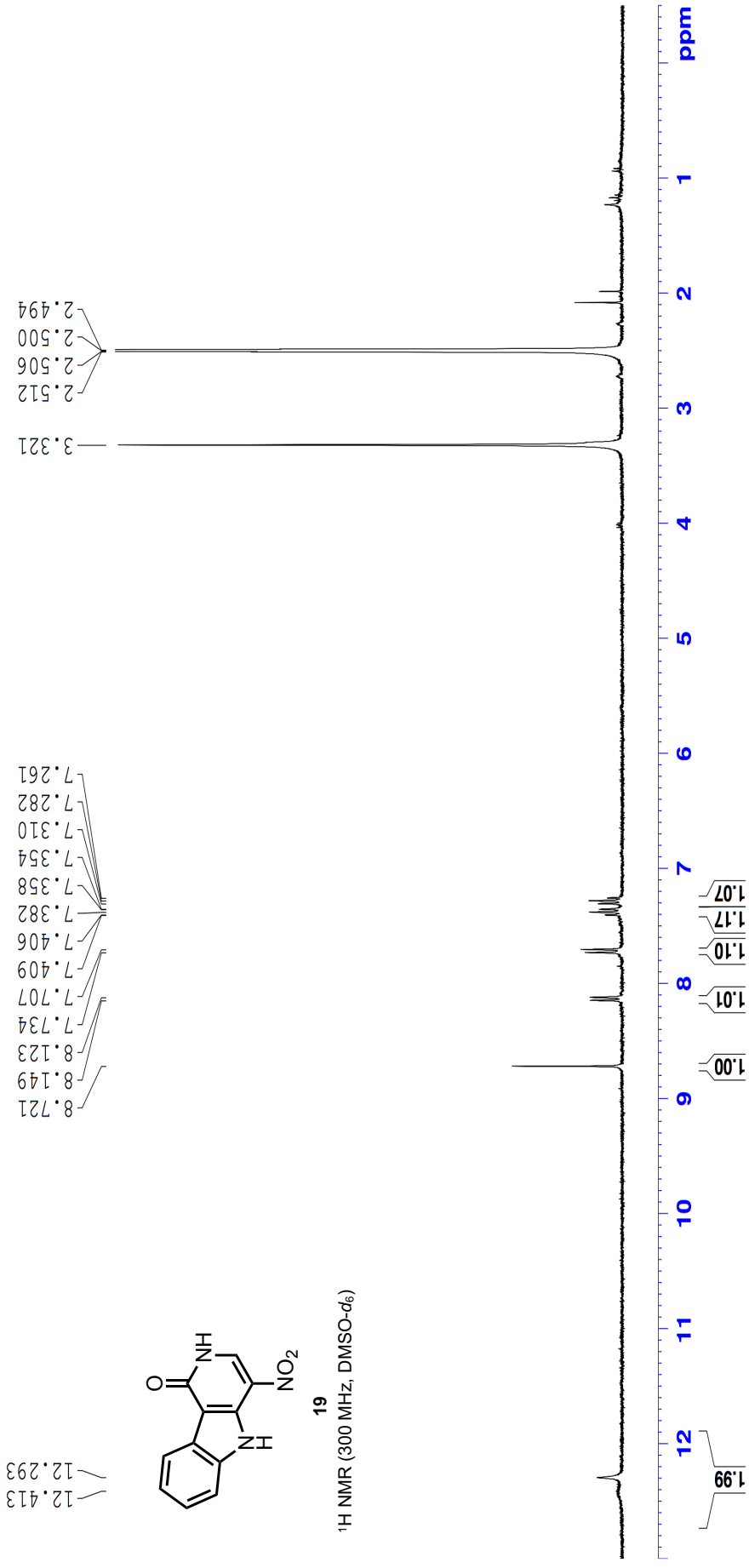

19

^{1}H NMR (300 MHz, DMSO-d_6)

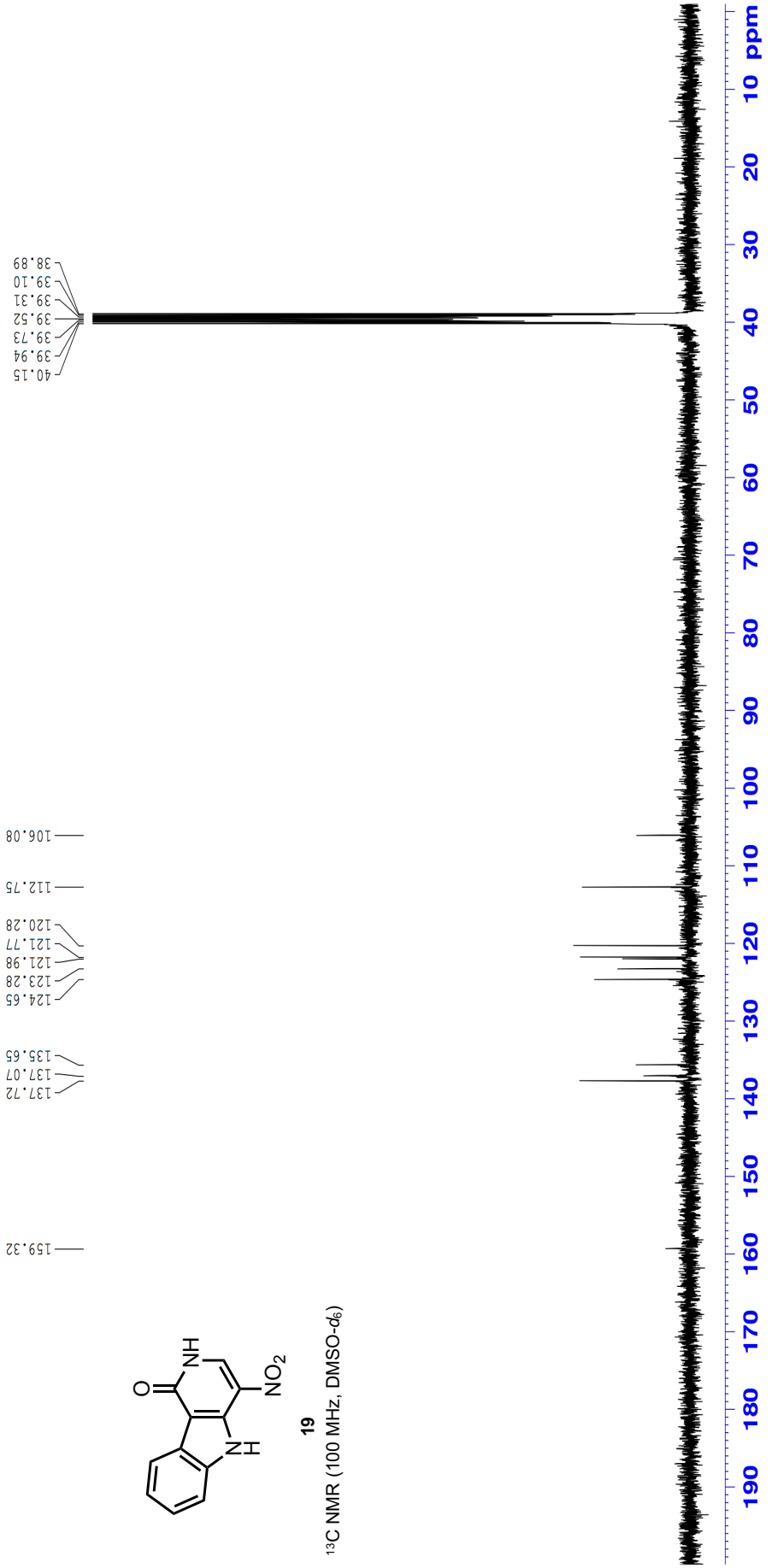

19

^{13}C NMR (100 MHz, DMSO-d_6)

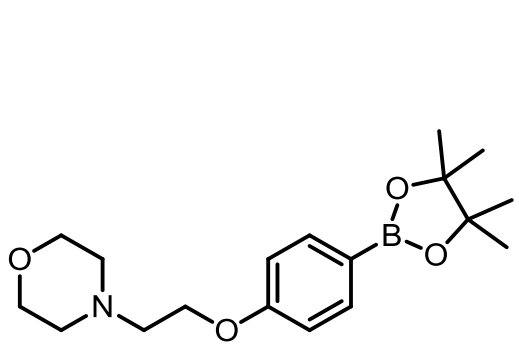

24

^{1}H NMR (400 MHz, DMSO-d_6)

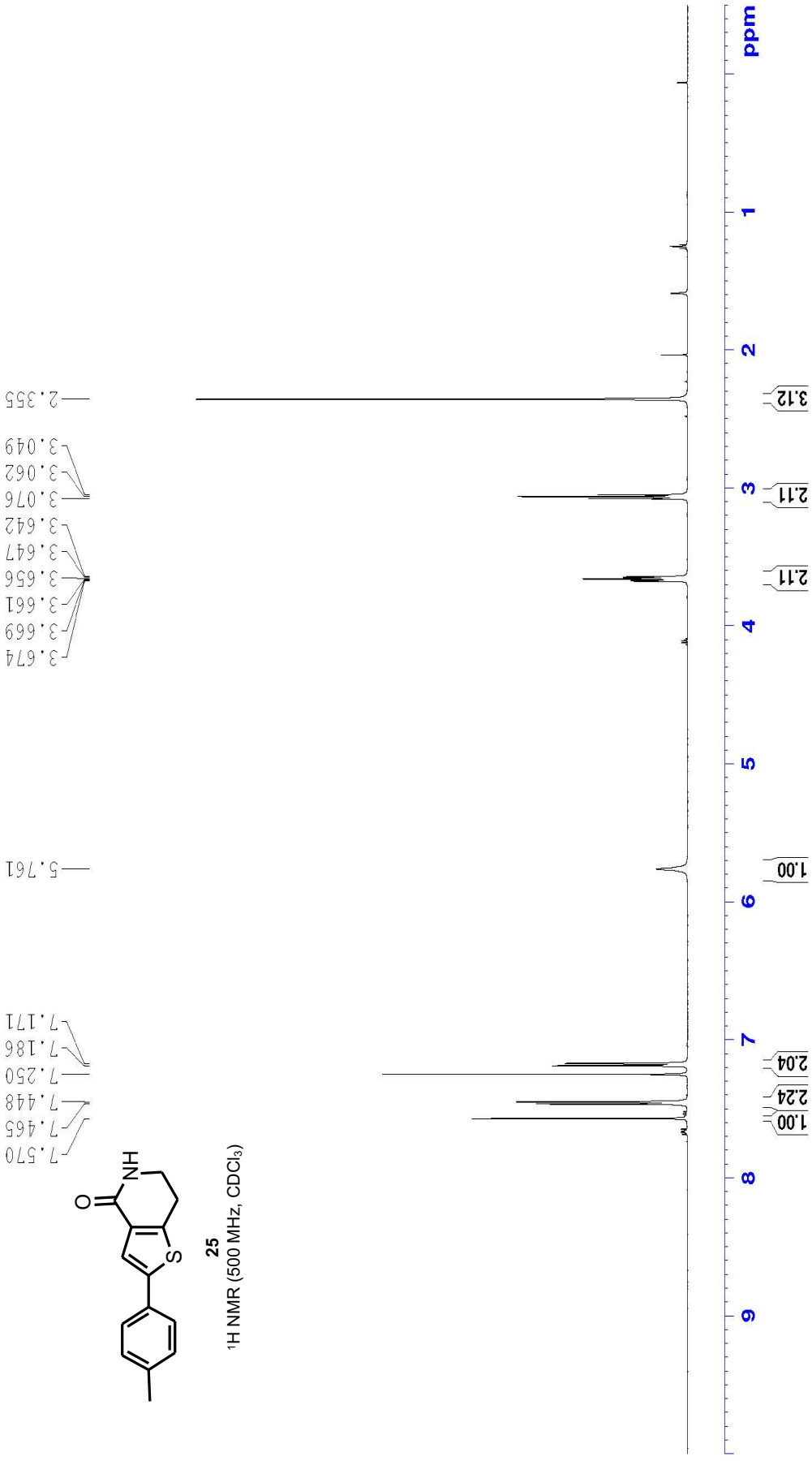

25

^{1}H NMR (500 MHz, $CDCl_3$)

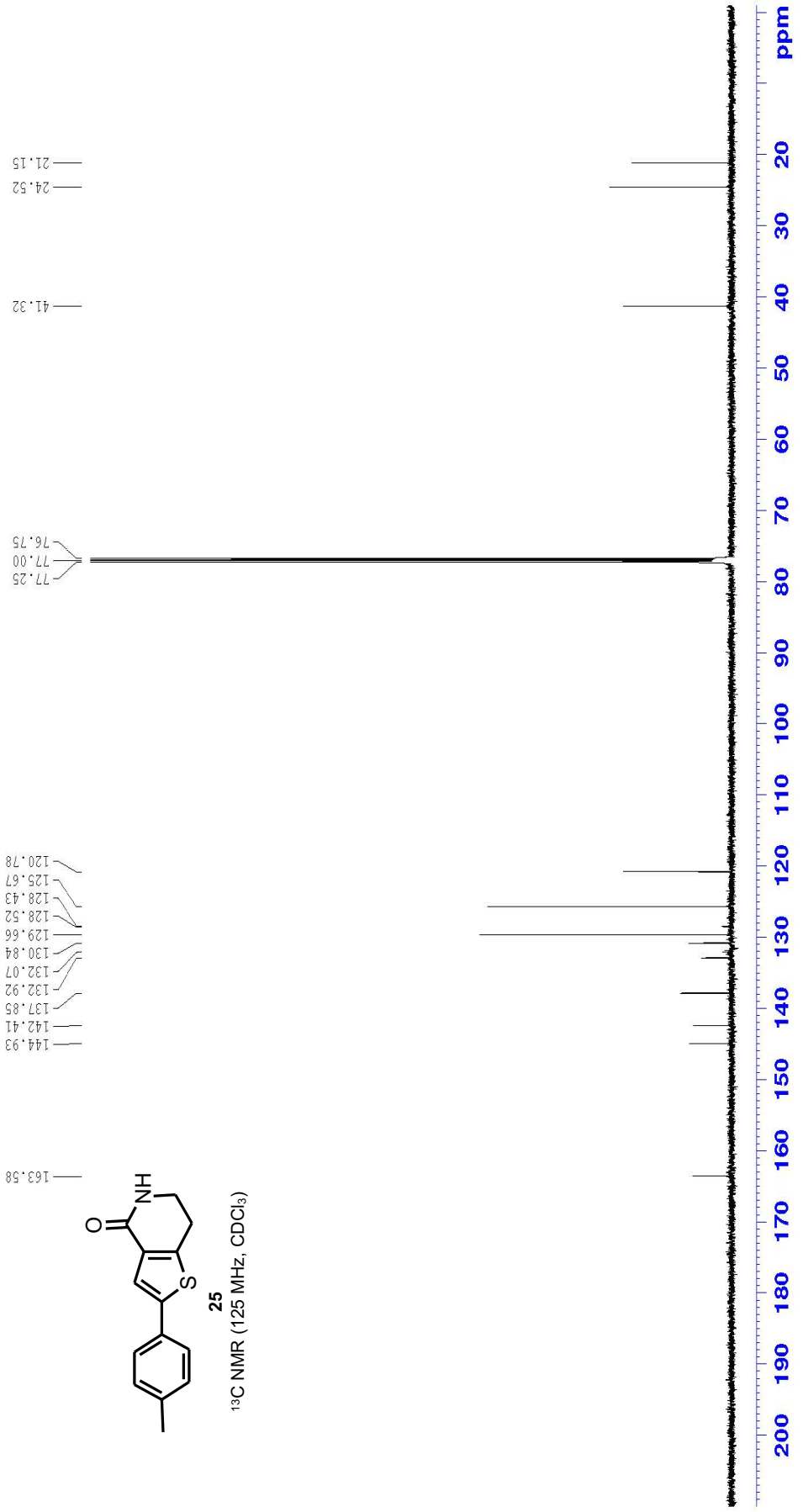

25

^{13}C NMR (125 MHz, $CDCl_3$)

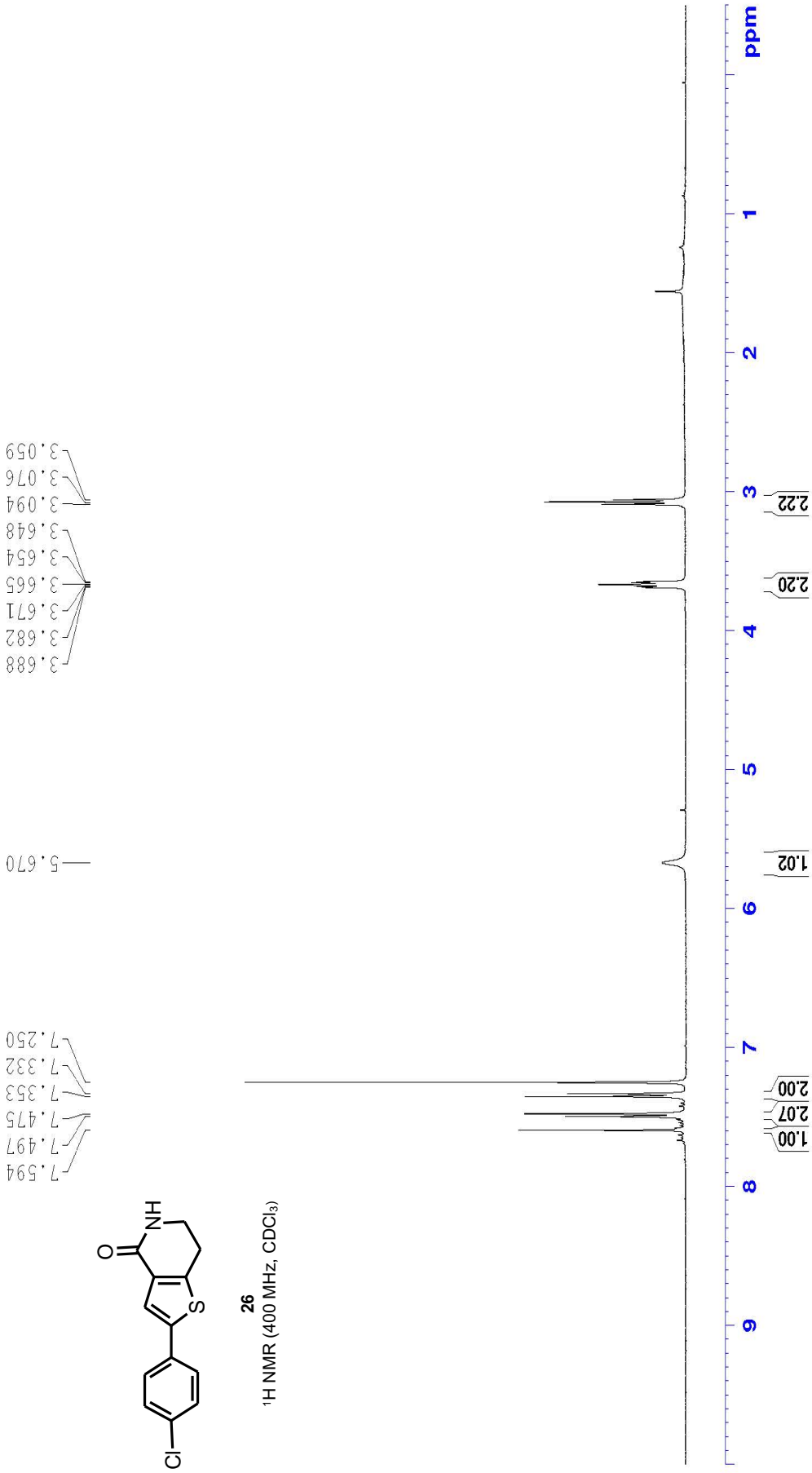
26
^{1}H NMR (400 MHz, $CDCl_3$)
ppm
1.00
2.07
2.00
1.02
2.20
2.22
7.594
7.497
7.475
7.353
7.332
7.250
5.670
3.688
3.682
3.671
3.665
3.654
3.648
3.094
3.076
3.059
NH
O
S
Cl

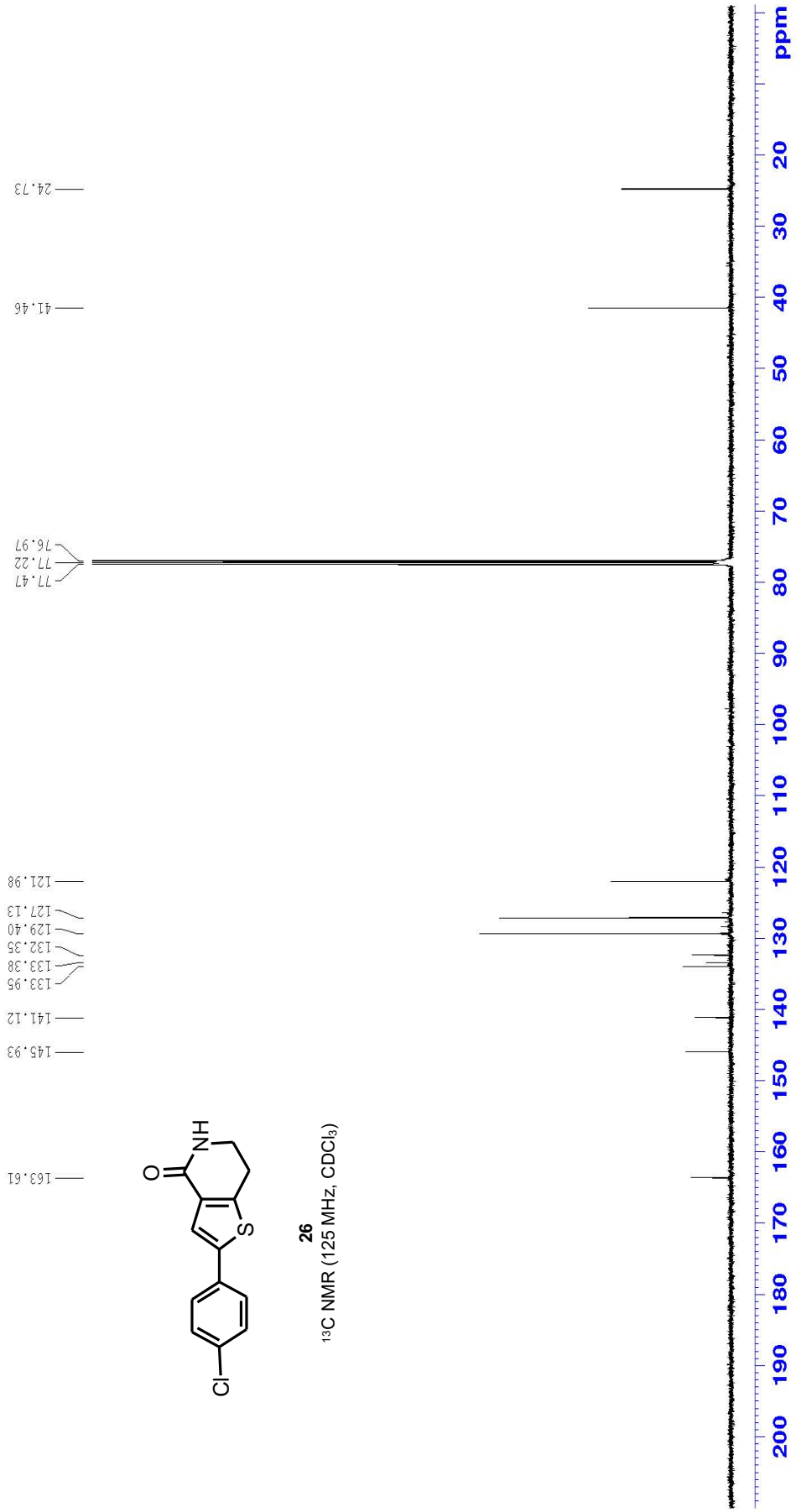

26

^{13}C NMR (125 MHz, $CDCl_3$)

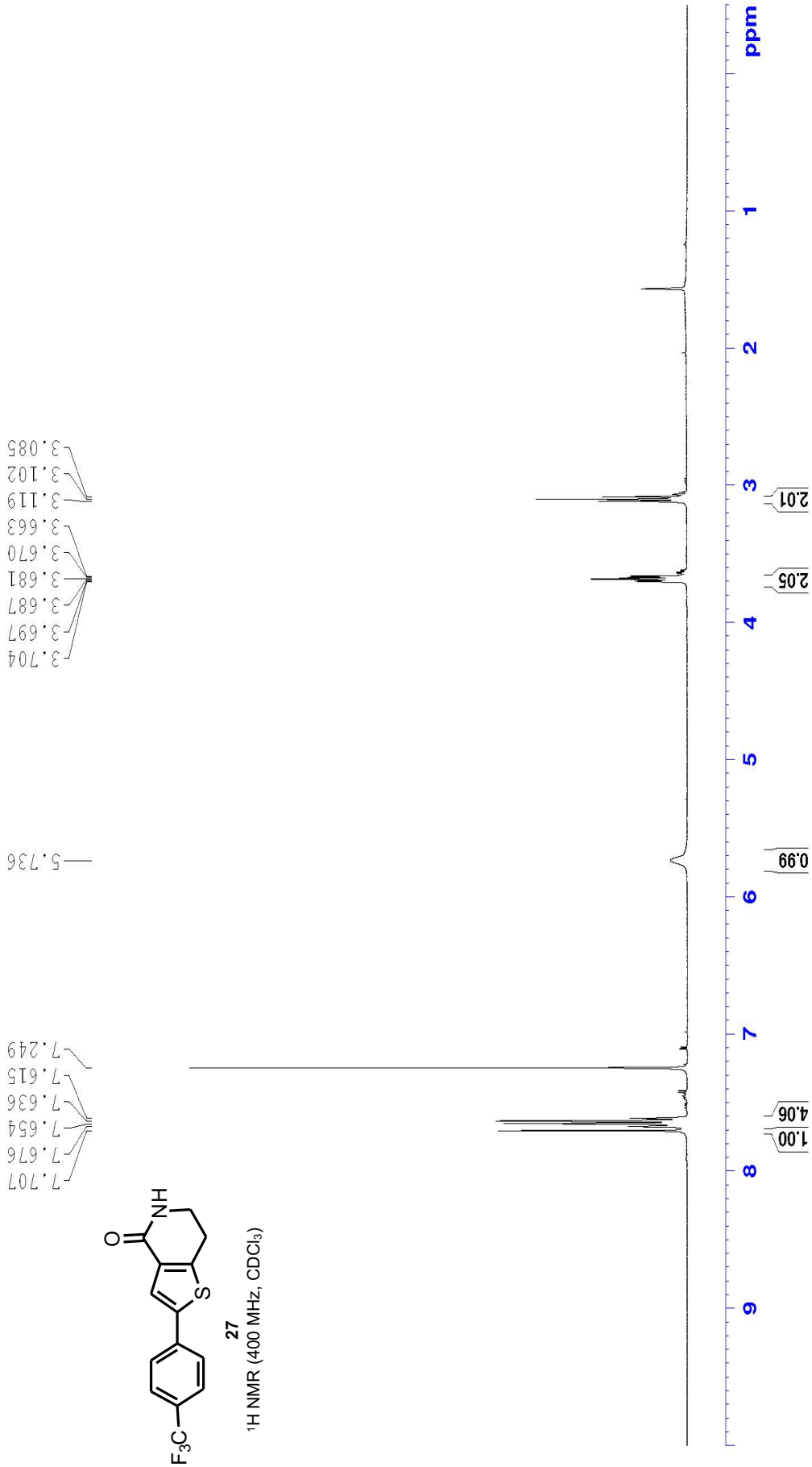

27

^{1}H NMR (400 MHz, $CDCl_3$)

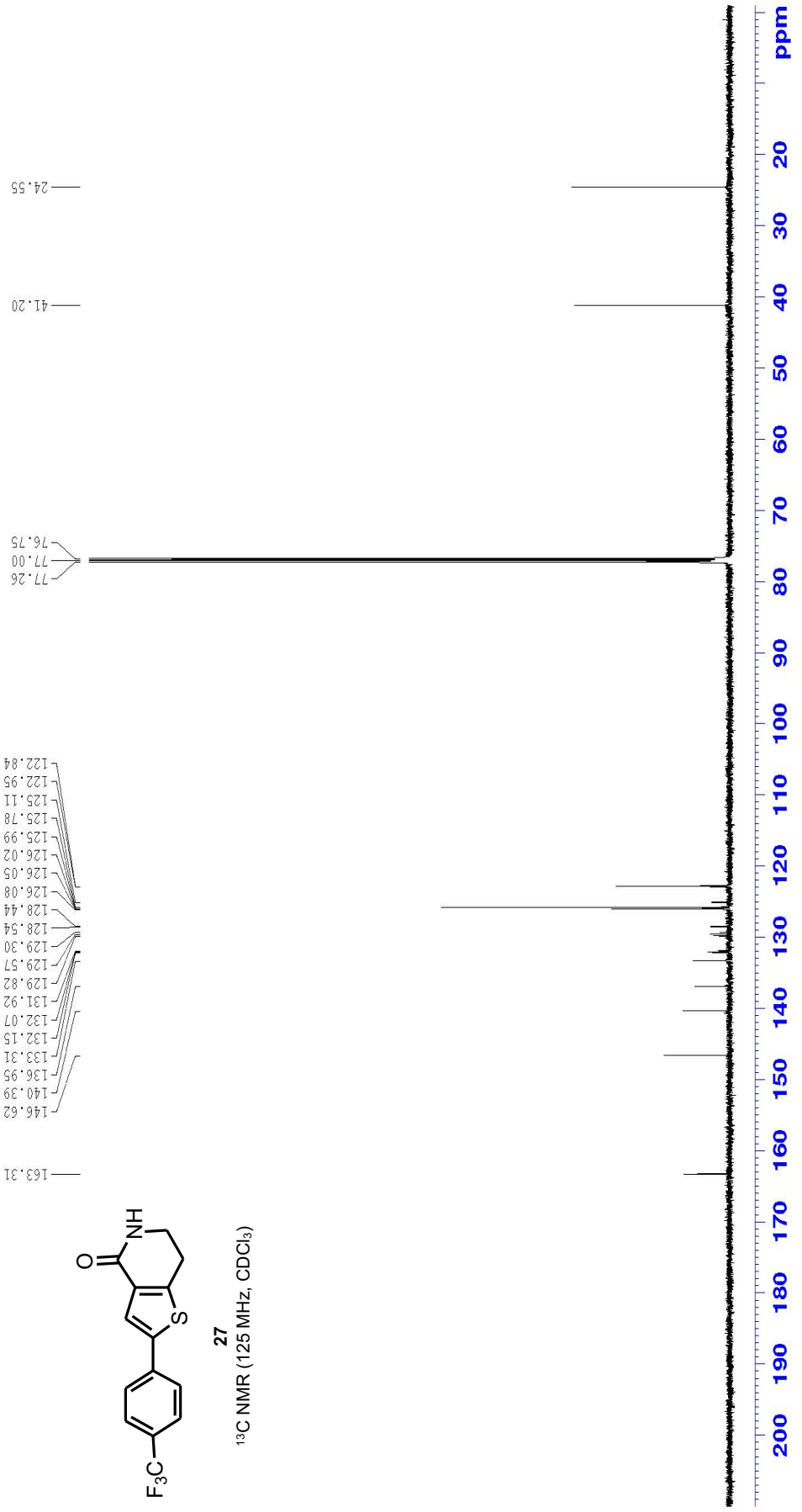

27

^{13}C NMR (125 MHz, $CDCl_3$)

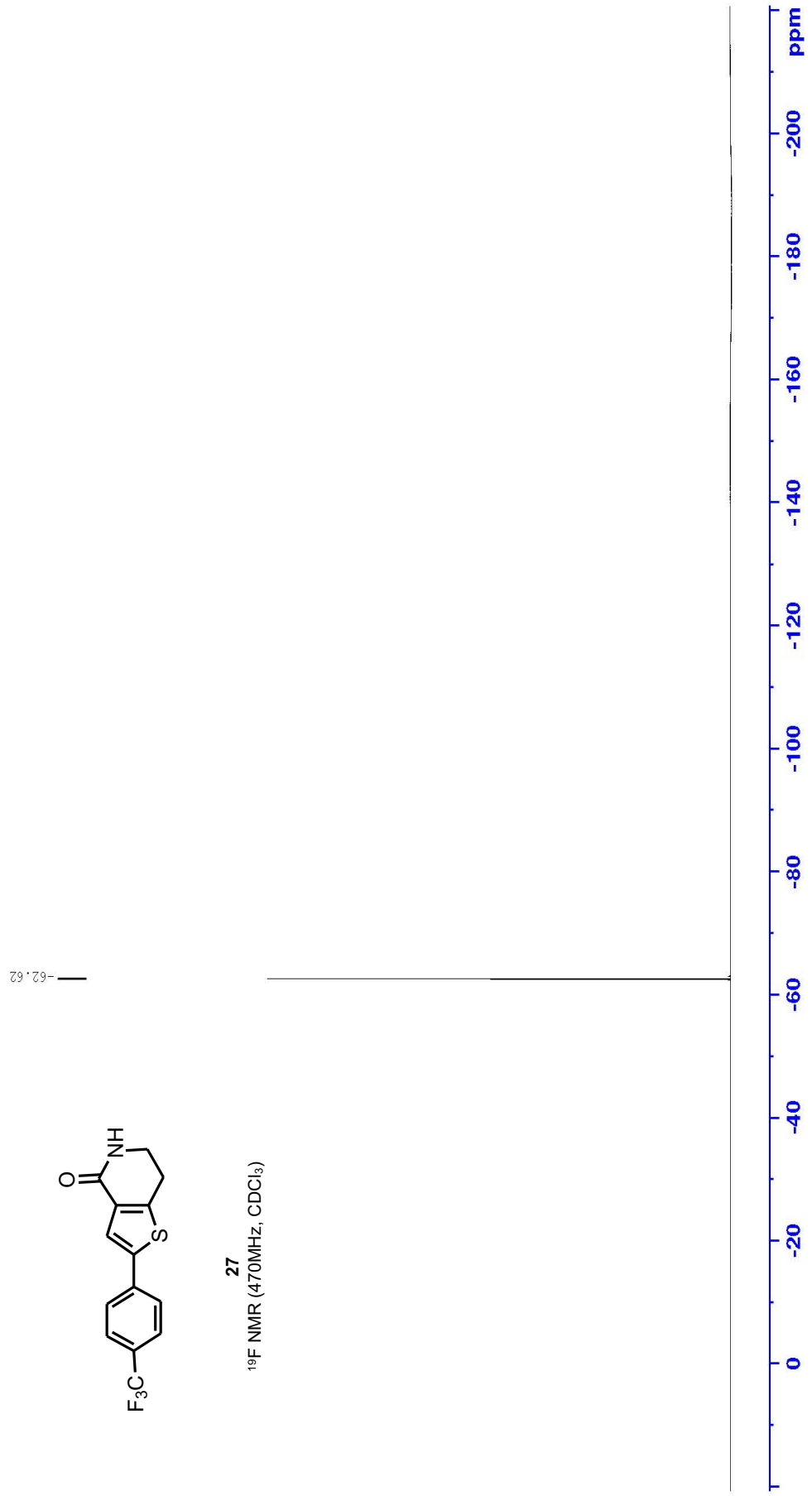

27

^{19}F NMR (470MHz, $CDCl_3$)

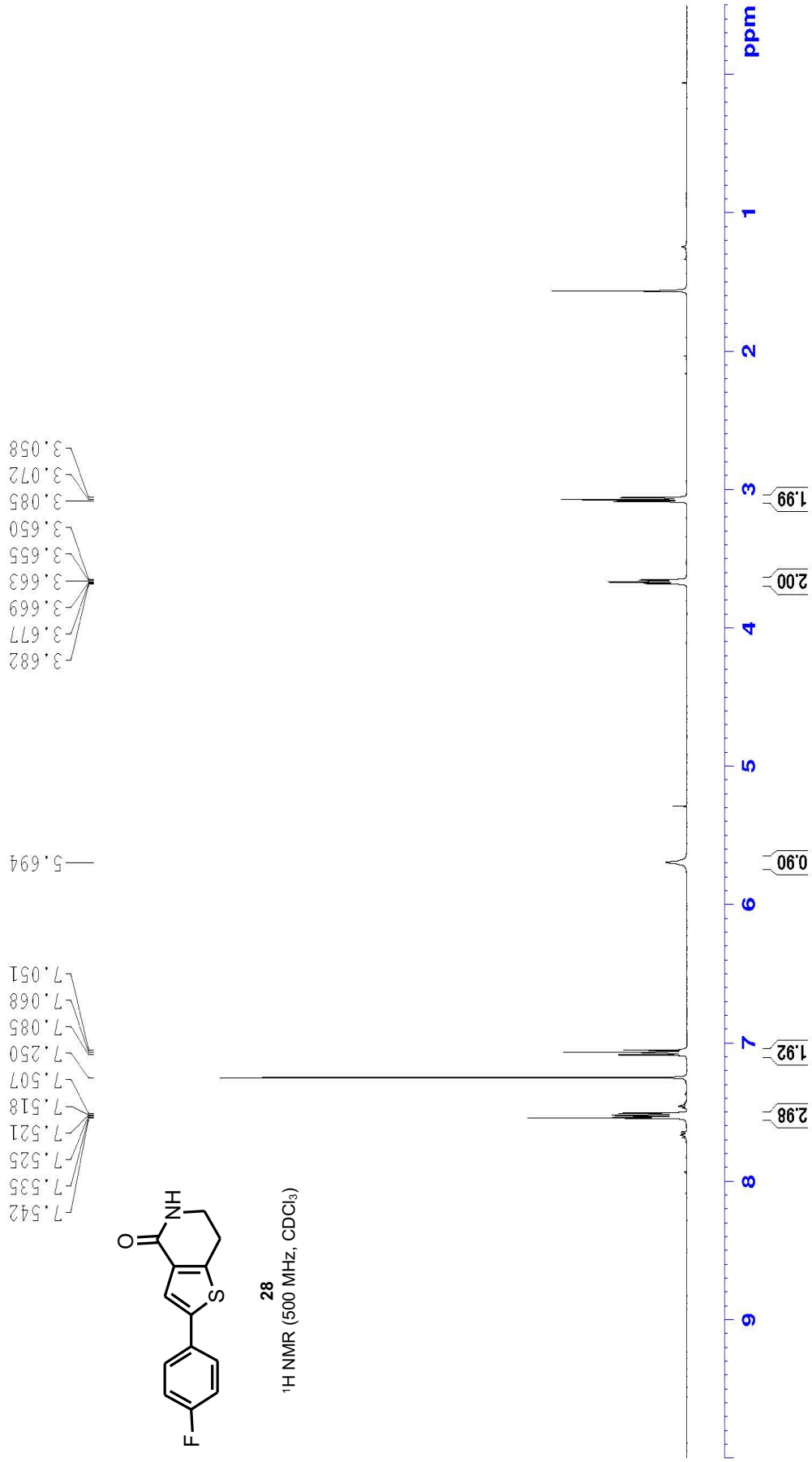

28

^{1}H NMR (500 MHz, $CDCl_3$)

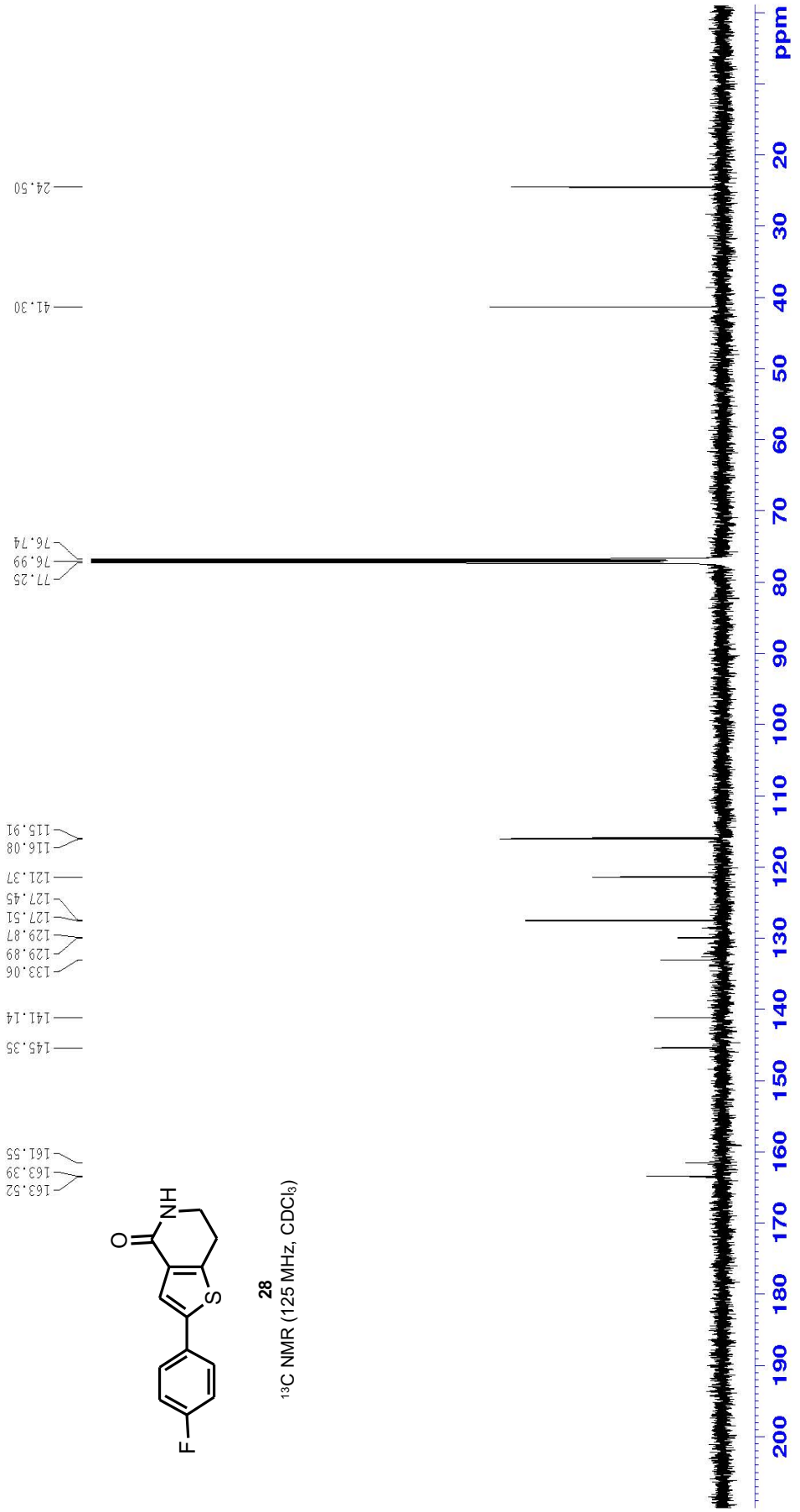

28

^{13}C NMR (125 MHz, $CDCl_3$)

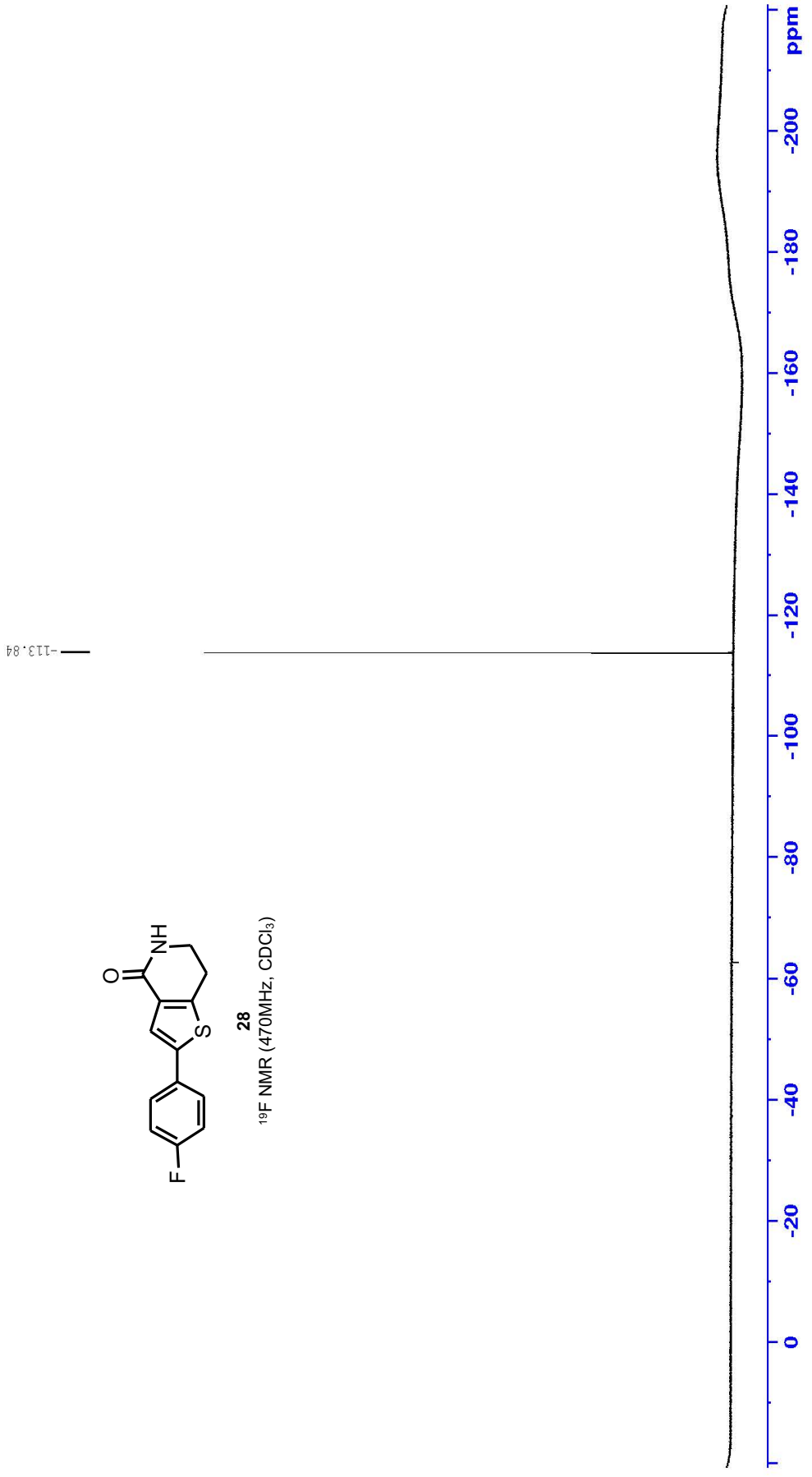

28

^{19}F NMR (470MHz, $CDCl_3$)

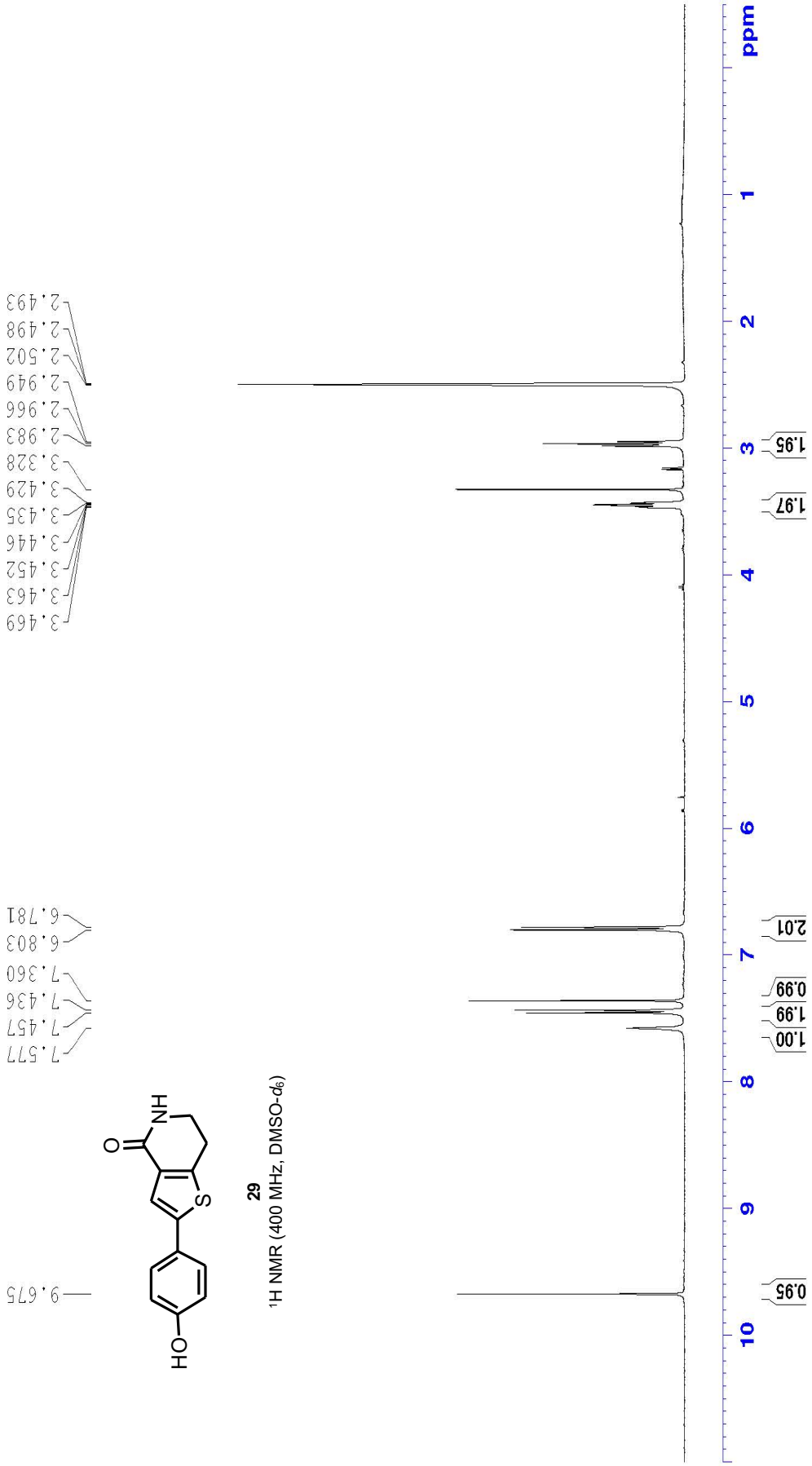
29
^{1}H NMR (400 MHz, DMSO-d_6)
ppm
1
2
3
4
5
6
7
8
9
10
0.95
1.00
1.99
0.99
2.01
1.97
1.95
9.675
7.577
7.457
7.436
7.360
6.803
6.781
3.469
3.463
3.452
3.446
3.435
3.429
3.328
2.983
2.966
2.949
2.502
2.498
2.493
NH
O
S
HO

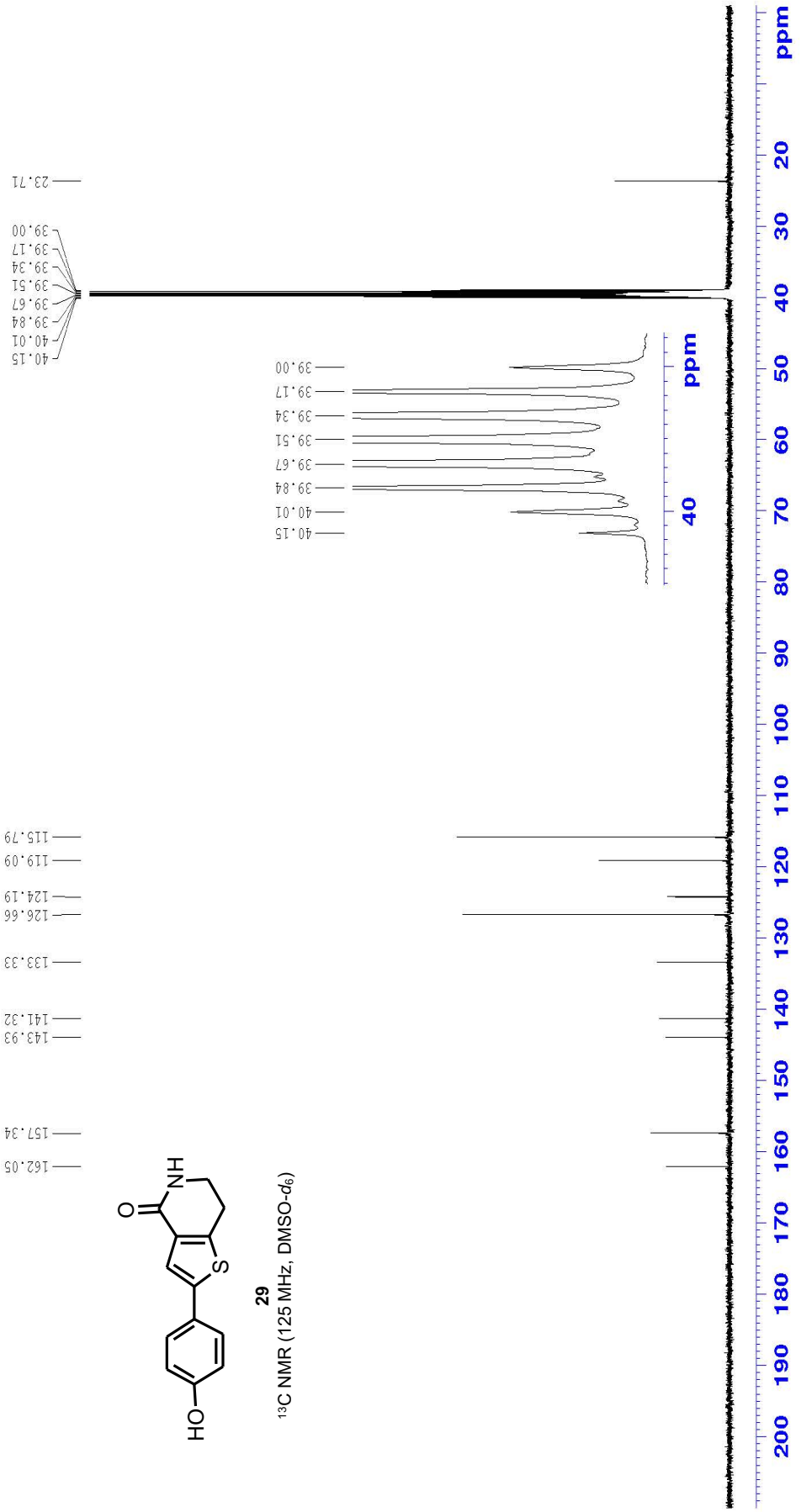

29

^{13}C NMR (125 MHz, DMSO-d_6)

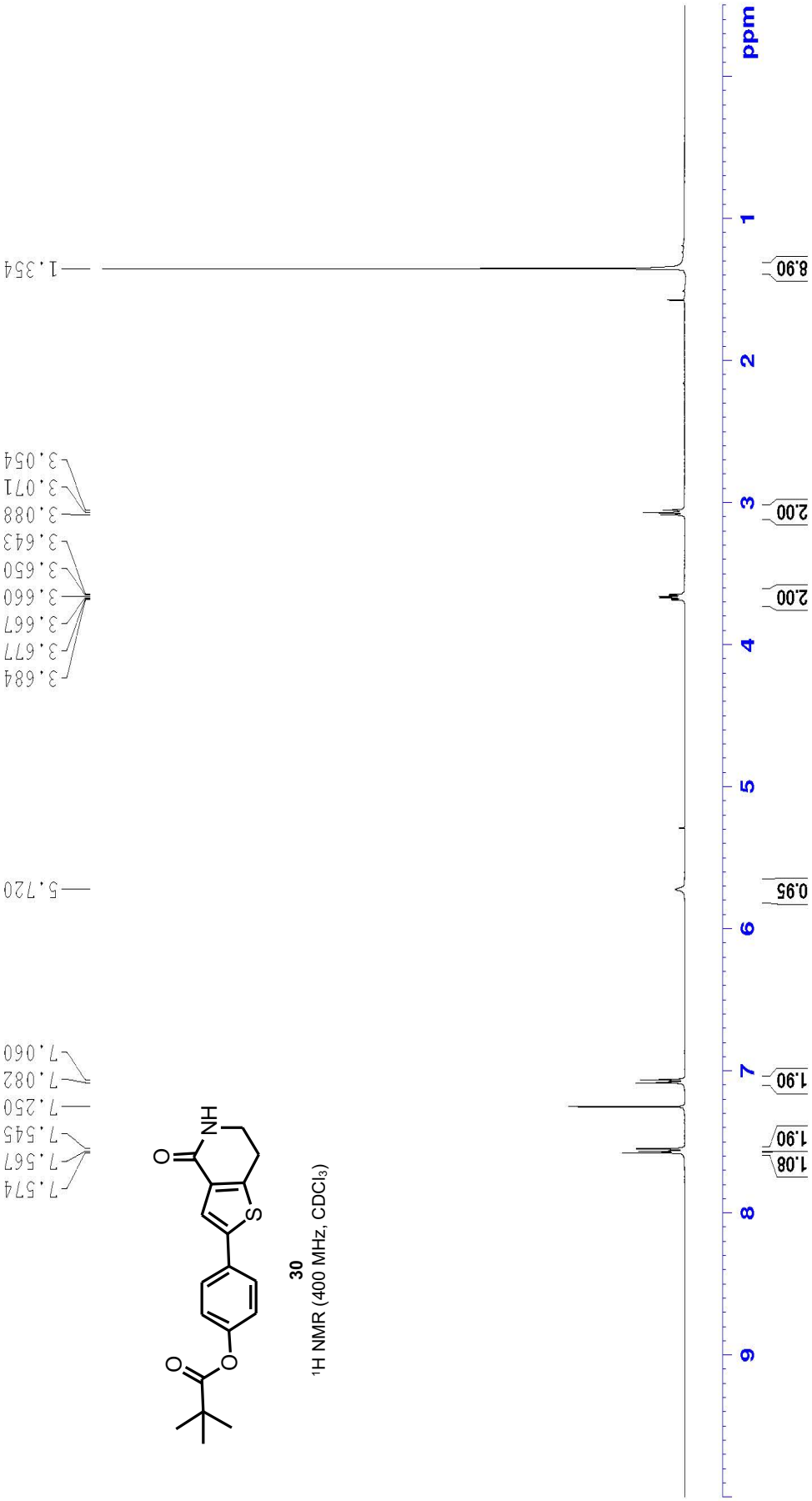

30

^{1}H NMR (400 MHz, $CDCl_3$)

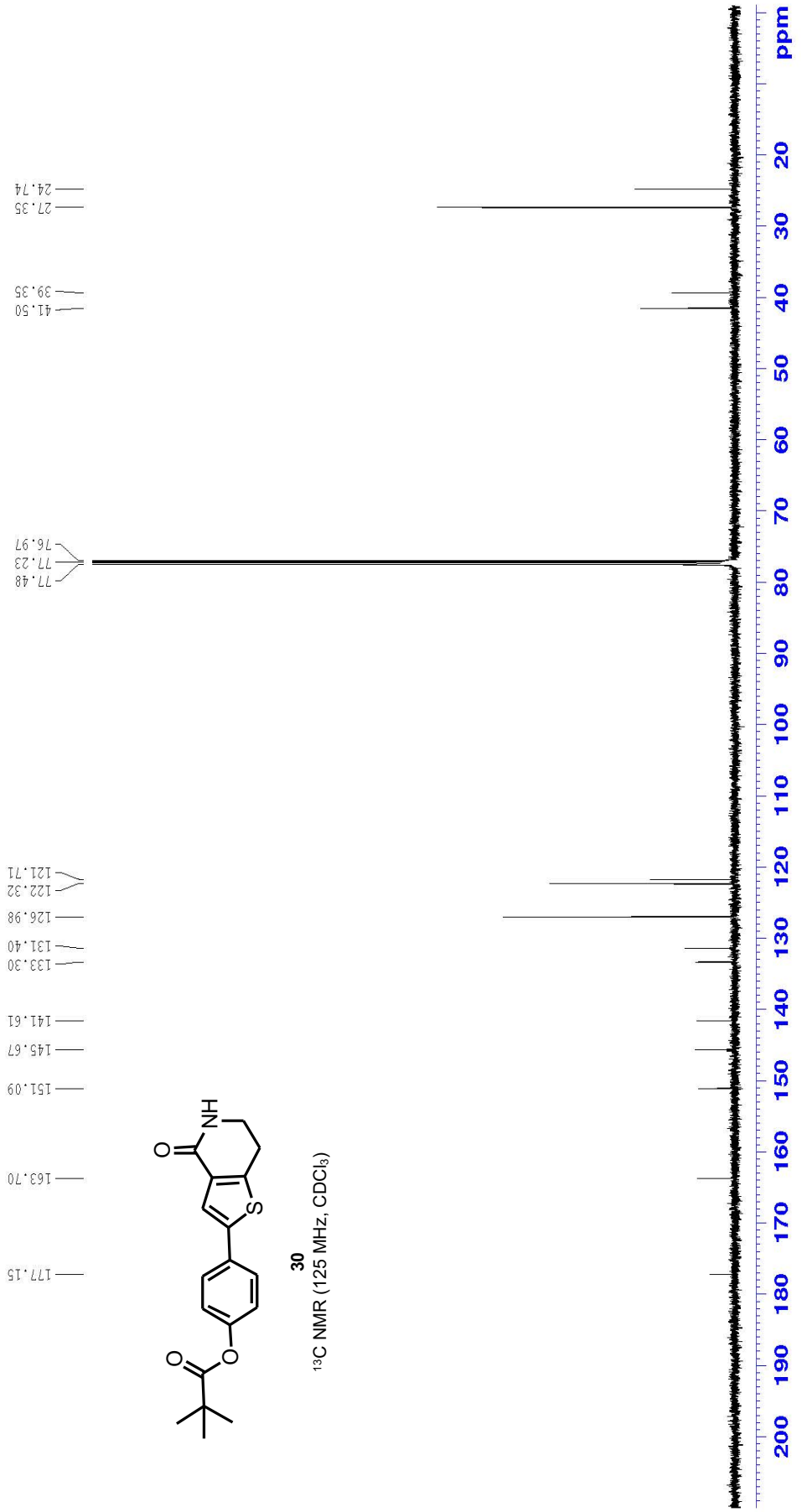

30

^{13}C NMR (125 MHz, $CDCl_3$)

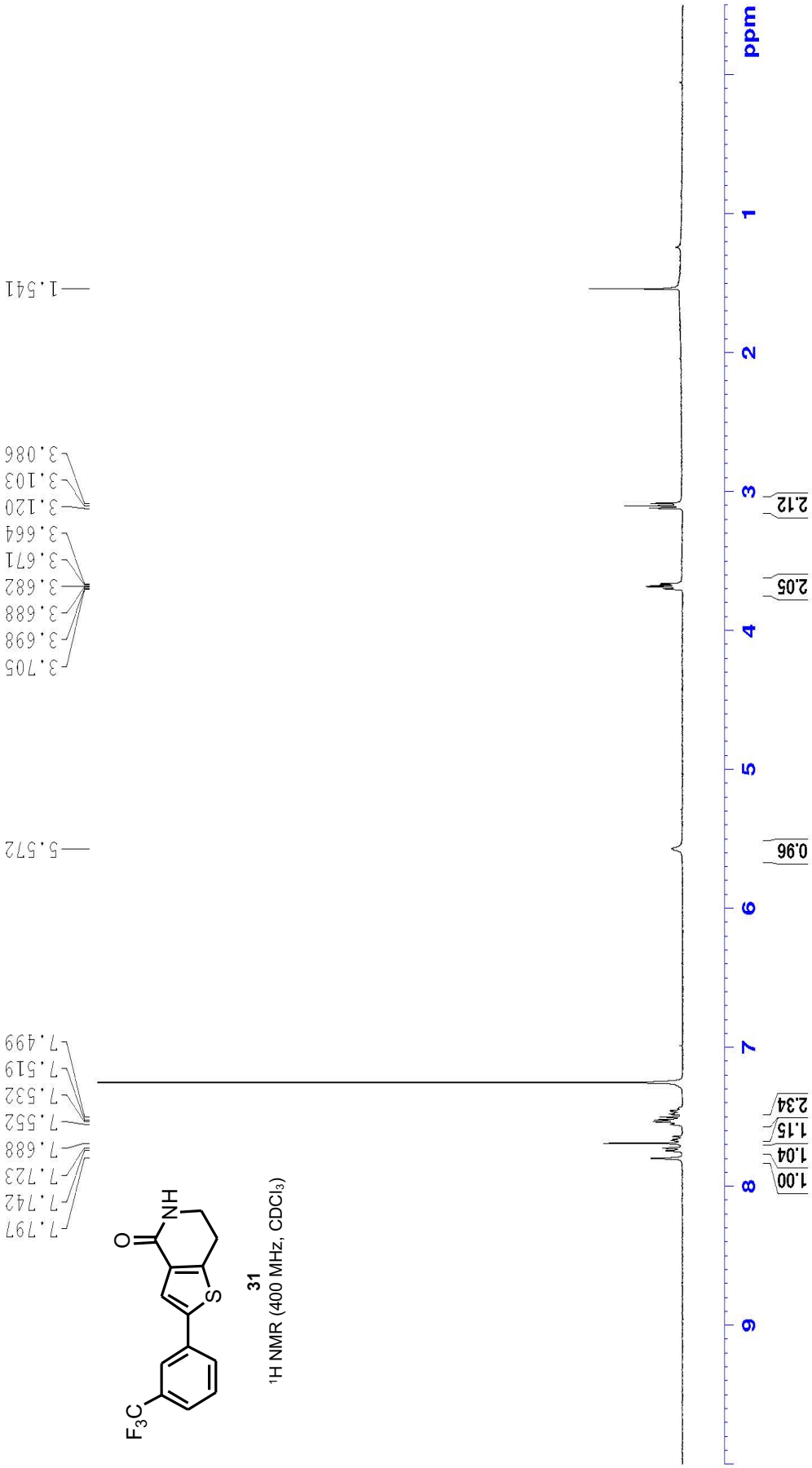

31

^{1}H NMR (400 MHz, $CDCl_3$)

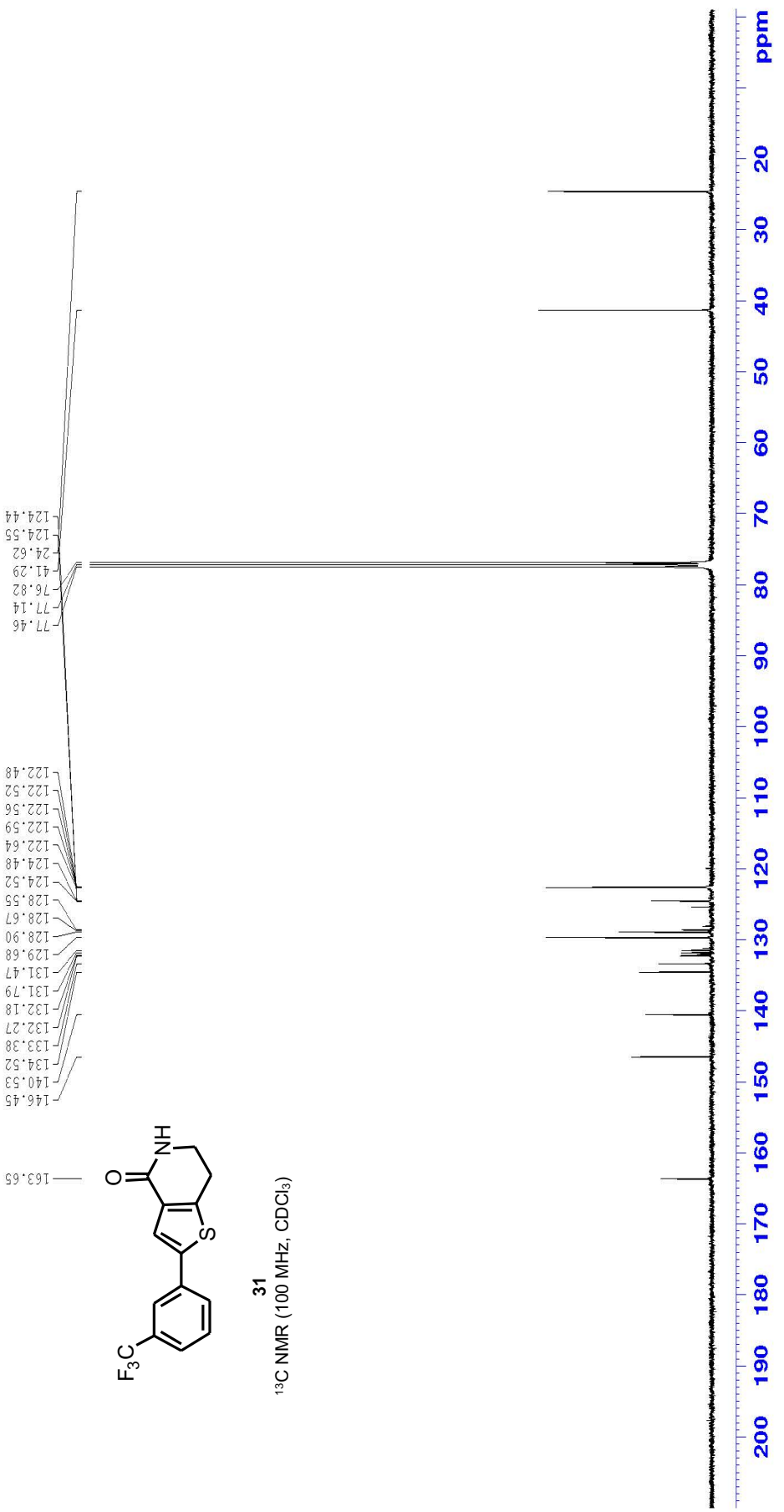

31

^{13}C NMR (100 MHz, $CDCl_3$)

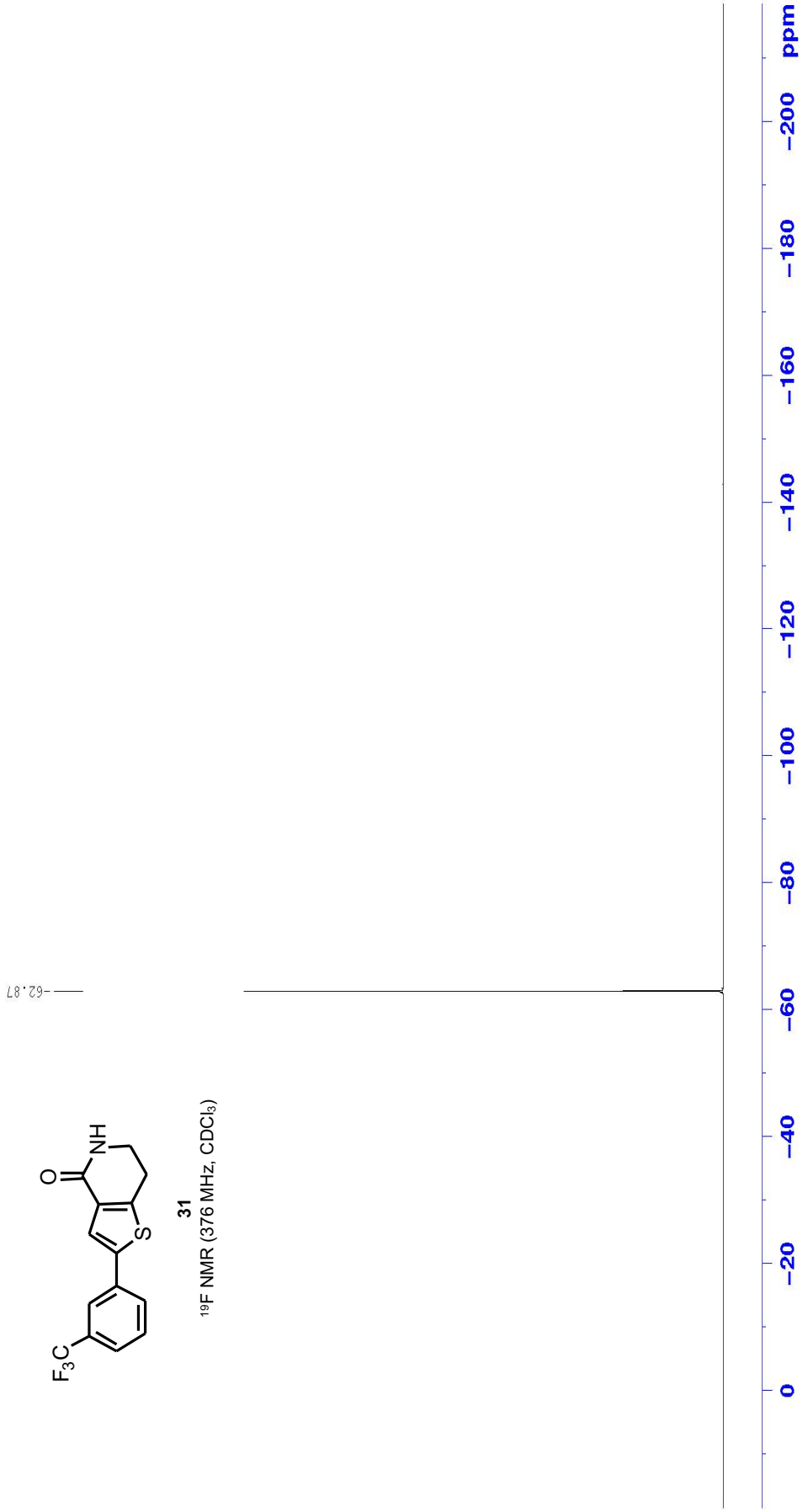

31

^{19}F NMR (376 MHz, $CDCl_3$)

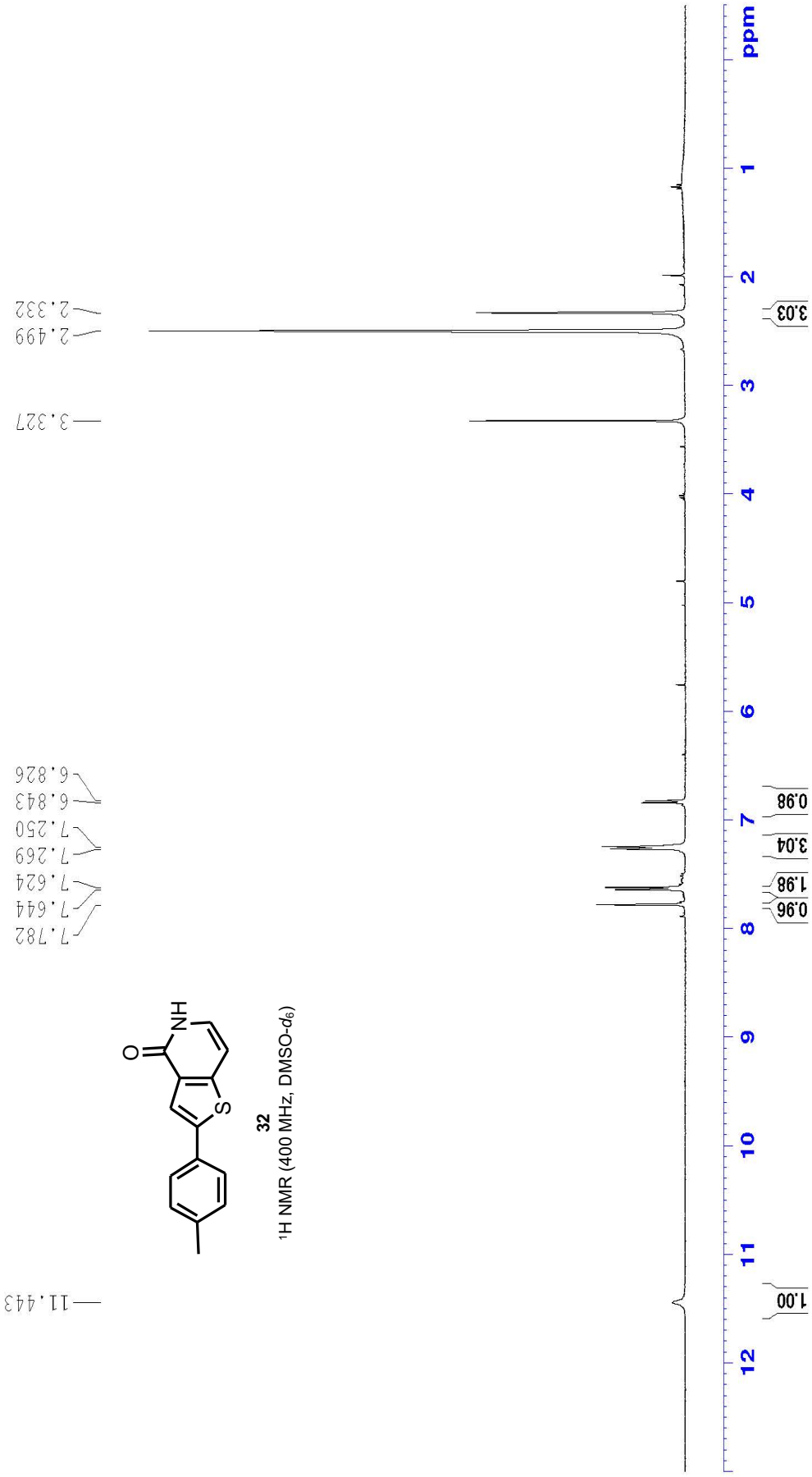

32

^{1}H NMR (400 MHz, DMSO-d_6)

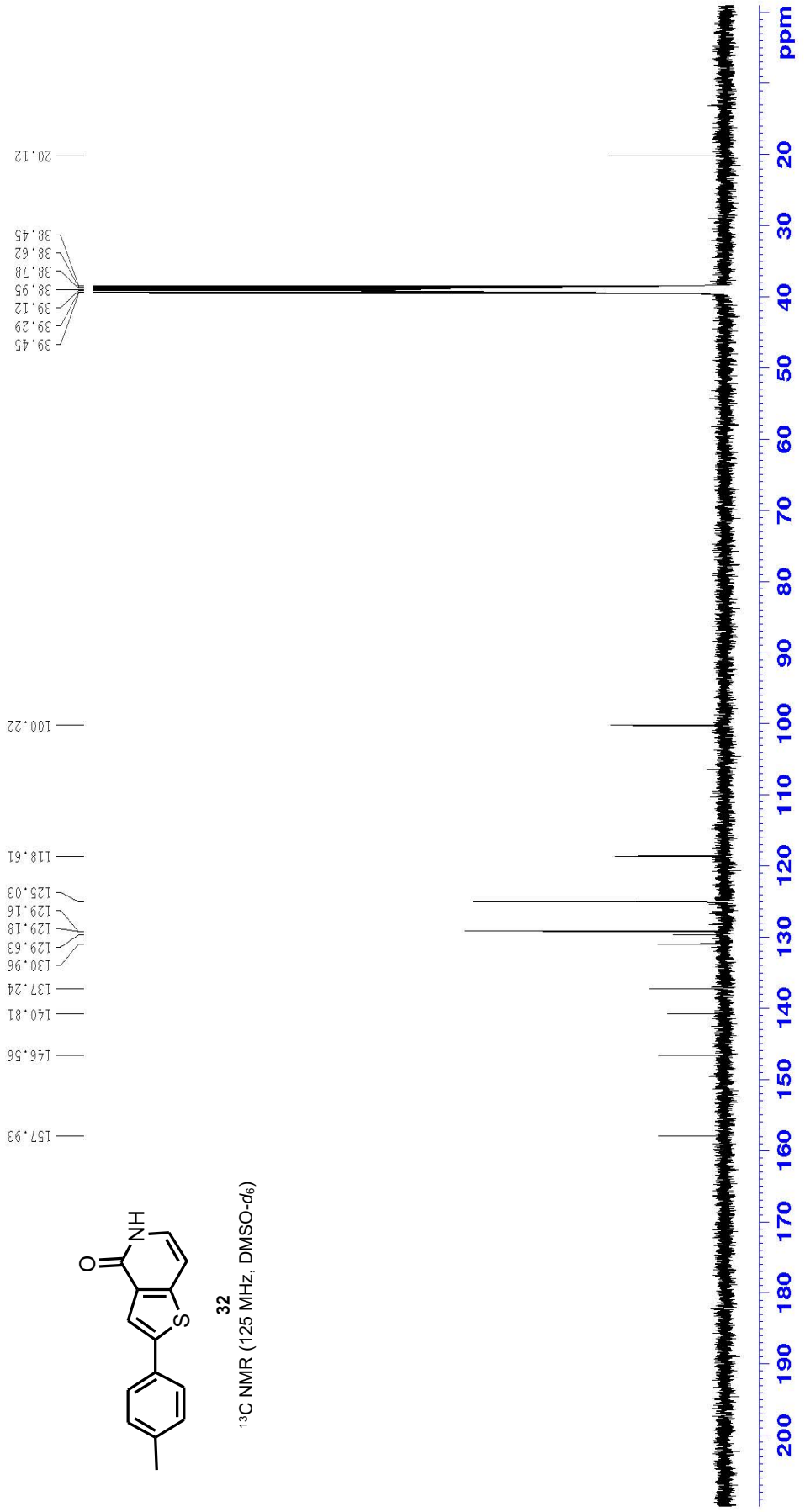

32

^{13}C NMR (125 MHz, DMSO-d_6)

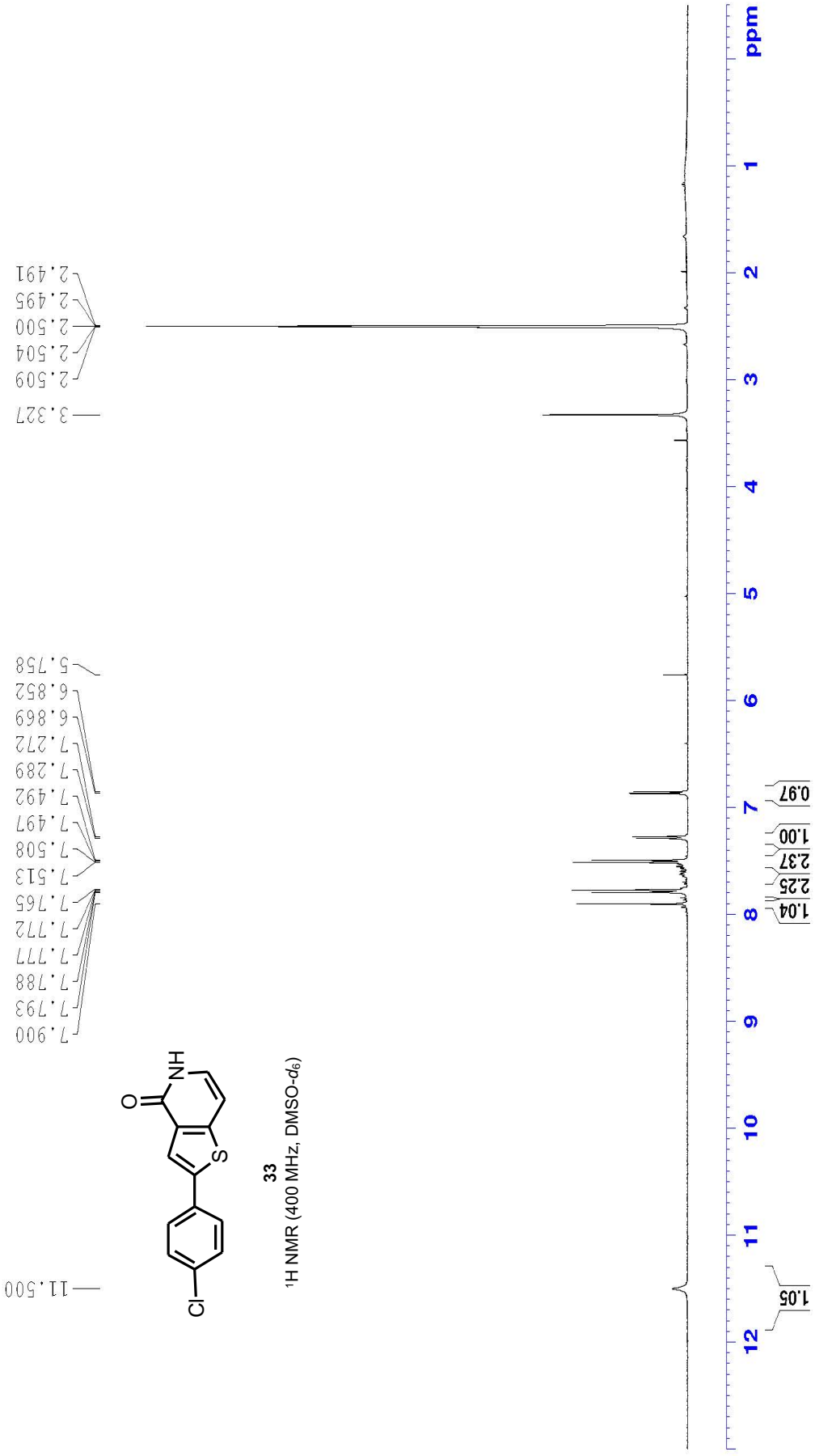

33

^{1}H NMR (400 MHz, DMSO-d_6)

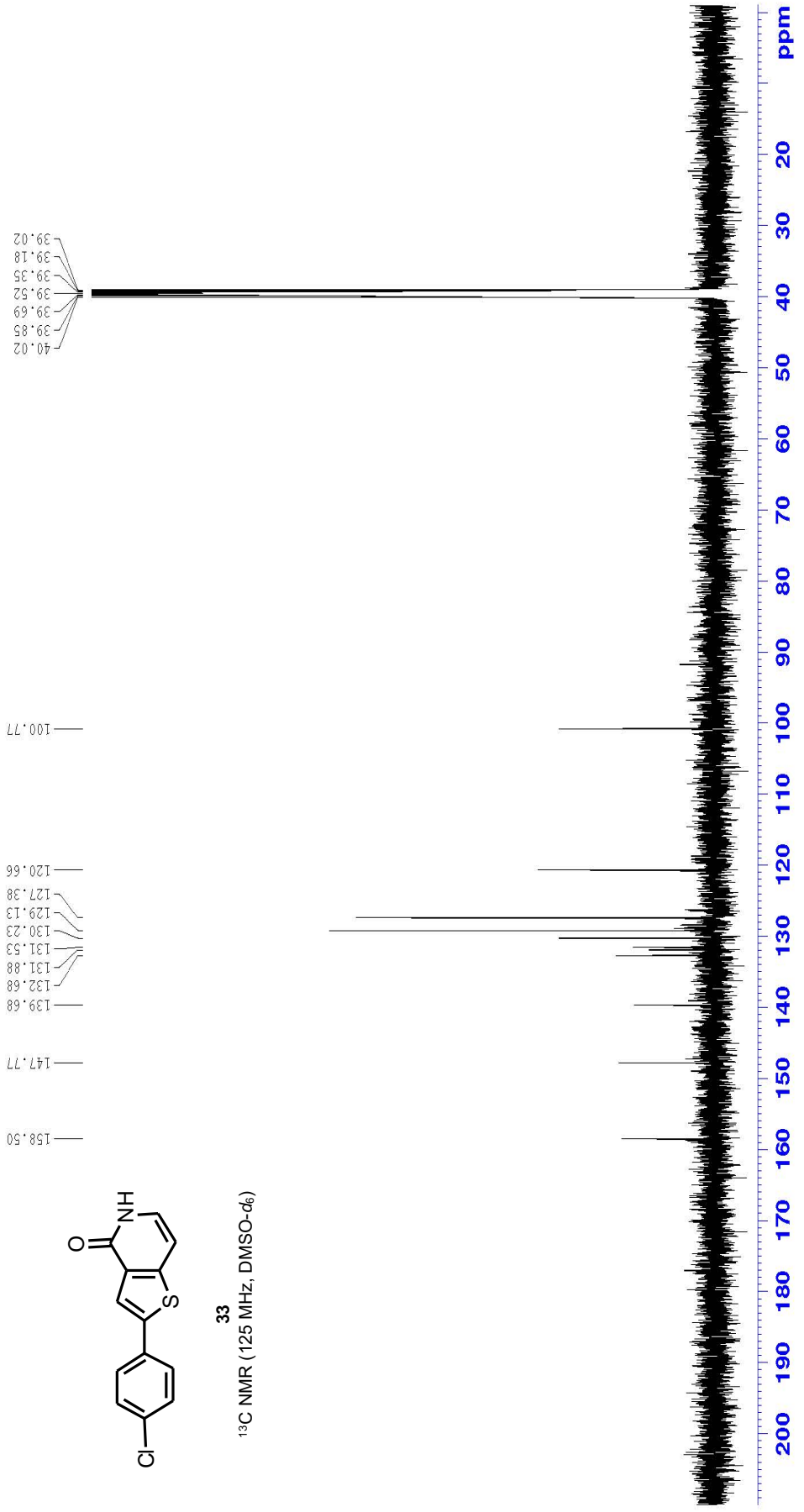

33

^{13}C NMR (125 MHz, DMSO-d_6)

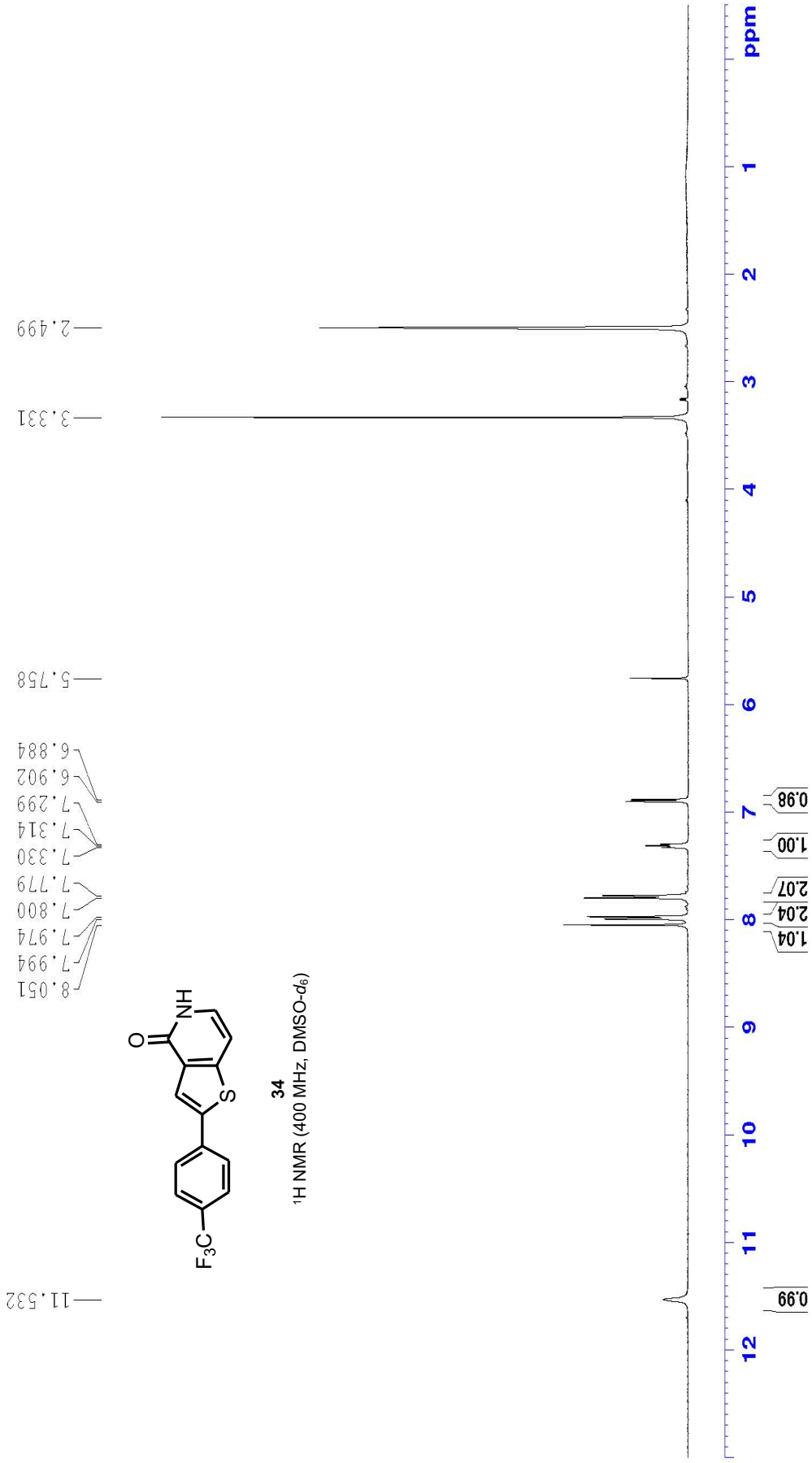
34
^{1}H NMR (400 MHz, DMSO-d_6)
NH
O
S
F_3C
11.532
8.051
7.994
7.974
7.800
7.779
7.330
7.314
7.299
6.902
6.884
5.758
3.331
2.499
0.99
1.04
2.04
2.07
1.00
0.98
ppm

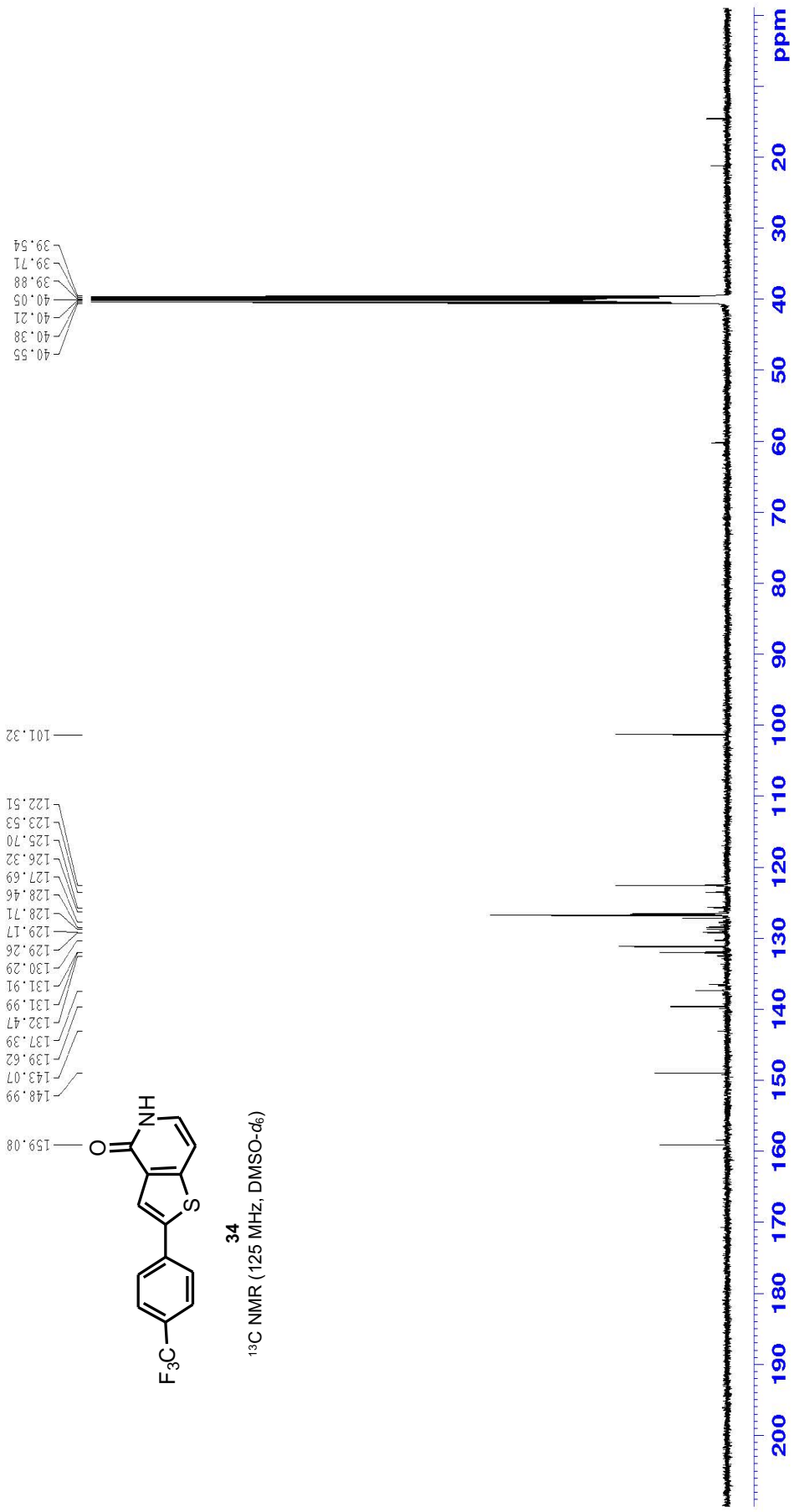

34

^{13}C NMR (125 MHz, DMSO-d_6)

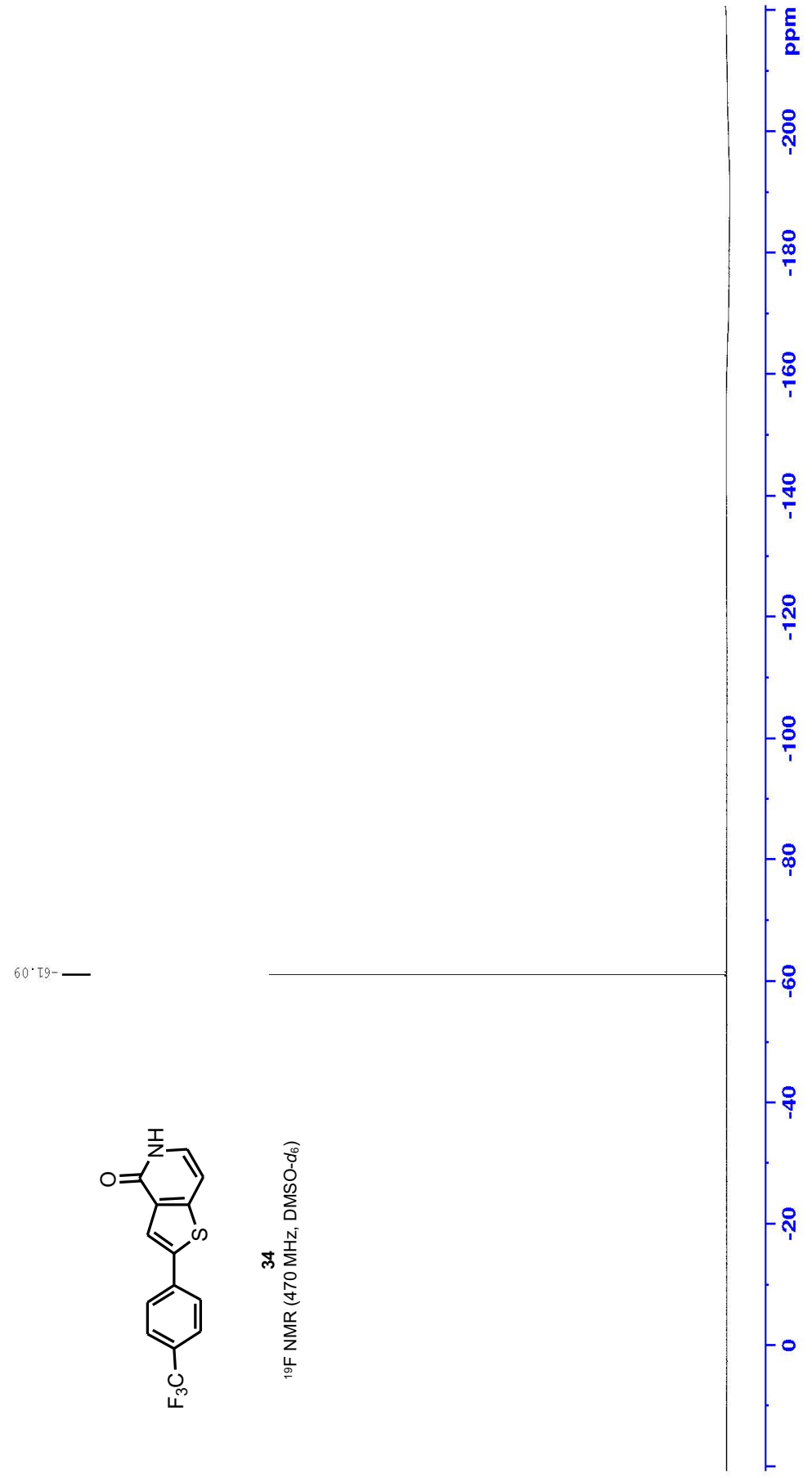

34

^{19}F NMR (470 MHz, DMSO-d_6)

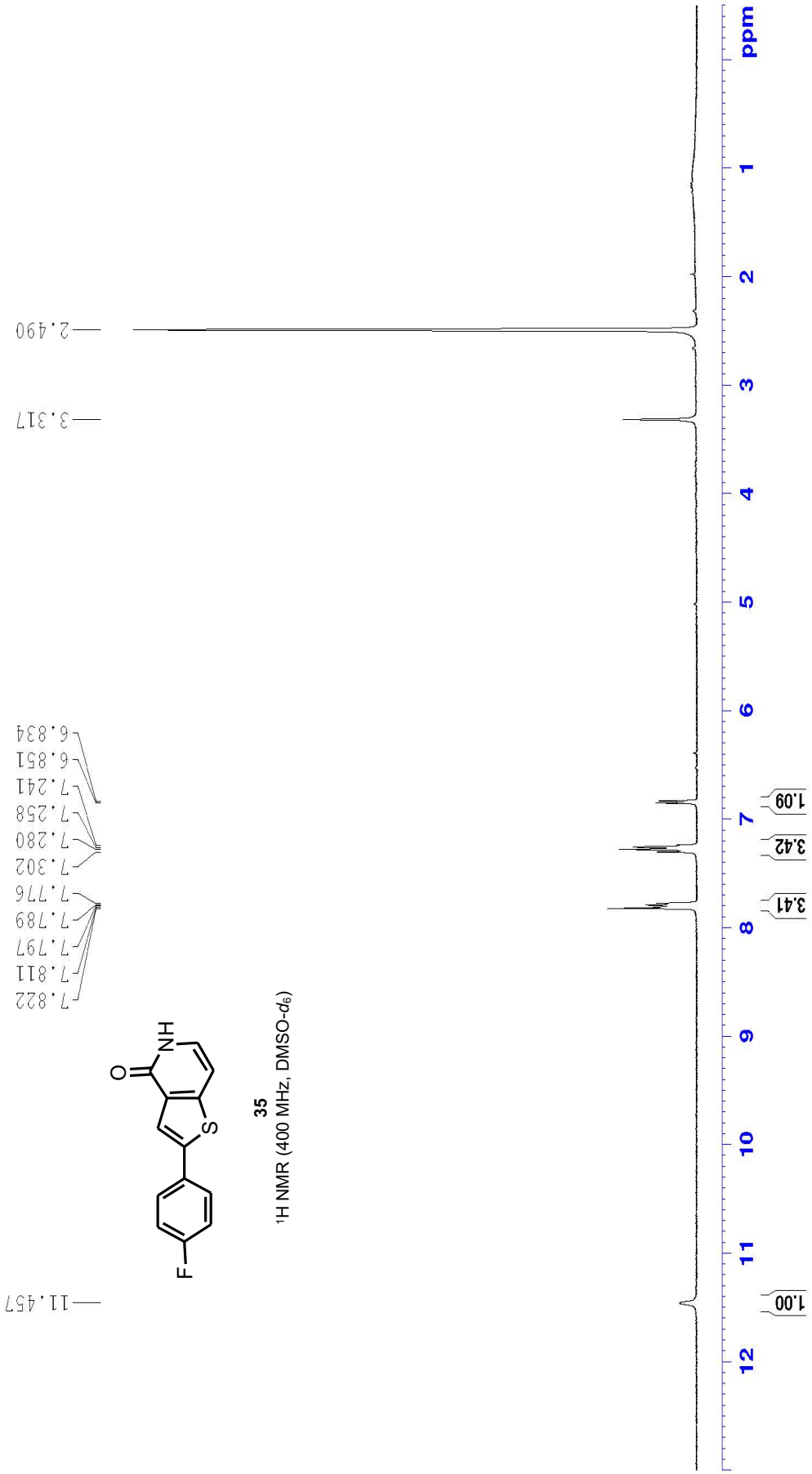
35
^{1}H NMR (400 MHz, DMSO-d_6)
11.457
7.822
7.811
7.797
7.789
7.776
7.302
7.280
7.258
7.241
6.851
6.834
3.317
2.490
1.00
3.41
3.42
1.09
ppm
NH
O
S
F

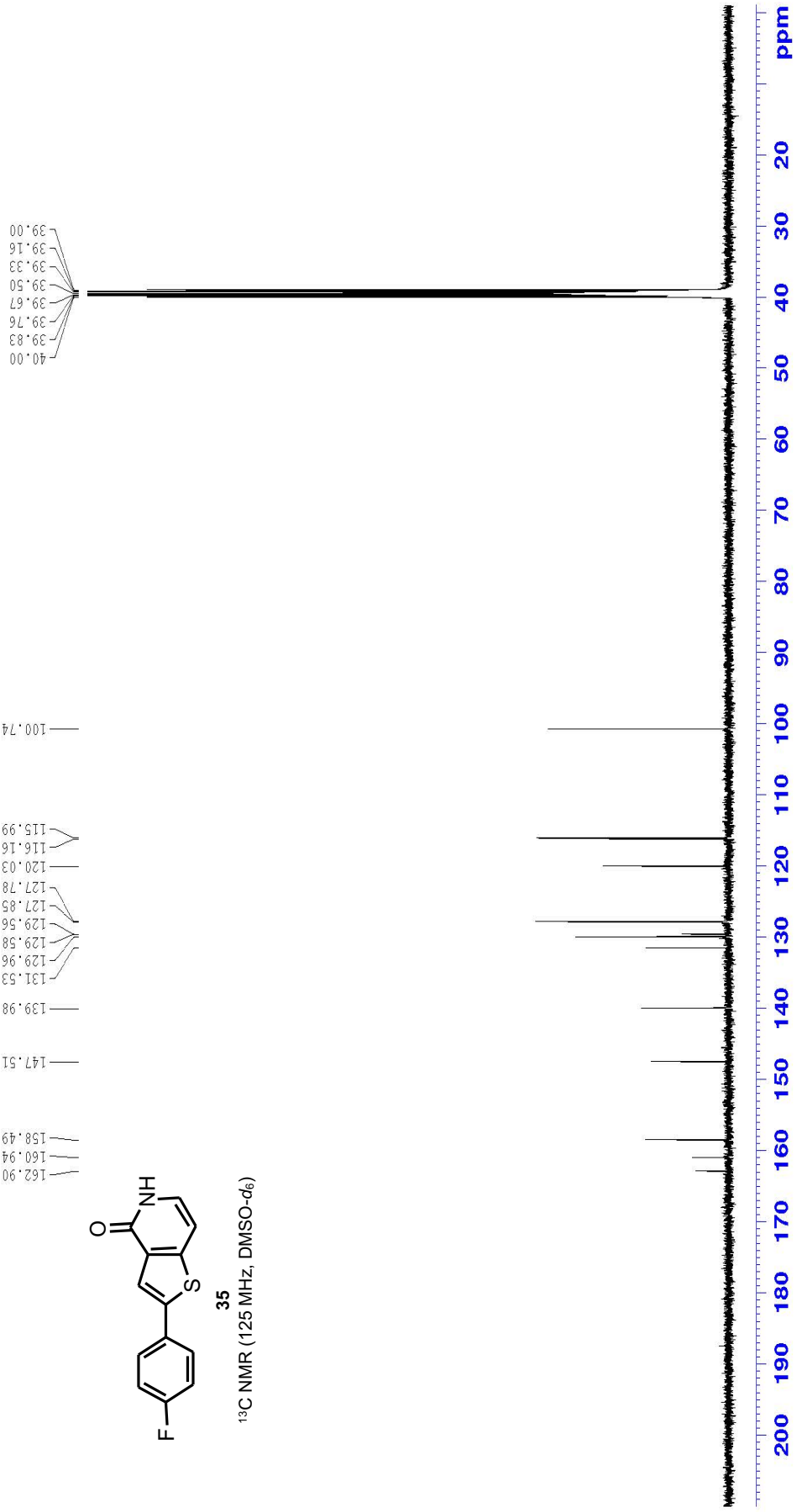

35

^{13}C NMR (125 MHz, DMSO-d_6)

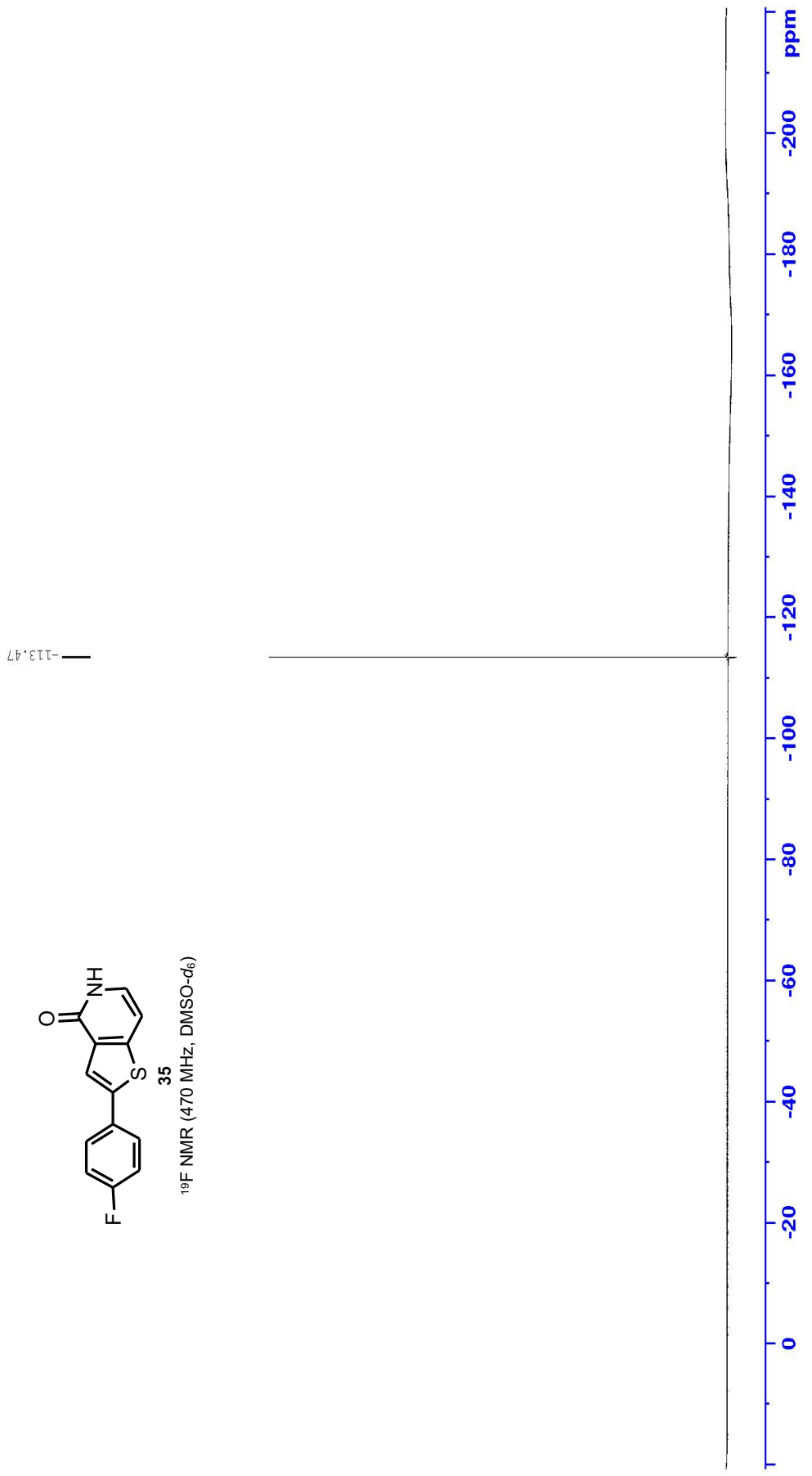

35

^{19}F NMR (470 MHz, DMSO-d_6)

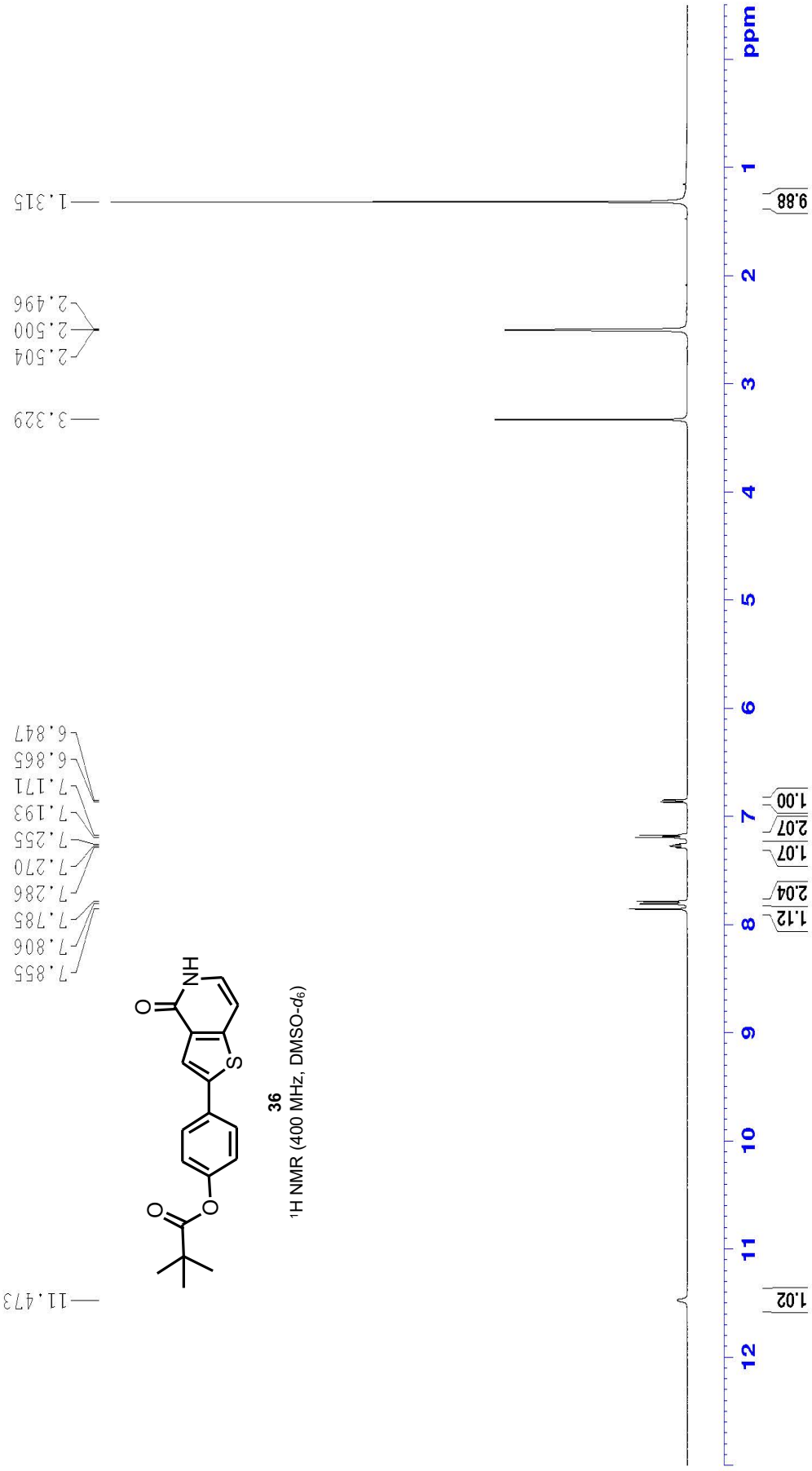

36

^{1}H NMR (400 MHz, DMSO-d_6)

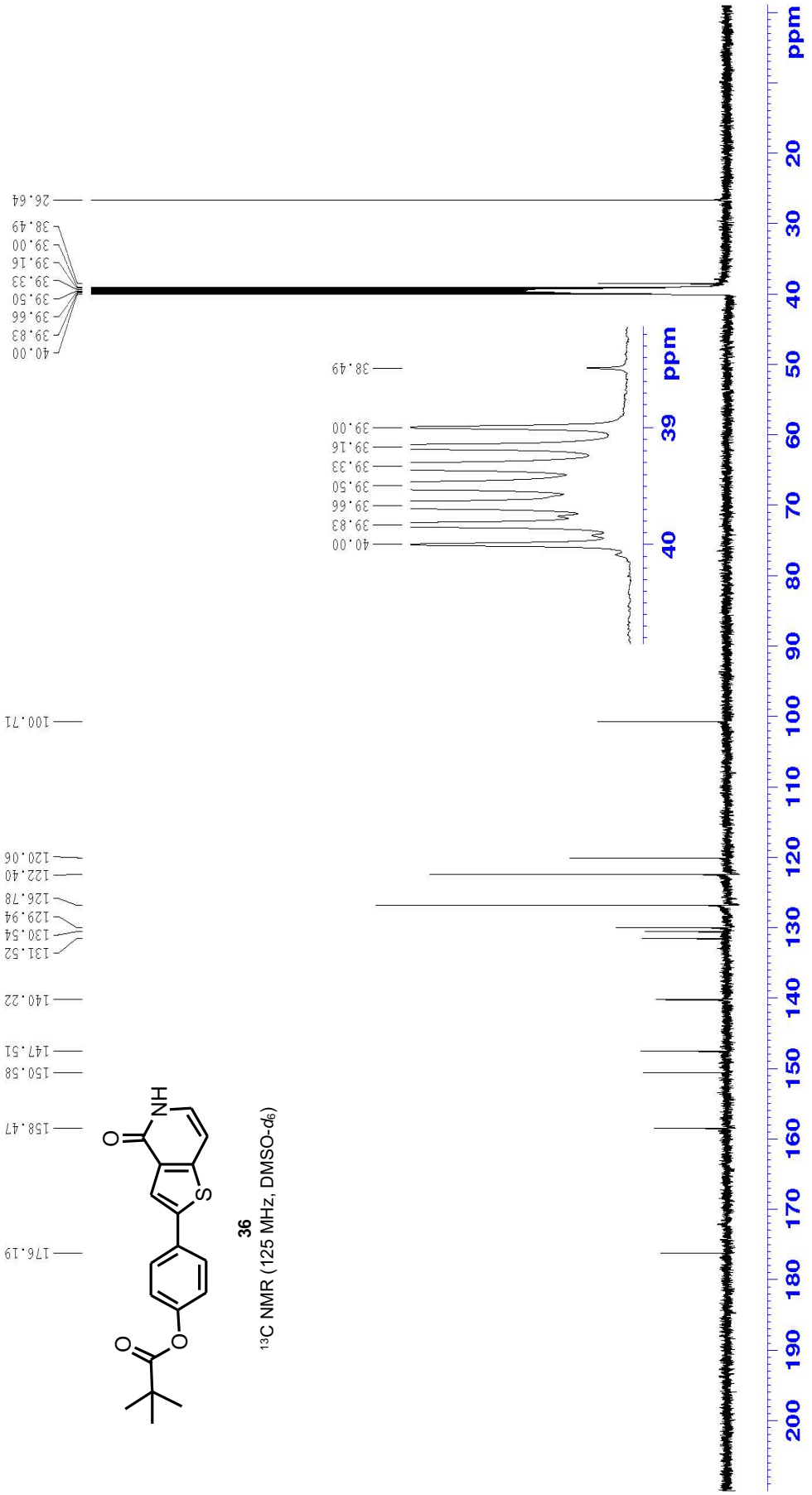

36

^{13}C NMR (125 MHz, DMSO-d_6)

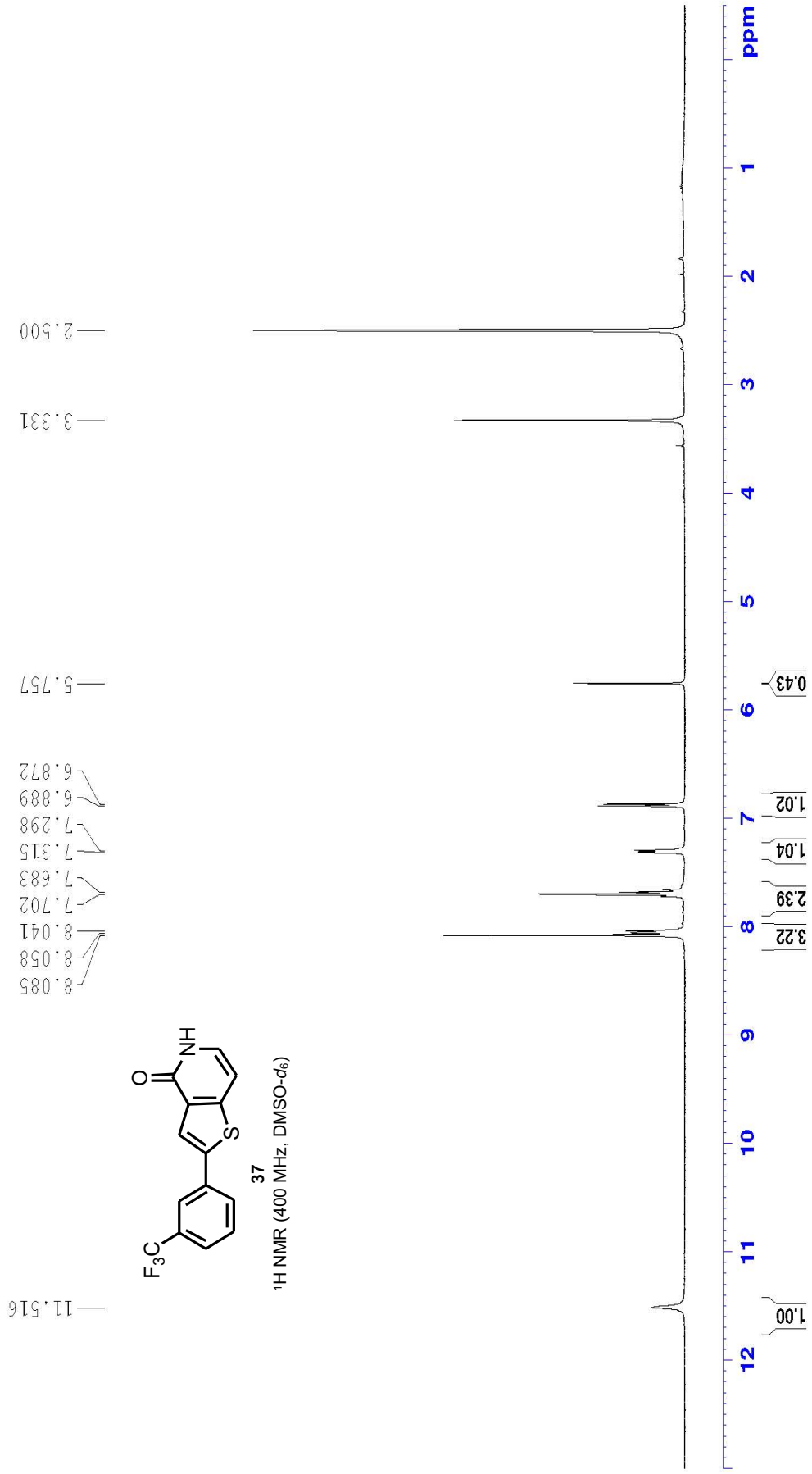

37

^{1}H NMR (400 MHz, DMSO-d_6)

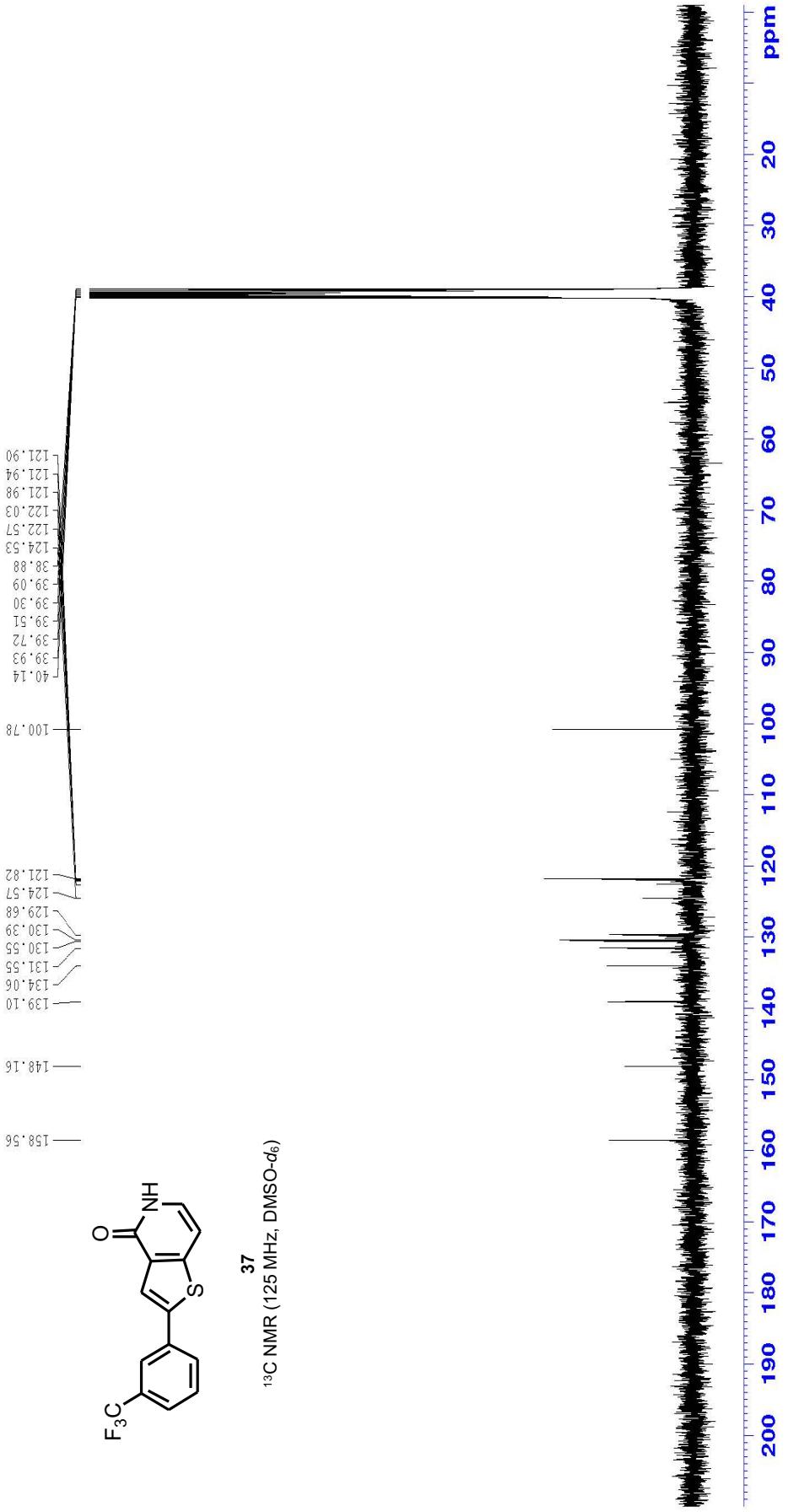

37

^{13}C NMR (125 MHz, DMSO-d_6)

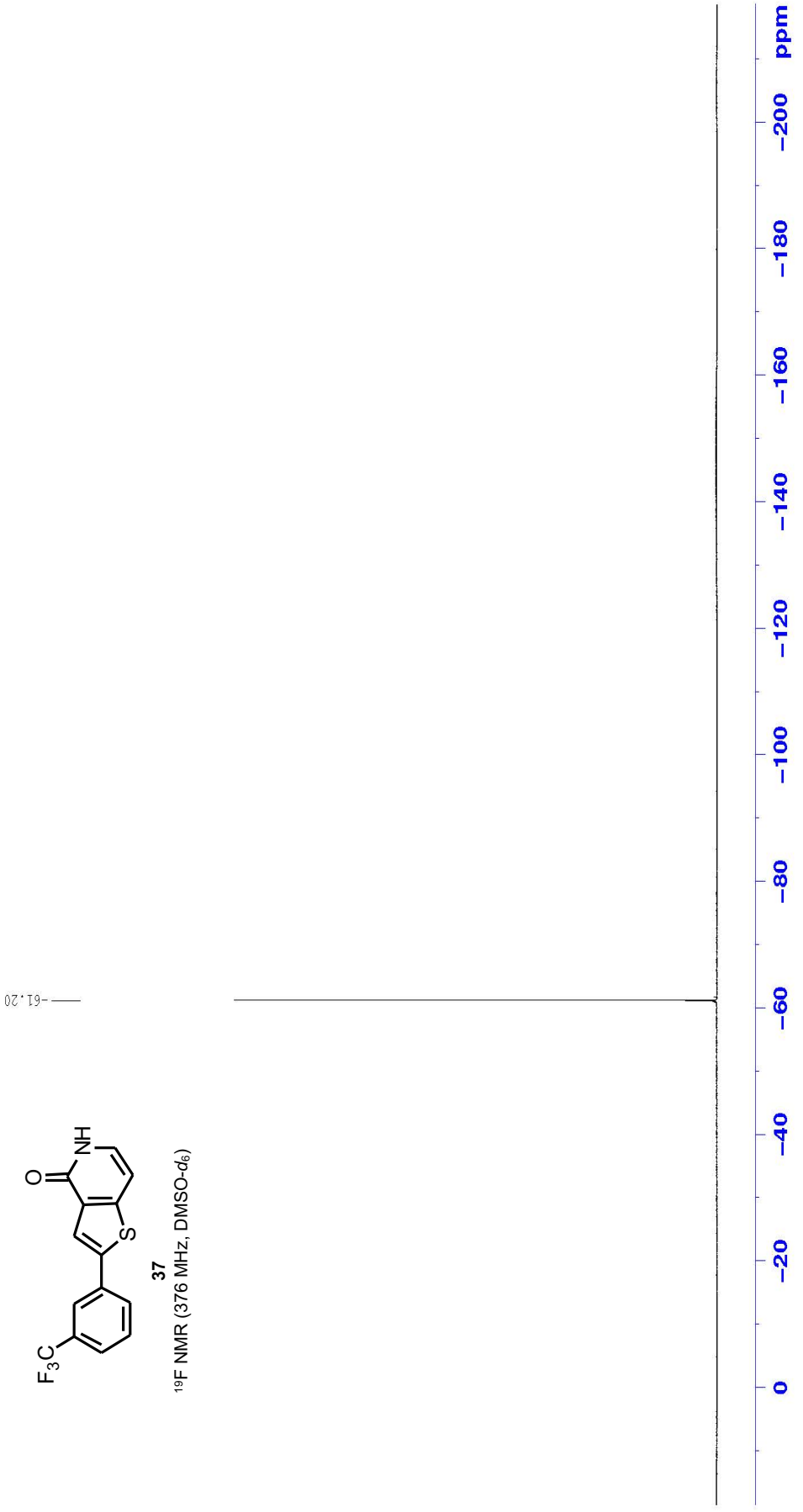

37

^{19}F NMR (376 MHz, DMSO-d_6)

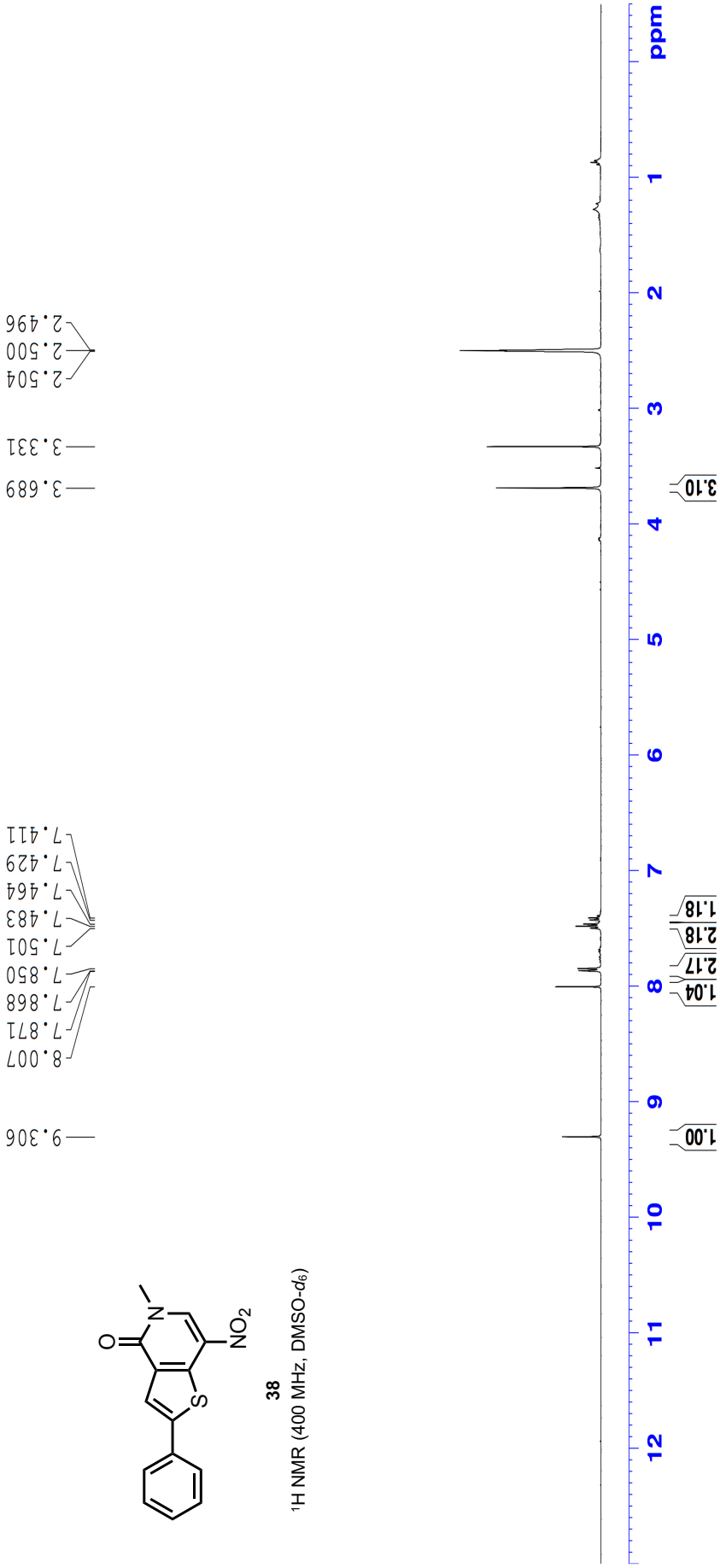

38

^{1}H NMR (400 MHz, DMSO-d_6)

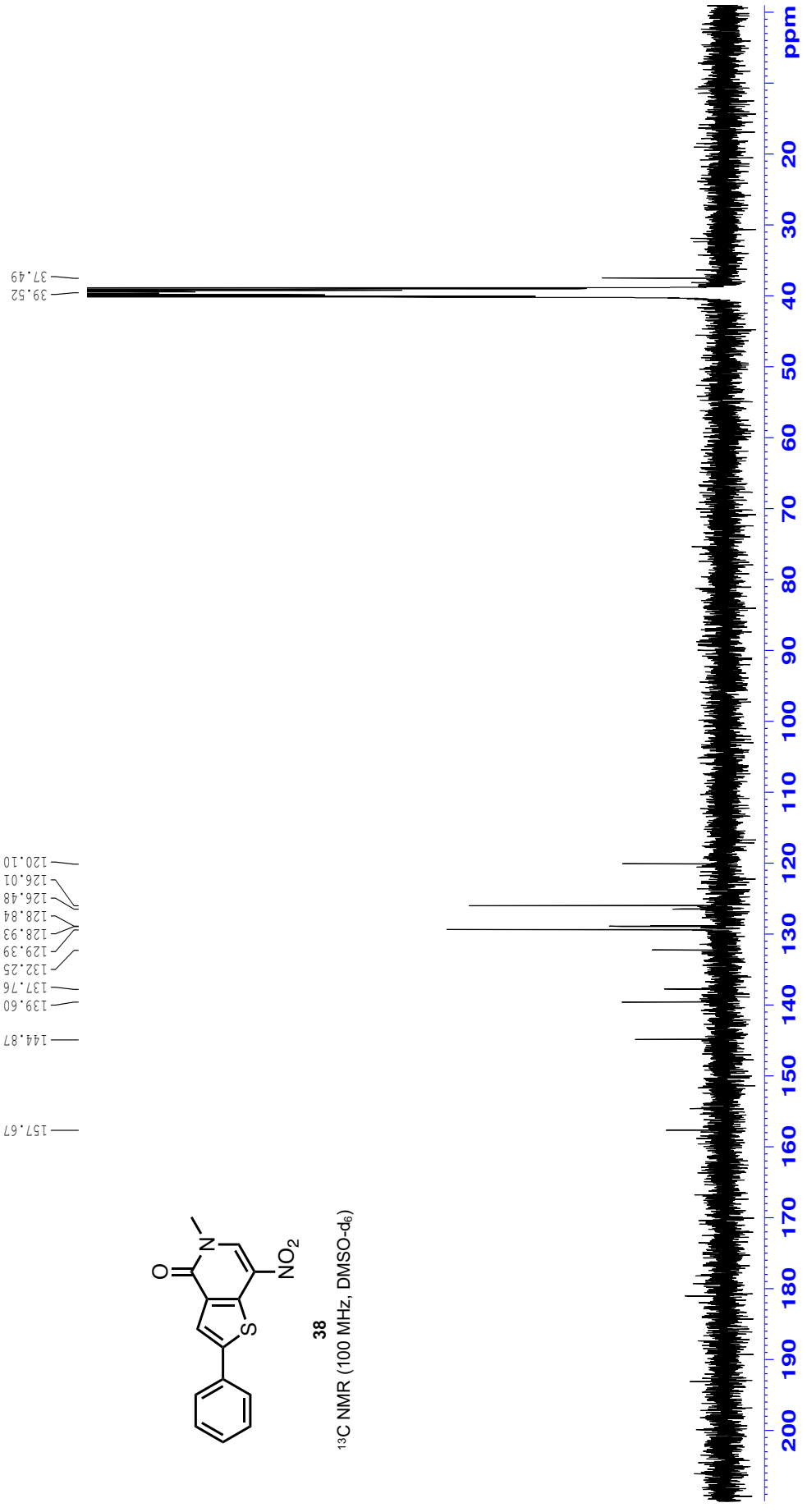

38

^{13}C NMR (100 MHz, DMSO-d_6)

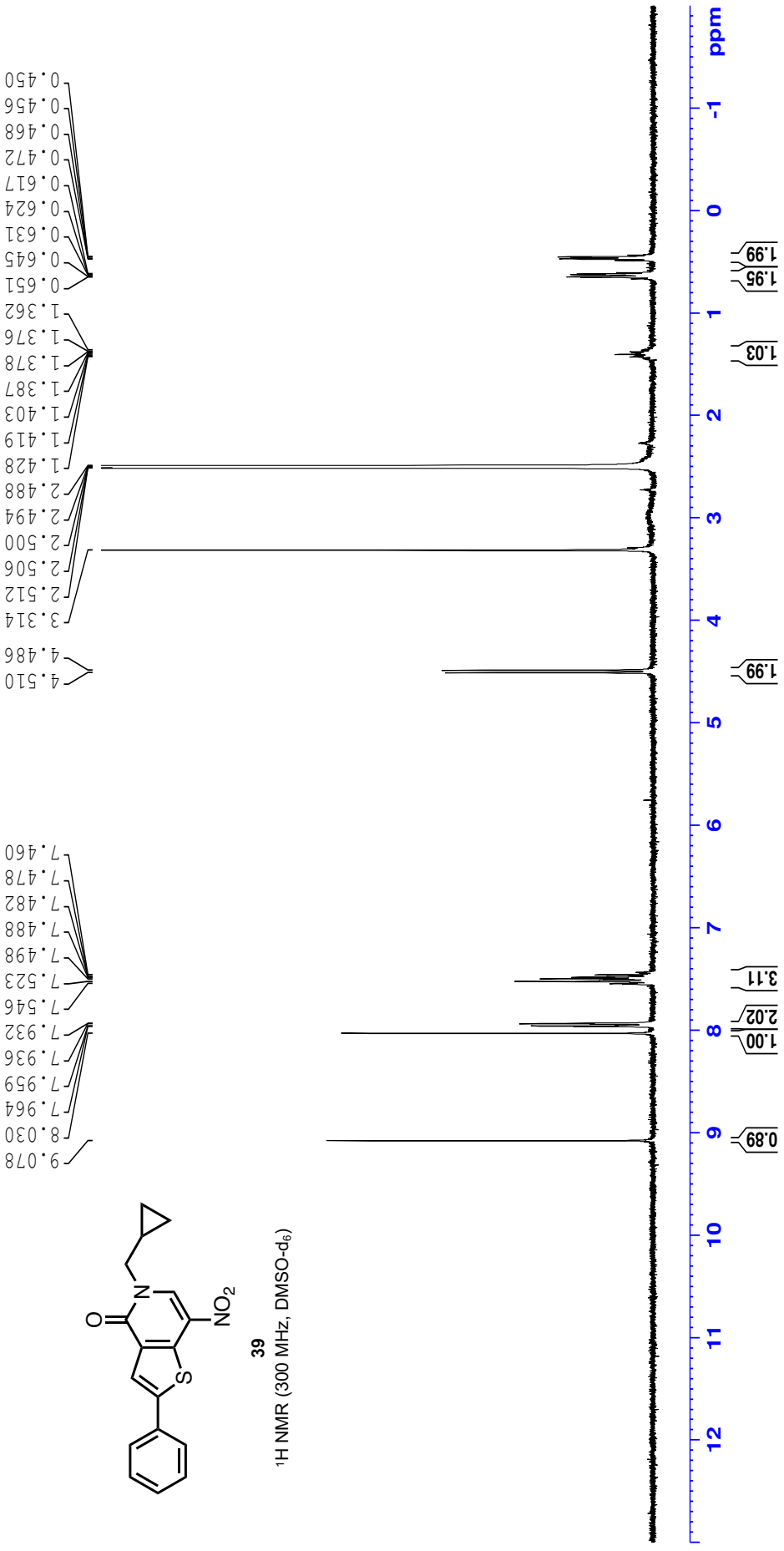

39

^{1}H NMR (300 MHz, DMSO-d_6)

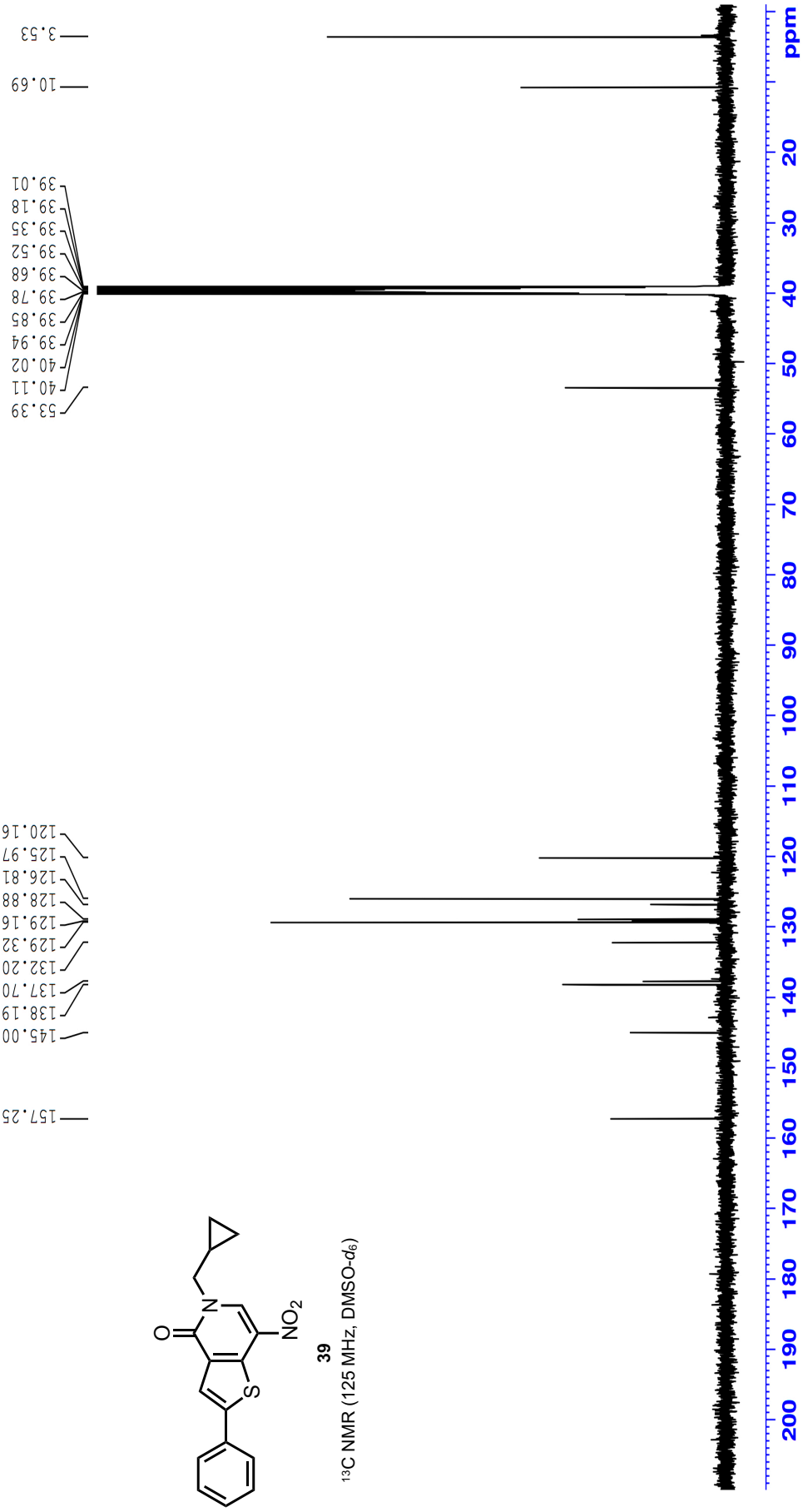

39

^{13}C NMR (125 MHz, DMSO-d_6)

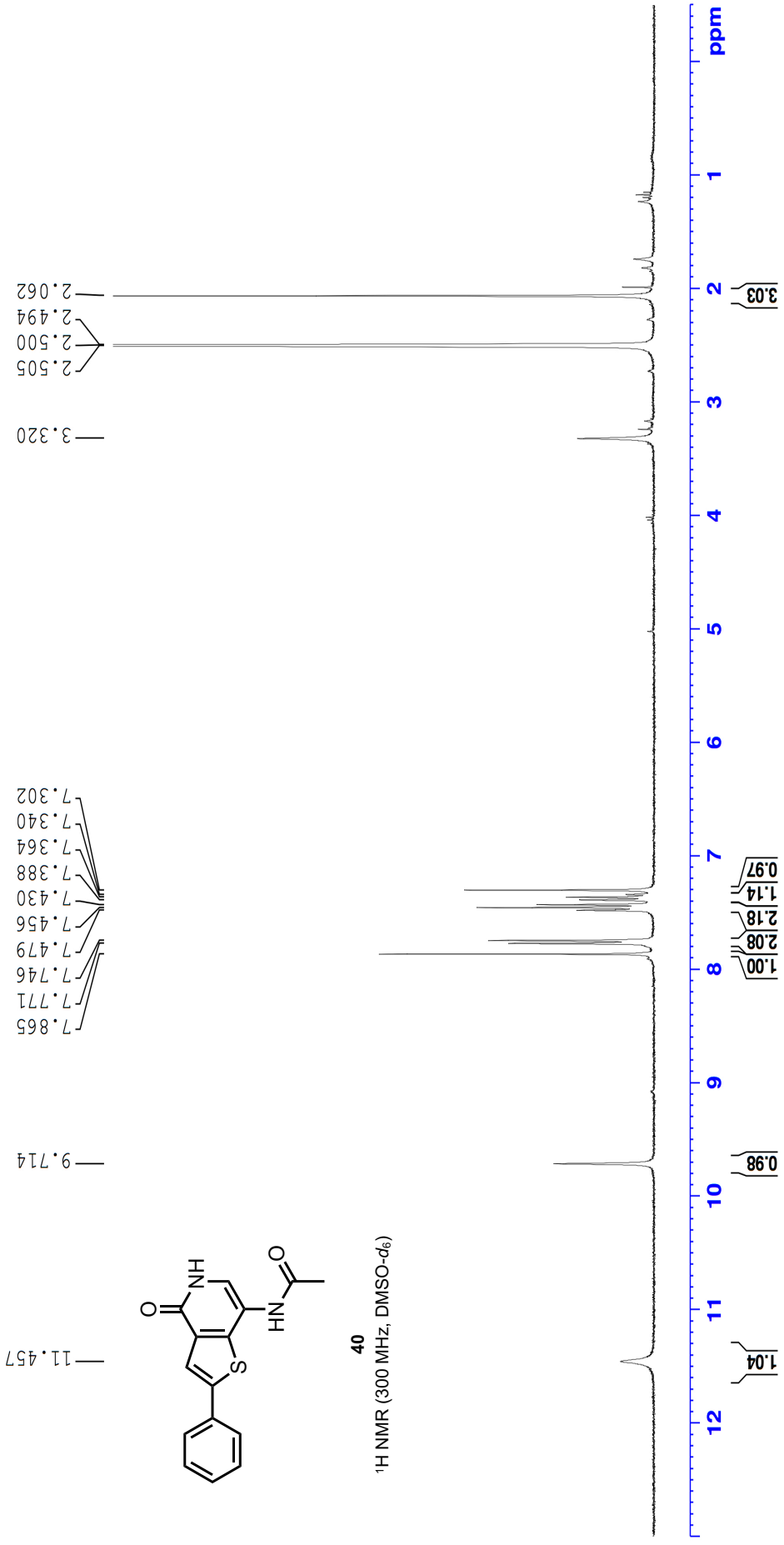

40

^{1}H NMR (300 MHz, DMSO-d_6)

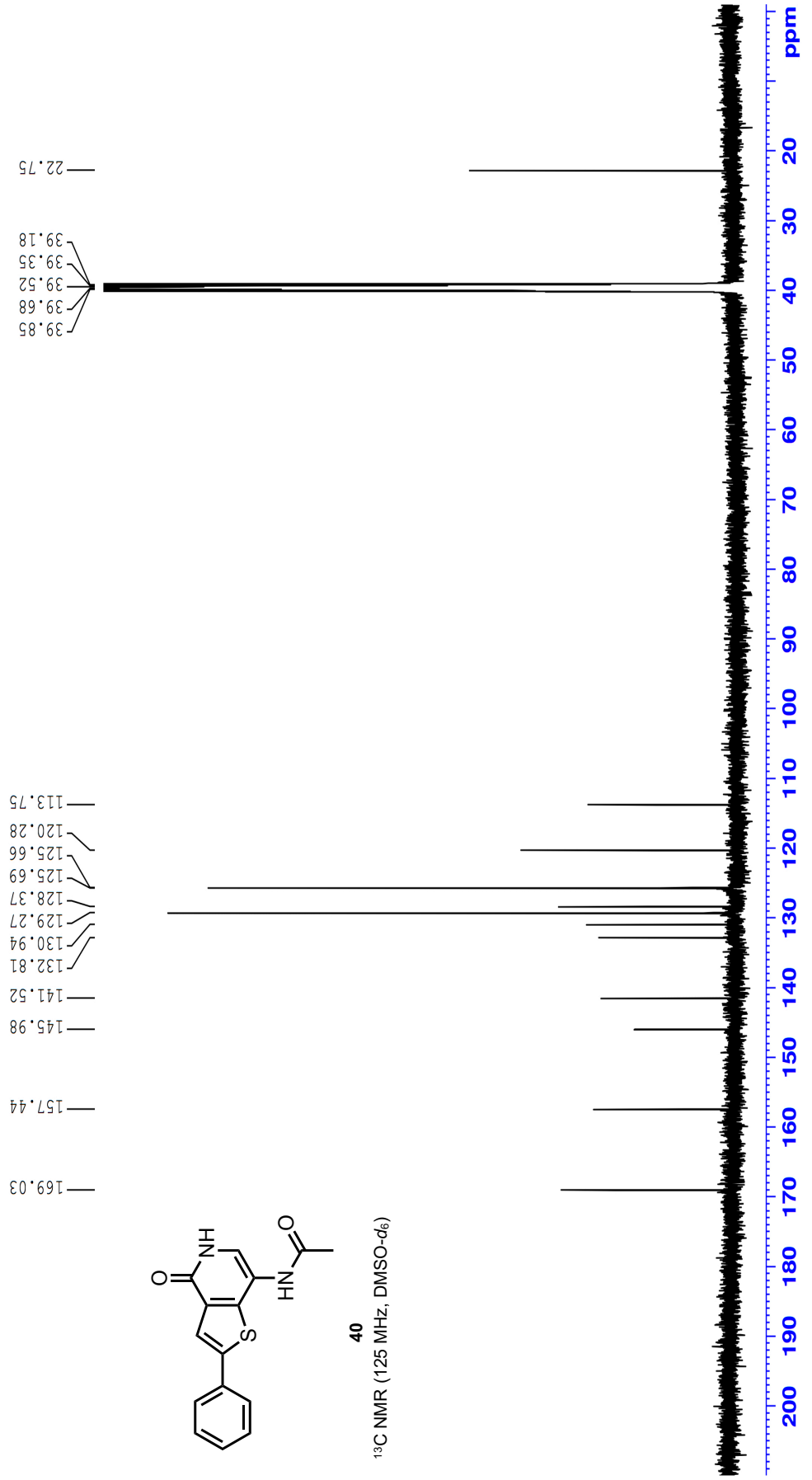

40

^{13}C NMR (125 MHz, DMSO-d_6)

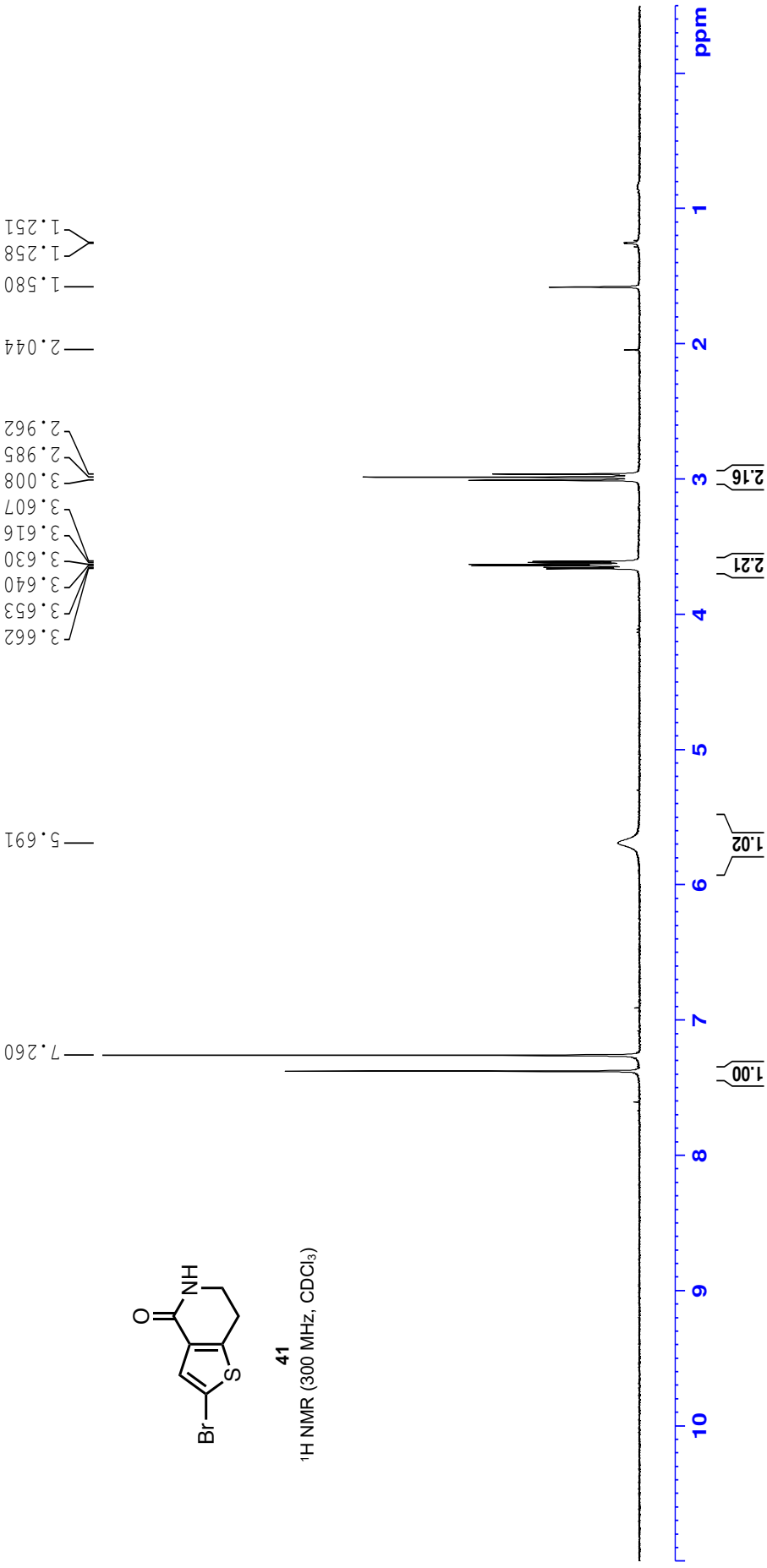

41

^{1}H NMR (300 MHz, $CDCl_3$)

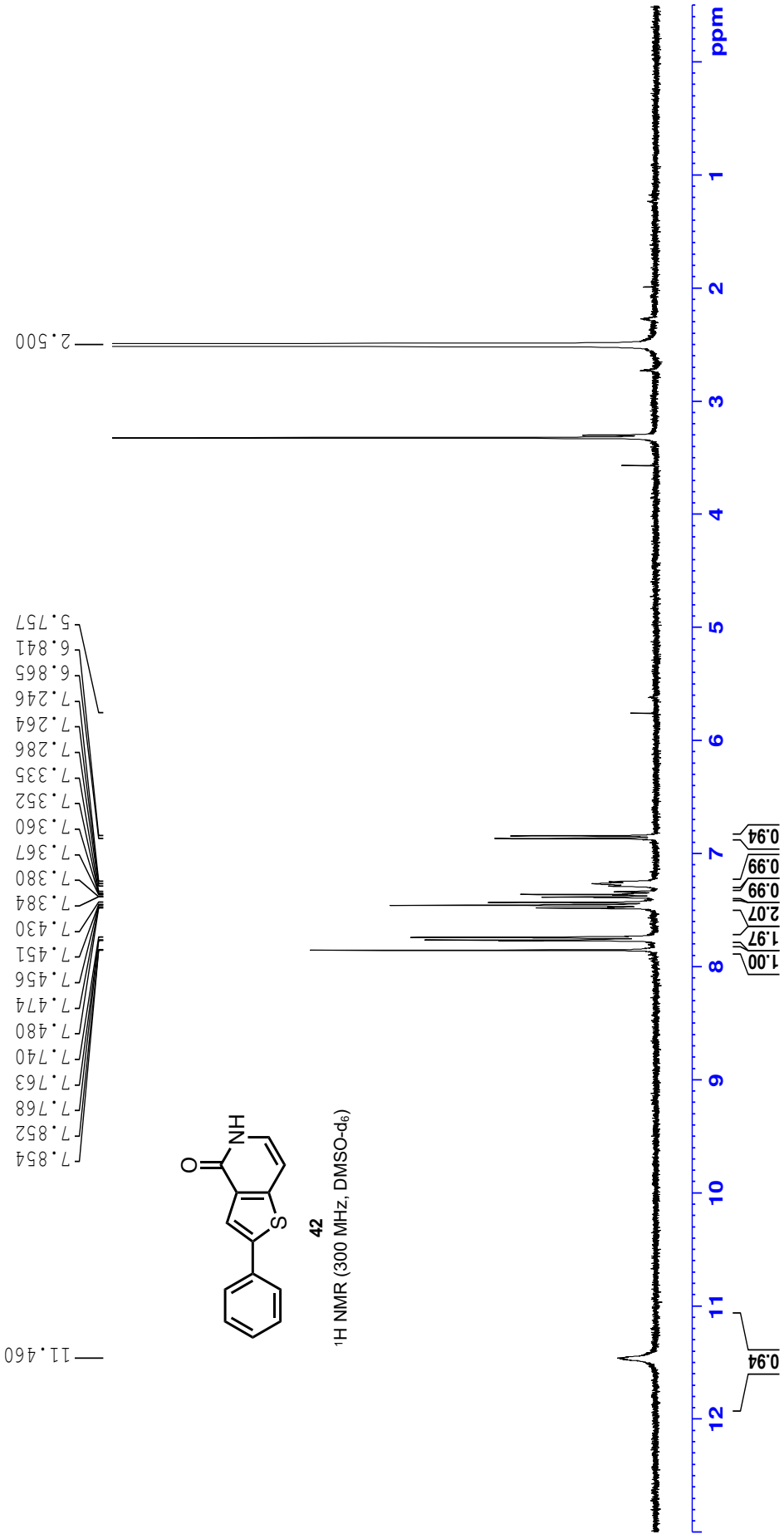

42

^{1}H NMR (300 MHz, DMSO-d_6)

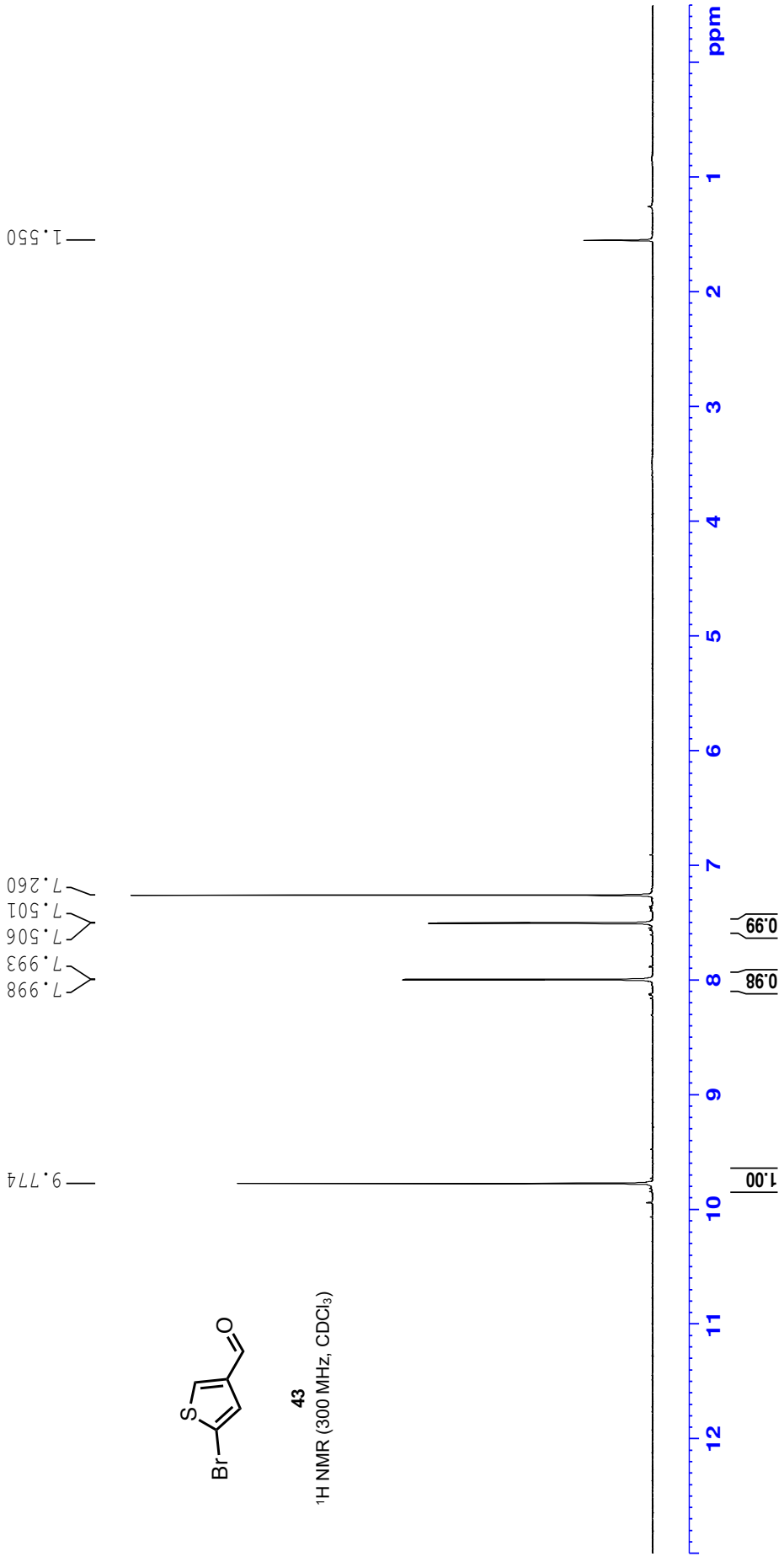

43

^{1}H NMR (300 MHz, $CDCl_3$)

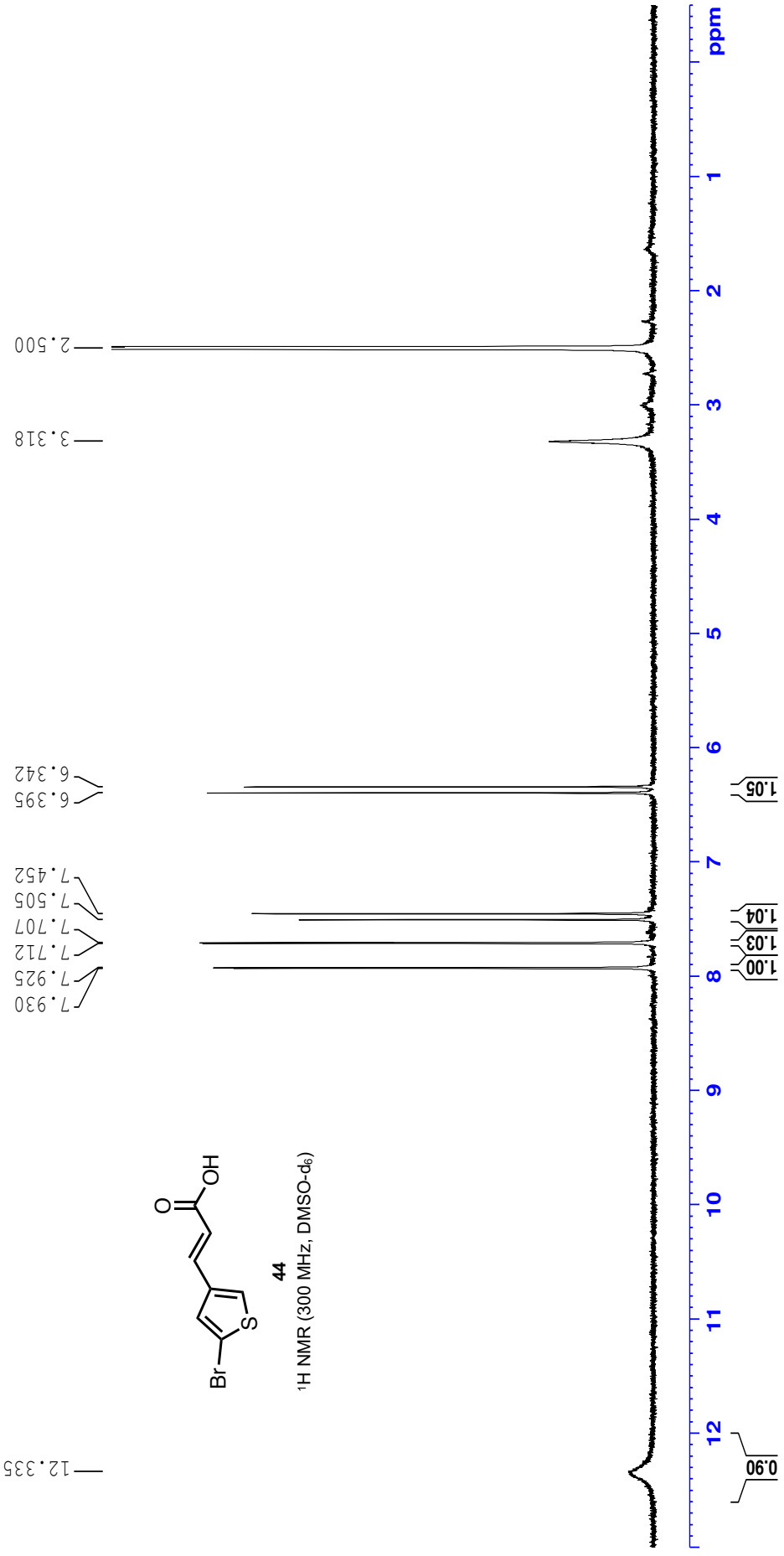

44

^{1}H NMR (300 MHz, DMSO-d_6)

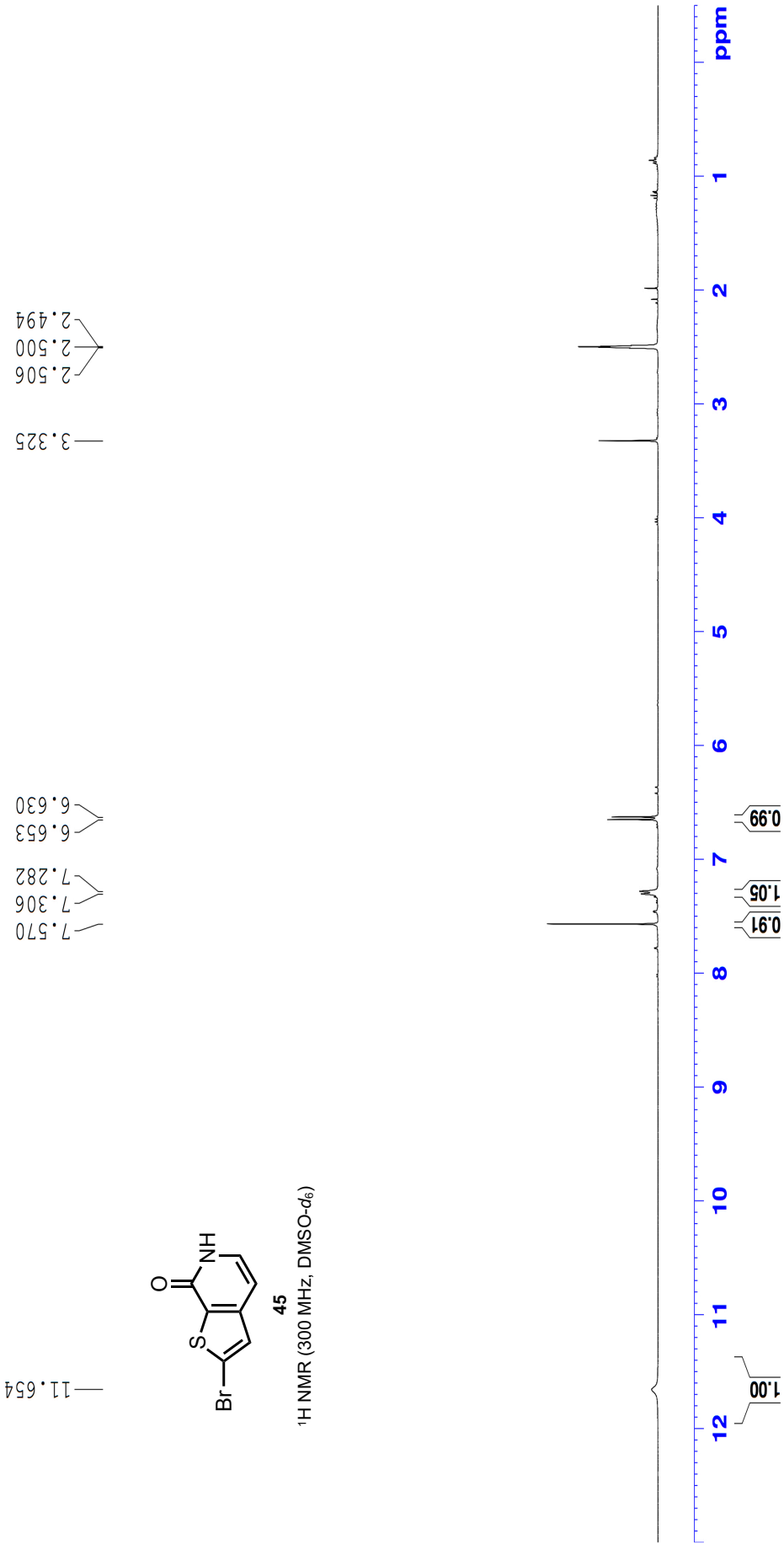
11.654
7.570
7.306
7.282
6.653
6.630
3.325
2.506
2.500
2.494
Br
S
O
NH
45
^{1}H NMR (300 MHz, DMSO-d_6)
ppm
1.00
0.91
1.05
0.99

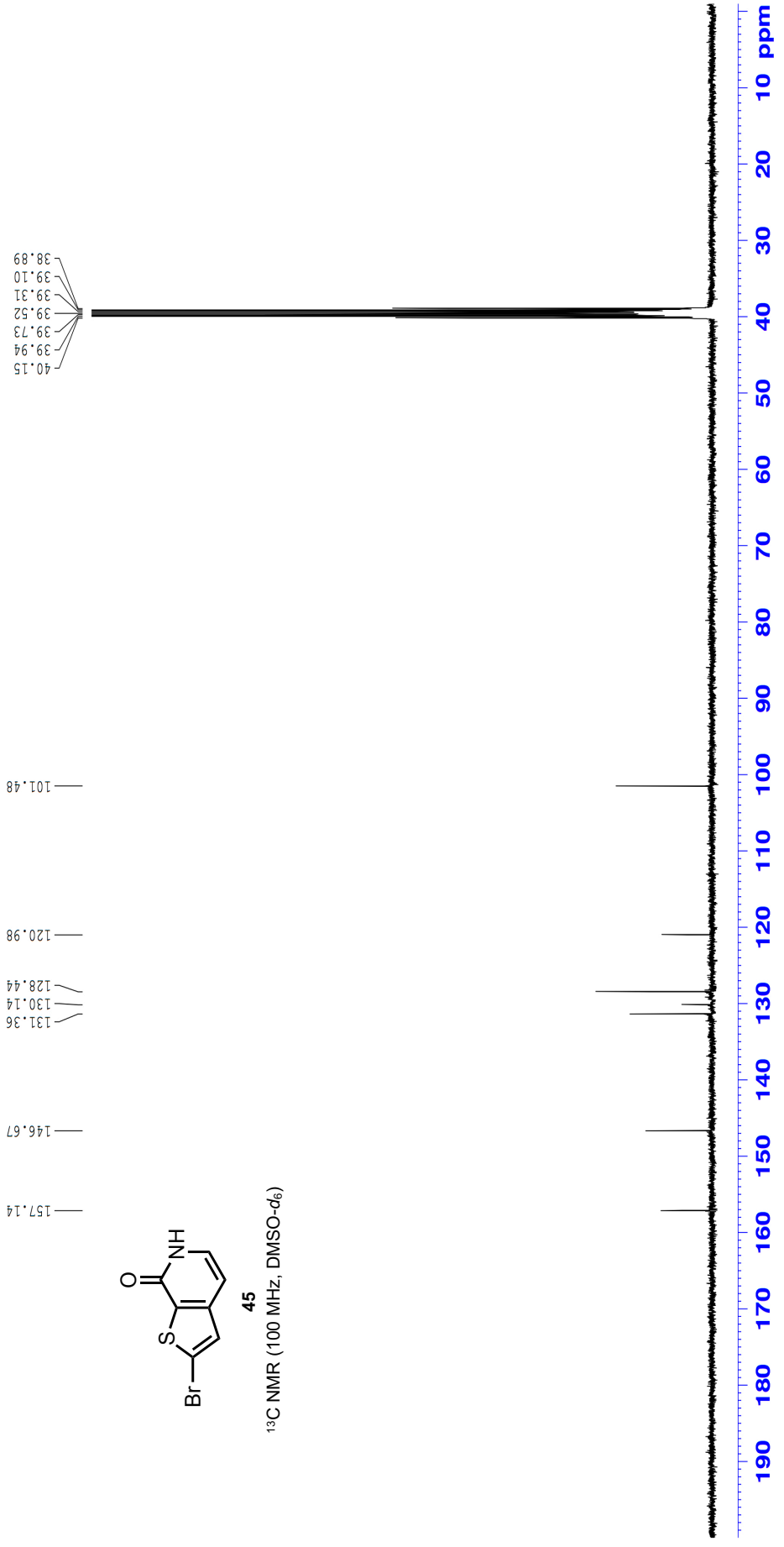

45

^{13}C NMR (100 MHz, DMSO-d_6)

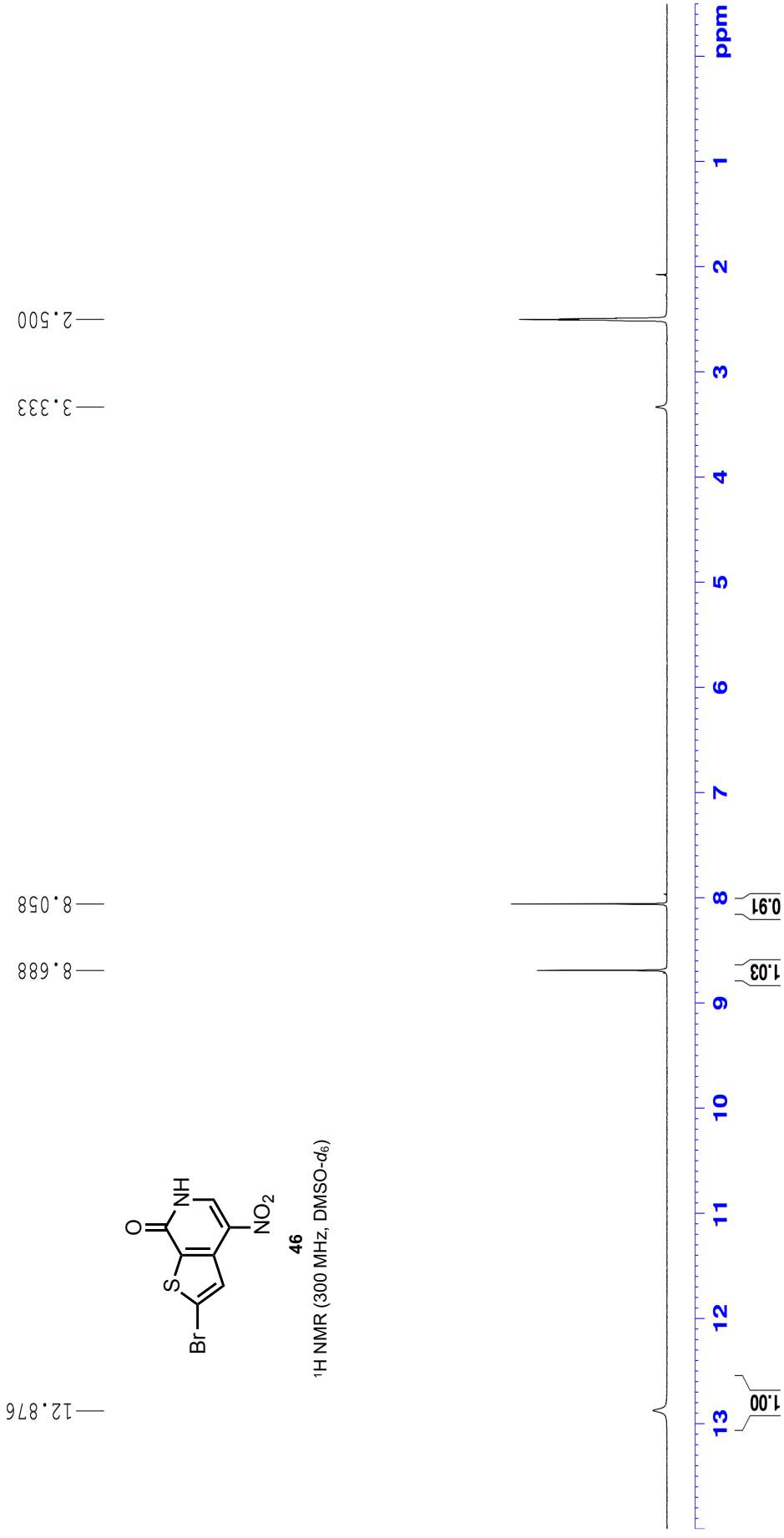

46

^{1}H NMR (300 MHz, DMSO-d_6)

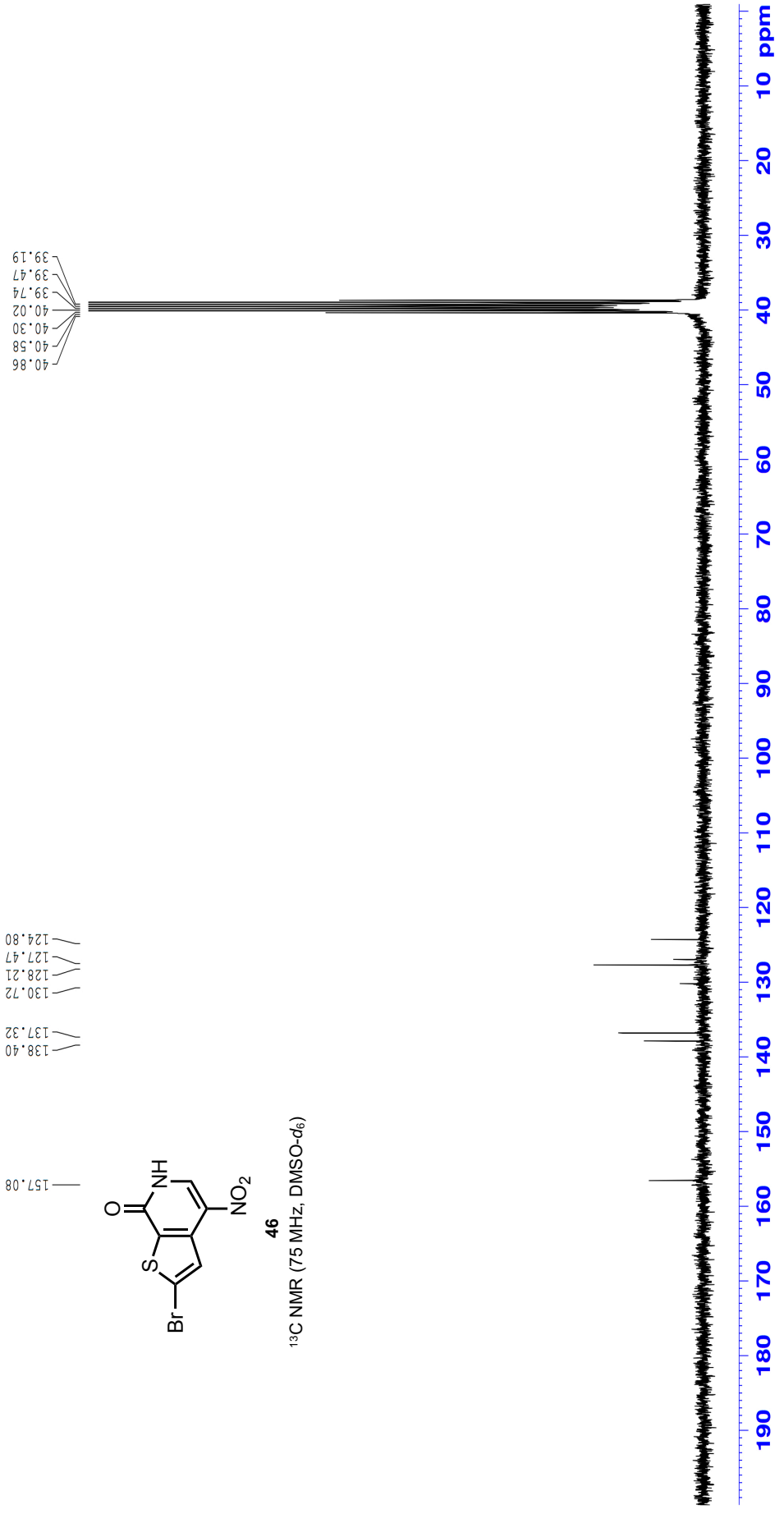
157.08
138.40
137.32
130.72
128.21
127.47
124.80
40.86
40.58
40.30
40.02
39.74
39.47
39.19
NH
O
S
Br
NO2
46
13C NMR (75 MHz, DMSO-d6)
190
180
170
160
150
140
130
120
110
100
90
80
70
60
50
40
30
20
10
ppm

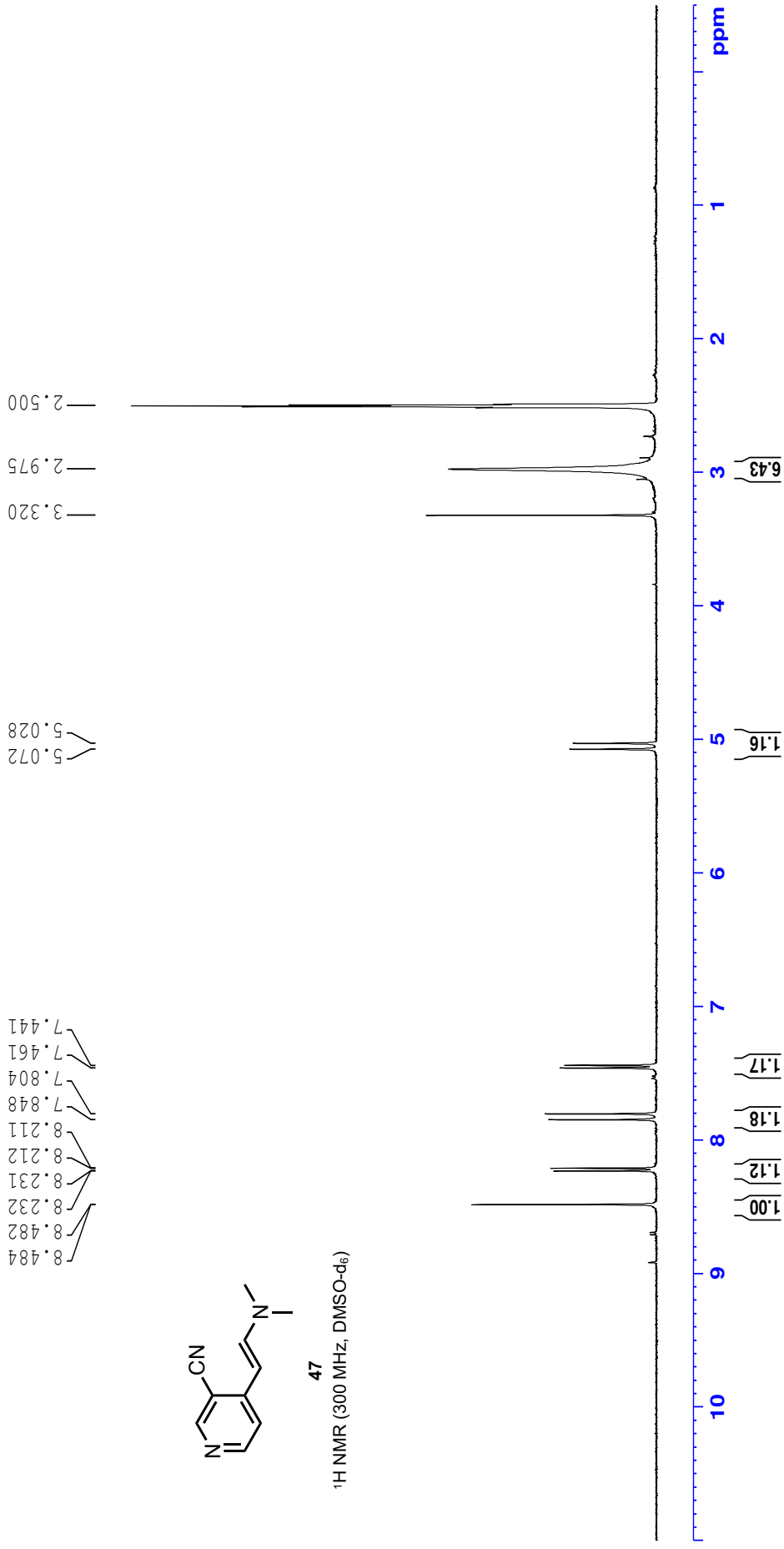

47

^{1}H NMR (300 MHz, DMSO-d_6)

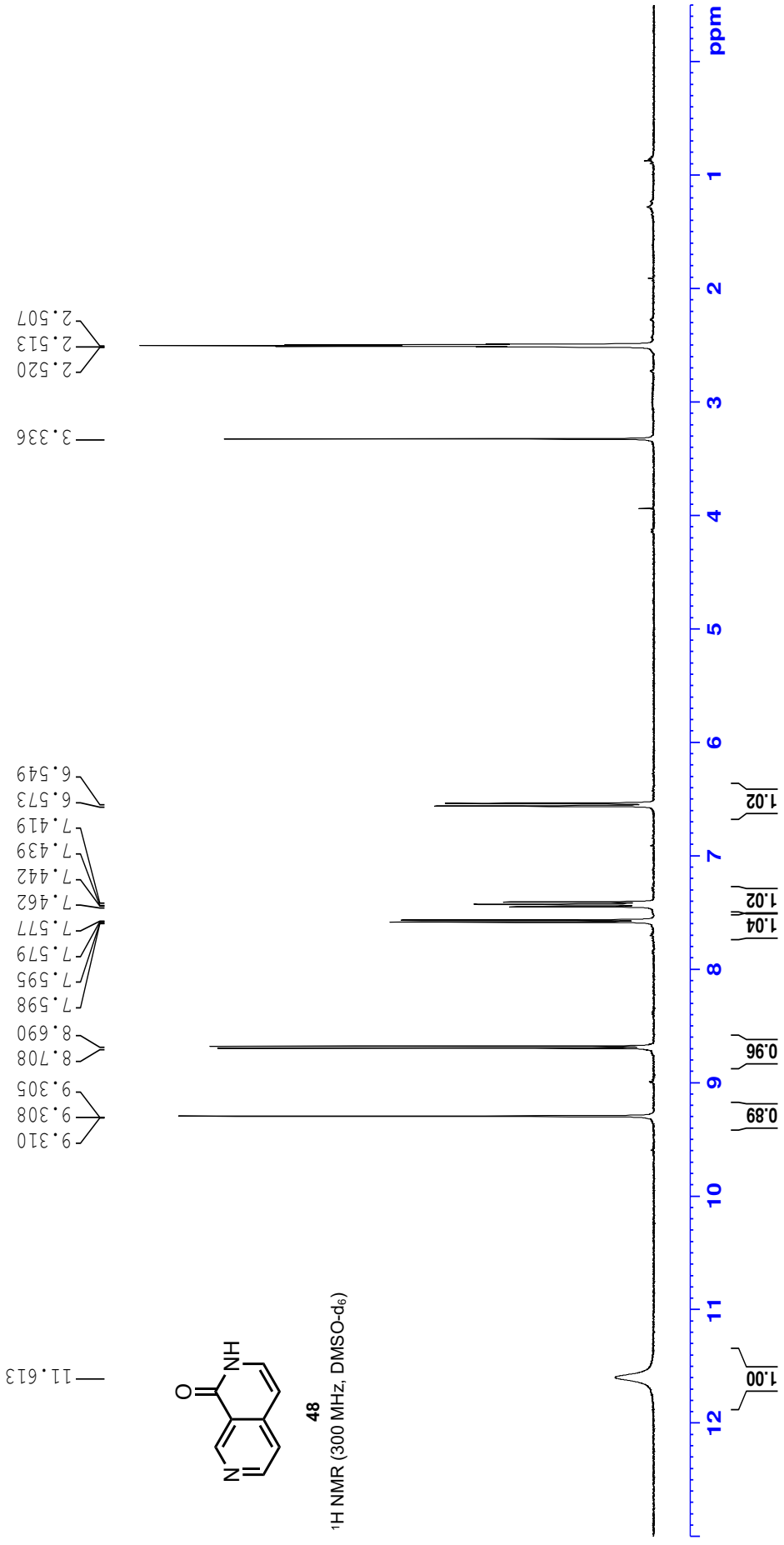

48

^{1}H NMR (300 MHz, DMSO-d_6)

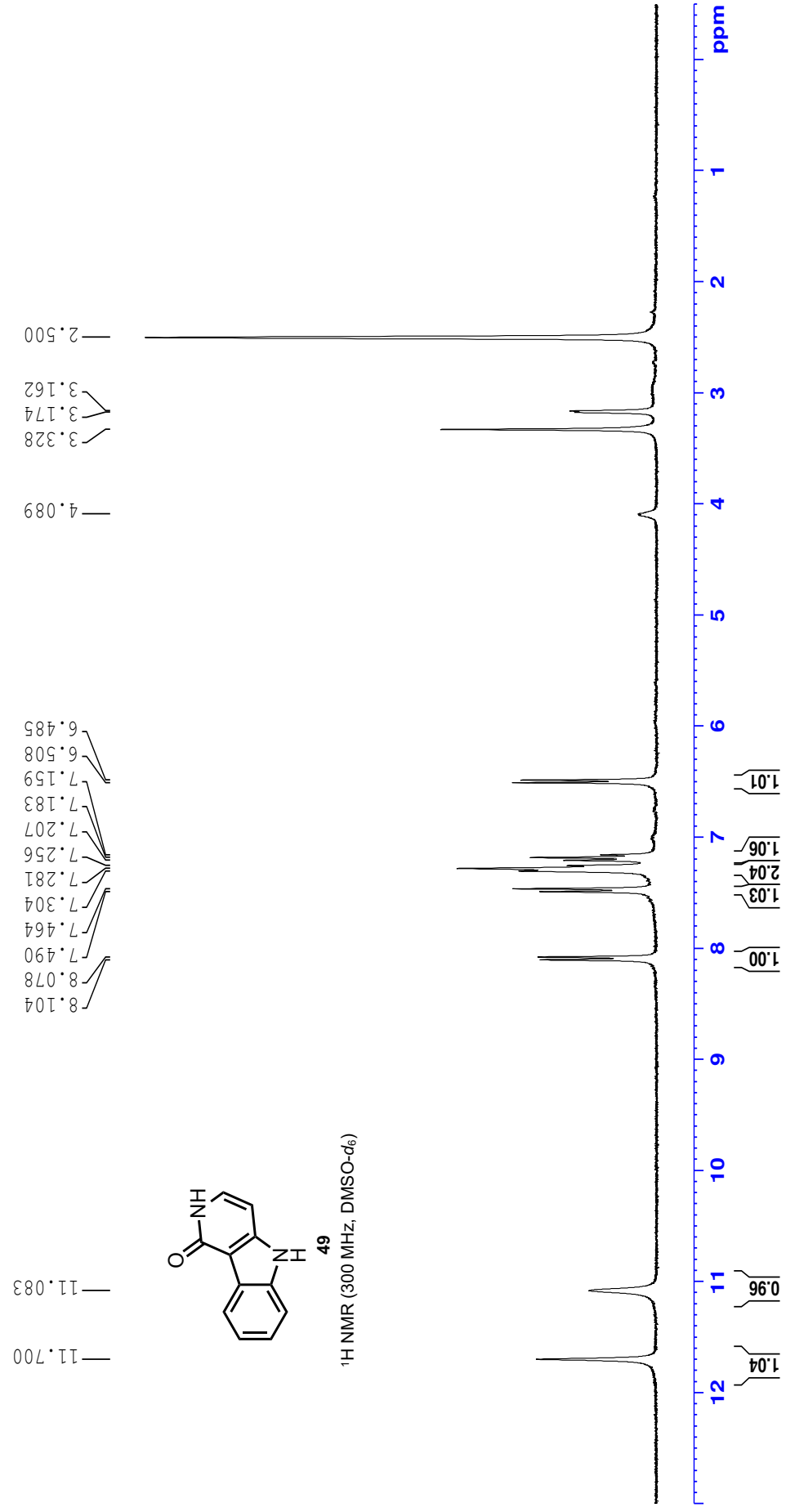

49

^{1}H NMR (300 MHz, DMSO-d_6)